Exploring the Gut-Brain Axis: The Impact of Gut Microbiota-Immune Interface on Mood and Multiple Sclerosis.

Andrea R. Merchak

Ph.D. Candidate
Neuroscience Graduate Program

University of Virginia
May 5, 2023

Mentor: Alban Gaultier

Table of Contents

Chapter 1:

Background

"There is no human endeavor I find more inherently optimistic than the efforts of scientists. The pursuit of understanding our universe, our planet, our bodies—to know the inner workings of humans and how we fit into the greater fabric that stitches us together with all living things and organic matter. Each new discovery is born from investigation, experimentation, recalibration, and new iteration, and sometimes, by just a stroke of luck mixed with the expertise to recognize the serendipity of a breakthrough."

-Kat J. McAlpine

excerpt from *A Science Editor's Love Letter to Hope*

This chapter expands on the publication authored by Andrea Merchak and Alban Gaultier. Brain, Behavior, & Immunity-Health, 2020.

1. Introduction to Depression

Mood disorders, which affect nearly 10% of the world population each year are undertreated and not well understood. Major depressive disorder (MDD) is the leading claim for disability aid in the United States, resulting in millions of dollars in federal unemployment costs[1]. Currently, most treatment plans include various types of counseling, but also rely heavily on pharmacological approaches, including selective serotonin reuptake inhibitors (SSRIs), serotonin-norepinephrine reuptake inhibitors (SNRIs), cyclic antidepressants, and less commonly monoamine oxidase inhibitors (MAOIs)[1]. Due to the heterogenous nature of depression, however, many individuals are treatment-resistant or forgo drug therapy due to adverse side effects. For these reasons, there is continued interest in the identification of novel therapeutic targets that have improved efficacy and safety profiles. Evidence linking the gut microbiome and mood has opened new avenues for potential therapies.

A noteworthy indication that peripheral activity may be influencing the brain during stress and depression is that blood brain barrier (BBB) permeability increases in these patients. This increase in permeability allows for increased immune signals and for other small molecules (some derived from the microbiome) to more easily cross into the brain. Some studies have shown that this effect is targeted to areas playing an important role in mood regulation like the nucleus accumbuns[2] while others have shown a more ubiquitous effect[3].

The novel tools available to investigate the gut-brain axis have revolutionized how we understand the impact of diet and microbes on brain function. Current work has shown that diet and microbiome not only affect the function of the periphery, but are also crucial for central nervous system (CNS) development and health. The link between the gut and the brain was first proposed by anatomists in the 18th century, but was pioneered and popularized by John Abernethy and his 1829 book *The Abernethian Code of Health and Longevity,* in which he traces all mental disorders to their ultimate cause of "gastric derangement"[4]. Since then, researchers have been able to use evidence-based, hypothesis-driven approaches to elucidate mechanistic links between the digestive and nervous systems for most known neurological and psychiatric disorders[5].

1.1 Microbiome Changes in Depression

About 90% of the bacterial species in the healthy, adult human gut fall within the *Bacterioidetes* and *Firmicutes* phyla[6]. Phyla refers to the broadest classification in the kingdom of bacteria. More specific taxonomy then includes class, order, family, genus, and species. The microbiome is established in the first 3-5 years of life and remains relatively stable thereafter. The primary influencing factors that establish a healthy gut microbiome are seeding of the microbiome by early exposure to the vaginal and skin microbiota of the mother and the diet. This stable gut microbiota is crucial for health. A strong colonization by a healthy microbiota can outcompete pathogenic bacteria, protozoa, and fungi, thus offering protection from the infiltration and compromise of the gut niche by pathogens. In addition, these bacteria are an important component in the proper digestion of food allowing efficient processing of essential nutrients and providing, through their metabolic processes, essential vitamins and nutrients.

Researchers have compared the bacterial families in the guts of patients with MDD to healthy controls. Fecal samples of patients suffering from depression, but not those whose depression was controlled by medication, had increased α-diversity, indicating increased number of bacterial families or genera able to inhabit a person's intestine[7]. Through fecal sequencing, increases have been observed in the proportion of *Coriobacteriaceae, Enterobacteriaceae, Rikenellaceae, Porphyromonadaceae, Thermoanaerobacteraceae, Acidaminococcaceae, and Fusobacterium.* There is evidence for decreases in the following bacterial families: *Bacteroidaceae, Ruminococcaceae, and Clostridiaceae.* Finally, there have been mixed findings when examining species of some families including *Prevotellaceae, Lachnospiraceae, Erysiopelotrichaceae, and Veillonellaceae*[7–9]*.*

Meta-analyses of probiotic studies as treatment for depression have not typically accounted for probiotic type. However, they are in agreement that the use of probiotics to improve mood, especially in patients with mild-to-moderate depression, is better than placebo and has fewer side effects than current treatment options[10,11]. One of the current drawbacks of probiotic treatment is that the effect size of the treatment is often not as great as that of neuromodulator therapies and therefore, its efficacy as a primary treatment has yet to be supported in clinical trials[12]. At this time, it is primarily proposed for use in conjunction with current therapies, for use in patients with mild-to-moderate depression, or as an additional therapy option for those with treatment-resistant depression.

Stress is one of the highest risk factors for depression and so most models of depression focus on different life stressors. Some of the strongest evidence for the role of the microbiome in regulating stress and mood responses comes from studies using animal models. The germ-free animal model lacks a microbiome, not only in the gut, but the skin and mouth as well. These mice have a striking increased response to a mild restraint stressor, a model where the mice are physically restrained for one hour. The increase in adrenocorticotropic hormone (ACTH) and corticosterone in response to the stressor are two-fold higher levels than those of a regularly colonized mouse undergoing the same procedure. This effect can be ameliorated by recolonizing germ free mice during development, indicating that the microbiome is vital to regulating the stress response[13]. The necessity of bacterial colonization for proper regulation of stress response has been supported in several other reports and has been expanded upon to show that anxiety- and depressive-like behavior are markedly decreased in response to stress in germ-free mice, which can be reversed by colonization[14]. Germ-free mouse

models have also led to the discovery of many microbially-derived metabolites that are only present in the CNS after recolonization with gut bacteria[15].

Early work in animal models has shown that stressors can change the gut microbiota composition in animals. For example in an early study of rhesus monkeys, the number of fecal *Lactobacilli* correlated with signs of behavioral stress in a maternal separation early life stress model[16]. Remarkably, depressive symptoms, including increased anxiety-like behavior and anhedonia, can also be transferred to rats using fecal transplants from severely depressed human patients[8]. Numerous studies have indicated specific bacterial strains are beneficial in reversing depressive- and anxiety-like behaviors in models of stress. For example, in the unpredictable chronic mild stress model of depression, *Lactobacillus reuteri*[17], *Lactobacillus rhamnosus*[18] and *Clostridium butyricum*[19] have shown antidepressant effects. *Lactobacillus* is commonly used as "antidepressant" bacteria, which is likely effective as it reverses the reduction of *Lactobacillus* that is seen in stress-induced depression[17]. While mechanisms mediating behavioral changes have been suggested in many of these studies and reviews have presented a wide variety of hypotheses based on decades of work, bacterial interaction with the host remains incredibly complicated. Here we examine the different modes of communication with the CNS that involve some of the small molecules produced by the commensal bacteria in the gut (**Figure 1.1**).

2. Introduction to Multiple Sclerosis

While mood disorders are the focus of this thesis, a portion of my work examines the impact of the microbiome on mouse models of multiple sclerosis (MS). MS is a chronic autoimmune disease that affects the CNS, resulting in a range of neurological symptoms. It is one of the most common neurological disorders affecting young adults, with an estimated 2.8 million people affected worldwide. MS is characterized by the destruction of the myelin sheath, which is the protective covering that surrounds nerve fibers in the CNS, leading to the formation of scar tissue and the disruption of signaling. Patients with MS and other autoimmune disorders are more likely to have depression than other disorders causing disability. In fact, about half of patients with MS will experience depression during their lifetimes[20–22]. This indicates that there are likely common physiologic risk factors for autoimmune diseases and mood disorders.

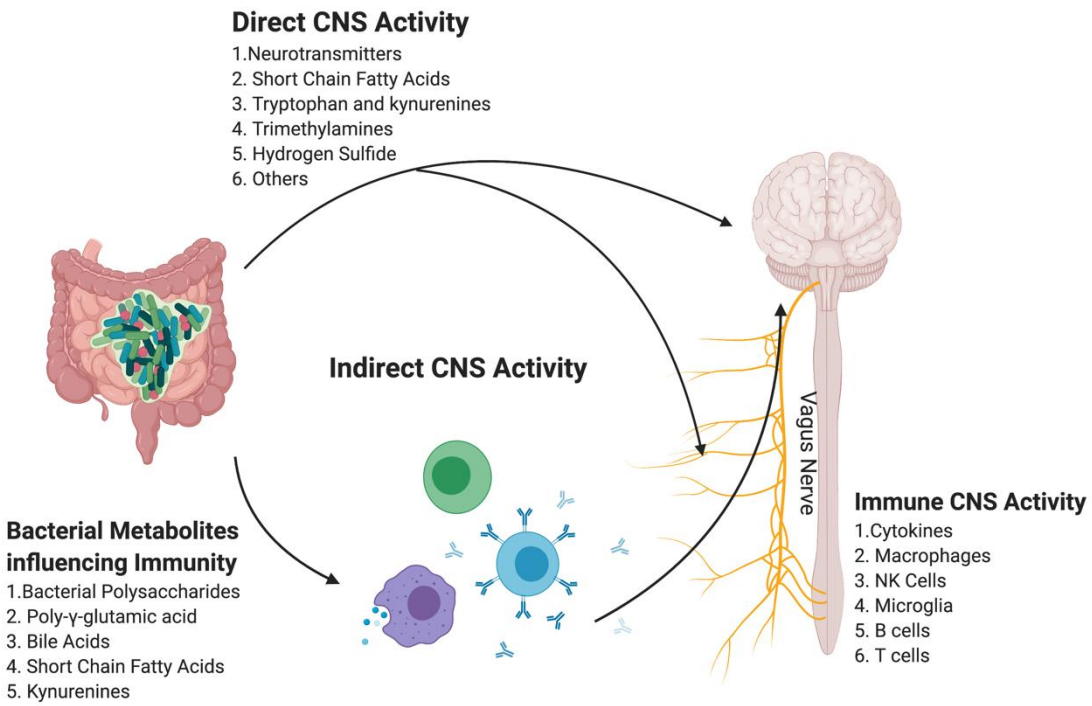

Figure 1.1: The gut microbiota produce diverse small molecules which can impact the central nervous system. Several act through neuromodulation directly on the vagus nerve which innervates the viscera, or by entering circulation and crossing the BBB to interact directly with the brain. While there are several modes of indirect communication with the central nervous system, modulation of the immune system has the greatest evidence for modulation of mood in stress and depression.

The exact cause of MS is still unknown, but it is widely believed to be a combination of genetic and environmental factors that trigger an abnormal immune response. There are several forms of the disorder including relapsing remitting (RRMS) which results in rapid onset of symptoms followed by periods of recovery and primary progressive (PPMS) which results in the gradual decline of motor and cognitive function. Current therapies for MS are most often immunosuppressant drugs which result in non-specific immune dampening. These have a number of harmful side effects ranging from increased susceptibility to infection to kidney damage. Because of these drawbacks, and that current therapies are aimed only at slowing progression rather than curing the disorder, novel therapies are necessary.

It is at this inflection point that I examine the environmental factors which contribute to MS. MS is most common in women and correlates with geography, the farther north one lives, the more likely one is to be diagnosed with MS. There also seem to be relationships with diet and the microbiome. As such I will further examine the known association between the microbiome and patients with MS.

2.1 Multiple sclerosis and the microbiome

The gut microbiota is known to change in patients with autoimmune diseases including MS[23]. MS patients tend to have lower abundances of *Chlostridia*[24]*, Bacteroides* and *Parabacteroides*[24–26] Prevotella[24–26]*,* and *Lactobacillus*[26] to name a few. Because of the heterogeneity of microbiota communities between patients, trends have been difficult to find across studies. There are many hypotheses as to why the gut microbiota is changed in these patients. Likely, there is a combination of several factors. There may be differences in host genetics that promote these gut microenvironments. There may also be direct effects of the autoimmune response on the digestive tract. Overall, studies are underway to determine whether probiotic supplements could be used in conjunction with current therapies to improve outcomes for patients.

Some of the most convincing data supporting a bidirectional cross talk between the gut and the immune system during MS comes from mouse models. For example, germ-free mice, who lack commensal microbiota completely, have mild forms of experimental autoimmune encephalomyelitis (EAE) or do not develop signs of the disease at all[27]. Th17 cells are one of the primary active immune mediators of EAE. Recent work has shown that in the absence of segmented filamentous bacteria (SFB), no Th17 cells develop and these animals have weak EAE[28,29]. While the studies described here use dramatic means to change the gut microbiota, we have also been able to track the more nuanced changes that occur through EAE[30]. For example, *Lactobacillus* is decreased during EAE in mice. Together these findings point to the gut microbiome as another angle to search for disease modifying and preventative therapies.

The rest of this chapter summarizes the known impacts of microbial products on the brain and immune system. I will provide information on mechanisms where available. I will present the current

state of our understanding of the microbiome-immune-brain axis in the context of depression and multiple sclerosis.

3. Direct Effects of Microbial Metabolites on the Nervous System

There is a high level of diversity in the molecules that are being produced in the gut. Many of them have direct neuromodulatory, neurotrophic, or neurotoxic activity. The nerve innervating the viscera, including the small intestine, is called the vagus nerve. The vagus nerve is responsible for significant portion of gut-brain communication. As it is geographically close to the gut, vagus nerve activity can be directly modulated by the small molecules released by the gut microbiota. These small molecules can also enter circulation and either be transported or freely diffuse across the blood brain barrier (BBB). When these small molecules enter the brain, they can influence metabolism or directly impact neurotransmitter signaling (**Figure 1.2**). Bacterially-derived short chain fatty acids act directly on the nervous system through histone deacetylase inhibition in the brain, changes in endocrine activity, and activation of the vagus nerve. Conversely, tryptophan and its metabolites act in the brain through modulation of several neurotransmitter receptors including NMDA and AMPA receptors. They also modulate the metabolic output of glial cells, which are essential for supplying nutrients and energy to neurons for proper firing. Both of these families of molecules have strong evidence indicating that they play a role in depression and stress. There are several other families of molecules including trimethylamines and ammonia which have been proven to be neuroactive but have yet to be implicated in depression. Those molecules should be a focus for future research to determine their impact on mood disorders.

Comparison of the Direct Pathway of Bacterial Metabolite-Brain Communication

Metabolite Family	Short Chain Fatty Acids	Trimethylamines	Kynurenines	Neurotransmitters
Examples	Acetate Proprionate Iso Butyrate Butyrate	Trimethylamin-N-oxide	Kynurenine Kynurenic Acid Xanthurenic Acid Quinolinic Acid	Seratonin Hydrogen Sulfide GABA Dopamine Epinephrine
Bacterial Producers	Bacteroides, Bifidobacterium Propionibacterium Eubacterium Lactobacillus Clostridium Roseburia Prevotella	Anaerococcus Clostridium Escherichia Proteus Providencia Edwardsiella	Clostridium Streptomyces Pseutodmonas Bacillus Burkholderia	Provotella Lactobacillus
Receptor Activation	FFAR2, FFAR3	None	NMDA, AMPA, GCPR35	Most Neurotransmitter Receptors
Vagus Nerve or Brain Activation	Vagus Nerve and Brain	Brain	Vagus Nerve and Brain	Vagus Nerve and Brain
Neurotoxicity?	No	?	Yes	No
Metabolic Regulatory Activity	Yes	?	Yes	No

Figure 1.2: Families of metabolites can be produced by a large number of different bacterial genera. Short chain fatty acids, kynurenines, and neurotransmitters produced in the gut all are implicated in stress and depression. Trymethylamines and others require further examination to determine their role in depression, though their impact on CNS activity has been established.

3.1 Short Chain Fatty Acids

The primary metabolic output of microbial fermentation of dietary fibers are 1-6 carbon chain saturated fatty acids, commonly known as short chain fatty acids (SCFAs). The bacterial genera that produce them include *Bacteroides, Bifidobacterium, Propionibacterium, Eubacterium, Lactobacillus, Clostridium, Roseburia, and Prevotella*[31]. This group of small molecules has a high absorption rate in the host body (up to 95%)[32] and are prime candidates for bioactive molecules that can affect host physiology. SCFA's can act on the immune, endocrine, and nervous systems showing their diverse

neuroactive potential[33]. Here, we will first examine the mechanism of bioactivity and then explore the translational potential of modulating SCFAs.

The most common SCFAs in the body are acetate (two carbon chain), propionate (three carbon chain), and butyrate (four carbon chain) which are found primarily in the colon. As anions they are responsible for the drop in pH in the colon, which results in a change in the microbial environment. This contributes to the colon having the highest quantity of microorganisms than any other part of the digestive tract and allows for unique organisms to inhabit this niche when compared to the small intestine. Other SCFAs found in lower amounts include formate, valerate and caproate [34]. Movement of SCFAs across the lamina propria by diffusion can occur, but the primary mode of movement into the host is via a variety of active transporters called monocarboxylate transporters (MCTs) expressed by colonocytes [35,36].

Once SCFAs enter the host cell, they can enter the citric acid cycle in the mitochondria and generate ATP. This is most common in colonocytes, but SCFAs also enter circulation through the portal vein, where they can be used for ATP production throughout the body [37]. While this is the primary use of SCFAs, they also exert other biologically activity beyond metabolism. For example, propionate-fed animals, when compared to standard-fed animals, have also been shown to have increased FOS activation in the C1 segment of the spinal cord, as well as in the parabrachial nucleus, the dorsal vagal complex, and parts of the hypothalamus demonstrating SCFA direct neuronal activity[38]. SCFAs can impact the CNS through several avenues. Beyond observations of this direct activity, SCFAs can promote the production of serotonin in the gut[39,40] as well as direct activation of the vagus nerve, which innervates the viscera,[41] and modulation of the immune system[42].

3.1.1 Histone Deacetylase Inhibition

The mechanisms by which SCFAs affect the cells are as diverse as the tissues on which they act. SCFAs serve as epigenetic regulators through histone deacetylase (HDAC) inhibition. HDAC modulation influencing the CNS has been well characterized and is implicated in a variety of neurodevelopmental and neuropsychiatric conditions, ranging from depression to schizophrenia[43]. Sodium butyrate is the primary model of SCFA activity as an HDAC inhibitor. As it has the most thoroughly studied SCFA for HDAC inhibition, it will be the focus here. However, work using other SCFAs and HDAC inhibitors is

becoming more prevalent and will provide further lines of evidence linking depression to HDAC inhibition. Strikingly, histone acetylation in the brain has been linked to several processes. Most specifically, it is important for learning and memory, as well as depressive-like behavior in mice. Learning and memory are impaired in patients with depression, so many of these processes may be linked; examination of memory in conjunction with mood may provide some unique insight.

Histone acetylation modulates the coiling of DNA around histones as well as histone compaction. Acetylation causes a less compact DNA structure which allows the genes in the area to be more accessible and more likely to be transcribed. In this way, HDACs are a key modulator of gene expression[44]. By removing the acetyl groups from histones, they induce a less transcriptionally active and more compact chromatin. Sodium butyrate is a non-specific inhibitor that has been primarily described to inhibit HDAC4, which is associated with synaptic plasticity, neuronal cell survival, and memory[43,45].

Histone acetylation of H3 and H4 in the cortex and hippocampus increases with environmental enrichment and improved long-term memory in a mouse model. In an attempt to mimic these effects, intraperitoneal injection of sodium butyrate led to results similar to environmental enrichment, including improved performance in the Morris water maze and in fear conditioning[46]. In another mouse model of memory loss that included amyloid pathology, histone hyper-acetylation of H3 and H4 in the hippocampus rescued memory loss. As a model of Alzheimer's disease, this study provides evidence that SCFAs may be used therapeutically. In this study, the transgenic mice were given a daily high intraperitoneal (i.p.) dose of sodium butyrate. There was no difference in plaque load or exploratory behavior; but, the mice showed stronger fear conditioning than control animals, which indicates better memory formation as they are able to remember the cues leading to an aversive stimulus. In addition, these animals had an upregulation of the genes associated with memory consolidation in the hippocampus, but not the cortex[47]. This gives further evidence for the link with depression, as volume loss in the hippocampus and other hippocampal abnormalities are associated with stress and depression.

Mouse models of stress using several different paradigms display increased HDAC expression or decreases in H3 and H4 acetylation in various brain regions. Social defeat stress[48–50], forced swim stress[51,52], or unpredictable chronic mild stress[53,54] have all been shown to correlate with a reduction

of acetylation. In addition, tricyclic antidepressants can operate as HDAC inhibitors[49]. This gives strong evidence that HDAC inhibition is important for mood regulation. In studies examining the antidepressant-like effects of sodium butyrate, depressive-like behavior was reversed in various behavioral tests for depressive-like behavior- including the tail suspension test[55] and the forced swim test[56]. Together, these studies illustrate the epigenetic modulation that occurs after stress and may lead to mood dysregulation. The regulation of histone deacetylase activity of sodium butyrate and other SCFAs may play a critical role in epigenetic modulation, a property which may be translated into novel therapies with further exploration.

3.1.2 Vagus Nerve Activation

The two most commonly studied SCFA receptors are the G Protein-coupled receptors (GPCR) free fatty acid receptor (FFAR) 2 and 3 previously known as GPR43 and GPR41 respectively. Both receptors are coupled to Ca+ release, ERK1/2 activation, inhibition of cAMP accumulation, and inositol 1,4,5-trisphosphate formation; however, they differ in their ligand specificity and expression profiles[57]. Crucial to communication between the brain and the gut, the vagus nerve afferent neurons express FFAR2 and FFAR3[58]. The length of the fatty acid chain seems to be relevant in the vagal response. Long chain fatty acids induce cholecystokinin, a hormone involved with digestion which acts on the vagus nerve. A study of the effects of intraluminal perfusate of sodium butyrate (short chain fatty acid) and sodium oleate (long-chain fatty acid) on vagal activation in rats reveals that sodium oleate activates the vagus nerve indirectly in a cholecystokinin dependent manner, while sodium butyrate activates the vagal nerve independently of cholecystokinin, supporting the hypothesis that sodium butyrate acts directly on the vagal afferent nerves[59]. These molecules may regulate a variety of behaviors- low-dose IP injection of three different short chain fatty acids (butyrate, propriate, and acetate) suppressed feeding behavior in mice. When the mice were vagotomized or when capsasin-denervation of vagus afferents was used, feeding behavior was increased, but not to baseline levels, indicating that this behavior was mediated partly by vagus nerve activation[41]. More work is needed to understand the full behavioral implications of SCFA-induced activation of these receptors on the vagus nerve. Evidence of other physiological effects have also been reported, such as SCFA-induced serotonin release and increased colon transit time[39]. While the SCFA binding to these receptors appears to have effects on

feeding behavior and may modulate neuronal firing, the full implications of this pathway are not yet understood.

Strikingly these receptors are also expressed in high levels in rat brains[60] and the sympathetic and sensory neurons in both the autonomic and somatic peripheral nervous system; expression has not been found in the brain or spinal cord of mice[61]. The expression and activity of these receptors is of interest in understanding species differences in neural modulation by bacterial metabolites; however, much work is needed to understand the evolutionary significance. These receptors may also give clues as to the physiological effects of SCFAs, but unfortunately receptor activation has not been studied to the same extent as HDAC inhibition.

3.2 Tryptophan and Tryptophan-Derived Metabolites

Tryptophan is an essential aromatic amino acid that is obtained from diet and from the metabolism of gut microbes. It is necessary for protein synthesis, but it is also catabolized in the human body to produce a number of biologically important molecules. In the gut and the peripheral adipose tissue, tryptophan hydroxylase (Tph1) initiates the transformation of tryptophan into 5-hydroxytriptamine (5-HT) or serotonin. A diverging catabolic pathway results in the degradation of about 95% of tryptophan, converting it into nicotinamide and NAD+ via the kynurenine pathway[62] (**Figure 1.3**). This pathway requires the activity of at least one of two enzymes, tryptophan 2,3-diozygenase (TDO) or indoleamine 2,3-dioxygenase (IDO). TDO is expressed primarily in the liver where circulating levels of tryptophan are regulated. When there is a deficit of tryptophan, almost all of it will be metabolized into nicotinamide and NAD+ in order to meet energy needs. When there is a surplus, the pathway will remain active, leading to the accumulation of metabolic intermediates in the circulation[63–65]. While the liver contains most of the TDO in the body, IDO is highly expressed in mucosal barrier tissues and is highly regulated by immune activation. It is expressed in immune cells and its activity is mediated by inflammatory cytokines like IFN-γ, TNF-α[66]. In addition to being regulated by immune activation, IDO can also play an active role in anti-pathogenic activity through

depletion of tryptophan availability to the pathogen itself[67]. Beyond what is produced by the human body, gut bacteria significantly contribute to the number of circulating kynurenines.

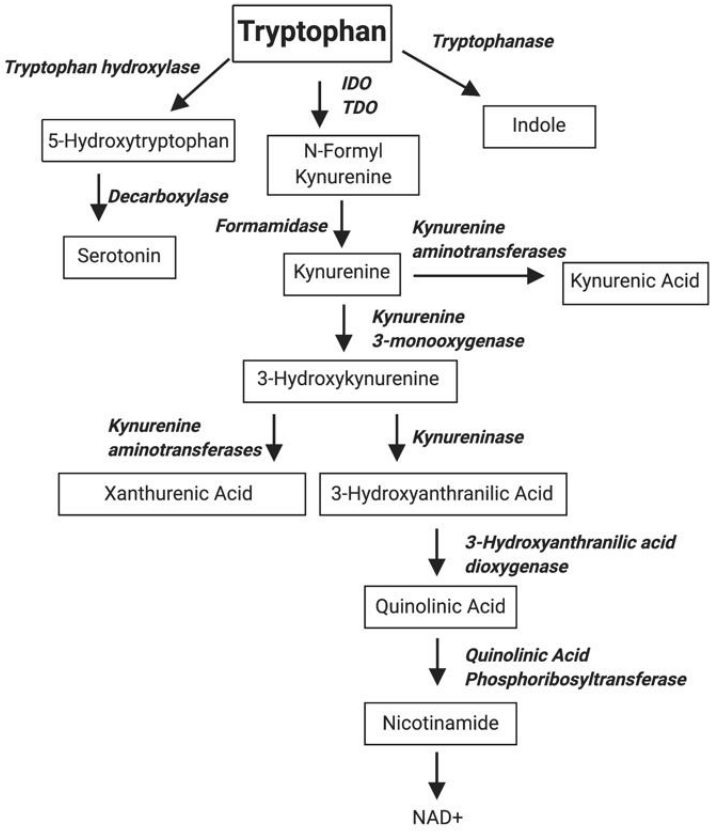

Figure 1.3: Tryptophan metabolism along the kynurenine pathway with select enzymatic steps shown. About 95% percent of dietary tryptophan is metabolized through kynurenine in order to produce NAD+.

Tryptophan is the only amino acid that exists in both an albumin-bound form and in a free form circulating in the serum, due to its mild affinity for albumin at the pH of the blood[68]. The free form, but not the albumin-bound, can diffuse across the BBB so dietary intake of tryptophan directly influences how much tryptophan is available in the brain[69,70]. This is crucial because tryptophan metabolism in the brain is necessary, in addition to peripheral metabolism, for healthy neuronal firing. Microglia, the brain's resident immune cells, are the most metabolically active brain cells along the kynurenic pathway. Changes in the CNS metabolism of tryptophan as measured by metabolite presence and relevant enzyme expression have been noted in the brains of deceased patients who

had been diagnosed with MDD. In the ventrolateral prefrontal cortex, depressed patients had a lower kynurenine to tryptophan ratio, indicating that there is excess tryptophan that is not being shuttled down an active kynurenine pathway. This was supported by the observation of lower expression of mRNA for IDO1, IDO2, and TDO and lower levels of the downstream product of the kynurenine pathway, quinolinic acid[71]. Another group showed that in the anterior cingulate cortex, an area of dysregulation in MDD, there is increased quinolinic acid as measured by IHC of the brains of depressed patients[72,73] and decreased quinolinic acid in the hippocampus[72]. This indicates that there is likely a region-specific difference in tryptophan metabolism in the brains of patients with MDD. Importantly, quinolinic acid can produce excitotoxicity and neurodegeneration[74–78], which can be prevented by endogenous levels of kynurenic acid[79–81]. Thus, the balance between these two metabolites central to neurologic outcomes.

While microglia and other cells of the brain metabolize tryptophan along the kynurenine pathway, their output is about 20-fold less than peripheral macrophages. This pattern is true for most immune cells, as peripheral macrophages are the primary producers of kynurenines. This highlights the disproportionate role of immune cell activation on levels of kynurenines in the brain[82]. Kynurenine and 3-hydroxykynurenine are actively transported into the brain while other members of the kynurenine pathway, including kynurenic acid, quinolinic acid, and 3-hydroxyanthranilic acid, are not able to cross the BBB through diffusion[83].

3.2.1 *Tryptophan and Serotonin*

The alternative tryptophan metabolic pathway to the kynurenine pathway leads to the production of serotonin. About 90% of the serotonin produced in the body is produced and stored in enterochromaffin cells in the gut[84]. Serotonin can be further converted to melatonin, a molecule integral in circadian rhythms[85]. The small intestine region closest to the stomach is responsible for most of the serotonin synthesis[86]. Indoles can promote serotonin conversion from tryptophan[87]. Serotonin is an integral player in MDD but, as its relevance to neuromodulatory activity is well documented elsewhere[88], it will not be a focus here.

3.2.2 *NMDA receptor*

A currently predominant explanation for the increase of quinolinic acid in certain brain regions during depression is that circulating proinflammatory cytokines induce a shift from microglial serotonin synthesis to kynurenine pathway metabolism through increase in IDO1 expression[89–91]. This is supported by studies showing increased in inflammatory cytokines IFNγ and TNFα in brain regions associated with increases in IDO1 expression[71]. Another line of evidence that supports this theory is that quinolinic acid (primarily produced by microglia[92,93])is an NMDA receptor agonist, while kynurenic acid (primarily produced by astrocytes) is an NMDA receptor antagonist[94]. Downstream kynurenine, xanthurenic acid is also able to attenuate both AMPA[95]. This may provide a mechanism by which ketamine, an NMDA antagonist that has unclear antidepressant properties, is effective for individuals with treatment-resistant depression.

The active transport and bioavailability in the brain indicate a strong link for peripheral levels of these molecules with mental health and mood[96]. Kynurenine's activity in the brain is regulated mostly by the degradation by astrocytes and microglia[93]. The metabolites generated by these cells types, kynurenic acid and quinolinic acid respectively, are both N-methyl-D- aspartate (NMDA) receptor antagonists while kynurenic acid is also an α7 nicotinic acetylcholine receptor (a7nAChR) antagonist. This is why they are shown to be relevant to major depressive disorder and schizophrenia[97]. Most of the data available on NMDA receptor activity is in vitro, so in vivo data examining kynurenine activity are necessary.

3.2.3 *AMPA receptor*

Kynurenic acid is able to compete with glutamate to different degrees in most glutamate-specific receptors. Specifically, kynurenic acid has been shown to act as an agonist to AMPA receptors and modulate glutamate release[98,99]. Strikingly, one study found that endogenous kynurenic acid has more robust effects on inhibiting neuronal firing in a model of epilepsy through AMPA receptors than through commercially available kynurenic acid, though both require very low concentrations of both are sufficient[100]. This may be due in part to increased concentrations around synapses as glia produce and localize more kynurenic acid than would be found in a bathing solution. Xanthurenic acid is also able to attenuate AMPA receptor activity[95]. The endogenous activity of kynurenins on AMPA activity

has yet to be explored. As all of these studies have so far show low-moderate affinities for AMPA receptor, there is not yet convincing evidence that endogenous AMPA modulation occurs in any appreciable way.

3.2.5 *Nicotinic Receptors*

In the 1980s and 1990s, several groups explored the neuromodulatory effects of kynurenines. Through these initial exploratory experiments, a body of electrophysiological evidence using a variety of different control agonists[101,102], and nicotine itself[103,104], demonstrated that kynurenic acid does not have any notable antagonistic effects on nicotinic receptors. This dogma was questioned in 2001 when a report emerged that kynurenic acid could antagonize nicotinic receptor activation by several canonical ligands, including acetylcholine[105]. Since then, for every study in support of antagonist activity by kynurenic acid on nicotinic receptors[106,107], there is one showing no activity[108–110]. Meta-analysis of these studies has concluded that, based on the lack of reproducibility in similar experiments across groups, the role of kynurenic acid remains unclear[111].

3.2.6 *GPCR35*

Kynurenic acid is a ligand for G protein-coupled receptor GPCR35. This receptor is highly expressed by gut-associated lymphocytes and in the CNS[82]. The activity of this receptor has not been as well characterized in the gut compartment during stress. However, a study in which peripheral levels of kynurenine were experimentally increased, it was found that GPCR35 metabolism contributed to analgesic effects during visceral pain. The investigators used a test of visceral pain called the writhe test, in which they gave mice an i.p. injection of acetic acid and measured how often the mice writhe. They used cAMP upregulation as a readout of GPCR35 activation and found that the addition of L-kynurenine administration before the writhe test decreased the number of writhes. They implicate the downstream metabolite kynurenic acid as the analgesic molecule by pharmacologically blocking the clearance of kynurenic acid, which synergistically increases the analgesic effect. This was attributed to the GPCR35 activation in the spinal cord[112].

In addition to the kynurenines discussed in detail here, there are other molecules in the kynurenine pathway that have been explored for their neuroactive potential. One of them is propionic-

acid, which is commonly used in high doses to induce autism-like behavior in rodents, but has not been examined thoroughly at physiologic levels[113]. As this metabolic pathway is ubiquitous and highly regulated, there are many avenues of future research on the bioactivity of different kynurenines.

3.3 Trimethylamines

Trimethylamines are microbial metabolites produced primarily from *Anaerococcus, Clostridium, Escherichia, Proteus, Providencia*, and *Edwardsiella*[114]. They result from the breakdown of choline and carnitine found in dairy products, meats, and fish[115]. They have primarily been studied in the context of cardiovascular disease[116]; In 2017, however, Del Rio et al found trimethylamine-N-oxide in the CSF so it is believed to be able to cross the blood brain barrier. While they found that trimethylamine levels in the CSF did not correlate with dementia or AD [117], others have suggested it as a biomarker of AD[118]. In vitro, trimethylamine-N-oxide promotes microtubule assembly of mutant tau protein [119], which is a foundational feature of AD supporting data, indicating it may be contribute to AD pathology[120]. Many of the bacterial groups associated with MS produce Trimethylamines, but no direct relationship has yet been drawn[121]. As this review was written, there were no published reports linking trimethylamines and depression or stress.

3.4 Neurotransmitters

Many of the metabolites produced by the bacteria in the gut are bonafide neurotransmitters. These molecules are able to interact directly with the vagus nerve, thus contributing to the pools of neurotransmitter in the brain. Hydrogen sulfide is a neurotransmitter that can be produced in the gut by the bacterial family *Provotella.* Both circulating hydrogen sulfide levels and *Provotella* population is decreased in patients with Parkinson's Disease[122]. One study has shown that hydrogen sulfide has a protective effect on dopaminergic pyramidal neurons in the rat and mouse models of Parkinson's disease[123,124]. Another bacteria, *Lactobacillus rhamnosus,* produces GABA, and monoamines, including noradrenaline, dopamine, and serotonin, are produced by a wide variety of bacterial families[125].

Beyond the direct contribution of neurotransmitters, the levels of host production of these molecules can be directly regulated by bacteria in the gut. For example, gut bacteria regulate the host

enzymatic activity of tryptophan hydroxylase 1, which is the rate-limiting step for enteric serotonin production[40]. While large quantities of neurotransmitter are induced by host tissue in the gut, the physiological importance of those produced by the bacteria are not as well characterized.

3.5 Other Bacterial Metabolites

There are numerous other small molecules that are produced by bacteria that have bioactive and neuroactive potential. Some have limited in vivo data, indicating a potential neuromodulatory role. For example, bacterially produced 4-ethylphenylsulfate, regulated by *Bacteroides fragilis,* appears to play a role in autism spectrum disorder[126]. Limited data showing neurotoxicity are available for a wide range of metabolites, like D-lactic acid and ammonia, but the impact at homeostasis has yet to be explored. D-lactic acid seems to rise in serum levels only when the gut barrier has been compromised[127–129]. Elevated serum levels of D-lactic acid have been found in patients with chronic fatigue syndrome, contributing to neurocognitive dysfunction[130]. Ammonia is a product of the catabolism of many amino acids, including glycine, lysine, arginine, leucine, isoleucine and valine. As a neurotoxin, it causes a loss of integrity of the BBB, as well as decreased dopamine and serotonin synthesis in the brain[131]. However, it is has only been documented at levels which impact the CNS during states of metabolic dysfunction, for example, liver cirrhosis[132], causing neurotoxic injury and hepatic encephalopathy characterized by intellectual deficits and psychomotor abnormalities. A final example is *Streptococcus*-produced streptokinase which is potentially neurotoxic[133] and may contribute to Parkinson's Disease[134]. Because all of these have limited data, their complete neuromodulatory effects need further exploration.

The vast majority of work examining mechanisms of bacterial metabolites acting on the CNS has been conducted on SCFAs and tryptophan and its derivatives. The scope of their activities is striking and evidence that they are necessary for homeostatic functioning is mounting. Much more work needs to be completed on the hundreds of other molecules produced by the gut bacteria that enter the host. It is estimated that about 10% of the metabolites found in mammalian blood are derived from or depend on the gut microbiota[135]. Of these only a few have been experimentally manipulated and studied. In addition to the metabolites in the CSF, there are dozens more in the periphery, at various levels, that have neuroactive potential. While work should continue examining

the impact of SCFAs and kynurenines in health and disease, we must begin to use unbiased metabolomics and creativity to pioneer the analysis of the bioactivity of these unexplored molecules.

4. Indirect Effects of Microbial Metabolites on the Central Nervous System

Indirect effects of the microbiome on the central nervous system range from peripheral metabolism control to activity in the vagus nerve. The most studied method of indirect communication between the gut and the brain is along the immune axis. The bidirectional communication between the microflora of the gut and the immune system of the host, both locally and systemically, is highly conserved and well-established. The nature of communication between the CNS and the immune system is less understood, but has been a focus of scientific study in recent decades. One of the most direct connections lies in the immune cells' recognition of stress signals as they express both adrenergic and glucocorticoid receptors[136]. Of primary importance, the glucocorticoid receptors that bind the stress hormones, are found on all circulating leukocytes including monocytes, neutrophils, T cells, eosinophils, and basophils. There have been noted sex differences in expression, which may be a contributing factor to the increased prevalence of MDD in females compared to males[136,137].

The immune system affects the CNS by 1) direct attack and autoimmunity, as in multiple sclerosis, 2) developmentally, as in autism spectrum disorder, and 3) in more nuanced and less well described ways for other conditions, including mood disorders. A higher incidence of depression occurs in people diagnosed with autoimmune disorders as compared to other disorders that have comparable quality of life changes[138]. Meta-analysis of immune cell populations of patients diagnosed with depression has shown that there are changes in the number of circulating immune cells of both the innate and adaptive immune systems, as well as a decrease in the proliferative potential of lymphocytes[139]. Here, we will give a brief overview of how major immune compartments are affected during MDD; a topic which has been reviewed in depth elsewhere[140].

4.1.1 *Innate immune system*

R. S. Smith first proposed that the patterns of MDD reflected an increase in immune cell activation, specifically, macrophage activation. He cited the *in vitro* activation of rat monocytes by

estradiol as an explanation for observed sex differences in MDD incidence[141]. He also cited the increased rates of depression in patients with coronary heart disease, rheumatoid arthritis, and stroke, all conditions with high macrophage activity, as support for this hypothesis[142]. Some mechanistic approaches of antidepressant therapy have been proposed to work through macrophage activation. Splenic macrophages have decreased cytotoxicity in response to antidepressants (desipramine, fluvoxamine, and fluoxetine)[143]. In addition, a non-pharmacological treatment-mindfulness- can decrease the macrophage migration inhibitory factor back to normal levels[144]. Finally, circulating natural killer (NK) cells, another subset of the classical innate immune cells, are reduced in patients with MDD[145].

Cytokine profiling can give a snapshot of the cumulative immune response in the body. It is most often measured from the serum as it is easy to sample and analyze. Some of the most studied cytokines in the context of depression are the pro-inflammatory cytokines TNFα and IL-6, as well as C-reactive protein (CRP), one of their downstream targets, all of which are risk factors for depression when upregulated[146]. Another family of cytokines likely to have a role in perpetuating depressive symptoms are the IL-1 family of cytokines that are primarily produced by peripheral mononuclear cells[147]. Polymorphisms in the genes encoding IL-1β, TNF and CRP have been found in patients with depression and are correlated with therapy outcomes[148]. Notably, there is a functional variant of the IL-6 receptor (IL-6R) that reduces the sensitivity to IL-6 in immune cells, thus leading to increased levels of circulating IL-6 but to decreases in circulating CRP. These patients are less likely to have an episode of major depression or psychosis[149].

Toll-like receptors (TLRs) are immune receptors that bind pathogen-associated molecular patterns (PAMPs), the danger signals that are often the first to trigger an inflammatory cascade. They are of primary importance for initiating the innate immune system, which acts quickly to initiate a strong inflammatory response. Depressed patients have increased TLR3, 4, 5, and 7 expression and decreased TLR1 and 6 mRNA expression levels. Increased TLR4 expression, however, which is critical to the immune response to bacterial polysaccharides, seems to be the most important risk factor of developing MDD[150].

4.1.2 *Adaptive Immune System*

By far, the most studied population of adaptive immune cells in MDD are T cells. There is an increase in total number of peripheral T cells with a higher inflammatory T helper (Th) to regulatory T cell (Treg) ratio in patients with MDD[151]. Specifically, there is an increase of circulating Th17 cells and proinflammatory cytokine IL-17 in patients with depression[137]. Medicated MDD patients have lower levels of Tregs, as well as impaired Th2 cell and Th17 cell maturation when compared to age matched controls[152]. Other cell types of the adaptive immune system also appear to play a role in depression, but no consensus on their roles exists. A metanalysis by Eyre et al. examined multiple cell types that were changed at different stages of clinical depression from sub-syndrome phase, through the acute clinical phase, and to the post-acute phase. They found that while many immune cell types have certain levels of dysfunction, the T cells are the most variable[153].

4.1.3 *Evolutionary Hypothesis*

A working hypothesis to describe the relationship between inflammation and depression looks back to an evolutionary advantage of stress-induced inflammation. The theory posits that in times of stress, including social stress, stress due to injury, or stress caused by harsh environment, having a primed and ready immune attack was advantageous, allowing the immune system to be better equipped to handle injury and sickness[140]. In addition, the sickness behavior that mirrors chronic depression was advantageous in that it results in resting the body, preventing spread of infectious pathogens, and preventing the of consumption of contaminated food. All of this is supported by a wealth of interconnected inflammatory and behavioral genetic changes in mammals that have yet to be fully understood[154].

4.1.4 *Impact of Bacteria on Immunity*

The balance between autoimmunity in the gut and preventing pathogenic infection of one of the largest and most regulated tissue barriers requires constant cross talk between the immune system and gut microbiota. Oral probiotics given therapeutically have the capacity to positively change the immune activity of peripheral blood lymphocytes, including mediating changes in cytokines associated with depression like IL-1, IL-8, and TNF-α[155]. The distal physiological effects effects non-

pathogenic bacteria can have on inflammatory markers shows their therapeutic potential. Here we examine a range of small molecules produced by non-pathogenic bacteria and their effects on the immune system. As the connection between the immune system and mood is already well-established, I will examine the other end of the microbiome-immune-brain axis- the impact of bacterial metabolites on the immune system (**Figure 1.4**).

Summary of Immune Cell Changes during Major Depressive Disorder

Immune Cell	Macrophages	NK Cells	Microglia	B Cells	T Cells
Innate or Adaptive Immune System	Innate	Innate	Innate	Adaptive	Adaptive
Established link with depression?	Yes	?	Yes	?	Yes
Number	No Change	No Change	No Change	↓	↑
Activity	↑	↑	↑	↓	↑
Do antidepressants reverse observed effects?	Yes	Some patients	?	Yes	Yes
Bacterially-Derived Small Molecules that act on this population	Bacterial Polysaccharide SCFAs Kynurenines	Bacterial Polysaccharide	Bacterial Polysaccharide	Bacterial Polysaccharide SCFAs Indoles Kynurenines	Poly-γ-glutamic acid SCFAs Indoles Kynurenines

Figure 1.4: Cells of both the innate and adaptive immune systems respond to stress and participate in bidirectional communication with the brain. Macrophages, microglia, and T cells have strong experimental evidence supporting their involvement in major depressive disorder while other cells like NK cells and B cells do not have the clinical evidence to support a strong relationship, but have been implicated in animal models. Citations for these outcomes can be found in the text.

4.2 Bacterial Polysaccharides

Bacterial lipopolysaccharide (LPS), a commonly used model of inflammation, causes an innate immune response and subsequent cytokine storm. Injection of LPS has also been used to model of sickness behavior and depression, because the resulting behaviors during the immune event closely

resemble those of depression and anxiety, even after vagotomy[156]. LPS, as well as other molecules that cause TLR activation, lead to a strong cytokine release both peripherally and by the epithelial cells of the blood-brain barrier, directly exposing brain resident cells to inflammatory cytokines[157]. While the validity of i.p. injection of PAMPs as a model for major depressive disorder is questionable, it can lead to clues to the milder inflammatory events observed in patients with MDD.

The increase in gut permeability in response to stress seems to be the result of a decreased number of tight junctions, as well as a weakened mucosal barrier caused by high levels of circulating cortisol[158]. Recent speculation has suggested that this observed decrease in gut barrier function leads to an increase in bacteria crossing the intestinal barrier, leading to higher exposure of the immune system to bacterial polysaccharides and other PAMPs, increasing TLR4 signaling and thus monocyte activation.

In animal models, evidence for this theory is strong, but there is limited clinical evidence. In a study of naturalistic stress using a public speaking paradigm, stress led to a leakier gut in humans. When these same subjects were exposed to an infusion of corticotropin-releasing hormone, a stress induced hormone, the same patterns of gut leakiness persisted[159]. There are also increases in the antibodies IgA and IgM against LPS in patients with MDD, supporting the hypothesis that that stress leads to increased gut permeability, and thus higher immune activation. Unfortunately, this study is limited by the low number of healthy control patients used and by a high variability among patients[160]. While these piecemeal studies have provided foundational data, we must gather more clinical evidence to support the theory that PAMPs are a contributing factor to the development of depressive episodes.

4.3 Poly-γ-glutamic Acid

Poly-γ-glutamic acid (γ-PGA) is produced primarily through fermentation by *Bacillus spp.* of soy and other legumes[161]. A γ-PGA supplemented diet increases GABA and glutamate in the brain, both neurotransmitters associated with mood[161]. γ-PGA also has the capacity to decrease Th17 migration and induce an anti-inflammatory phenotype by increasing differentiation of Tregs in a partially TLR4 dependent manner[162]. As TLR4, Tregs, and Th17s are all mediating factors of depression, γ-PGA most

likely plays a role in mood disorders, and may have the potential to treat depression via TLR4 inhibition.

4.4 Short Chain Fatty Acids

There are differences in fecal SCFA levels in patients with disparate CNS disorders including Parkinson's disease[163], multiple sclerosis[164], and autism spectrum disorder[165]. Many studies have reported differences between fecal SCFA in patients with symptoms of stress or depression compared to healthy controls. One study, for example, found increases in fecal sodium butyrate[166]. This remains controversial, however, as another study found no differences in fecal acetate, proprionate, isobutyrate, or butyrate in depressed patients when compared to controls[8]. It is important to recognize, however, that the fecal levels of SCFAs are not necessarily reflective of the levels that are present in the intestinal lumen or that are being absorbed by the body.

In a wide range of animal models of stress and depression, including chronic mild stress, early-life stress, and fear conditioning, sodium butyrate was shown to reduce anxiety and depression-like phenotypes[167]. One study examined the interaction of sodium butyrate with SSRIs. When the SCFA was administered in conjunction with fluoxetine, an SSRI, in a mouse model of depression, the mice treated with both the drug and SCFA displayed less despair behavior, as measured by the tail suspension test, than either group receiving fluoxetine or SCFAs alone[55]. While these preclinical experiments are promising, there is a lack of clinical trials examining the safety and efficacy of sodium butyrate and other SCFAs as a primary or supplemental therapy for depression.

The most common SCFAs in the body are acetate (two carbon chain), propionate (three carbon chain), and butyrate (four carbon chain) which are found primarily in the colon[34]. Free Fatty Acid Receptor 2 (FFAR2) is the most abundant SCFA receptor in the gut and is present predominantly on immune cells. It is also present in high levels on enteroendocrine cells expressing PYY and on gut associated mast cells that contain serotonin, and it is thought to promote serotonin release in the colon[168]. FFAR2 is crucial to regulating the immune response, specifically neutrophil activation and recruitment in the gut. *Ffar* knockout mice were found to have exacerbated and extended colitis, arthritis, and asthma as well as increased levels of ROS in the colon[169]. FFAR3 is much less abundant, but is also found on small intestine and colonic enteroendocrine cells. No cells have yet been found

to express both receptors. FFAR3 seems to have different responses to different SCFAs and to mediate contractility of the smooth muscle of the colon[170]. FFAR3 is found on the afferent nerve fibers on the portal vein and are necessary for propionate-induced glycogenesis in the intestines. FFAR2 and 3 are the best described receptors, but there are a variety of other SCFA receptors that are located on different organs with different specificities[171]. Most of the receptors, including FFAR2 and FFAR3, have a primary role in regulating metabolic output and glycogenesis with secondary roles modulating the immune system. Evidence of SCFAs affecting the immune system is extensive and well documented[172]. Here we will present a brief overview of SCFA immunomodulatory mechanisms and review the literature linking SCFAs to changes in the CNS via the immune system.

Luminal-derived butyrate is a primary form of energy for the epithelial cells of the colon. As such, presence of butyrate is vital to maintaining a strong barrier in the gut[172]. This barrier strength has a substantial impact on the circulating cytokine levels as well as immune cell activation as any bacteria that can cross into the host tissue will initiate a strong innate immune response. SCFAs are able to locally regulate the chemoattractants CXCL1 and CXCL8, both important for neutrophil recruitment. Neutrophils are the first responders to an inflammatory event whether that be injury or infection. They proliferate dramatically in response to cytokines and then just as quickly undergo controlled cell death as other immune cells take over. Neutrophils express FFAR2, which, when activated, decreases chemotaxis. In addition to neutrophil trafficking, SCFAs cause neutrophils to have a decrease in the proinflammatory cytokine TNF[172]. These data indicate that neutrophil inflammatory response seen in patients with depression can be tempered by SCFAs, which will have downstream immune effects. This regulation of the immune response may be another checkpoint for mediating mood.

High concentrations of SCFAs cause histone deacetylase (HDAC) inhibition in innate immune cells including monocytes, dendritic cells (DCs), and macrophages. When these cells are exposed to SCFAs, they do not differentiate as readily resulting in reduced production of pro-inflammatory cytokines IL-12 and TNF[172,173]. The decrease of TNFα and the anti-inflammatory changes evident in macrophage activity indicate that SCFAs tend to reverse the patterns that are evident in patients with MDD. This supports the theory that SCFA anti depressive-like effects may operate in part through innate immune regulation.

The effect of SCFAs on the adaptive immune system is complex as there are numerous contributing factors. Exposure of dendritic cells (DCs) to butyrate causes an increase in the expression of enzymes indolamine 2,3-dioxygenase (IDO1) and aldehyde dehydrogenase 1A2 which, in turn, push T cells to a more regulatory phenotype[174]. In addition, SFCAs affect the differentiation of T cells by inhibiting the maturation of DCs, causing impaired IL-12 and TNF production in T cells[175]. T cell differentiation can also be mediated directly by activity of SCFAs. They do not have the FFAR2 and FFAR3 receptors[176], however, SCFAs can modulate mTOR activity in CD4 helper cells which promotes differentiation into Th1, Th17 or IL-10 producing Tregs[177]. mTOR modulation can occur through two different SCFA-dependent pathways. First, mTOR activation can be mediated through HDAC inhibition, and second, the SCFAs can be converted into acetyl-coA which increases the metabolic activity of the CD4 T cells and increases mTOR activity[178]. Changes in systemic immunity are also seen with oral administration of SCFAs. With mice fed butyrate, there was a measurable increase in circulating T regulatory cells[179]. Together these studies show that signaling by SCFAs can modulate gut homeostasis through diverse immune signaling mechanisms. As such, they can be seen as a sort of master regulator, impacting diverse swaths of immune activity. SCFAs have robust therapeutic potential for mediating mood through a variety of mechanisms both direct and indirect.

4.5 Indoles

Indoles are small molecules derived from tryptophan whose synthesis in mammals is rare. As such, most of the indoles in the body are a result of gut bacteria metabolism through the shikimate pathway[180]. One of the direct downstream metabolites of indoles is the uremic toxin indoxyl sulfate, which is low in animal models of depression[181] and in MDD patients[182]. Indoles are just beginning to be studied in the context of depression, but one of the first promising studies shows that 1-methyl-3-(phenylselanyl)-1*H*-indole reverses stress induced depressive-like behavior in mice[183]. Indoles derived from bacteria and plants are potential novel targets for anti-depressant therapy and are in need of further investigation[184].

Like SCFAs, indoles can act on the first line of defense from pathogens by increasing the mucus production of endothelial cells, as well as strengthening tight junctions[185]. Tryptophan catabolites, including kynurenine, kynurenic acid, indoles, and others are principle ligands for the aryl hydrocarbon receptor (AHR) (**Figure 1.5**). The AHR, also known as the dioxin receptor, binds planar exogenous small molecules in the barrier tissues as well as endogenous ligands[186]. The characterized list of bacteria that produce these and other AHR ligands is extensive and includes several species of *Lactobacillus, Bacteroides, Fusobacterium, Kleibsella,* among others[187]. It is a cytoplasmic receptor and transcription factor that exists in complex with the proto-oncogene c-SRC and heat shock protein 90 (HSP90), which stabilize it in a conformation that increases the affinity of its ligand binding domain. Once a ligand binds, part of the AHR complex translocates to the nucleus, associating with the AHR nuclear translocator (ARNT), and promoting transcriptional control of a variety of genes with disparate functions[188].

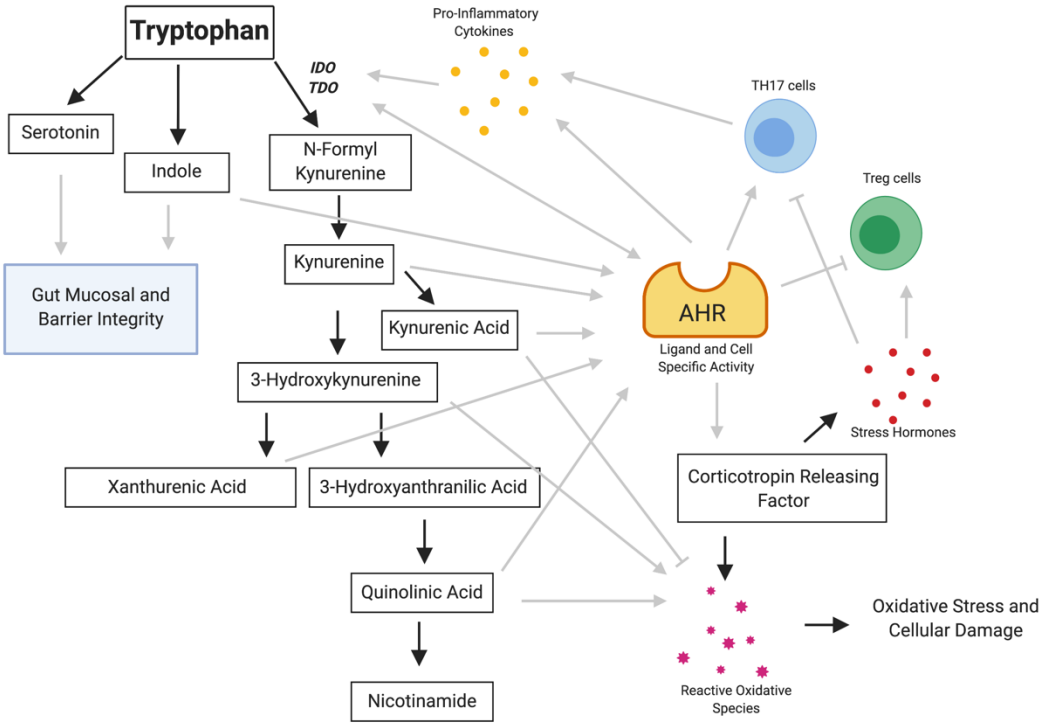

Figure 1.5: The aryl hydrocarbon receptor (AHR) has a complex ligand and cell specific repertoire of activity. The nuance of its function depends on the affinity of the ligands available

as well as the presence of antagonists (not pictured). Most members of the kynurenine metabolic pathway act as AHR agonists leading to changes in the T cell compartment as well as stress hormone release.

Transcriptional patterns can be further modified by interaction with other nuclear proteins, for example, RORgt[189] and c-Maf[190], which differentiate CD4+ cells to become Th17 or induced Tregs respectively. Several other transcription partners that lead to a variety of cell-type-specific transcriptional activities. In all cell types, the activation of AHR leads to the transcription of cytochrome p450 enzymes. These include Cyp1A1 and Cyp1B1, which both degrade the small molecules that activate AHR[191]. In this way, there is consistent negative feedback with AHR activation. AHR interaction with nuclear factor-κB (NF-κB) leads to increased transcription of inflammatory regulators CCL1, interferon responsive factor, and B cell-activating factor (BAFF)[192]. The interaction of AHR with other transcription factors has been documented but the downstream effects have not yet been thoroughly described.

In addition to these modulatory elements, AHR activity can also be mediated by microbially derived antagonistic ligands, thereby preventing homeostatic cell responses, such as cell cycle regulation and migration[193]. Another mechanism of AHR suppression is through the binding of certain ligands that can change the conformation of the cytoplasmic complex. This allows for the ubiquitination and subsequent proteasome-mediated degradation of AHR[194]. A final regulatory mechanism is the AHR repressor (AHRR) that binds to the downstream elements of AHR signaling, including ARNT, and suppresses the ability of AHR to conduct transcriptional activity in a ligand-dependent manner[195]. Because of the promiscuous nature of the AHR and the diversity of its ligands, it is difficult to predict the transcriptional readout of any single AHR-ligand interaction, especially in the context of the complex metabolism of the microbiome.

In Th17 cells, the interaction between AHR and RORgt in the nucleus leads to an increase in production of IL-22. In addition, in Th17 cells, AHR inhibits STAT1 and STAT5 transcriptional activity. However, the c-Maf/AHR interaction in Tregs leads to increased production of IL-10, IL-21, and AHR, leading to positive feedback loop. AHR's mediation of the balance between Th17 cells and Treg cells is important for homeostasis because a lack of Th17s causes an increase in microbial translocation

across the epithelial barrier of the intestine[196]. The presence of immunogenic material that can induce a strong immune response can then influence mood and other CNS functions. Type 3 innate lymphoid cells (ILC3s) are a group of innate immune cells crucial for barrier function which have similar immune activity to Th17 cells. They are also highly influenced by AHR and can change the inflammatory state of the lamina propria of the small intestine via local cytokine release[197]. These effects also seem to have a light-dependent circadian component showing the integration between the CNS and gut immune system[198]. These studies emphasize that Th17 and ILC3s are regulated and highly responsive to changes in the bacterial microenvironment through AHR.

Corticotropin-releasing factor (CRF) regulates the stress response and it appears that AHR can upregulate the transcription of *Crf* in a ligand-dependent manner. In this way AHR activation by exogenous ligands can directly impact the stress hormone response[199]. Most of the current literature, however, is focused on how it impacts the immune system.

In humans, a mutation that decreases the transcription of AHR mRNA is associated with MDD[200]. This mutation leads to a decrease in mRNA levels in the cerebellum, colon, and esophagus, but it probably affects most tissues. This decrease in AHR expression is associated with an increase in expression of many enzymes that are critical for the kynurenine pathway, including TDO2. These genetic changes in patients with MDD strengthens the argument that dysregulation of this immune-metabolic connection, genetically or through changes in the AHR ligands in the gut lumen, may contribute to mood dysregulation in some patients.

Indole-induced activation of AHR regulates the adaptive immune system by mediating maturation and differentiation of T helper cells and T regulatory cells[201] and their cytokine release[202]. Recently, it has also been shown to regulate the cross talk between astrocytes and microglia in the brain[203]. This novel finding strikingly mediates clinical scores in a mouse model of multiple sclerosis, but likely plays a part in homeostatic immune function in the brain itself. There may soon be evidence for glial AHR activity playing a role in amyloid clearance in Alzheimer's and neuroprotection in Parkinson's Disease.

4.6 Kynurenines

Tryptophan metabolism is completed by both the cells of the gut as well as the microbiota. Kynurenines are the most commonly investigated tryptophan-derived metabolites in the context of the peripheral immune system. Examples include kynurenic acid, quinolinic acid, and 3-hydroxykynurenine to name a few. While the majority of the kynurenic acid used by the body is produced in the gut (with highest concentrations near the colon), it is also found in food products and some traditional medicines at very high concentrations[204]. Patients with disparate etiologies of depression have shown increases of kynurenines in the peripheral blood[205], especially with respect to circulating tryptophan[8]. In a clinical trial using *Lactobacillus* as a probiotic therapy for depression, those treated with the probiotic had an increased 3-Hydroxykynurenine to Kynurenine ratio compared to those who received placebo[206]. 3-Hydroxykynurenine, another member of the kynurenine family of metabolites, acts much like quinolinic acid. As it crosses the blood-brain barrier, it increases the oxidative stress and contributes to apoptosis in the brain[207]. Kynurenine can also contribute to macrophage activation through an increase CCL2-mediated migration by monocytes that can target most tissues, including the brain[208].

Kynurenine activates AHR in CNS cells like astrocytes and peripheral cells including monocytes. In fact, kynurenine AHR activation can mediate monocyte trafficking to the brain as well as rescue depressive-like behavior in the mice[208]. The aryl hydrocarbon receptor also exhibits bidirectional communication with IDO, the primary initiator of the kynurenine pathway outside of the liver. IDO is highly regulated by the inflammatory state of the environment. Normal basal activity of T regulatory cells (the primary producers of IL-10) plays a critical role in regulating both IDO1 and mood[209]. IDO1 is highly upregulated by cytokines including TNFα and IFNγ[210] and is downregulated by IL-4 and IL-13[211]. It is also regulated by SCFAs, specifically butyrate[212]. The interplay between IDO and AHR further emphasizes the role of kynurenines in tightly modulating both the immune response and metabolic activity.

4.6.1 Additional Consequences of Aryl Hydrocarbon Receptor Activation

While the majority of the research examining AHR activation has focused on its complex activity in the gut and immune cells, AHR is also expressed by cells in the CNS. Recently, there is

increased work in looking at AHR activation in the CNS. AHR activation in the brain by microbial metabolites has been implicated in communication between microglia and astrocytes[203]. AHR can also act as an E3 ubiquitin ligase that can target the estrogen receptor for degredation[213]. As depression can be tightly linked to estrogen, including in post-partum depression and peri-menopausal depression, it is prudent to examine what effect estrogen receptor degradation has on hormonally regulated mood changes. AHR has also been reported to recruit DNA methyltransferases and thus induce hypermethylation and silencing of both BRCA1[214] and CDKN2A[215], both important for cell cycle regulation. Studies have focused on colorectal cancers, but cell cycle regulation is critical for maintaining homeostasis. Although these effects have been studied in the context of cancer, these genes are also vital for mounting and resolving an appropriate immune response, suggesting implications in autoimmunity and depression that have yet to be discovered.

The complexity of AHR activation and regulation require thorough and well controlled experiments to tease apart its diverse functions. As the cell type and ligands all determine the transcriptional outcome of AHR nuclear translocation, each of these will have to be systematically examined. In addition, computer modeling will help to understand the impact of competition between ligands in a microenvironment filled with agonists of different specificity.

5. Open Questions

Because of the ubiquitous nature of AHR expression, its diverse functions that are tissue and ligand specific, and its promiscuous binding, AHR provides a great target to examine the intercommunication between the gut microbiome and the immune system.

One of the primary group of bacteria that has been shown to decrease during depression is *Lactobacillus*. *Lactobacillus* can also modulate behavior-given orally it can prevent anxiety- and depressive- like behavior in mice exposed to stress[17]. Importantly, *Lactobacillus* has been shown to produce a variety of AHR agonists in vitro. Because of these observations, we hypothesized that the mechanism of communication between the host and *Lactobacillus* and the gut microbiome as a whole is occurring through AHR activation.

Chapter 2:

Stress-induced Despair Behavior Develops Independently of the Ahr-RORγt axis in CD4+cells

Real depression

Is when you stop loving the things you love.

-Atticus

This chapter expands on the publication authored by Andrea Merchak, Courtney Rivet-Noor, Sihan Li, Rebecca Beiter, Sangwoo Lee, Jalon Thomas, Anthony Fernández-Castañeda, Jung-Bum Shin, and Alban Gaultier. Scientific Reports, 2022.

Abstract:

Current treatments for major depressive disorder are limited to neuropharmacological approaches and are ineffective for large numbers of patients. Recently, alternative means have been explored to understand the etiology of depression. Specifically, changes in the microbiome and immune system have been observed in both clinical settings and in mouse models. As such, microbial supplements and probiotics have become a target for potential therapeutics. A current hypothesis for the mechanism of action of these supplements is via the aryl hydrocarbon receptor's (Ahr) modulation of the T helper 17 cell (Th17) and T regulatory cell axis. As inflammatory RORγt+ CD4+ Th17 T cells and their primary cytokine IL-17 have been implicated in the development of stress-induced depression, the connection between stress, the Ahr, Th17s and depression remains critical to disease understanding. Here, I utilize genetic knockouts to examine the role of the microbial sensor Ahr in the development of stress induced despair behavior. I observe an Ahr-independent increase in gut-associated Th17s in stressed mice, indicating that A is not responsible for this communication. Further, we utilized a CD4-specific RAR Related Orphan Receptor C (*Rorc)* knockout line to disrupt the production of Th17s. Mice lacking *Rorc* produced IL-17 did not show any differences in behavior before or after stress when compared to controls. Finally, we utilize an unsupervised machine learning system to examine minute differences in behavior that could not be observed by traditional behavioral assays. Our data demonstrate that neither CD4 specific *Ahr* nor *Rorc* are necessary for the development of stress-induced anxiety- or depressive-like behaviors. These data suggest that research approaches should focus on other sources or sites of IL-17 production in stress-induced depression.

2.1 Introduction

In the United States, an estimated 17.3 million adults are diagnosed with major depressive disorder (MDD). With over 60% struggling with severe impairments, MDD is the number one cause of disability in the U.S.[216]. Dogma states that depression and other mood disorders are caused by an imbalance in neurotransmitters[217–219]. As such, the majority of existing treatments target neurotransmitter uptake (SSRIs, SNRIs, etc.)[220]. However, a significant number of patients do not benefit from these therapeutics, suggesting alternate etiologies for MDD[220].

The microbiome has emerged as an important contributor to many neurological conditions, ranging from Parkinson's disease to autism spectrum disorder[221,222]. Thus, it is unsurprising that the microbiome has also been found to play a crucial role in the development and maintenance of MDD. For example, patients with depression have altered microbiomes when compared to control patients[223]. Microbiome dysbiosis is also present in animal models of MDD[17,224–226] and therapeutic administration of probiotics has been found to be beneficial[17]. However, the mechanism by which the microbiome contributes to the etiology of depression remains under investigation. One postulated route is through the immune system[227].

While there are many ways in which inflammation and the microbiome can interact in depression, a microbiome-responsive regulator of the immune system called the aryl hydrocarbon receptor (Ahr) has the potential to serve as a lynchpin in this pathway. Indeed, metabolomics, GWAS, and epigenetic studies have indicated that dysfunction of the Ahr is associated with both MDD and post-traumatic stress disorder[200,228]. The Ahr is a cytoplasmic receptor that can bind microbiome produced metabolites, including tryptophan-derived molecules[227]. Ahr activation induces transcription factor activity that can modulate the inflammatory environment of the gut. In particular, the Ahr has been shown to regulate T helper cell 17 (Th17) and T regulatory cell (Treg) function in response to microbial metabolites[229]. This represents an important connection between the microbiome and immune system as IL-17 produced by RORγt + Th17s have been shown to contribute to depression- and anxiety-like behaviors[230,231] Studies have shown that the number of Th17s in the gut associated lymphoid tissue (GALT) increases in response to stress and correlates with depressive-like behavior[232]. Additionally, the transfer of Th17 cells into mice has been found to induce depressive-like behaviors[230]. Administration of IL-17A blocking antibodies has also been found to reduce learned helplessness behaviors in mice[230]. However, the evidence for the role of IL-17 in MDD remains controversial, with some reports claiming a positive correlation between the inflammatory cytokine and depression and others reporting no differences in IL-17 levels between those with MDD and controls[233–238] These conflicting results highlight the need for further investigation into the mechanism and role of the Ahr and increased inflammatory Th17 cells in depression.

Here, for the first time, we use genetic tools and artificial intelligence driven behavior analysis to assess the contribution of T cell specific Ahr and RORγt to the development of anxiety- and

depressive-like behaviors in a murine model of stress. While our data confirm that stressed mice present with a larger number of Th17 cells in the gut, our behavioral analyses show that the deletion of either *Ahr* or *Rorc* in T cells does not impact anxiety- or depressive-like behaviors in mice. Taken together our data suggest that RORγt induced IL-17 in T cells is not necessary for the pathological development of depressive-like behaviors induced by unpredictable chronic restraint stress.

2.2 Results

Absence of the Ahr in T cells does not influence baseline behaviors

We and others have previously shown that microbiome dysbiosis induced by unpredictable chronic stress (UCS) is a contributing factor to depressive- and anxiety-like behaviors in mice[17,239,240] Furthermore, therapeutic reconstitution with *Lactobacillus* is sufficient to correct behaviors induced by UCS[17]. *Lactobacillus* is known to produce metabolites that engage the Ahr receptor, such as tryptophan metabolites which can modify the immune environment[241]. Given the emerging role of T cells and their cytokines in depression[230,242,243] I wanted to determine whether T cell-specific Ahr sensing of the microbiome leads to the immunological and behavioral changes associated with stress. I generated *Cd4 Cre Ahr*$^{flox/flox}$ mice (*Ahr* KO) to examine depressive- and anxiety-like behaviors in the absence of this important receptor in the T cell compartment. As expected, *Ahr* expression was significantly reduced in CD4 + T cells isolated from *Ahr* KO mice by qPCR (**Figure 2.1A**). Furthermore, in vitro generated Th17 cells prepared from *Ahr* KO animals failed to upregulate the Ahr downstream transcription factor *Cyp1b1* in response to idoxyl-3-sulfate (I3S) induced Ahr activation[244]. *Ahr* KO levels of *Cyp1b1* expression were consistent with those of Ahr competent cells treated with an Ahr antagonist CH223191. This confirmed a robust functional deletion of Ahr in T cells (**Figure 2.1B**). Next, I explored whether lacking Ahr in T cells could influence behaviors at baseline. Both depressive- and anxiety-like behavioral assays were performed on *Ahr* KO mice and age-matched controls. No differences were observed in the forced swim, tail suspension, or nestlet shredding tests (**Figure 2.1C**). These results show that mice lacking Ahr in T cells do not present with baseline depressive- or anxiety-like behaviors.

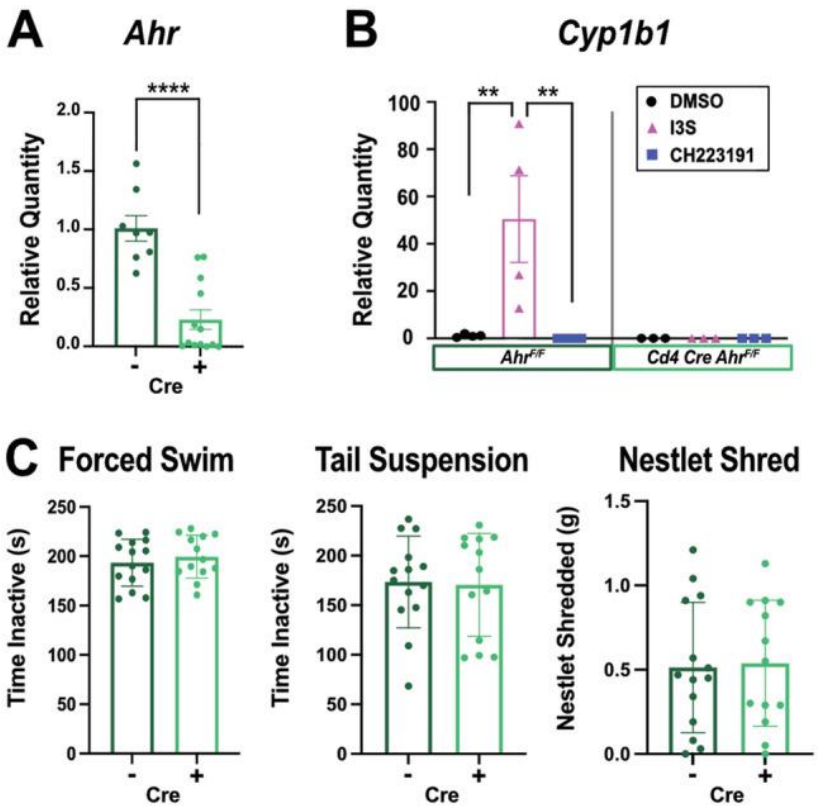

Figure 2.1: Absence of *Ahr* in T cells does not Influence Baseline Behavior. (A) Relative quantity of *Ahr* expression from *in vitro* skewed Th17 cells in *Ahr* KO and *Ahr* competent cells was determined by qPCR (n=8 or 13/group). T test (p= <0.0001). (B) Relative quantity of *Cyp1b1* expression from *Ahr* KO and competent cells skewed *in vitro* to become Th17s and treated with an Ahr agonist (I3S), antagonist (CH223191), or control media (DMSO) (n= 3-4/group). Combined N=2. Two-way ANOVA (DMSO to I3S: p=0.0019; I3s to CH223191: p=0.0016, interaction statistics in supplemental table 1). (C) Baseline behavioral comparisons between *Ahr* KO and littermate controls (n= 13-14/group). T tests. Male mice.

UCS drives a specific expansion of Th17 cells in the lamina propria in an Ahr-independent manner

To test the role of the T cell Ahr in response to stress, I subjected *Ahr* KO or age-matched controls to 3 weeks of UCS, as previously described[17] (**Figure 2.2A**). Surprisingly, no differences in anxiety- or depressive-like behaviors were observed between groups after stress (**Figure 2.2B**). While

classic behavioral assays may detect strong phenotypic differences, they may not detect more subtle behavioral changes. To circumvent this limitation, I applied an unsupervised machine learning approach to analyze behaviors in both genotypes using DeepLabCut[245]. First, I validated this computational approach using a preclinical murine model of multiple sclerosis (MS) known as experimental autoimmune encephalomyelitis (EAE). EAE produces significant locomotor changes and should produce detectable motor differences between groups to act as a positive control. DeepLabCut was able to detect robust behavioral differences between groups in nearly 40% of behavioral motifs characterized by the software (**Sup Figure 2.1A-F**). However, in our *Ahr* KO vs control groups, Kullback–Leibler Divergence, a measure quantifying variance within and between groups (**Figure 2.2C** and **Sup Figure 2.1B**), showed more variance within a group than between groups, suggesting that individual mice have a stronger impact on behavior than the genotype. Similarly, the generated PCA plot showed large overlap between groups (**Figure 2.2D**). Of all behavioral motifs analyzed, only one showed a significant change between groups (2.8% of all behaviors), suggesting the overall behaviors of *Ahr* KO mice are very similar to control animals in response to stress (**Sup Figure 2.1C,D**). Finally, immunophenotyping revealed no differences in the measured immune compartments between *Ahr* KO and control mice (**Sup Figure 2.2A**). Interestingly, both the *Ahr* KO animals and controls showed an increase in the number of CD4 + RORγγt + Th17 cells in the GALT that was significantly impacted by stress (**Figure 2.2E**). I also observed a genotype independent decrease in Th17s in the inguinal lymphnodes. I believe this is due to cells migrating out of the lymphnodes and into the GALT. Together, these data suggest that the microbiome changes and increases in Th17 cells observed in response to stress are not mechanistically linked by Ahr activation in CD4 + cells.

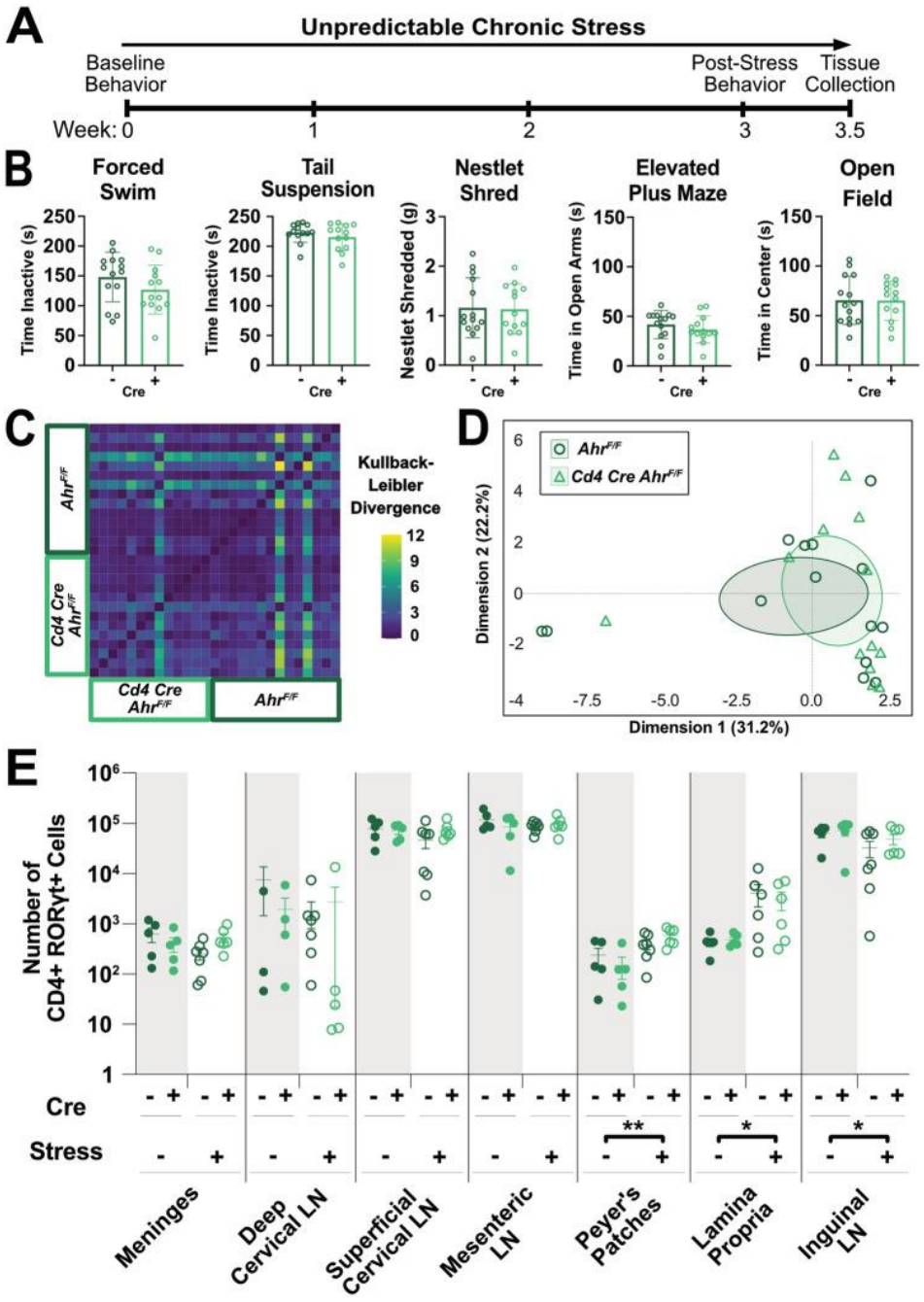

Figure 2.2: Unpredictable Chronic Stress (UCS) Drives Expansion of Th17s in the Lamina Propria in an *Ahr* Independent Manner. (A) Schematic representing timeline for unpredictable chronic stress in mice. (B) Measures of learned helplessness and anxiety-like behaviors between *Ahr* KO and littermate controls (n= 13-14/group). T tests, male mice. (C) Kullback-Leibler divergence heatmap and (D) PCA plot of DeepLabCut analyzed behaviors between groups (n= 13-14/group). A single representative experiment is shown (N=2). (E) Number of

CD4+ RORγT+ cells in various immune tissues between stressed and naïve *Ahr* KO and littermate controls (n= 5-7/group). Two-way ANOVA (Peyer's Patches: p= 0.0026, Lamina Propria: p= 0.0359, Inguinal LN: p= 0.0440), N=1, male mice. LN= lymphnode.

Deletion of *Rorc* in T cells does not induce spontaneous anxiety- or depressive-like behaviors

To explore the role Th17 cells in anxiety- and depressive-like behaviors, *Cd4 Cre Rorc*$^{flox/flox}$ (*Rorc* KO) mice were generated. Knock down of RORγt was confirmed using in vitro-derived Th17s by examining levels of *Il17* and RAR Related Orphan Receptor (*Rorc)* by qPCR (**Figure 2.3A**) and IL-17 secretion by ELISA quantification (**Figure 2.3B**). Immunophenotyping on the spleen revealed the absence of CD4 + RORγγt + T cells in vivo (**Sup Figure 2.3A-C**). Baseline behaviors were compared between male *Rorc* KO mice and controls. No differences between the *Rorc* KO mice or age matched controls were observed in tasks used to assess depressive- (**Figure 2.3D**) or anxiety- like behaviors (**Figure 2.3F**). As Th17 cells are also known to contribute to autism-like behaviors in male mice[231], we analyzed the marble burying (**Figure 2.3C**), social preference (**Figure 2.3E**) and novel object recognition (**Figure 2.3G**) tests at baseline. No differences between genotypes were observed in these behavior tests. Lastly, to ensure there were no subtle behavior differences between groups that could not be quantified with known behavioral tasks, we again used machine learning to examine unbiased behavioral clusters. The Kullback–Leibler Divergence plot showed individual variance had a larger impact on behavior than genotype effects (**Figure 2.3H** and **Sup Figure 2.3D**) and a large overlap in the PCA plot was observed (**Figure 2.3I**). Additionally, only 3 of 35 behavioral motifs demonstrated significant differences between groups after DeepLabCut analysis (**Sup Figure 2.3C-F**). Together, these data suggest that at baseline, a lack of *Rorc* from development does not impact autism-, depression-, or anxiety-like behaviors in male mice.

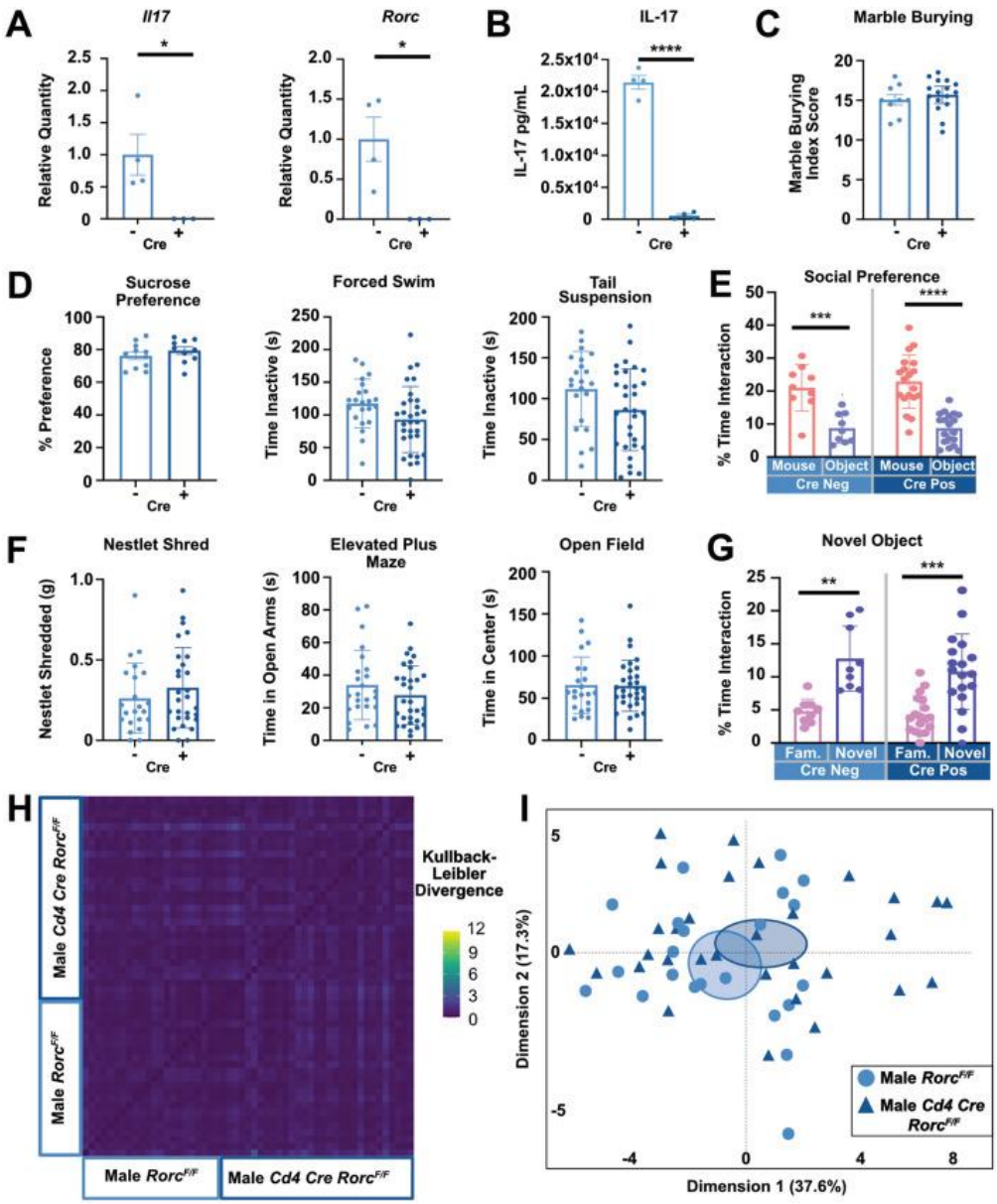

Figure 3.3: Depletion of *Rorc* does not Induce Spontaneous Behavioral Changes in Male Mice. (A) Loss of gene expression of both *Il17* and *Rorc* in *in vitro* skewed Th17s from *Rorc* KO mice and littermate controls by qPCR (n=3-4/group). T tests (*il17*: p= 0.0450, *rorc*: p= 0.0281). (B) ELISA representing loss of IL-17 in *in vitro* skewed Th17s from *Rorc* KO animals (n= 3-4/group). T test (p= <0.0001). (C) Baseline marble burying (n= 9 or 16/group), (D) depressive-like (sucrose preference: n=9/group, forced swim and tail suspension: n= 22 or 37/group), (E) social preference (n= 9 or 19/group), (F) anxiety-like (nestlet: n=22 or 28/group, elevated plus maze:

n= 24 or 31/group, open field: n= 22 or 31/group), and (G) novel object recognition (n= 9 or 19/group) behaviors in *Rorc* KO mice vs littermate controls. T tests used in D and F. Two-way ANOVA used in E (Cre Neg: p= 0.0010, Cre Pos: p<0.0001) and G (Cre Neg: p= 0.0014, Cre Pos: p=0.0002). (H) Kullback-Leibler divergence heatmap and (I) PCA plot of DeepLabCut analyzed behaviors between groups (n=22 or 32/group). Combined N=2, male mice.

UCRS induced anxiety- or depressive-like behaviors are not affected by the lack of *Rorc* in Th17 cells

While no behavioral differences in male mice were observed between groups at baseline, females experience depression at a higher rate than males[246]. Thus, we aimed to examine the impact of *Rorc* in Th17 cells in female mice. No differences in escape behavior, anhedonia, or anxiety-like behaviors were observed between female *Rorc* KO mice and controls at baseline (**Figure 2.4A, B**). Similarly, our machine learning approach was not able to detect differences in behaviors as shown through the Kullback–Leibler Divergence plot (**Figure 2.4C** and **Sup Figure 2.4C**), PCA plot (**Figure 2.4D**), and motif usage breakdown plots (**Sup Figure 2.4A, B**). To examine the impacts of *Rorc* KO in a stressful environment, female mice were exposed to 3 weeks of Unpredictable Chronic Restraint Stress (UCRS), a stronger model of stress known to induce anxiety- and depressive-like behaviors and changes in spine density of the basolateral amygdala[247]. After exposure to stress, no differences between groups were observed in escape behavior (**Figure 2.4E**). The nestlet shred test revealed that *Rorc* KO mice demonstrate a significant increase in anxiety-like nesting behaviors, whereas the elevated plus maze showed a significant decrease in anxiety-like behaviors, and the open field test showed no difference between groups (**Figure 2.4F**). Ultimately, our unbiased computational approach also did not detect any genotype driven differences as seen in the Kullback–Leibler Divergence plot (**Figure 2.4G** and **Sup Figure 2.4F**) and the PCA plot (**Figure 2.4H**). No differences in groups were detected in any of the 35 behavior motifs identified between groups. In summary, although we saw a significant increase in anxiety-like behavior in the nestlet shredding test between *Rorc* KO and control animals, our other behavioral tests did not support this trend and our unbiased behavioral analysis showed no changes between groups. Based on these data, *Rorc* KO in T cells does not significantly impact anxiety- and depressive-like behaviors in female mice before or after UCRS.

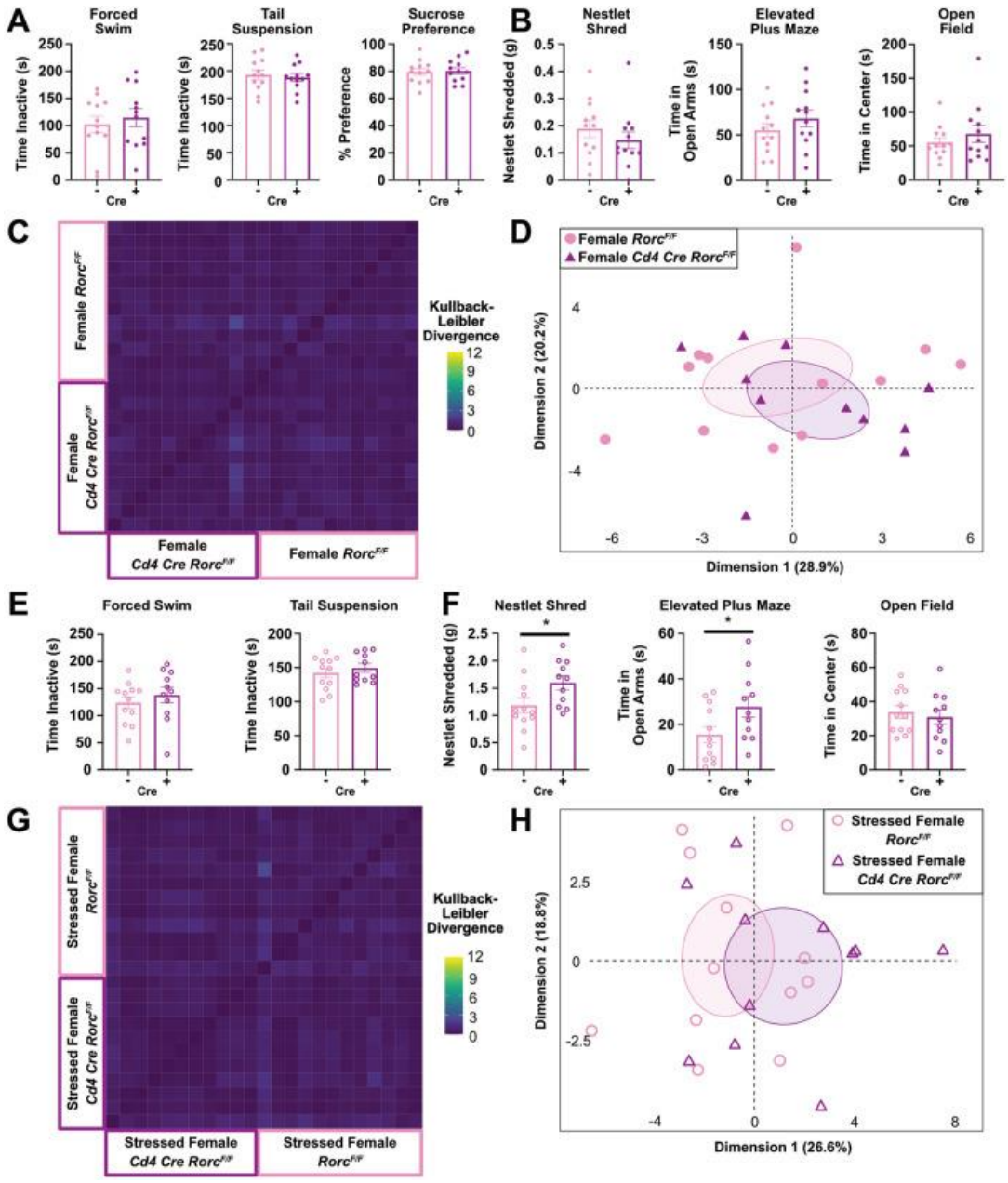

Figure 4.4: Loss of *Rorc* in T cells does not Impact Depressive- or Anxiety- like Behaviors in Female Mice. No differences in (A) depressive-like (n= 12/group) or (B) anxiety-like (n=12/group) behaviors between female *Rorc* KO and littermate controls at baseline. No differences in the (C) Kullback-Leibler divergence heatmap or (D) PCA plot of DeepLabCut analyzed baseline behaviors between groups (n=12/group). (E) Depressive-like (n=12/group) and (F) anxiety-like (n= 12/group) behaviors after 3 weeks of UCRS between female *Rorc* KO and littermate controls (Nestlet Shred: p= 0.0392, Elevated Plus Maze: p= 0.0453). (G) Kullback-

Leibler divergence heatmap and (H) PCA plot of DeepLabCut analyzed behaviors after 3 weeks of UCRS between groups (n=12/group). T tests, N=1, female mice.

2.3 Discussion

Depression presents a major social, health, and economic concern across the world, representing the most common cause of disability[248]. The root causes of this debilitating disorder have yet to be elucidated. With treatments remaining inconsistent and new options lacking, new research is needed to further our understanding of this disorder. Both the microbiome and T lymphocytes have been gaining support as potential mediators of MDD pathology. Here, I examined the role of T cell specific RORγt and Ahr in a mouse model of depression. I demonstrate that deletion of the *Ahr* gene does not impact anxiety- or depressive-like behaviors at baseline or after chronic stress exposure. Additionally, while we see an increase in the number of RORγt + cells in the lamina propria of stressed mice, it occurs independently of the Ahr. This indicates that there is another mechanism for Th17 cell expansion in response to stress other than environmental sensing through the Ahr.

Further, when *Rorc* is deleted from CD4 + T cells, no changes in anxiety or depressive-like behaviors are observed at baseline or after stress exposure. This is supported by previous work showing that increasing Th17s is not sufficient to change the susceptibility of mice to social defeat stress[242]. Others have suggested that increased Th17s are responsible for stress-induced depressive-like behaviors and have supported this claim by transferring Th17s into mice and finding increases in depressive-like behaviors[230]. However, this only suggests that an increase in Th17s may be sufficient to drive these behaviors[230], not that it is necessary. Additionally, while Th17's signature cytokine IL-17 is implicated in mood disorders, the origin of IL-17 is not precisely defined. IL-17 can be produced from many cell types and be induced in alternative ways that may contribute to depression outside of Th17s[249,250] Supporting this concept, it has been found that IL-17 from $\gamma\delta$ T cells regulates anxiety-like behaviors in mice[243]. Additionally, multiple transcription factors (STAT3, NF-κB, KLF4, etc.) and microRNA can act on IL-17 producing cells to induce IL-17 production[251]. This regulation can act in synergy with RORγt or independently of it, as with KLF4[251], suggesting that IL-17 could be produced without *Rorc* and outside of Th17 cells. These data and our own work suggest that if there is a role of

IL-17 in the onset of depression, this cytokine does not solely originate from CD4 + cells or is produced by alternative cell type (ILC3s, $\gamma\delta$T cells, or others).

The notion that Th17 cells play a critical role in the onset of depression has been growing in popularity but remains controversial. Several human studies have demonstrated that changes in IL-17 are correlated with depression[234,236,238,252] while others have not[233237]. While further work is needed to fully understand the role of IL-17 in the onset of depressive symptoms, our work demonstrates that the Ahr is not responsible for the observed stress-induced increase in intestinal Th17s and that these cells are not necessary for the induction of stress-induced depression. Instead, I suggest there are alternative means or sites of IL-17 production in stress-induced depression. Further investigation of the mechanisms and potential causes of depression symptoms, including the microbiome and other inflammatory signals, is required.

Chapter 3:

Immune Education by *Lactobacilli* is required for Resilience to Environmental Stressors

The Fury of Rainstorms

The rain drums down like red ants,
each bouncing off my window.
The ants are in great pain
and they cry out as they hit
as if their little legs were only
stitched on and their heads pasted.
And oh they bring to mind the grave,
so humble, so willing to be beat upon
with its awful lettering and
the body lying underneath
without an umbrella.
Depression is boring, I think
and I would do better to make
some soup and light up the cave.
-Anne Sexton

This chapter expands on the manuscript authored by Andrea R. Merchak, Samuel Wachamo, Lucille C. Brown, Alisha Thakur, Ryan M. Brown, Courtney Rivet-Noor, Tula Raghavan, and Alban Gaultier.

Forward:

In the previous manuscript, we addressed two leading candidates as lychpins in the immunogenic theory of stress induced depression. As both AHR and RORγt are not necessary for the development of stress induced depression, we next aimed to manipulate the microbiome itself to better answer these questions.

3.1 Introduction

The gut microbiota consists of the collection of bacteria, viruses, and fungi that maintain a symbiotic homeostasis within the digestive tract. This community is important for proper immune development, digestion, as well as many other functions[253,254]. The connection between the gut microbiota and the brain has re-emerged as an area of focus for biomedical research related to psychological disorders[17,227,255,256].

Dysbiosis, or a disruption of the microbial community, is commonly reported in patients with psychological stress exposures or mood disorders[257,258]. Several groups, including our own have found *Lactobacillus* to be one of the primary bacterial families to be diminished [17]. In fact, in clinical trials and animal preclinical research, *Lactobacillus* has been found to be a psychobiotic which aids in stress resistance, reduces disordered behavior in mice and reduces self-reported depression and anxiety in patients [17,206,259–262]. Interestingly, the beneficial effect of *Lactobacillus* has been observed using different species and strains of *Lactobacillus* suggesting that this is a generalized phenomenon to the bacterial family *Lactobacillacea.* Due to the difficulty of executing gnotobiotic studies, and that *Lactobacilli* are a ubiquitous commensal, almost all work thus far has been done in an additive manner--there is a fundamental lack of understanding of how complete loss of *Lactobacilli* could affect host physiology.

To circumvent these limitations, I have capitalized on the underutilized gnotobiotic consortia known as the Altered Schaedler Flora (ASF). This bacterial consortium was standardized in 1978 and consists of eight known, well-characterized bacterial strains passed from mother to pup during birth and development[263]. These bacteria include two strains of *Lactobacillus,* two strains of *Clostridium,* one strain of each of *Bacteroides, Mucispirillum, Eubacterium and Pseudoflavonifactor.* I have

harnessed this powerful tool and removed the two species of *Lactobacillus* to better understand their role in behavior, immune development, and mood.

By utilizing healthy mice lacking *Lactobacilli* from birth, I have found that Type 1 adaptive immunity is important as a primary mediating factor in stress resistance. I show that *Lactobacillus* is necessary for the development of sufficient systemic IFNγ and that it is likely occurring through indirect communication with CD4 T cells. Here I show that both *Lactobacilli* and IFNγ are necessary for resilience against environmental stressors.

3.2 Results

The transfer of microbiota from stressed mice to germ-free (GF) mice is sufficient to induce depressive- and anxiety-like behaviors.

Microbiota changes are well documented in both mice and humans exposed to environmental stress[7–9,16]. Here I used a previously characterized unpredictable chronic mild stress (UCRS) paradigm to induce depressive- and anxiety- like behaviors[17,264]. Mice were exposed to two randomized mild stressors each day for a period of 3 weeks. As reported, stressed mice spend more time inactive than naïve mice in the tail suspension test (**Figure 3.1A**) and had more repetitive behavior in the nestlet shred test (**Figure 3.1B**). Furthermore, these mice presented with microbiome dysbiosis (**Figure 3.1C-E**) and lower levels of *Lactobacillus* as measured by 16S sequencing when compared to naïve mice, replicating our previously published results [17]. There was no single group of bacteria that replaced the ecological niche created by the decrease of *Lactobacillus* (**Figure 3.1D**). To explore if microbiome dysbiosis is a marker or an active contributor to anxiety- and depression-like behaviors, I transferred the microbiota from naïve and stressed animals to germ-free mice. In order to do so, I transferred bedding from the donor cages to the germ-free cages daily for two weeks. The mice were then left for two weeks to allow for the microbiota to fully engraft before behavioral testing (**Figure 3.1F**). Strikingly, the depressive- and anxiety-like behaviors transferred to the ex-germ-free mice. The mice receiving bedding from stressed mice spent more time inactive during tail suspension than the ex-germ-free mice housed with bedding obtained from naïve animals (**Figure 3.1G**). Mice colonized with the microbiome from stressed mice also presented with more anxiety-like behaviors than the naive recipients as measured with the elevated plus maze (**Figure 3.1H, I**). These data indicate that bacterial transfer is sufficient to drive behaviors associated with mood disorders and environmental

stress exposure and support a growing body of evidence showing that the microbiota can directly modulate behavior[8,17–19,239,265,266].

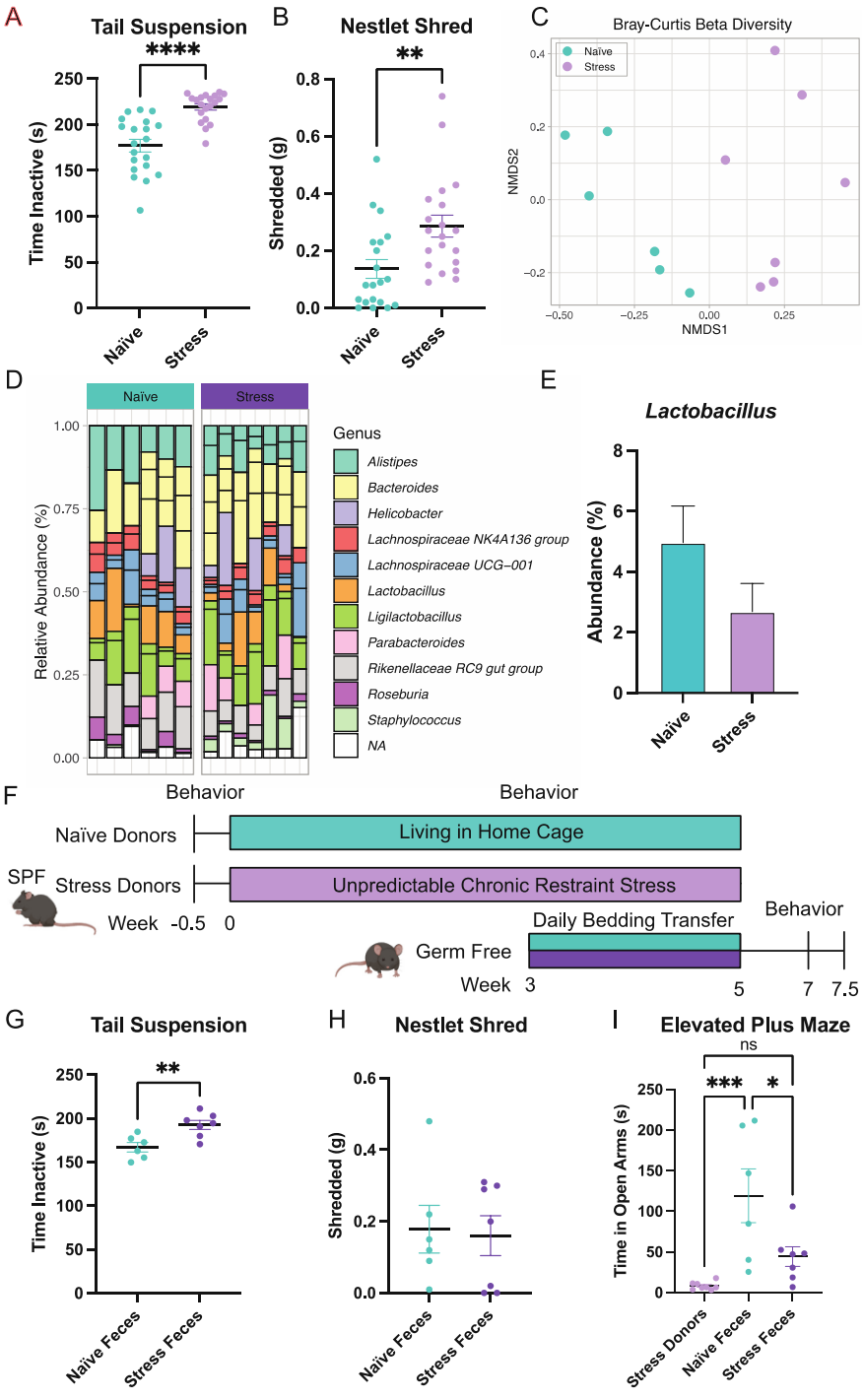

Figure 3.1: Gut microbiota drives anxiety- and depressive-like behavior. SPF B57Bl/6J mice underwent the Unpredictable chronic mild stress (UCMS) paradigm. After three weeks of

stress, behavior was performed and mice had increased (**A**) time inactive in the tail suspension test and (**B**) increased nestlet shred (Male mice; n=20 mice/group; N= 1 experimental replicate; Student's T tests). These mice also had dysbiosis as measured by 16S sequencing. (**C**) The samples from stressed and naïve mice clustered separately by Bray-Curtis analysis. (**D**) There were no significantly changed genera of bacteria except for (**E**) *Lactobacillus* which was confirm with qPCR (Male mice; n=6-7 mice/group; N= 1 experimental replicate; Student's T tests). The stressed SPF mice and naïve mice served as fecal donors for germ-free mice. (**F**) Bedding was transferred daily for two weeks to ensure engraftment and after two additional weeks, behavioral analysis was performed on the ex-germ-free recipient mice. (**G**) The ex-germ-free mice who received the microbiome from stressed animals had increase time inactive by the tail suspension test, (**H**) no difference in the nestlet shred, and (**I**) decreased time in the open arms of the elevated plus maze in comparison with mice who received the microbiome from the naïve donors (Feale mice; n=6-7 mice/group; N= 1 experimental replicate; Student's T tests).

Microbiota from stressed animals can suppress systemic IFNγ production

To understand how microbiota from stressed mice may initiate anxiety- and depressive-like behaviors in germ-free mice, I first performed untargeted metabolomics on the serum from recipients. This revealed higher levels of stress hormones (**Figure 3.2A**) than the naïve microbiome recipients as expected. Numerous changes in other metabolic pathways were also evident, however, no trends were evident to the authors. As germ-free mice are often described as having a "leaky gut", I aimed to ensure this was not confounding our results. I began by analyzing the gut physiology and function. I first analyzed the expression of several ion channels as markers for proper digestion and function and found no differences between the two groups (**Figure 3.2B**)[267,268]. Since germ-free mice have been reported to present with disturbed gut barrier integrity, I next examined markers of barrier junctions by qPCR and also found no differences (**Figure 3.2C**)[269]. Together, I conclude that there are no gross disruptions to gut permeability and stability.

In recent years, the adaptive immune system and in particular, tissue resident CD4+ T cells, have emerged as a key player responsible for communication between the gut and brain in

stress[137,151–153]. I performed Luminex analysis to quantify the concentrations of cytokines in the serum. The only cytokine that changed was IFNγ which was reduced in recipients of the stressed microbiome (**Figure 3.2D**). I next probed select immune markers in the meninges, a site recently shown to host numerous immune cells and influence behaviors[270]. I noted a decrease in the expression of *Tbet* in dural meninges, the transcriptional factor most commonly associated with Type 1 anti-viral adaptive immunity and IFNγ expression. I also found a reduction *FoxP3*, the T regulatory transcription factor, by qPCR (**Figure 3.2E**). Expression of transcription factors linked to Type 2 (*Gata3*) or Type 17 immunity (*Rorc*) were not altered (**Figure 3.2E**). I followed up by analyzing expression of the signature cytokines of each of the T cell subsets and found that only *Ifng* was decreased (**Figure 3.2F**). Taken together, mice receiving the microbiome of stressed animals presented with a reduction in markers associated with Type 1 immunity, especially IFNγ which is a cytokine that has recently been linked to sociability by acting directly on neurons[270].

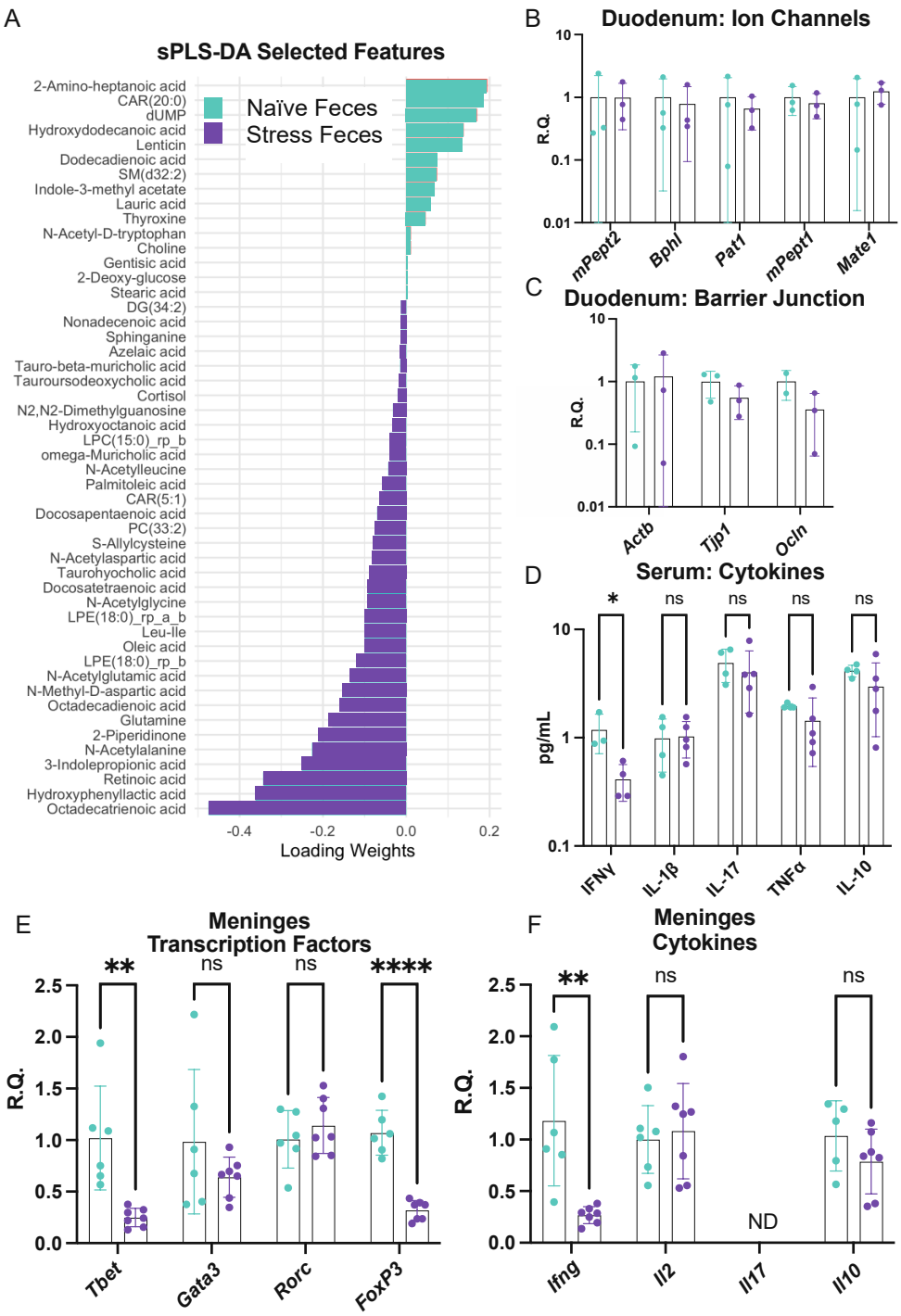

Figure 3.2: Ex-germ-free mice who received microbiome from stressed mice have lower Th1-associated molecules. (**A**) Untargetted metabolomics performed on the serum of ex-germ-free mice who were colonized with the gut microbiota from either naïve or stressed donors. Data presented represent the significantly different annotated molecules by concentration as established by partial least squares analysis (Female mice; n=4-5 mice/group; N= 1

experimental replicate). qPCR on the duodenum of ex-germ-free mice targeting (**B**) ion channels and (**C**) epithelial tight junction associated transcripts (Female mice; n=2-3 mice/group; N= 1 experimental replicate; unpaired T tests corrected for multiple comparisons using the Benjamini, Krieger, and Yekutieli two-stage linear step up procedure). (**D**) Luminex analsyis was performed on the serum from ex-germ-free mice. (Female mice; n=3-5 mice/group; N= 1 experimental replicate; unpaired T tests corrected for multiple comparisons using the Benjamini, Krieger, and Yekutieli two-stage linear step up procedure). Examination of the dural meninges from ex-germ-free mice by qPCR on (**E**) transcription factors associated with four types of CD4+ T helper cells and (**F**) their associated cytokines(Female mice; n=5-7 mice/group; N= 1 experimental replicate; unpaired T tests corrected for multiple comparisons using the Benjamini, Krieger, and Yekutieli two-stage linear step up procedure). .

Mice without *Lactobacillus* have fewer Th1 cells and are more susceptible to stress

So far, I have shown that stress leads to a decrease in *Lactobacillus.* I have also shown that the transfer of microbiome from stressed animals was sufficient to drive anxiety and depressive-like behaviors and a decrease in IFNγ. To explore whether *Lactobacillus* was responsible for the changed IFNγ production, ASF animals were used. ASF mice have a known community of gut commensals consisting of a collection of eight bacteria including two strains of *Lactobacillus.* These gnotobiotic mice allow for the examination of a more complex gut microbiome than germ-free mice. These mice have a digestive and immune system that are closer to an SPF mouse than their germ-free counterparts[263]. To probe our hypothesis that *Lactobacillus* is responsible for IFNγ changes, I generated gnotobiotic mice that have the complete ASF or ASF lacking the two species of *Lactobacillus- L. intestinalis* and *L. murinus.* From here they will be referred to as ASF (+L) and ASF (-L), respectively. These mice were reared in colonies that perpetuated these two gut microbial compositions. By flow cytometry, ASF(+L) and ASF(-L) mice have no differences in the number or percent of CD8+ T cells or CD4+ T cells (**Figure 3.3A, B**). However, of the CD4+ T cells there is a lower proportion of cells that are Tbet+ in the small intestine (**Figure 3.3C**). These data support the hypothesis that *Lactobacillus* are regulator of Tbet expression and perhaps Type 1 immune

responses. To further characterize these cells, I found that a lower proportion of the CD4+Tbet+ cells in ASF(-L) express CD69, a marker for activation and memory (**Figure 3.3D**).

To see if the presence or absence of *Lactobacillus* would alter the stress response, I exposed ASF(+L) and ASF(-L) mice to a mild acute stressor- restraint. I then performed c-Fos staining and quantification in areas of the brain involved in the stress response (**Figure 3.3D**). After a single restraint, ASF(-L) mice had higher activation in the stress response regions of the amygdala and the periventricular nucleus of the thalamus (PVT) than the ASF(+L) mice (**Figure 3.3F, G**). Notably, these trends were maintained in both the naïve and stressed mice. In the cortex, I observed increased c-Fos expression after stress in both groups, but no difference between groups (**Figure 3.3H**). These data show that *Lactobacillus* can influence Th1 cells and neuronal activation after acute stress.

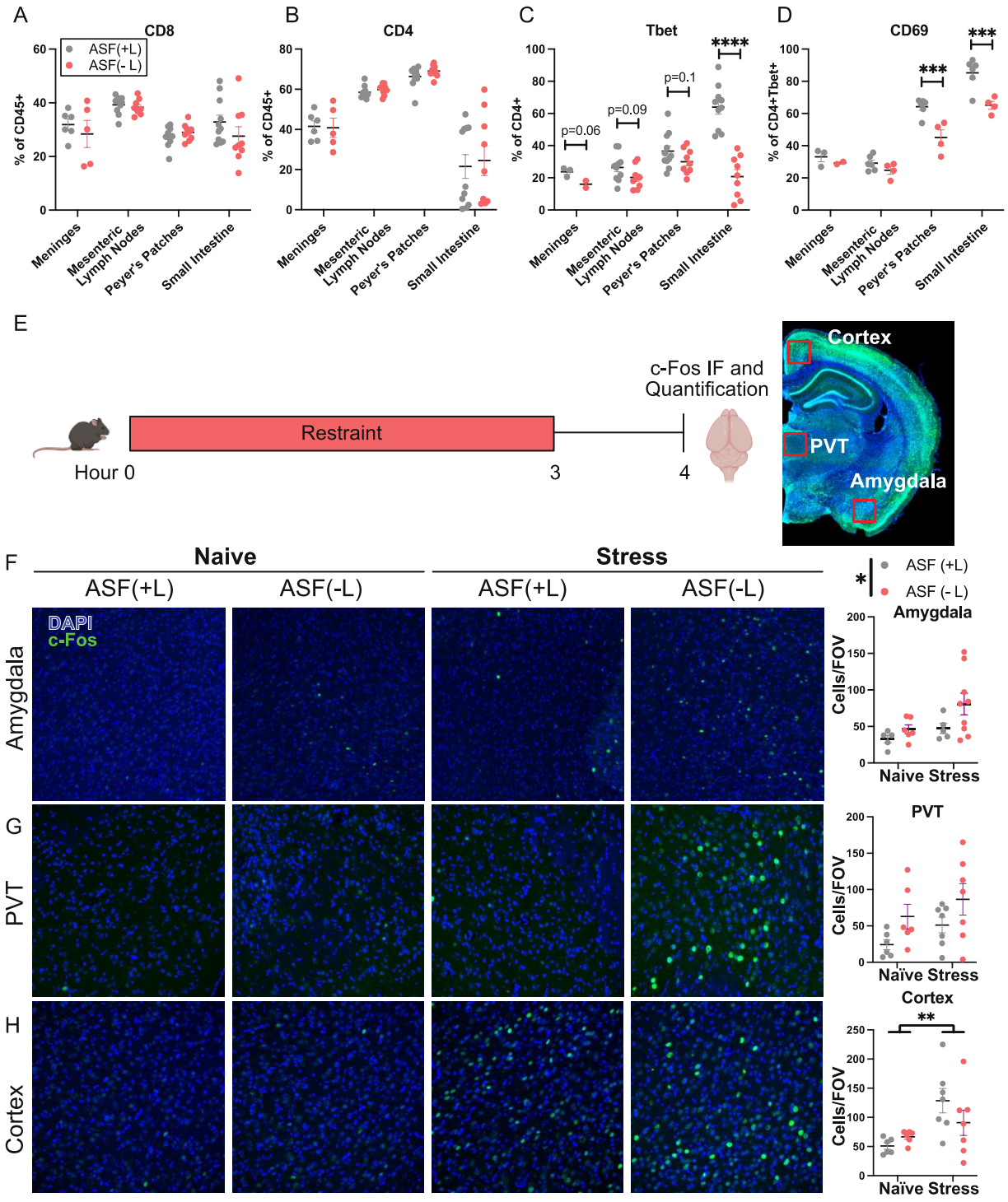

Figure 3.3: Mice without *Lactobacillus* from birth mirror immune and behavioral phenotypes of stressed mice. Flow cytometry analysis of dural meninges, mesenteric lymph nodes, Peyer's patches, and lamina propria of the small intestine in either ASF (+L) or ASF(-L) mice. Cells gated

on singlets, live cells, CD45+ and (**A**) CD4 or (**B**) CD8. CD4+ cells were further gated on (**C**) Tbet followed by (**D**) CD69. (Male and female mice; dural meninges from 2-3 mice were pooled leaving n=3-5 biological replicates. CD4, CD8, and Tbet had n=9-10 mice/group and N=2 experimental replicates; CD69 had n=4-5mice/group and N=1 experimental replicate; Two-way ANOVA followed by Sidak's multiple comparison test with a single pooled variance). (**E**) Schematic of experimental design for F-H. After three hours of restraint c-Fos expressing cells were counted in the (**F**) Amygdala, (**G**) periventricular nucleus of the thalamus, and (**H**) Cortex. (Male and female mice; n=6-7 mice/group; N= 2 experimental replicates; Two-way ANOVA followed by Sidak's multiple comparison test with a single pooled variance).

Lactobacillus modulates IFNγ indirectly

Th1 cells can be primed to respond to components of the gut environment through indirect education via M cells and dendritic cells or they can be directly exposed to bacterial material. Th1 cells have the ability to directly detect bacterial components through pattern recognition receptors (PRRs)[271]. *Lactobacillus* and other commensal bacteria are known to produce extracellular vesicles (EVs) that contain a variety of bacterial materials from cellular envelope components, DNA, and other intracellular components. The primary purpose of bacterial EVs is thought to be intercellular communication and horizontal gene transfer[272], however, they are known to cross the lamina propria of the gut via transcellular transport and through disruptions in the epithelial barrier. In order to determine whether this direct contact was responsible for increased IFNγ production and activation of Th1 cells I utilized an in vitro system. I isolated EVs from cultured *L. reuteri* and cultured ASF(+L) and ASF(-L) intestinal material. EVs from pure *L. reuteri* cultures ranged in size from 200-400nm in diameter (**Figure 3.4A**). A population of EVs of this size were also evident in the cultures from ASF(+L) but not ASF(-L) consortia. Th1 cells were differentiated from naïve CD4+ T cells from C57Bl/6J mice in the presence of the EVs and simulated for 24 hours. After stimulation, there was no difference in IFNγ secreted as measured by ELISA (**Figure 3.4B**) nor were there any differences in the RNA expression of activation markers as measured by qPCR (**Figure 3.4C**). Together, these data indicate that there is likely an indirect pathway of activation and proliferation of Th1 cells in vivo via endogenous cells types. Identification of this mechanism will require further investigation.

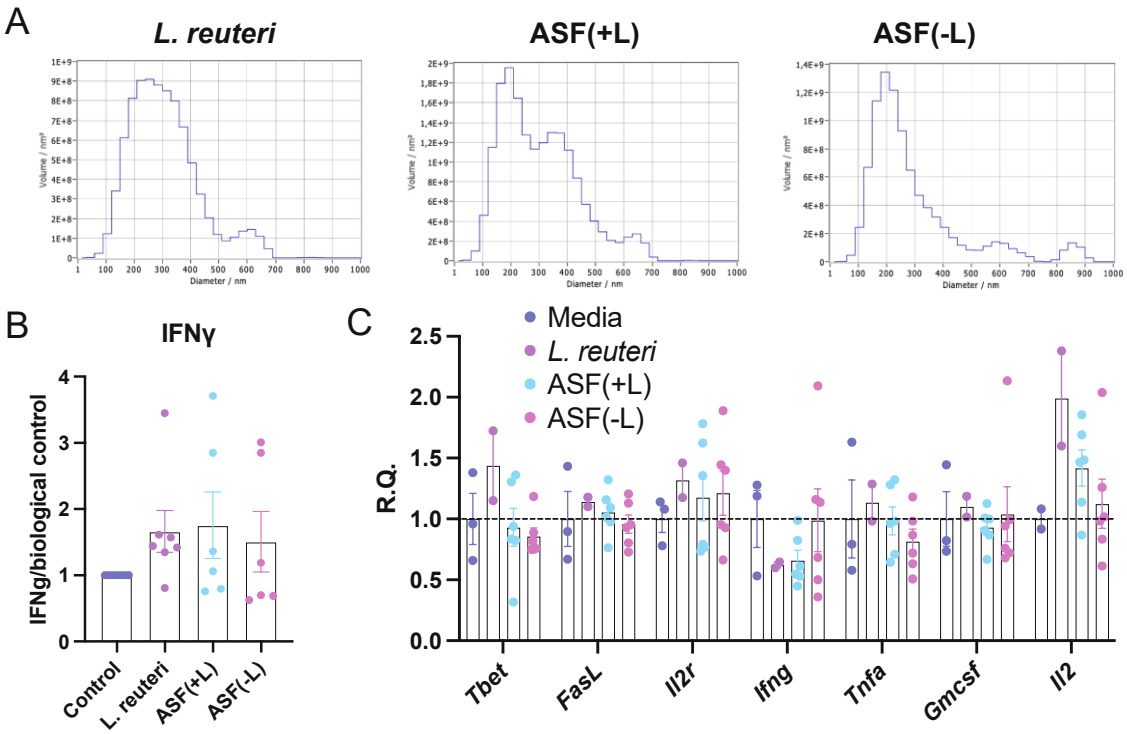

Figure 3.4: *Lactobacillus* derived extracellular vesicles do not induce IFNγ response more than control bacteria. (**A**) Size characterization of EVs isolated from a pure culture of *L. reuteri,* community culture of the intestinal contents of ASF(+L) mice or the intestinal contents of ASF(-L) mice. (**B**) EVs were added to cultures of naïve CD4+ T cells during in vitro differentiation and during a 24-hour anti-CD3/anti-CD28 stimulation. Supernatant was collected for an ELISA for IFNγ. (**C**) Cell pellets were collected for qPCR analysis of genes associated with Th1 activation EVs were collected from n=2 individual mice/group (T cells were isolated from n=3 C57Bl/6J mice; N=2 experimental replicates; One-way ANOVA followed by Dunnett's multiple comparison test with a single pooled variance).

Mice lacking *Lactobacillus* have amplified behavioral responses to subclinical stress

While our data suggest that mice lacking *Lactobacillus* present with higher stress-induced neuronal activity as determined by c-Fos expression, it may not translate into long term behavioral changes. To test if absence of *Lactobacillus* leads to a change in depression- and anxiety-like behaviors, I developed a stress paradigm adapted from the unpredictable chronic mild stress paradigm previously

used. This subclinical chronic stressor only uses restraint based on space constraints in the gnotobiotic isolators. For this stress paradigm, mice were restrained for 2 hours daily for 7 days (**Figure 3.5A**). Behavioral changes using this paradigm in SPF only appear after three weeks. There were no differences in anxiety or depression measures at baseline, however, after the subclinical stressor, only mice without *Lactobacillus* exhibited anxiety-like behavior as measured by the nestlet shred (**Figure 3.5B**). The tail suspension test, a measure of depression-like behavior, also showed that the mice without *Lactobacillus* responded to the mild stressor (**Figure 3.5C**). A third measure of anxiety-like behavior, the elevated plus maze, revealed that both groups spent less time in the open arms after stress, though this may be an artifact of multiple testing as other anxiety-like tests did not corroborate these results (**Figure 3.5D**). Together these data indicate that mice lacking *Lactobacillus* in a simplified gnotobiotic microbiome are more susceptible to stress when compared to similar microbiomes that contain *L. intestinalis* and *L. murinus.*

To determine whether the serum concentrations of IFNγ followed what was observed in mice colonized with the gut microbiota from stressed mice (**Figure 3.2E**), I tested serum levels of cytokine before and after stress. As hypothesized ASF(-L) mice have lower concentration of serum IFNγ than ASF(+L) mice (**Figure 3.5E**). After stress, serum IFNγ decreases only in the ASF(+L) mice. These data indicate that a reduction in IFNγ (and thus a higher homeostatic concentration of IFNγ) may be necessary for psychological resilience to environmental stressors. To confirm that the concentrations of IFNγ were not simply a result of overall changes in the pro-inflammatory environment, I also measured other cytokines associated with environmental stressors-IL-6 and IL-2 [273,274]. Neither are reliant upon the presence of *Lactobacillus* indicating that this is likely an IFNγ specific effect (**Figure 3.5F, G**). In further support of the hypothesis that Type 1 immunity is modulated during stress, I also observe that the intestinal differences in the proportion of Tbet+ and Tbet+CD69+ cells between ASF(+L) and ASF(-L) mice at baseline (**Figure 3.3C, D**) equilibrate after stress (**Figure 3.5H, I**). Overall, by utilizing ASF mice, I have shown that systemic IFNγ is dependent on the presence of *Lactobacillus* in the gut microbiota and that in the absence of *Lactobacillus* and IFNγ mice are more susceptible to environmental stress.

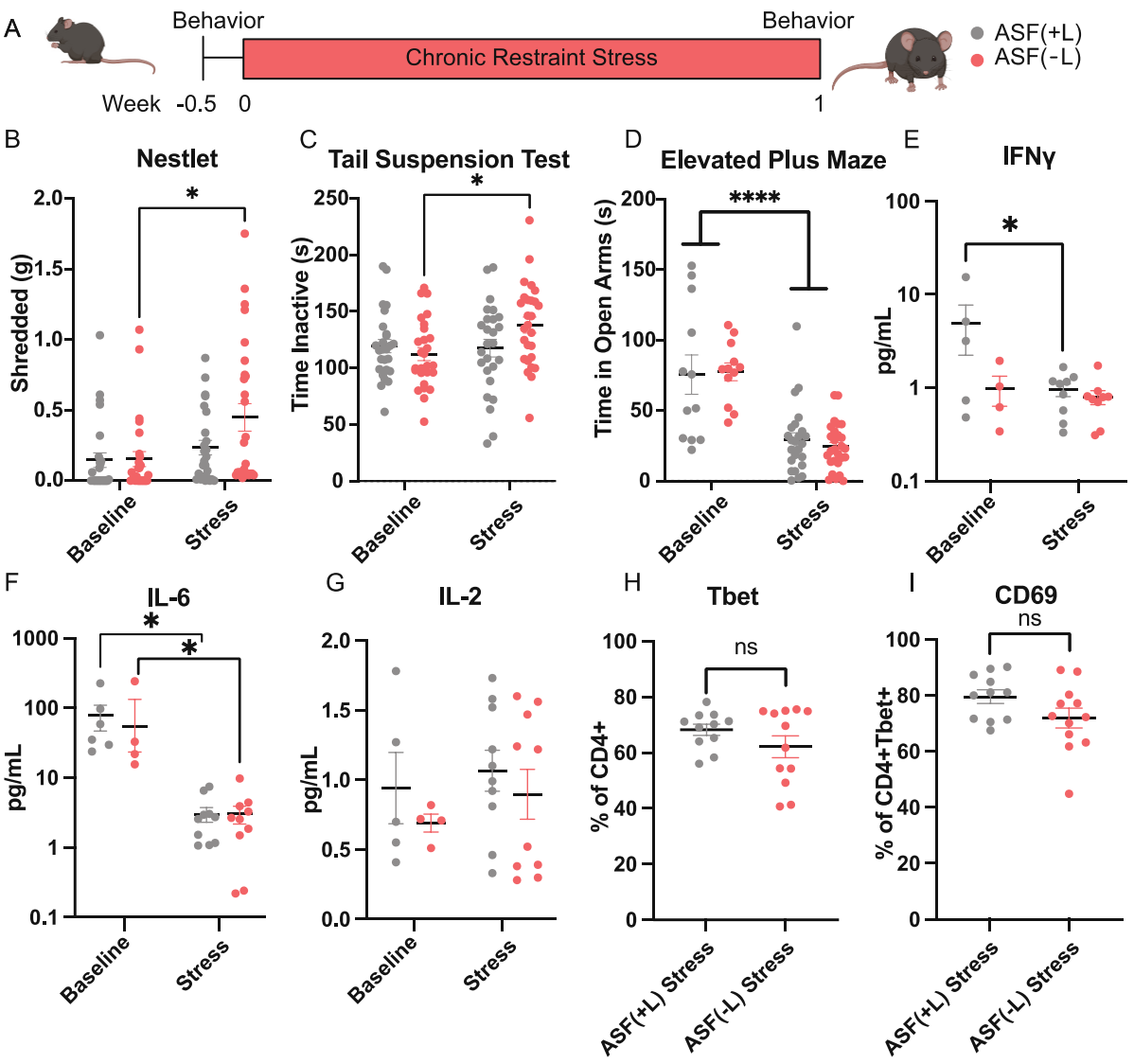

Figure 3.5: Mice without *Lactobacillus* are more behaviorally susceptible to subclinical stressors than mice with *Lactobacillus*. (**A**) Schematic representing the modified subclinical stressor aimed at preventing bacterial contamination. ASF(+L) and ASF(-L) were restrained for two hours daily for one week in sterile tubes flanked by behavior testing. Behavioral testing at baseline and after stress included (**B**) the nestlet shred, (**C**) tail suspension test, and (**D**) the elevated plus maze (Male and female mice; n=24-26 mice/group; N=3 experimental replicates; One-way ANOVA followed by Dunnett's multiple comparison test with a single pooled variance). (**E**) Luminex analysis on the serum of ASF(+L) and ASF(-L) mice before and after stress

(Male mice; n=4-10 mice/group; N=2 experimental replicates; One-way ANOVA followed by Dunnett's multiple comparison test with a single pooled variance). IFNγ, (**F**) IL-6, and (**G**) IL-2 are shown. (**H**) Flow cyotometric analysis of the lamina propria of the small intestine in stressed ASF(+L) and ASF(-L) mice gated on singlets, live cells, CD45+, CD4+, and Tbet+ followed by (**I**) CD69 (Male and female mice; n=11-12 mice/group; N=2 experimental replicates; Student's T tests).

Circulating IFNγ may reduce stress susceptibility

Other groups have previously shown that genetic knockout of IFNγ increases anxiety-like behavior, but little work has focused on more physiological systems[275]. In order to determine a causative relationship between circulating IFNγ and stress responses, I administered either IFNγ or anti-IFNγ neutralizing antibody to animals exposed to the acute stress paradigm (**Figure 3.6A**). I found that in the amygdala, there was a significant difference in c-Fos expression between naïve animals and stress animals (**Figure 3.6B**). Animals given IFNγ i.p. before stress appeared to have lower c-Fos expression after the acute stressor than controls while those given the neutralizing antibody seemed to have heightened responses to the acute stressor both in the amygdala and the periventricular nucleus of the thalamus (**Figure 3.6C**). The cortex showed similar patterns to the manipulation of *Lactobacillus* (**Figure 3.6H**)- there was an increase in c-Fos expression in response to stress, but no difference based on manipulation of IFNγ (**Figure 3.6D**). Overall these data support previous work that circulating IFNγ can regulate behavioral responses and may be produced in response to the gut microbiota.

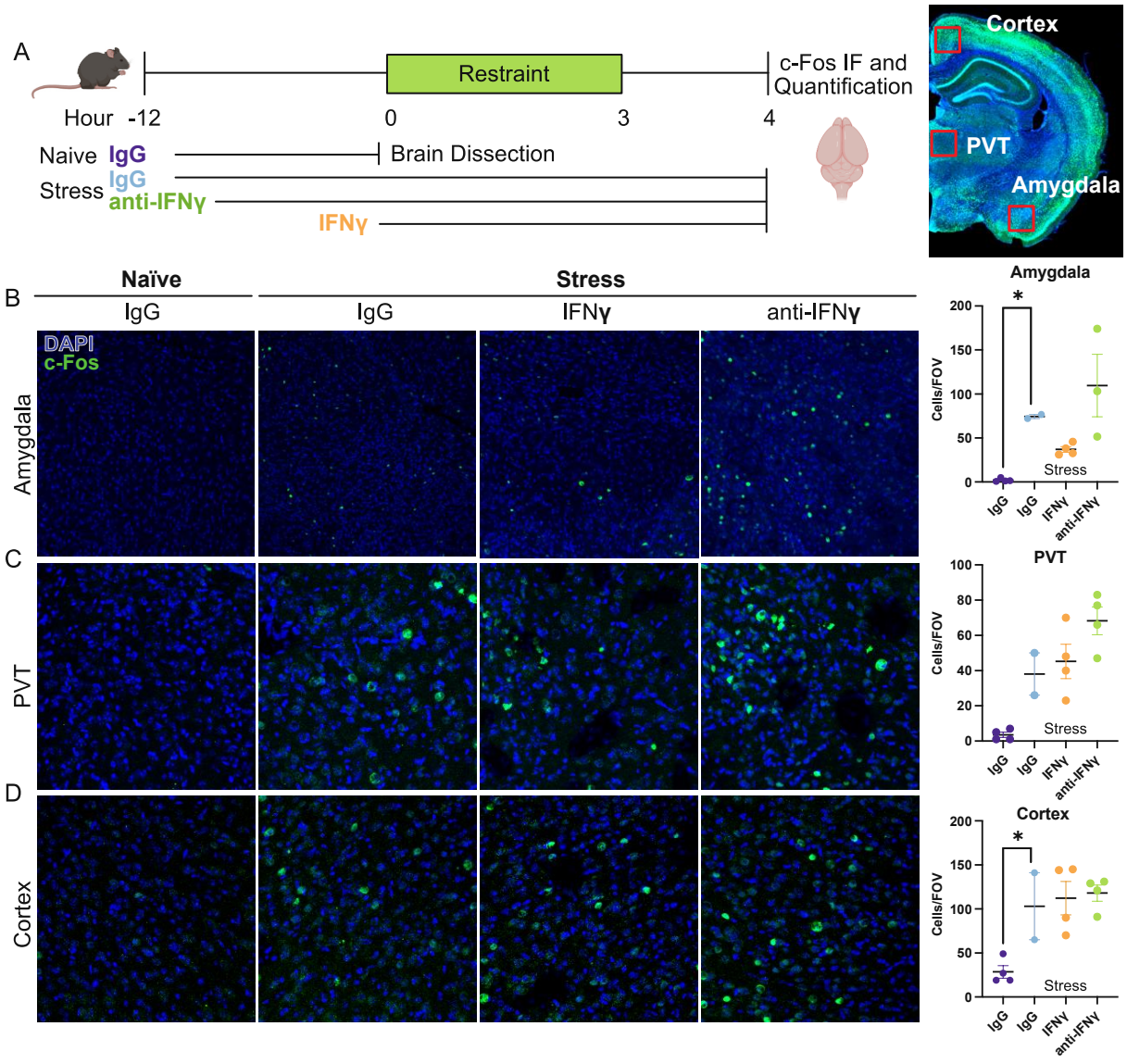

Figure 3.6: Circulating IFNγ may drive susceptibility to stress. (**A**) Schematic of experimental design. Mice were treated i.p. with anti-INFγ neutralizing antibody or IgG 12 hours before a three-hour acute restraint stress. One group was given recombinant IFNγ immediately before acute restraint stress. Brains were dissected for c-Fos quantification before or after stress. (**B**) c-Fos quantification in the amygdala, (**C**) periventricular nucleus of the thalamus, and (**D**) cortex (Male mice; n=2-4/group; N= 1 experimental replicate; One-way ANOVA followed by Dunnett's multiple comparison test with a single pooled varience).

3.3 Discussion

Historically, researchers have used fairly blunt tools in order to study the gut microbiota. Germ-free rodents were developed in the early 1940s and can be reconstituted with the microorganisms of interest, however they pose significant problems for extrapolating results[276]. They are immunocompromised, have high levels of anxiety-like behavior and do not respond to novel microorganisms in the same way a specific pathogen free (SPF) mouse would[269,277]. Another common method to study commensal bacteria is to disrupt the microbiome of SPF mice by using antibiotics and colonizing with the microorganism of interest, however this comes with other issues-antibiotic use can cause off target effects and the engraftment of the target microbe is not stable[278,279]. Due to these challenges, I have been unable to understand the mechanistic relationship between *Lactobacillus* residing in the gut microenvironment and mood until now.

Here I have shown that the gut microbiome is changed in mice subjected to environmental stress and this change is sufficient to drive anxiety- and depressive-like behavior when transferred to germ-free mice. I have also shown that mice raised with a known consortium of gut bacteria that contains *Lactobacillus* are more resistant to both acute stressor and more chronic mild stressors than mice without *Lactobacillus*. This difference seems to be in an IFNγ dependent manner and likely results from indirect exposure of Th1 cells to bacterial components.

While the exact mechanism of Th1 sensing of *Lactobacillus* is unclear, I have been able to determine that it is not through direct contact between Th1 cells bacterial EVs. This is in support of previous work[272]. However, there is evidence that EVs from *Lactobacillus* administered in vivo can reduce environmental stress responses indicating that they still may be acting on another cell type, including macrophages or even neurons as previously proposed[280]. Beyond EVs, there is likely increased Th1 activation and IFNγ production occurring through canonical intestinal immune development through sampling by M cells and antigen presentation by dendritic cells or interaction with small molecules excreted by the bacteria[281,282].

Our work supports previous work implicating IFNγ in the stress response and behavior[275]. Stress, depression and IFNγ have previously been correlated in the clinic, but the causative relationship and mechanism have not been established[283,284]. Recent studies have also shown that meningeal sources of IFNγ are can act directly on neuronal IFNγ receptors to promote the normal development

of social behavior[270]. In addition to neurons, astrocytes and premyelinating oligodendrocytes also have IFNγ receptors indicating that there may be several responding cell types in the brain[285,286]. Overall, there are likely direct both direct and indirect mechanisms of IFNγ influence on neuronal circuits and behavior.

Our results provide a novel framework to understand the roles of the bacterial gut microbiome and the immune system in mood disorders. I have used novel methods to show that *Lactobacillus* are indeed driving IFNγ production-likely via antigen presentation and not due to direct PRR activation. I have also shown that the IFNγ produced in response to *Lactobacillus* is sufficient to provide resilience in response to environmental stressors as had been previously observed in clinical settings. This work is an important step for understanding the role of homeostatic physiology in developing psychological resilience.

Chapter 4:

The Activity of the Aryl Hydrocarbon Receptor in T cells Tunes the Gut Microenvironment to Sustain Autoimmunity and Neuroinflammation

My body betrays me

My body betrays me
I have MS you see
From one day to the next
I wake up quite perplexed
Will this be a good day
To accomplish all that might come my way
Or will I feel out of sorts in complete disarray
There was a time my body was in perfect tune
Then one morning poof all was gone too soon
Never have I recovered in fact have gotten worse
Sometimes I think to myself surely I've been cursed
See here you foot or hand
You must move at my command
Alas no matter how hard I try or wish
Nothing happens right for this to be accomplished
Yup, sadly I've been betrayed
That forever I fear will be shaken
By a disease in my body so over taken

by Lynne

This chapter expands on the publication authored by Andrea Merchak, Hannah Cahill, Lucille Brown, Ryan Brown, Courtney Rivet-Noor, Rebecca Beiter, Erica Slogar, Deniz Olgun and Alban Gaultier. PLOS Biology, 2023.

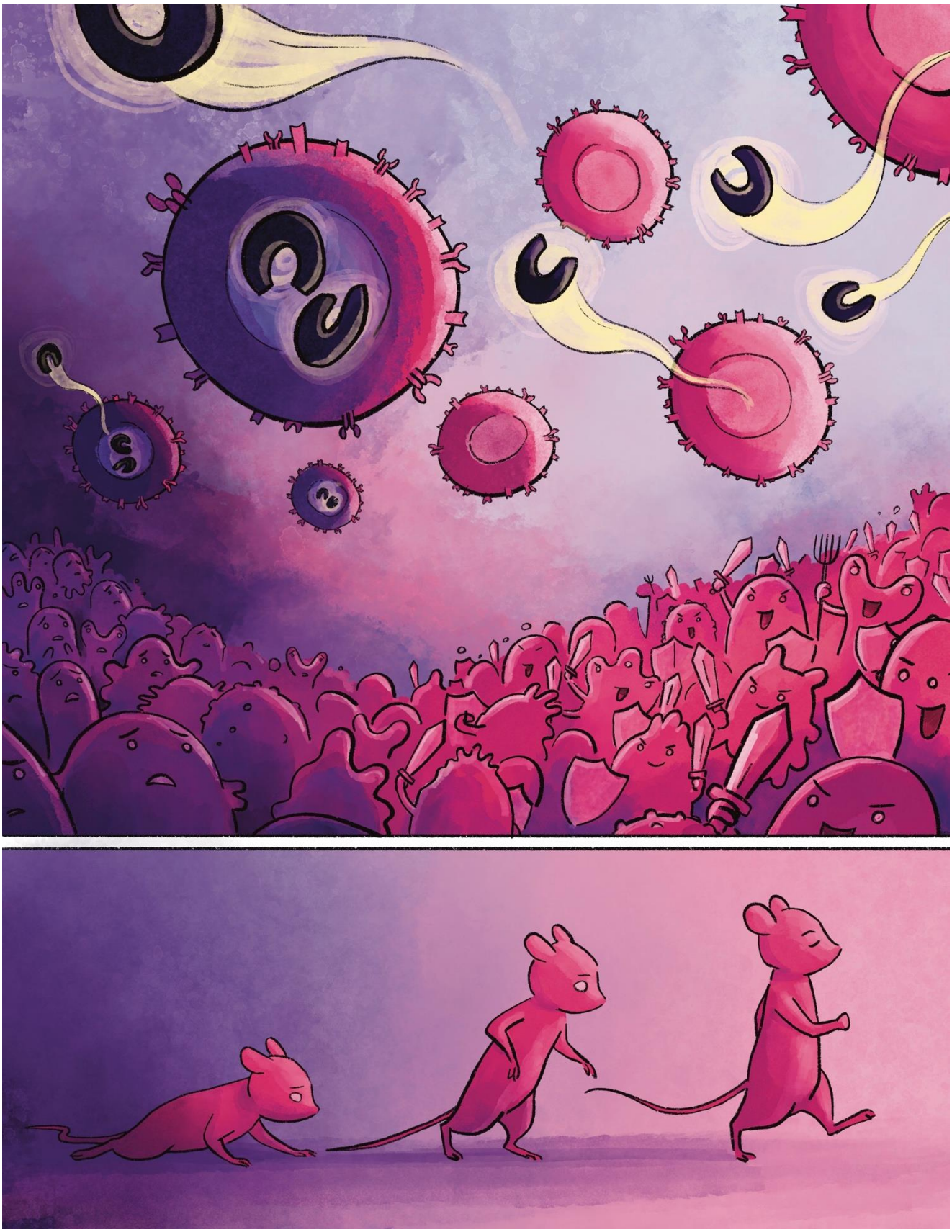

Forward:

Because we had previously developed T cell specific AHR deficient mice, and both AHR and T cells are key drivers of pathogenesis in EAE, I harnessed those tools to expand into multiple sclerosis research.

Abstract:

Multiple sclerosis (MS) is a T cell driven autoimmune disease that attacks the myelin of the central nervous system and currently has no cure. MS etiology is linked to both the gut flora and external environmental factors but this connection is not well understood. One immune system regulator responsive to non-pathogenic external stimuli is the aryl hydrocarbon receptor (AHR). The AHR, which binds diverse molecules present in the environment in barrier tissues, is a therapeutic target for MS. However, AHR's precise function in T lymphocytes, the orchestrators of MS, has not been described. Here I show that in a mouse model of MS, T cell specific *Ahr* knockout leads to recovery driven by a decrease in T cell fitness. At the mechanistic level, I demonstrate that the absence of AHR changes the gut microenvironment composition to generate metabolites that impact T cell viability, such as bile salts and short chain fatty acids. Our study demonstrates a newly emerging role for AHR in mediating the interdependence between T lymphocytes and the microbiota, while simultaneously identifying new potential molecular targets for the treatment of MS and other autoimmune diseases.

4.1 Introduction

Multiple sclerosis (MS) is a chronic inflammatory demyelinating disease that affects 2.3 million people worldwide. MS etiology and pathology are linked to both genetic and environmental factors[287]. A primary environmental factor impacting disease pathology lies with the gut microbiota[24,26,288,289]. Indeed, the connection between the microbiota and the immune system in autoimmune disorders such as MS is well established[290]. The gut flora, composed of bacteria, fungi, and viruses, aids food digestion and maintains pathogen control, but recent studies have also highlighted the integral role of the microbiome in modulation of the homeostatic immune state both locally and systemically[227]. Gut dysbiosis is a hallmark of disease in both patients with MS and in experimental animal models of MS[24,25,291–293]. The dysbiotic microbiome can cause earlier onset and increase disease severity in mice [25]. Furthermore, germ-free mice lacking a microbiome are resistant to experimental autoimmune encephalomyelitis (EAE), an animal model of MS[27]. These findings spurred the examination of various

bacterial supplements in mouse models of MS, and numerous potential candidates have been identified[30,290]. However, the mechanism(s) of action is not well understood. The importance of the microbiome in MS is well described, but a better understanding of the cross-talk between the immune system and the microbiome is required to translate these findings to the clinic. Further, discoveries in the context of MS provide a foundation for understanding environmental factors impacting many other autoimmune disorders.

The aryl hydrocarbon receptor (AHR) is a prime candidate for understanding the microbiome-immune interface. The AHR is a cytoplasmic receptor that, when activated, traffics to the nucleus to execute downstream transcriptional programing[294]. While canonical immune sensors have been primarily characterized based on their response to pathogenic material, the AHR is a homeostatic regulator that is activated by a variety of nonpathogenic exogenous ligands present in barrier tissues. These ligands include indoles[295], kynurenines[296], and other small molecules[297]. Downstream immune effects are dependent on the cell type and ligand. The AHR has also been directly tied to MS. AHR activation is the suspected mechanism by which the novel MS therapeutic, Laquinimod, acts[298,299]. It is thought that AHR activation by Laquinimod in antigen presenting cells reduces the ratio between inflammatory T cells and regulatory T cells (Treg). Microbiome changes have been identified in AHR null mice and in mice treated with a potent AHR agonist 2,3,7,8-tetrachlorodibenzo-p-dioxin (TCDD), further supporting the connection between AHR, the microbiome and MS [300–304]. While AHR activity in response to microbiome derived metabolites is well described, a gap of knowledge remains about the impact of AHR expression on the microbiota composition and function.

Here, I explore the role of AHR activity in CD4+ T cells using EAE. I have demonstrated that deleting *Ahr* from CD4+ T cells increases recovery in EAE in a microbiome-dependent manner. This improved recovery was the result of increased T cell apoptosis after activation in the central nervous system (CNS). While AHR deficiency did not grossly alter the composition of the microbiome, it significantly impacted the production of microbiome-mediated metabolites. In particular, AHR deficiency in T cells led to an increase in bile acids (BA) and a subset of short-chain fatty acids (SCFA) that ultimately impacted T cell viability. Our study aimed to understand how a microbiota response element can act in the inverse in the context of autoimmunity. This is the first demonstration, to our knowledge, of a role for AHR in T lymphocytes as a regulator of the microbiome activity that ultimately

influences the outcome of CNS autoimmunity. Our discovery builds a foundation for further work that could lead to a microbiome centric approach to dampen the overactive immune system in MS and related autoimmune disorders.

4.2 Results

Separately housed CD4+ specific *Ahr* knockout mice recover from active EAE:

Given the emerging role of the microbiome and the well accepted contribution of T cells to MS pathology, AHR is ideally positioned to influence the pathology of CNS autoimmunity. Here I explored the role of AHR in CD4+ T cells in EAE. For this study, I used the previously validated *Cd4*^{cre}*Ahr*$^{fl/fl}$ and littermate control *Ahr*$^{fl/fl}$ mouse strains[264]. Cohoused adult littermate mice were immunized with myelin oligodendrocyte glycoprotein (MOG)$^{35-55}$ to induce active EAE. The cohoused mice showed no difference in EAE clinical score when *Ahr* expression was removed from CD4+ cells (**Figure 4.21A, Sup Figure 4.1A**, Females; **Sup Figure 4.1B-C,** Males). Further, I observed no difference in myelin content in the spinal cord, as revealed by Luxol Fast Blue staining at the chronic phase of disease (**Figure 4.1B-C**). To assess the role of AHR driven microbiome changes in EAE, I separated mice by genotype at weaning (3 weeks) and induced EAE between 8 and 16 weeks of age. In this condition, while the time of onset and the peak clinical scores of EAE were not impacted, mice lacking *Ahr* expression in T cells presented with a significant recovery when compared to wild type animals (**Figure 4.1D, Sup Figure 4.1D**, Females). Furthermore, the change in recovery does not appear to be driven by sex as it was conserved in both sexes (**Sup Figure 4.1E-F**, Males). Supporting the clinical scores, the demyelination of the spinal cords was not different between the two groups at the peak of disease (day 16); however, I noted a significant increase in myelin staining at the chronic phase (day 31) in the *Cd4*^{cre}*Ahr*$^{fl/fl}$ animals when compared to the control (**Figure 4.1E-G**). Together, these data indicate that the lack of *Ahr* expression in CD4+ cells promotes EAE recovery in a microbiome-dependent manner that can be reversed by cohousing.

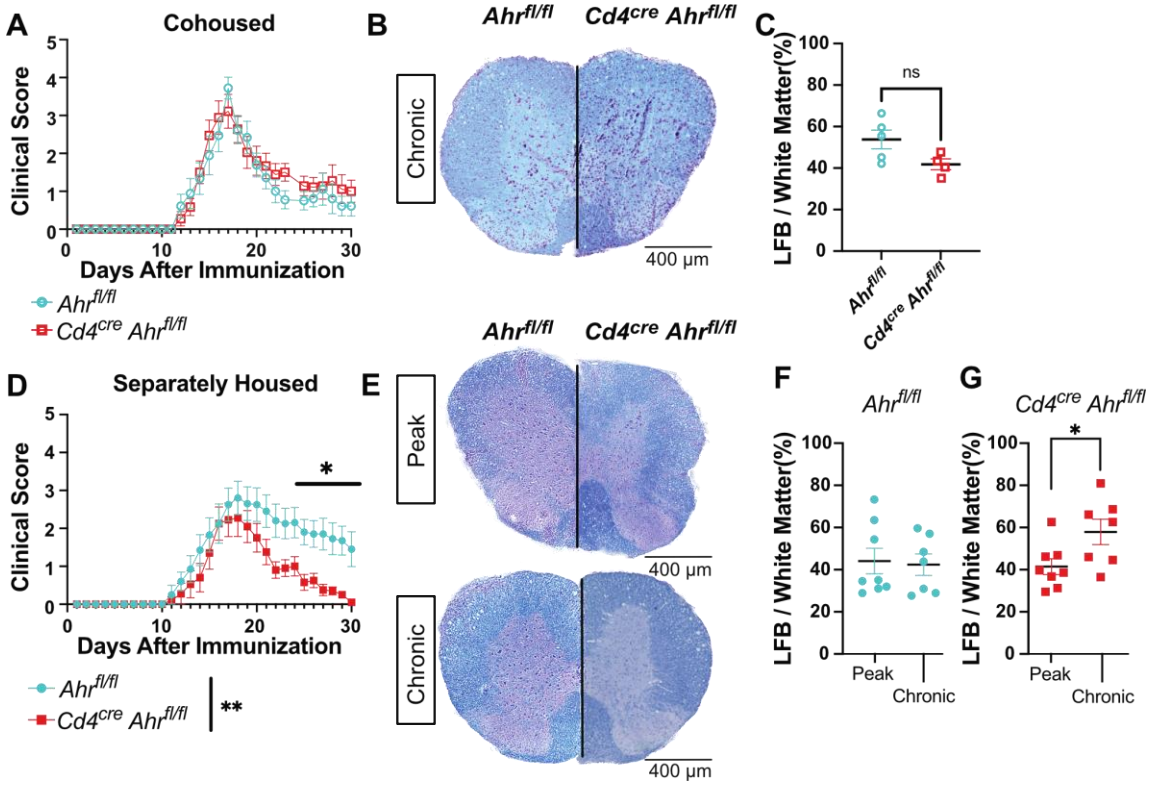

Figure 4.1. Separately housed *Cd4^{cre}Ahr$^{fl/fl}$* recover from EAE with increased myelin staining at chronic phase. (**A**) Clinical score of *Cd4^{cre}Ahr$^{fl/fl}$* and *Ahr$^{fl/fl}$* mice cohoused (Females; Representative plot includes n= 9 mice/group; total replicates of N=2 experiments). Spinal cords sections of *Cd4^{cre}Ahr$^{fl/fl}$* and *Ahr$^{fl/fl}$* were stained with Luxol Fast Blue and Hematoxylin/Eosin stain a day 31 post EAE induction (**B**) Representative images and (**C**) quantification of myelin stain. Images from four equally spaced spinal cord levels were averaged for each mouse. (n=5 mice/group; Unpaired T test p=0.0706) (**D**) Clinical score of *Cd4^{cre}Ahr$^{fl/fl}$* and *Ahr$^{fl/fl}$* littermate controls separated at weaning (3 weeks of age). (Females; Representative plot includes n=8-9 mice/group; total replicates of N=2 experiments; Mann-Whitney U Test on total scores reported in legend [p=0.0096] and on single days reported on plot) (**E**) Luxol Fast Blue with Hematoxylin/Eosin stain at the peak stage of EAE (day 16) and at chronic phase (day 31). (**F**) Quantification of myelin stain by Luxol Fast Blue alone in *Ahr$^{fl/fl}$* mice

and (**G**) *Cd4*^{cre}*Ahr*$^{fl/fl}$ mice. (n=7-8 mice/group; N=2 experiments; Unpaired T tests [p=0.8343, 0.0322]) Scale bars represent 400µm. Error bars represent standard error from the mean.

T cell differentiation and activity are unchanged in *Cd4*^{cre}*Ahr*$^{fl/fl}$ mice:

CD4+ T cells are responsible for orchestrating EAE pathology, and defects in these cells have been shown to impact disease outcomes[305]. Additionally, AHR agonists can modulate T cell skewing in a ligand dependent manner *in vivo*[306]. I aimed to explore the role of AHR in T cells differentiation and cytokines production. First, I examined T cell differentiation and the production of cytokines in cohoused *Cd4*^{cre}*Ahr*$^{fl/fl}$ mice. I found that the deletion of AHR in T cells did not impact their capacity for *in vitro* differentiation as determined by expression of lineage transcription factors by flow cytometry (**Figure 4.2A-E**) or production of the signature cytokine for each lineage by ELISA (**Figure 4.2F-I**). This was mirrored in separately housed animals (**Sup Figure 4.2A-G**). Furthermore, there were no differences in the immune cell composition between the knockout and control animals at baseline (**Figure 4.2J-M**). I next measured several cytokines important to EAE induction in the spinal cords of mice at the peak of disease. I expected to see significant reduction in the pathological cytokines in the separately housed *Cd4*^{cre}*Ahr*$^{fl/fl}$ mice that ultimately recover, but surprisingly I found minimal differences (**Figure 4.2N-S**). The only change was a small reduction in TNFα which may warrant further investigation. These findings suggest that CD4 cell intrinsic AHR activity is not necessary for normal T cell development and cytokines expression supporting published work indicating that AHR activation of the antigen presenting cell may be more important to T cell subset generation *in vivo*[307–309]. Further, these data reinforce the hypothesis that the T cell-intrinsic reduction of AHR activity in *Cd4*^{cre}*Ahr*$^{fl/fl}$ mice is not responsible for EAE recovery described in separately housed mice.

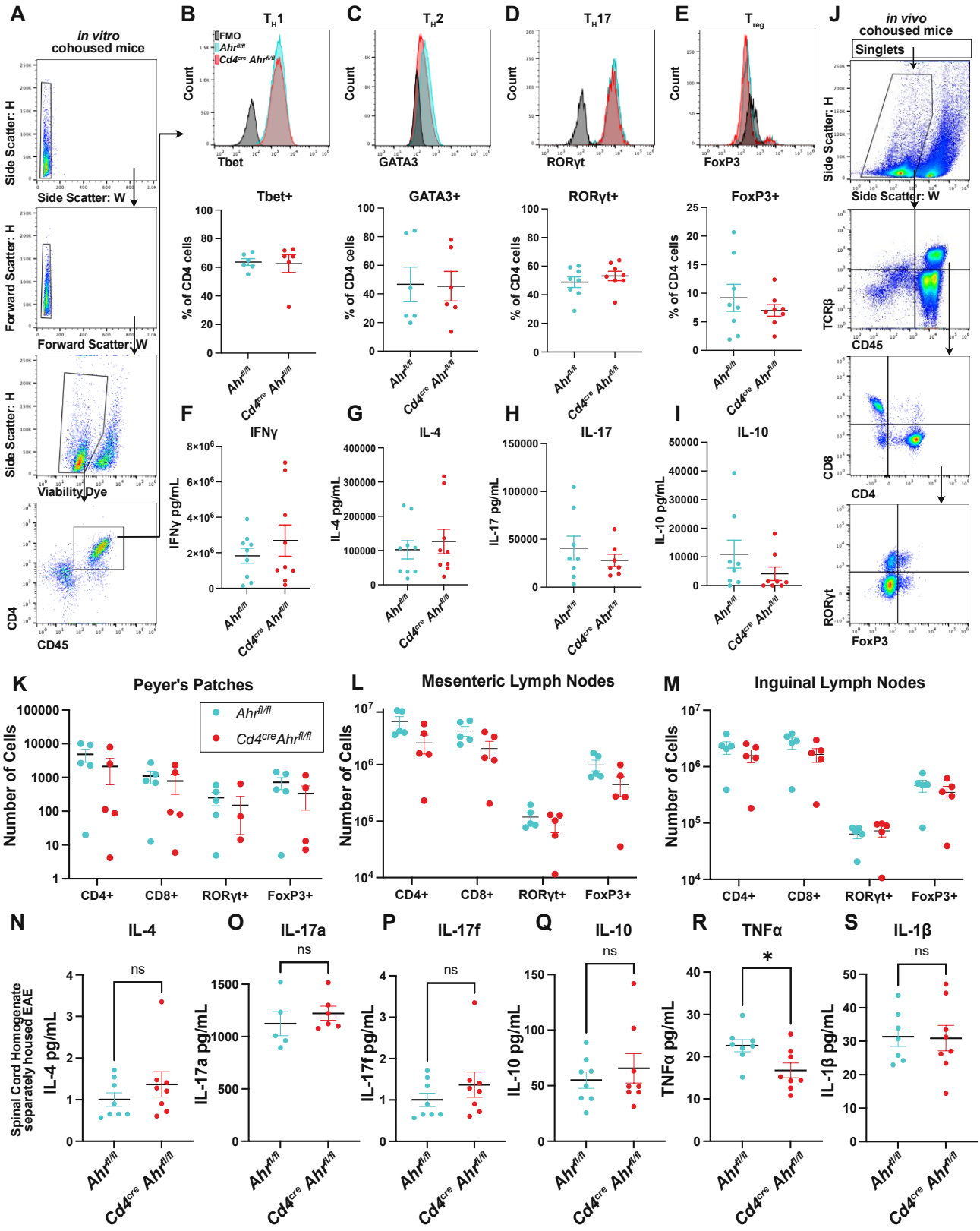
A
in vitro
cohoused mice
Side Scatter: H
Side Scatter: W
Forward Scatter: H
Forward Scatter: W
Viability Dye
CD4
CD45
B
TH1
FMO
Ahrfl/fl
Cd4cre Ahrfl/fl
Count
Tbet
Tbet+
% of CD4 cells
C
TH2
GATA3
GATA3+
D
TH17
RORγt
RORγt+
E
Treg
FoxP3
FoxP3+
F
IFNγ
IFNγ pg/mL
G
IL-4
IL-4 pg/mL
H
IL-17
IL-17 pg/mL
I
IL-10
IL-10 pg/mL
J
in vivo
cohoused mice
Singlets
Side Scatter: H
Side Scatter: W
TCRβ
CD45
CD8
CD4
RORγt
FoxP3
K
Peyer's Patches
Ahrfl/fl
Cd4creAhrfl/fl
Number of Cells
CD4+
CD8+
RORγt+
FoxP3+
L
Mesenteric Lymph Nodes
M
Inguinal Lymph Nodes
N
IL-4
Spinal Cord Homogenate
separately housed EAE
IL-4 pg/mL
ns
O
IL-17a
IL-17a pg/mL
P
IL-17f
IL-17f pg/mL
Q
IL-10
IL-10 pg/mL
R
TNFα
TNFα pg/mL
*
S
IL-1β
IL-1β pg/mL

Figure 4.2. *Ahr* knockout in CD4+ cells does not influence T cell differentiation. (**A**) Naïve CD4+ T cells were isolated from cohoused *Cd4*^{cre}*Ahr*$^{fl/fl}$ and littermate control animals and treated to promote differentiation. Flow cytometry gating strategy to measure percent of cells expressing the transcription factors specific to each cell type is shown. (**B**) Representative histogram and quantification of Tbet+ cells after *in vitro* differentiation of naïve CD4+ cells to T_H1 cell type, (n=6 mice/group; N=2 experiments; Unpaired T test [p=0.8715]) (**C**) GATA3 staining of T_H2 differentiated cells, (n=6 mice/group; N=2 experiments; Unpaired T test [p=0.9356]), (**D**) RORγt staining of T_H17 cells (n=8 mice/group; N=3 experiments; Unpaired T test [p=0.3989]) (**E**), and FoxP3 staining for T_{regs}.(n=8 mice/group; N=3 experiments; Unpaired T test [p=0.4078]). (**F**) ELISA analysis of culture supernatant after 24 hours of anti-CD3 stimulation in $T_H1$cells (n=9 mice/group; N=3 experiments; Unpaired T test [p=0.3924]) (**G**) T_H2 cells(n=8 mice/group; N=3 experiments; Unpaired T test [p=0.5917]) (**H**) T_H17 cells (n=7-8 mice/group; N=3 experiments; Unpaired T test [p=0.4013]) (**I**) or Treg cells. (n=8 mice/group; N=3 experiments; Unpaired T test [p=0.2278]) (**J**) Gating strategy for (**K**) flow cytometry of single cell suspensions of Peyer's patches from cohoused *Cd4*^{cre}*Ahr*$^{fl/fl}$ and *Ahr*$^{fl/fl}$ mice. (Multiple T tests with Welch correction [p=0.070748, 0.081520, 0.325104, 0.080798]) (**L**) Analysis of cell compositions from mesenteric lymph nodes (Multiple T tests with Welch correction [p=0.127038, 0.179526, 0.444670, 0.118472]) (**M**) and the inguinal lymph nodes from cohoused *Cd4*^{cre}*Ahr*$^{fl/fl}$ and *Ahr*$^{fl/fl}$ mice (Multiple T tests with Welch correction [p=0.381964, 0.224164, 0.664161, 0.465348]) (**N-S**) Luminex assay on whole spinal cord homogenate of separately housed *Cd4*^{cre}*Ahr*$^{fl/fl}$ and *Ahr*$^{fl/fl}$ mice at the peak of disease (day 16 after immunization; n=8 mice/group; N=2 experiments; Unpaired T test) (N) [p=0.3087] (O) [p=0.4580] (P) [p=0.8313] (Q) [p=0.4941] (R) [p=0.0215] (S) [p=0.9333] Error bars represent standard error from the mean.

Cd4^{cre}*Ahr*$^{fl/fl}$ mice have fewer T cells in the spinal cord during EAE:

To determine whether EAE recovery in *Cd4*^{cre}*Ahr*$^{fl/fl}$ was linked to a difference in immune cell number during pathology, I quantified CD45+ immune cells in the spinal cord tissue using immunohistochemistry at the peak and chronic stages of EAE progression (**Figure 4.3A-B**). While the

quantity of CD45+ cells was equivalent at the peak of the disease, I observed a decrease in the number of CD45+ cells in the *Cd4*^{cre}*Ahr*$^{fl/fl}$ spinal cord compared to controls at the chronic phase (**Figure 4.3B**). I next aimed to determine whether this reduction was a result of changes in the number of infiltrating T cells or macrophages. To accomplish this, I quantified expression of CD3, a pan-T cell marker, by immunohistochemistry. I saw no difference in the CD3+ cells in the spinal cord at the peak of disease (**Figure 4.3C**); however, at the chronic phase, significantly lower CD3+ T cell coverage was observed in the *Cd4*^{cre}*Ahr*$^{fl/fl}$ mice compared to the separately housed littermate controls (**Figure 4.3D**). Meanwhile, monocytes and macrophages, the other primary effector cells in EAE, showed no differences at either peak or chronic phase as shown by CD11b expression (**Figure 4.3E-F).** I confirmed this outcome using flow cytometry on percoll-isolated immune cells from the spinal cord. At the peak of disease, I again observed no differences in infiltrating T cells (CD4+ or CD8+), T cell subsets (RORgt+, Tbet+ GATA3+ or FoxP3+) or macrophages (CD11b+) (**Figure 4.3G-H**). At the chronic phase of disease, I found that the loss of T cells was limited to the CD4+ compartment and not the CD8+ compartment. Of the classic CD4 helper cell subtypes, all trended down in *Cd4*^{cre}*Ahr*$^{fl/fl}$ mice with no one subtype constituting a significant decrease, indicating a pan-CD4+ phenotype, not associated with a specific subtype of CD4+ T cells (**Figure 4.3F**). Taken together, our data suggest that in separately housed mice, EAE recovery observed in *Cd4*^{cre}*Ahr*$^{fl/fl}$ mice is not due to a difference in cytokine expression or T cell differentiation. Instead, recovery correlates with an overall reduction in CD4+ T cell numbers at the chronic phase of disease and suggests an impact for AHR and the microbiome on CD4+ T cell fitness.

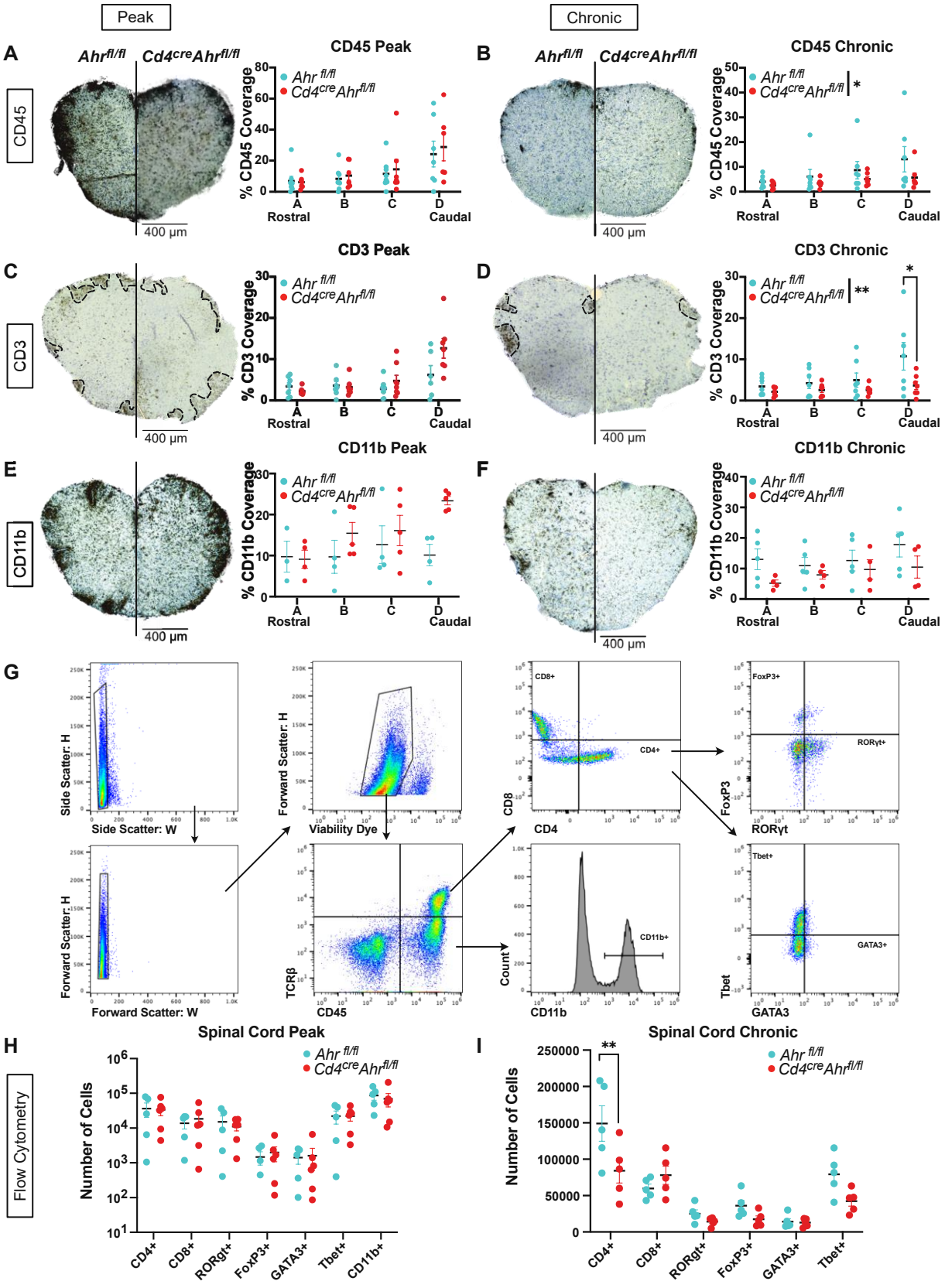
Peak
Chronic
A
B
C
D
E
F
G
H
I
CD45
CD3
CD11b
Flow Cytometry
Ahrfl/fl
Cd4creAhrfl/fl
400 μm
CD45 Peak
CD45 Chronic
CD3 Peak
CD3 Chronic
CD11b Peak
CD11b Chronic
% CD45 Coverage
% CD3 Coverage
% CD11b Coverage
Rostral
Caudal
Side Scatter: H
Side Scatter: W
Forward Scatter: H
Forward Scatter: W
Viability Dye
TCRβ
CD45
CD8+
CD4+
CD8
CD4
FoxP3+
RORγt+
FoxP3
RORγt
Tbet+
GATA3+
Tbet
GATA3
CD11b+
Count
CD11b
Spinal Cord Peak
Spinal Cord Chronic
Number of Cells
CD4+
CD8+
RORgt+
FoxP3+
GATA3+
Tbet+
CD11b+

Figure 4.3. Reduced CD3+ cells in the spinal cord of *Cd4^{cre}Ahr$^{fl/fl}$* mice correlate with clinical signs. (**A**) Spinal cords of separately housed *Cd4^{cre}Ahr$^{fl/fl}$* and *Ahr$^{fl/fl}$* littermate controls were stained for total immune cells (CD45+) by immunohistochemistry at four levels at the peak of disease (day 16 after immunization) (Each dot represents a mouse n=7 mice/group; N=2 experiments; Two-way ANOVA[p=0.5336]) (**B)** or at the chronic phase of disease (day 31 after immunization). (Two-way ANOVA [p=0.0419]; Sidak's multiple comparisons test [p=0.9896, 0.9209, 0.7898, 0.1753]) (**C**) Spinal cords of separately housed *Cd4^{cre}Ahr$^{fl/fl}$* and *Ahr$^{fl/fl}$* littermate controls were stained for T cells (CD3+) by immunohistochemistry at four levels at the peak of disease (day 16 after immunization) (n=7 mice/group; N=2 experiments, Two-way ANOVA [p=0.0830]) (**D**) or at chronic phase of disease (day 31 after immunization). (n=7 mice/group; N=2 experiments, Two-way ANOVA [p=0.0054]; Sidak's multiple comparisons test [p=0.9578, 0.9029, 0.7095, 0.0070]) (**E**) Spinal cords of separately housed *Cd4^{cre}Ahr$^{fl/fl}$* and *Ahr$^{fl/fl}$* littermate controls were stained for macrophages (CD11b+) by immunohistochemistry at four levels at the peak of disease (day 16 after immunization) (n=4-5 mice/group; N=2 experiments; Two-way ANOVA [p=0.1271]) (**F**) or at chronic phase of disease (day 31 after immunization). (n=5 mice/group; N=2 experiments, Two-way ANOVA [p=0.2269]) (**G**) Gating strategy for flow cytometry analysis of immune cells isolated from dissociated spinal cord tissue (**H**) at peak of disease (day 16 after immunization) (n=5-6/group; Multiple Unpaired T Tests with Benjamini and Yekutieli corrections [p values listed in supplement (S1 Data)]). (**I**) or chronic phase of disease (day 31 after immunization) (n=5 mice/group; Multiple Unpaired T Tests with Benjamini and Yekutieli corrections [p values listed in supplement (S1 Data)]). Scale bars represent 400µm. Error bars represent standard error from the mean.

Apoptosis of *Ahr* deficient CD4 T cells is dependent on gut-derived small molecules:

I next investigated the mechanism behind the reduced T cell numbers in the spinal cords of *Cd4^{cre} Ahr$^{fl/fl}$* mice during chronic EAE. I performed a gene expression analysis on whole spinal cord tissues isolated from two *Cd4^{cre}Ahr$^{fl/fl}$* and two *Ahr$^{fl/fl}$* animals at the peak of EAE using a qPCR array composed of 384 genes associated with neuroinflammation. I found that the expression of many genes involved in apoptosis were modulated in the spinal cord tissue of *Cd4^{cre}Ahr$^{fl/fl}$* mice; in particular I

noted increased expression of *Fas, GrB, Casp3,* and *Casp9* and decreased expression of the antiapoptotic transcript of *Xiap,* indicating an increase in apoptosis in CD4 specific *Ahr*-deficient mice (**Sup Figure 4.3A-B**). To test if T cells lacking AHR were undergoing apoptosis in EAE, I stained spinal cords sections for CD3 expression by immunofluorescence and TUNEL assay (**Figure 4.4A**). While I could detect some apoptotic T cells in the spinal cords of control mice subjected to EAE, CD3+TUNEL+ cell numbers were significantly increased in the spinal cords of *Ahr* deficient animals (closed triangles; **Figure 4.4B**). I confirmed this observation by quantifying cellular death of isolated immune cells from the spinal cord at the peak of disease using flow cytometry. I observed a significant and specific increase in the percentage of dead CD4+ T cells without change in the percentage of dead CD8+ and or total TCRB+ cells between genotypes (**Figure 4.4C**). To further understand the mechanisms behind these observations, I focused examination on the primary pathogenic subset of CD4+ cells in EAE, the type 17 T helper cell (T_H17)[310]. To obtain T_H17 cells I isolated naïve CD4+ cells from the lymph nodes and spleen, then cultured the cells in T_H17 differentiation conditions. Similar to the *in vivo* observations, $Cd4^{cre}Ahr^{fl/fl}$ T_H17 cells have a significant increase in apoptosis after mild *in vitro* stimulation by anti-CD3 as measured by Annexin V staining compared to littermate controls (**Figure 4.4D**). Increased T_H17 cell death was only observed in cells isolated from $Cd4^{cre}Ahr^{fl/fl}$ animals separated at weaning, as T cells isolated from cohoused $Cd4^{cre}Ahr^{fl/fl}$ mice did not display elevated apoptosis (**Figure 4.4E**). Taken together, these results support the hypothesis that gut microenvironment may be implicated in the *Ahr*-dependent T cell fitness phenotype. To directly test this hypothesis, I isolated metabolites (<3kDa) from cecums of separately housed $Cd4^{cre}Ahr^{fl/fl}$ and $Ahr^{fl/fl}$ mice, and added them to *in vitro* skewed T_H17 cells prepared from C57BL6/J mice during the 24 hour stimulation period. I next analyzed apoptosis by flow cytometry. T_H17 cells exposed to metabolites derived from the gut of $Cd4^{cre}Ahr^{fl/fl}$ mice had elevated apoptosis compared to cells exposed to metabolites from $Ahr^{fl/fl}$ microbiome (**Figure 4.4F**). Collectively, these data demonstrate that exposure to the microbial metabolites from $Cd4^{cre}Ahr^{fl/fl}$ mice is sufficient to induce early T cell apoptosis which likely contributes to recovery in EAE.

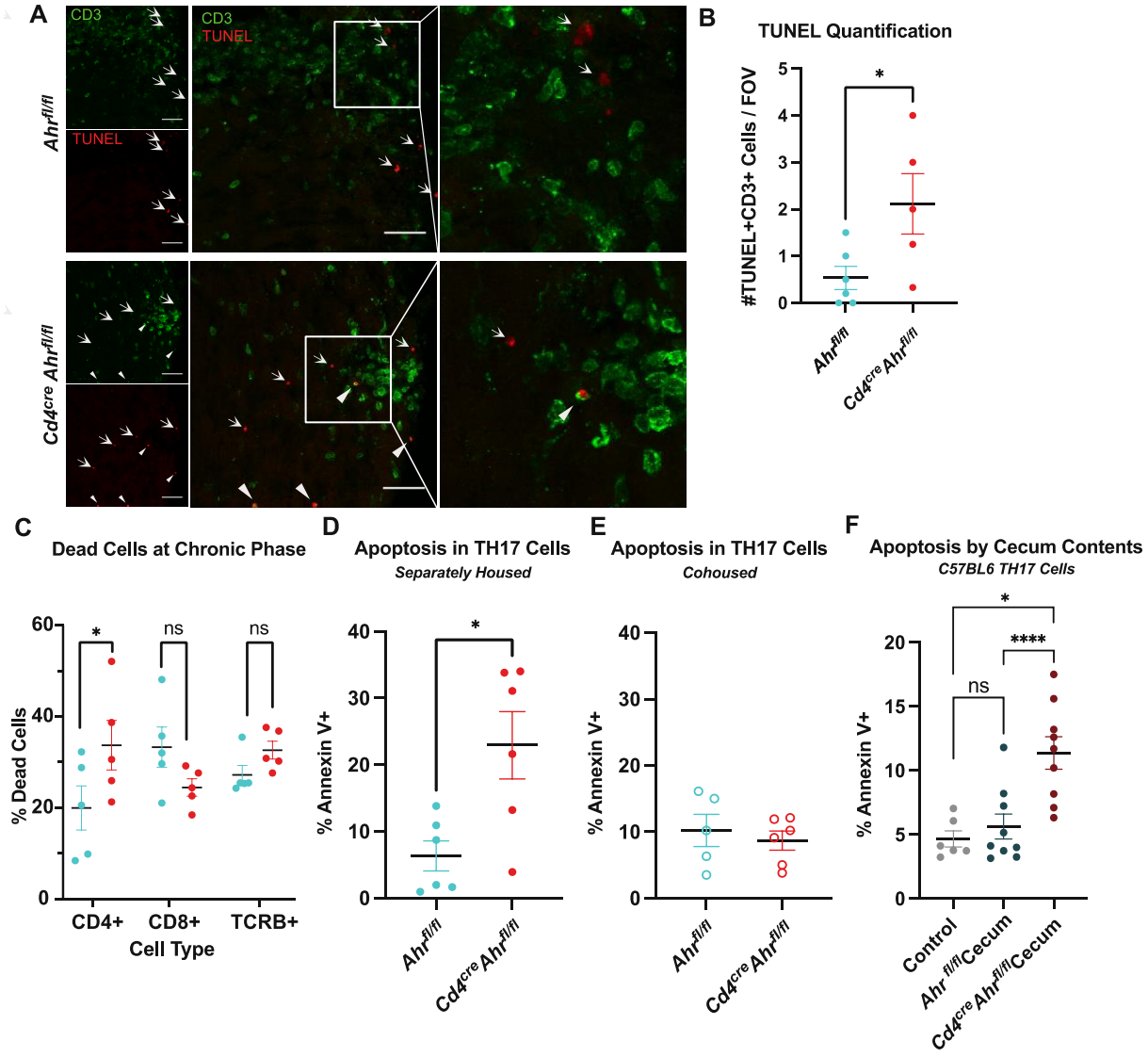

Figure 4.4. T cell apoptosis is increased in animals who recover from EAE. (**A**) Representative image of spinal cords stained with TUNEL assay and T cell marker at the peak of disease (CD3). Closed triangles indicate TUNEL+CD3+ cells and arrows indicate TUNEL+CD3- cells. Scale bar = 400µm. (**B**) Quantification of the number of TUNEL+ T cells (2-6 lesion sites averaged per animal; n=5-6 mice; N=2 EAE experiments; Unpaired T test [p=0.0357]). (**C**) T cells isolated from the spinal cord at the peak of disease stained with viability dye and measured by flow cytometry. Cells gated on singlets, CD45+, gate shown on x-axis, then dead cells (n=5 mice/group; Two-way ANOVA [p=0.0192] with Sidak's Multiple Comparison Tests [p=0.0465,

0.2862, 0.6800]). (**D**) T cells skewed to T_H17 *in vitro* from separately housed *Cd4*^{cre}*Ahr*$^{fl/fl}$ mice stained for apoptotic marker Annexin V 24 hours after stimulation with anti-CD3 antibody. (n=6 mice/group; N=2 experiments; Unpaired T test [p=0.0133]). (**E**) T_H17 cells from cohoused *Cd4*^{cre}*Ahr*$^{fl/fl}$ and *Ahr*$^{fl/fl}$ mice show no differences in the number of Annexin V positive cells 24 hours after stimulation with anti-CD3 antibody. (n=5-6 mice/group; N=2 experiments; Unpaired T test [p=0.5851]). (**F**) *In vitro* differentiated T_H17 cells from C57BL6/J mice were exposed to the <3kDa fraction of cecal contents from *Ahr*$^{fl/fl}$ and *Cd4*^{cre}*Ahr*$^{fl/fl}$ mice for 24 hours with anti-CD3 stimulation. (n=6-9 mice/group; N=3 experiments; Mixed-effects analysis, with Geisser-Greenhouse correction [p=0.0013]; Tukey's post hoc analysis [Ctr v Fl p=0.7729; Ctr v Cre p=0.0333, Fl v Cre p<0.0001]). Error bars represent standard error from the mean.

Metabolomic differences in the gut microenvironment are evident in separately housed *Cd4*^{cre}*Ahr*$^{fl/fl}$ mice:

To identify the impact of CD4+ cell AHR loss on the gut microenvironment, I began by performing 16S sequencing of DNA isolated from fecal pellets and cecal contents of *Ahr*$^{fl/fl}$ or *Cd4*^{cre}*Ahr*$^{fl/fl}$ mice. Neither cohoused nor separately housed animals saw differences in fecal or cecal microbial signatures (**Sup Figure 4.4A-D**). Given the marked effect of the metabolites prepared from the cecums of *Cd4*^{cre}*Ahr*$^{fl/fl}$ and *Ahr*$^{fl/fl}$ on T cell apoptosis (**Figure 4.4F**), I next conducted untargeted metabolomics by LC-MS on these preparations (<3kDa). Two-dimensional clustering of the annotated products revealed distinct clustering of genotypes, indicating different chemical profiles (**Figure 4.5A**). This difference occurred despite there being no significant difference in the 16S microbial signatures of the cecal contents suggesting that AHR activity in T cells modify microbial metabolism without altering the microbe composition to a degree that can be captured by 16S sequencing (**Sup Figure 4.4E-F**). Impact analysis of biological pathways identified primary bile acid biosynthesis as the most significantly upregulated pathway with six primary (cholic, taurocholic) or secondary (glycocholic, sulfocholic, dehydrocholic, lawsonic) bile acids significantly increased in the cecal microenvironment of *Cd4*^{cre}*Ahr*$^{fl/fl}$ mice (**Figure 4.5B-C**). Bile acids are dysregulated systemically in patients with MS and adding back primary bile acid is sufficient to reduce the severity of EAE[311]. Bile acid biosynthesis is known to be dependent on the gut microbiota composition[312,313]. Of the changed bile acids,

taurocholic acid was the most highly upregulated with over a 10-fold increase in *Cd4*^{cre}*Ahr*$^{fl/fl}$ compared to control mice (**Figure 4.5C**). Increased bile acid accumulation in these mice may be due to the downregulation of bile acid transporters in the small intestine of the *Cd4*^{cre}*Ahr*$^{fl/fl}$ mice (**Figure 4.5D**). In addition to changes in bile acids, alanine, aspartate, and glutamate metabolism were also upregulated, whereas purine metabolism and tryptophan metabolism were downregulated in *Cd4*^{cre}*Ahr*$^{fl/fl}$ mice. As short chain fatty acids (SCFAs) have been reported to impact the viability of inflammatory T cell and cannot be captured through untargeted metabolomics, I next performed targeted SCFA metabolomics [314,315]. Isovaleric acid was the only SCFA with a significantly higher abundance in the *Cd4*^{cre}*Ahr*$^{fl/fl}$ cecums compared to controls (**Figure 4.5E**).

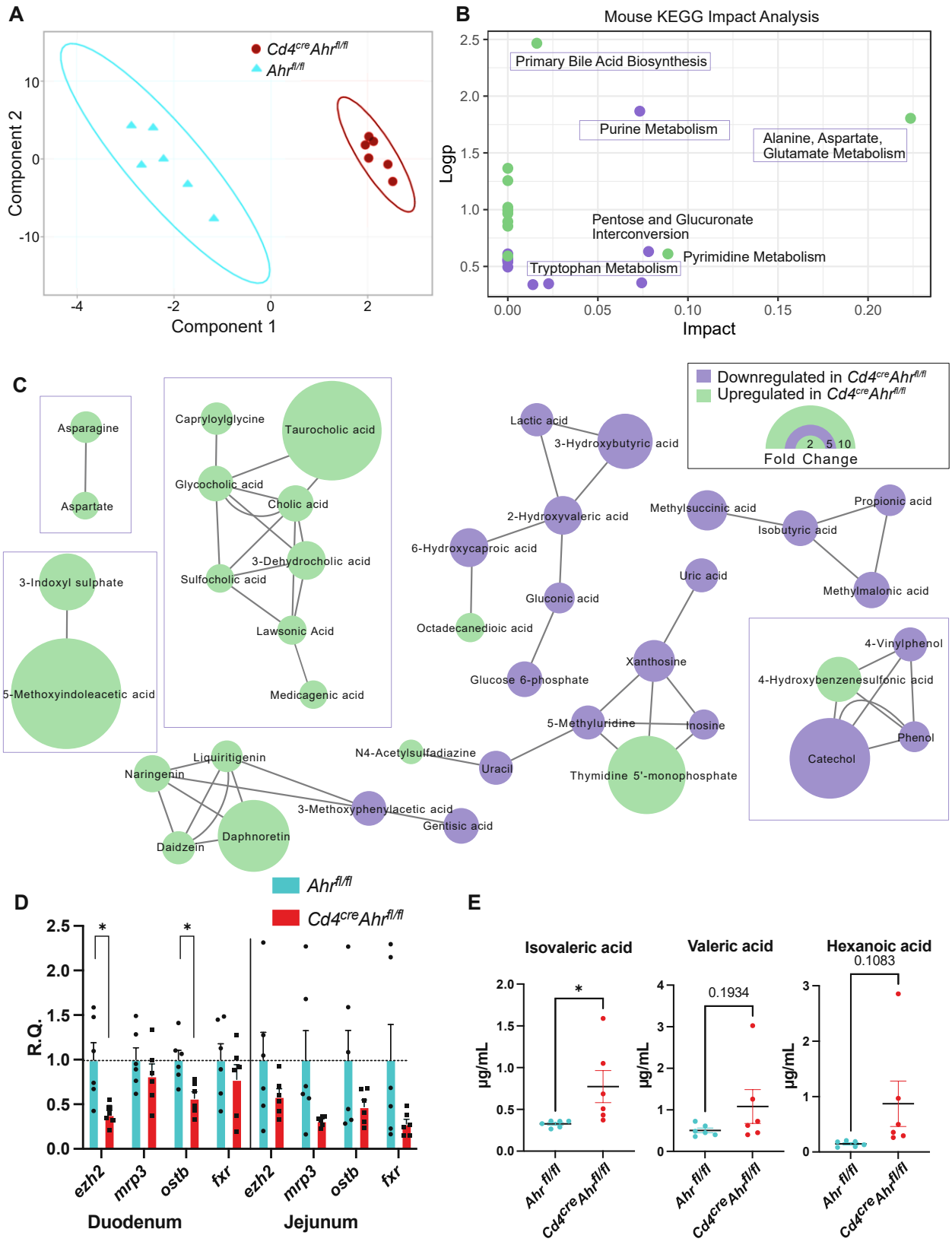
A
Cd4cre Ahrfl/fl
Ahrfl/fl
Component 2
Component 1
B
Mouse KEGG Impact Analysis
Primary Bile Acid Biosynthesis
Purine Metabolism
Alanine, Aspartate, Glutamate Metabolism
Pentose and Glucuronate Interconversion
Pyrimidine Metabolism
Tryptophan Metabolism
Logp
Impact
C
Downregulated in Cd4cre Ahrfl/fl
Upregulated in Cd4cre Ahrfl/fl
Fold Change
Asparagine
Aspartate
3-Indoxyl sulphate
5-Methoxyindoleacetic acid
Caprylolylglycine
Taurocholic acid
Glycocholic acid
Cholic acid
3-Dehydrocholic acid
Sulfocholic acid
Lawsonic Acid
Medicagenic acid
Lactic acid
3-Hydroxybutyric acid
2-Hydroxyvaleric acid
6-Hydroxycaproic acid
Gluconic acid
Octadecanedioic acid
Glucose 6-phosphate
Methylsuccinic acid
Propionic acid
Isobutyric acid
Methylmalonic acid
Uric acid
Xanthosine
5-Methyluridine
Inosine
Thymidine 5'-monophosphate
Uracil
N4-Acetylsulfadiazine
4-Vinylphenol
4-Hydroxybenzenesulfonic acid
Phenol
Catechol
Liquiritigenin
Naringenin
Daidzein
Daphnoretin
3-Methoxyphenylacetic acid
Gentisic acid
D
Ahrfl/fl
Cd4cre Ahrfl/fl
R.Q.
ezh2
mrp3
ostb
fxr
Duodenum
Jejunum
E
Isovaleric acid
Valeric acid
Hexanoic acid
0.1083
0.1934
μg/mL
Ahr fl/fl
Cd4cre Ahrfl/fl

Figure 4.5. Elevated bile salts and SCFA detected in the cecum of AHR deficient mice. (**A**) Partial least-squares plot of LC-MS untargeted metabolomics of the <3kDa fraction of the cecal contents from *Cd4*^{cre}*Ahr*$^{fl/fl}$ and *Ahr*$^{fl/fl}$ mice. (**B**) Metaboanalyst mouse KEGG pathways significantly changed by genotype. (**C**) MetaMapp network analysis visualizing the chemically or biologically related significantly changed molecules. (**D**) qPCR of bile acid transporters (*mrp3, ostb*) and bile acid response elements (*ezh2*, *fxr*) in bulk tissue of the duodenum and jejunum of separately housed animals illustrated as relative quantity (R.Q.) from *Ahr*$^{fl/fl}$ tissue . (n=6 mice/group; N=2 experiments; Multiple T Tests with Welch correction [duodenum p=0.0104, 0.3591, 0.0071, 0.3828; jejunum p=0.2230, 0.0623, 0.1487, 0.1004]). (**E**) Quantitative targeted metabolomics for short chain fatty acids show a significant increase in isovaleric acid, and a trending increase in valeric and hexanoic acid in *Cd4*^{cre}*Ahr*$^{fl/f}$ mice. (n=6 mice/group; N=1 experiment; Unpaired T tests [p=0.0427, 0.1934, 0.1083]) Error bars represent standard error from the mean.

Taurocholic acid induces T_H17 cell apoptosis and protects from EAE:

The chemical composition of the cecal microenvironment between separately housed *Cd4*^{cre}*Ahr*$^{fl/fl}$ and *Ahr*$^{fl/fl}$ animals is significantly changed. I next aimed to determine what functional differences arose from the chemical differences both *in vitro* and *in vivo*. I first examined the most highly increased bile acid in *Cd4*^{cre}*Ahr*$^{fl/fl}$ mice, taurocholic acid. When administered to C57BL6/J derived T_H17 cells *in vitro,* taurocholic acid was sufficient to drive apoptosis similarly to cecal content isolates (**Figure 4.6A-B**). I also examined isovaleric acid, the short chain fatty acid, elevated in the absence of AHR. Similarly to taurocholic acid, isovaleric acid could induce apoptosis of *in vitro* generated T_H17 cells (**Figure 4.6C**). Similar results were obtained with hexanoic acid, which was also trending higher in *Cd4*^{cre}*Ahr*$^{fl/fl}$ mice (**Figure 4.6C**). Collectively, our data suggest that the combined effects of the cecal milieu of *Cd4*^{cre}*Ahr*$^{fl/fl}$ mice could induce changes in T cell fitness, ultimately resulting in recovery from paralysis in EAE. As such, I aimed to determine whether this held true *in vivo* by conducting a fecal microenvironment transfer to C57BL/6 wildtype mice. The mice were given a cocktail of oral antibiotics for two weeks followed by a series of three oral gavages of the flushed contents of the intestinal tract from separately housed *Cd4*^{cre}*Ahr*$^{fl/fl}$ and *Ahr*$^{fl/fl}$ animals. During this time

the animals were also cohoused with an untreated member of the respective genotype to promote lasting engraftment of the microbiome (**Figure 4.6D**). When these mice underwent EAE, the wildtype mice given FMT from *Cd4*^{cre}*Ahr*$^{fl/fl}$ animals had a similar, but less pronounced reduction in severity as the donor mice (**Figure 4.6E-F**). Because the FMT resulted in an intermediate phenotype, I next aimed to determine whether an individual component of the gut microenvironment could act as a therapeutic for EAE. As taurocholic acid was the most efficient driver of apoptosis *in vitro* (**Figure 4.6B**) I chose this as our prime candidate. I administered taurocholic acid orally for seven days after EAE induction (**Figure 4.6G**). Compared to mice given saline, those receiving taurocholic acid had decreased peak EAE scores (**Figure 4.6H**) and delayed onset (**Figure 4.6I**). These data are in support of recent work showing that bile acid receptor agonists and bile acid cocktails can reduce T cell activation and suppress EAE [316,317].

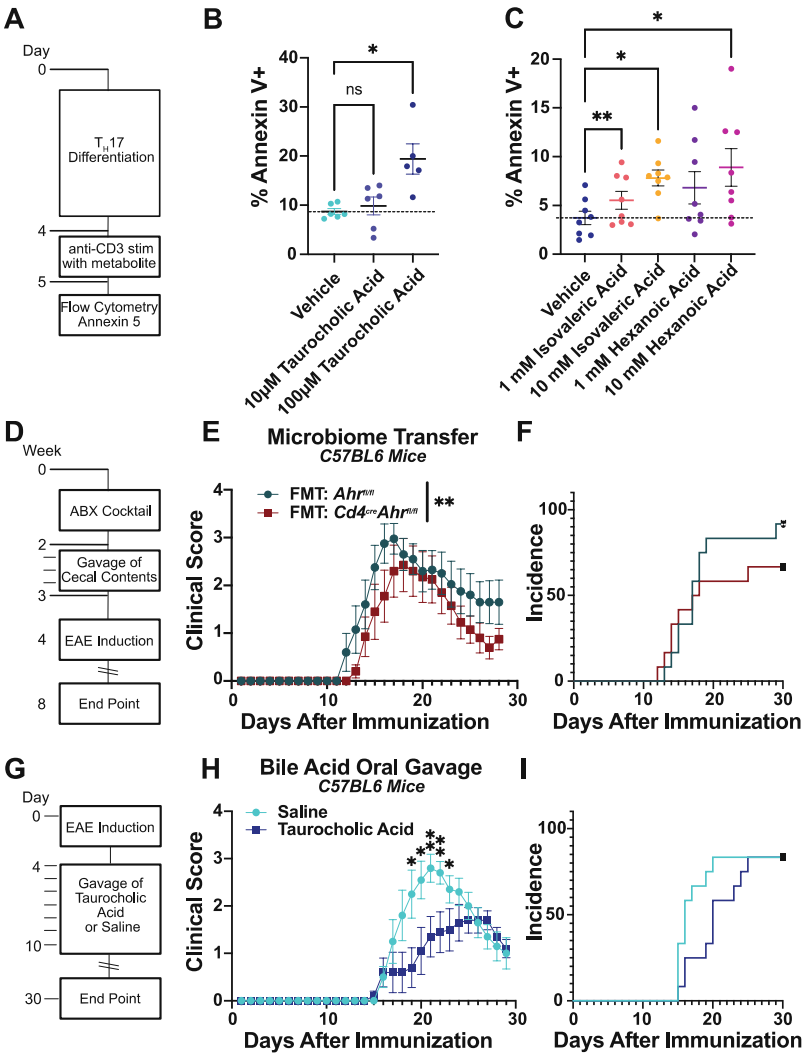

Figure 4.6. Gut Microenvironment and bile salts can drive EAE recovery and T cell apoptosis

(**A**) Schematic representation of experiments in B and C. *In vitro* derived T_H17 cells from C57/BL6/J mice were treated with a metabolite in addition to mild anti-CD3 stimulation for 24 hours. (**B**) Taurocholic acid (10µM and 100µM) was administered during anti-CD3 stimulation and apoptosis of T_H17 cells isolated from C57BL6/J mice was measured using Annexin V staining by flow cytometry. (n=5-6 mice/group; N=2 experiments; Mixed effects analysis with Geisser-Greenhouse correction [p=0.0070]; Dunnett's multiple comparison test [Veh vs 10µM p=0.8178, Veh vs 100µM p=0.0233]) (**C**) Administration of isovaleric acid and hexanoic acid (short chain fatty acids that are increased in mice that recover) are sufficient to drive apoptosis in T_H17 cells isolated from C57BL6/J mice. (n=8 mice/group; N=2 experiments; RM one-way ANOVA with the Geisser-Greenhouse correction[p=0.0399] Dunnett's multiple comparisons

test [Veh vs 1mM Hexanoic p=0.0764, Veh vs 10mM Hexanoic p=0.0352, Veh vs 1mM Isovaleric p=0.0026, Veh vs 10mM Isovaleric p=0.0254]). (**D**) Schematic depicting approach to FMT. (**E**) EAE clinical scores of C57BL6/J mice receiving FMT from separately housed *Ahr*$^{fl/fl}$ or *Cd4*^{cre}*Ahr*$^{fl/fl}$ mice. (Females; Representative plot includes n=11 mice/group; total replicates of N=2 experiments; Mann-Whitney U Test on total scores reported in legend [p=0.0096]. (**F**) Incidence of clinical sign development in mice treated with FMT. (**G**) Schematic depicting approach to oral supplement of 12.5 mg taurocholic acid/day in C57BL6/J mice immunized for EAE. (**H**) EAE clinical scores of C57BL6/J mice receiving 7 days of oral taurocholic acid from separately housed *Ahr*$^{fl/fl}$ or *Cd4*^{cre}*Ahr*$^{fl/fl}$ mice. (Females; n=12 mice/group; total replicates of N=1 experiment; Mann-Whitney U Test on single days reported on plot). (**I**) Incidence of clinical sign development in mice treated with taurocholic acid. Error bars represent standard error from the mean.

4.3 Discussion

Here I demonstrate that the deletion of the aryl hydrocarbon receptor (AHR) in CD4+ cells can promote recovery in chronic EAE while having no impact on the onset nor the initial magnitude of the disease. I further show that this phenotype is dependent on the microbiome, as cohousing littermate *Cd4*^{cre}*Ahr*$^{fl/fl}$ and *Ahr*$^{fl/fl}$ mice abrogates recovery in EAE. These data are in support of previous work in similar models has shown no difference in EAE recovery after T cell-specific *Ahr* deletion [318]. At the mechanistic level, our data suggest that specific metabolites elevated in the cecum of *Cd4*^{cre}*Ahr*$^{fl/fl}$ mice reduce T cell fitness and viability. In particular, the cecal environment of *Cd4*^{cre}*Ahr*$^{fl/fl}$ animals is characterized by high levels of isovaleric acid and taurocholic acid, which induce T cell apoptosis *in vitro,* suggesting a potential mechanism for EAE recovery.

AHR activity can regulate autoimmunity via natural killer (NK) cells[319], macrophages[320], dendritic cells[321], and T cells[306,309,322]-all contributors to EAE pathogenesis. By utilizing CD4 cre mice, I will be targeting all cell types that are affected by CD4 expression at any time-including CD8 T cells which express CD4 during thymic development. AHR activation is a known regulator of T cell differentiation and inflammatory to regulatory T cell ratios. Importantly, T cell activity is dependent on the specific ligand activation with some promoting a pro-inflammatory environment, and others having the opposite effect[306]. It has been postulated that T cell intrinsic AHR activity is necessary for

differentiation but several groups have shown that AHR antagonists do not have a cell intrinsic effect on T cell differentiation leaving remaining questions in the field[323]. Here I demonstrate that T cell-specific AHR expression is not necessary for the differentiation of T cells *in vitro* supporting the hypothesis that the AHR activity in antigen presenting cell is the necessary factor influencing T cell differentiation *in vivo*[307–309]. Beyond T cells, AHR activation in glial cells regulates the pathogenic effects of microglia and astrocytes in EAE via changed cytokine production [203,324]. AHR's ubiquitous expression in barrier tissues coupled with its complex ligand binding profile warrants further study of AHR function in autoimmunity. I have identified that the changes of the luminal microenvironment of the intestine resulting from *Ahr* knockout in CD4+ cells lead to decreased post-activation lifespan in T cells; however, the impact of these changes on other cell types and other models of autoimmunity have yet to be determined. Though I aimed to target T cells using the CD4 cre line, I acknowledge that other CD4 expressing cells including some gut macrophages may also be contributing to the observed phenotype.

Bile acids, SCFAs, and other small molecules I identified can move into circulation and some can gain entry into the central nervous system by crossing the blood brain barrier[325]. There are likely systemic effects that have yet to be described. For example, our data suggest that significant remyelination is taking place in the chronic phase of EAE in CD4 specific *Ahr* knockout animals. Given the described impact of the microbiome and SCFA on myelination [326,327], it would be critical to test if the metabolic signature generated by the lack of *Ahr* in T cells can influence oligodendrocyte generation.

The data presented here support a bidirectional communication between T cells and the microbiome via AHR. However, it remains to be understood how T cells can modulate the metabolic signature of the cecum. I hypothesize that there are many mechanisms that could be mediating the change. For example, I show that the expression on bile acid transporters are reduced in the intestines of mice with *Ahr* deletion. This could lead to heightened levels of bile acids which have an impact on microbial viability, metabolism, and community structure. Additionally, it is possible that *Ahr* deletion in T cells may lead to modulation of IgA secretion by B cells[328,329]. IgA is the primary mechanism by which the adaptive immune system can directly modulate mucosal microbial communities[328]. An alternative hypothesis is that immune cell activity is modulating antimicrobial peptide release

indirectly through communication with Paneth cells[330,331]. Most work on these systems thus far has focused on models of severe microbiome dysbiosis. Less is known about the subtler changes in the microbiome subject to homeostatic regulation. Therefore, the mechanism by which the adaptive immune system can interface with the microbiota is of great interest for understanding the basis of autoimmune disorders.

Ahr knockout in T cells results in a change in both primary and conjugated bile acids in the cecum. Bile acids are produced by the host for digestion and are normally reabsorbed by transporters (primary) or passively (primary conjugated) in the ileum while secondary bile acids are not as easily absorbed [332]. There is an increase in conjugated bile acids in *Ahr* knockout mice, but lower levels of secondary bile acids. This is the inverse of patients with MS indicating that there may be a causative connection in both patients and mice with EAE[311]. Further studies are needed to understand which step of this pathway: production, conversion or absorption are influenced by the gut flora and/or the T cells. Our results support the existing work in synthetic bile acid receptor agonists showing that T cell fitness and activity can be mediated by bile acid receptor activation[316,317]. As previous groups have shown that T cells traffic to the gut before the CNS during EAE, I hypothesize that exposure to these factors during priming in the lymph node may lead to the early apoptosis after trafficking to the CNS[333]. This evidence that bile acids can have a direct influence on T cell function warrants further study in the context of autoimmune diseases.

Microbiome-modulated immune responses become particularly important in patients with chronic and relapsing autoimmune conditions like MS[334–338]. I have described a novel function for the environmental sensor AHR in T cells as a regulator of the gut microenvironment. As we further understand the complexities of harnessing the gut microbiome, I predict tools for controlling host-derived microbe modulation will be a new frontier for therapeutics. Our work is an important step in the discovery of a targetable endogenous modulator of the microbiome opens a potential new therapeutic avenue for MS patients.

Chapter 5:

IL-12 Mediates OPC Maturation and Myelin Morphogenesis in Females

Up to me

I cannot be the only one
Who doesn't have a clue
About where I am heading
Nor what I'm meant to do
But time will not wait for me
And as the days go passing by,
One thing I know that I control;
It's up to me to try.
-Ms. Moem

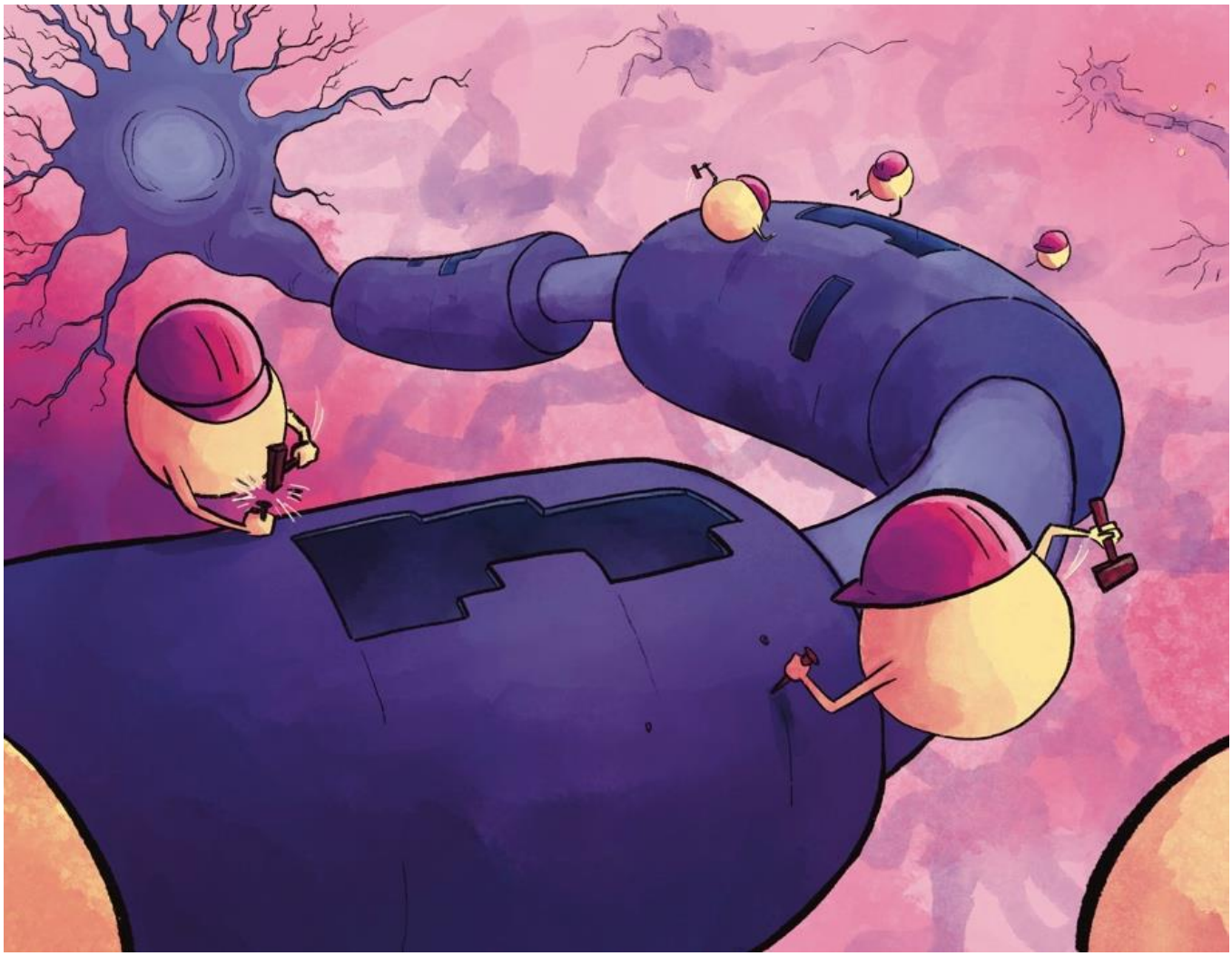

Forward

The work presented in the previous chapter resulted in the collection of much data that never made it into the final manuscript. One such piece of data was cytokine analysis of the spinal cord that revealed a reduction in IL-12 and IL-27 in mice who recovered from EAE (**Figure 5.0A**). These data inspired the work that follows in this chapter. Thankfully, I began this work before I ever bothered to replicated the findings from EAE. Upon a second run, it became clear that IL-12 was not in fact changed (**Figure 5.0B**). Let this be a lesson that sometimes it is okay to get ahead of yourself.

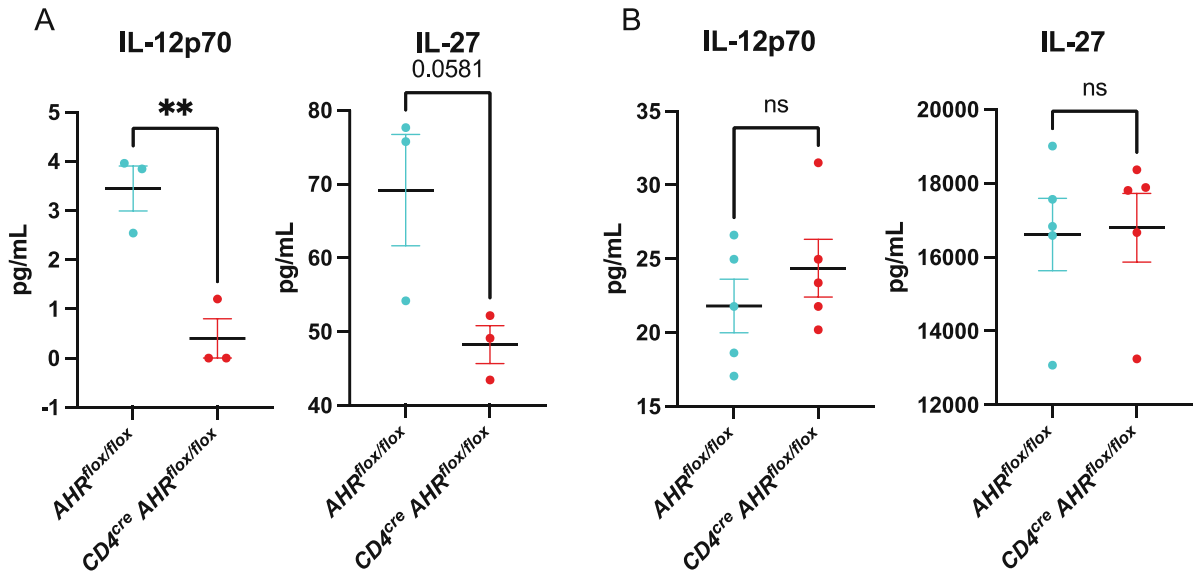

Figure 5.0: Scientists get ahead of themselves occasionally. (**A**) Luminex analysis on spinal cord homogenate from EAE mice at day 16 post immunization. *CD4^{cre}AHR$^{flox/flox}$* mice tend to recover from EAE by day 30 post immunization (n=3 mice/group; N=1 experimental replicate; Student's T Test). (**B**) A repeat of the experiment in (A) (n=5mice/group; N=1 experimental replicate; Student's T Test).

5.1 Introduction

Relapsing remitting multiple sclerosis (MS) is the most common neurodegenenerative disorder affecting young people. Onset is generally between 25-50 years of age and is characterized by periods of autoimmune mediated damage to the central nervous system (CNS). Myelin is the primary target of the autoimmune attack on the CNS therefore leaving axons vulnerable to permanent damage. After the autoimmune events, there is a period of remission which is characterized by partial recovery of motor and cognitive function, but it is unclear the degree to which remyelination occurs. Disease

modifying therapy currently targets quieting the autoimmune response, and pharmaceutical aids for remyelination remain elusive.

Research around remylination is two pronged. The first approach is supported by reports that damaged adult oligodendrocytes survive myelin breakdown and can maintain original myelin structure[339]. Therapies can target promoting remyelination in existing oligodendrocytes that may or may not be damaged or senescent. The second approach promotes the maturation and differentiation of oligodendrocyte progenitor cells (OPCs) into new myelin forming oligodendrocytes[340]. Effective remyelination therapies will likely take advantage of both approaches by harnessing intrinsic signaling in oligolineage cells.

Oligolineage cells, especially OPCs have recently been characterized as having immune properties, including phagocytosis and antigen presentation, so it follows that these cells may utilize classical immune signaling cascades[341–343]. Here, we propose that oligolineage cells may use Interleukin 12 (IL-12) signals to establish maturation and myelin formation programming. In the brain, Il-12 is produced by microglia and is regulated by astrocytes[344]. Receptors for IL-12 family cytokines have been documented in neurons of the central (CNS) and peripheral nervous systems and in neuroectoderm cells of the CNS[345–347]. The IL-12 family cytokines are primarily produced by macrophages, neutrophils, and dendritic cells at the site of tissue damage or pathogen infiltration. The primary target of IL-12 is T cells which in turn differentiate, have enhanced cytotoxicity, and produce other cytokines. In addition to immune cell signaling, IL-12 is also known to have anti-angiogenic activity[348].

IL-12 family cytokines are a family of hetero- and homo-dimeric proteins. They include IL-23, IL-27 and IL-35- each having a unique dimeric receptor. The receptors activate the JAK-STAT cascade in T cells promoting immune responses. Other functions, including the anti-angiogenic activity, have been found to operate through alternative signaling cascades[348]. Here, we suggest that oligolineage cells are sensitive to IL-12 family cytokines during development.

5.2 Results

IL-12 related response genes correlate with myelin formation in development and disease.

Myelin formation is a life-long process. It begins with the formation of OPCs from 6-9 weeks of age which occurs in three waves[349,350]. These cells undergo differentiation which starts between 15-19 gestational weeks. Finally, mature myelin formation begins at 20-25 gestational weeks[351]. Myelin formation continues to develop quickly in a brain region-specific manner, starting with the motor cortex with the majority of myelin formation occurring within the first year of life, after which formation appears to slow [352]. Myelin continues to form throughout life in response to life experience, learning, and development[353,354]. Strikingly, bulk RNA sequencing data produced by Miller and colleagues shows that IL-12 family receptors are upregulated during the prime myelin formation period from 21 weeks of gestation to 10 months of age[355] (**Figure 5.1A**). *Il12rb2* and *Il27r* are especially temporally tied to mature myelin formation. Conversely, in brain tissue throughout development, there are very low or undetectable transcript levels of *Il12rb1, Il23r, Il12a* and *Il12b*. To investigate further, we next data mined a single nucleus sequencing data set collected by Jäkel and colleagues containing white matter samples from healthy controls, as well as several demyelinating regions in patients diagnosed with multiple sclerosis[356]. We first clustered the cells according to establish cell types by signature transcripts (**Figure 5.1B**). Next, we separated the groups based on tissue phenotype and examined several downstream IL-12 receptor response elements. Transcripts for *Ifngr1, ifngr2, and Socs3* were all increased in active lesion sites and chronic active lesion sites in oligodendrocytes and OPCs (**Figure 5.1C-E**). Surprisingly, there was no difference in the number of cells expressing these transcripts, rather there was increased expression in each individual cell. Overall, these data indicate that there is likely IL-12 or Type 1 immune signaling occurring in oligodendrocytes and OPCs in lesion sites of multiple sclerosis patients, leading to increased transcription of inflammatory response elements.

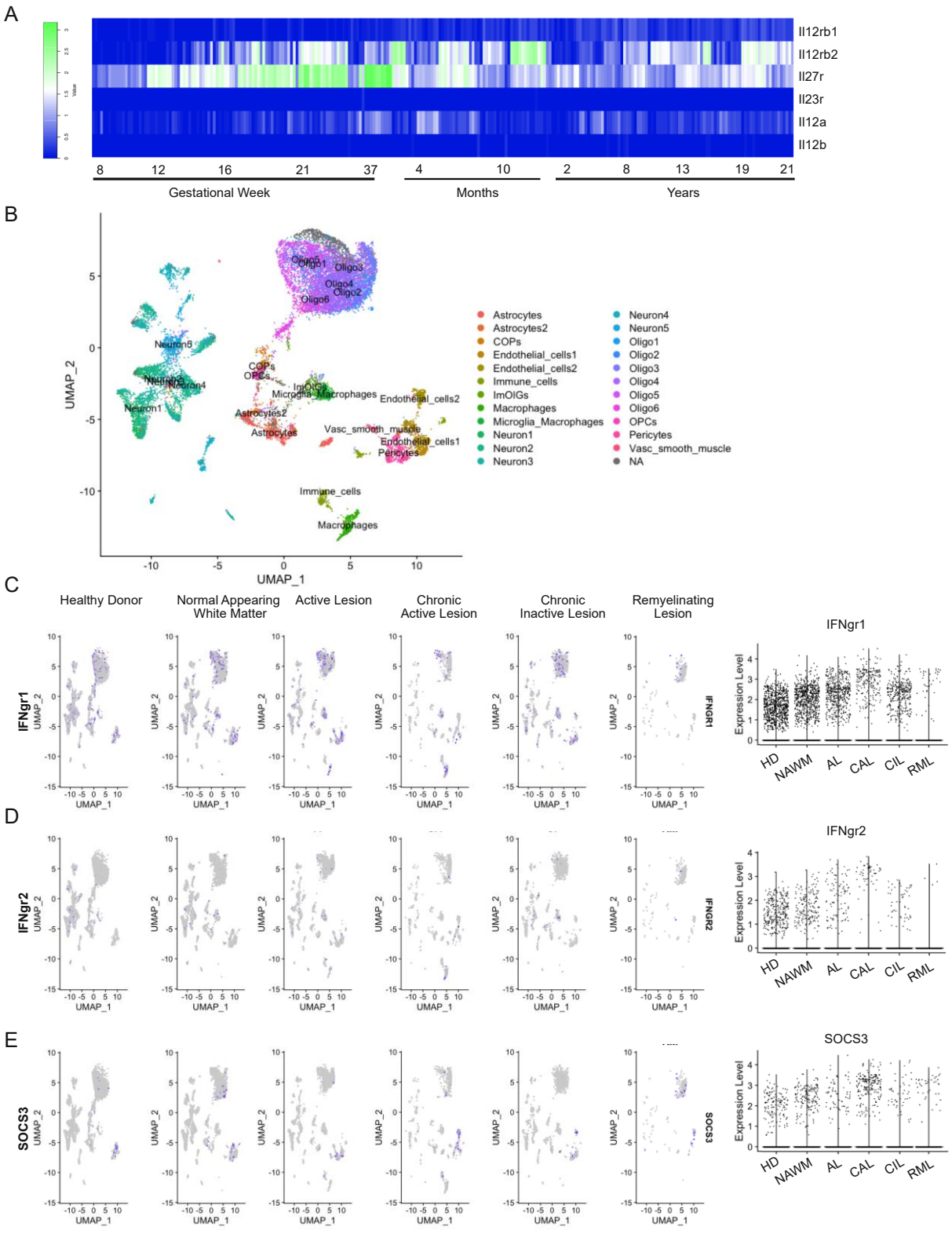
A
Il12rb1
Il12rb2
Il27r
Il23r
Il12a
Il12b
8
12
16
21
37
4
10
2
8
13
19
21
Gestational Week
Months
Years
B
UMAP_1
UMAP_2
Astrocytes
Astrocytes2
COPs
Endothelial_cells1
Endothelial_cells2
Immune_cells
ImOlGs
Macrophages
Microglia_Macrophages
Neuron1
Neuron2
Neuron3
Neuron4
Neuron5
Oligo1
Oligo2
Oligo3
Oligo4
Oligo5
Oligo6
OPCs
Pericytes
Vasc_smooth_muscle
NA
C
Healthy Donor
Normal Appearing White Matter
Active Lesion
Chronic Active Lesion
Chronic Inactive Lesion
Remyelinating Lesion
IFNgr1
IFNGR1
Expression Level
HD
NAWM
AL
CAL
CIL
RML
D
IFNgr2
IFNGR2
E
SOCS3

Figure 5.1: IL-12 receptor expression correlates with myelin development. (**A**) Publicly available bulk RNAseq was obtained from the Allen Developing Human Brain Atlas[355]. Gene levels for IL-12 family signaling molecules were mapped from 8 gestational weeks through 21 years of age. (**B**) Publicly available single nucleus RNAseq data was obtained from Jäkel and colleagues[356]. We validated and replotted the cell type clustering performed by the authors, and then extracted the expression levels of the following genes of interest: (**C**) *Ifngr1,* (**D**) *Ifngr2,* and (**E**)*Socs3.* Overall, samples from nine patients were used, with multiple sclerosis patients contributing tissue to several groups depending on lesion types.

Aberrant IL-12 signaling leads to impaired OPC differentiation in vitro.

Sequencing data in patients indicates a role for IL-12 signaling both during development and in pathological demyelination. To further probe the mechanism of IL-12 signaling, we moved to an in vitro system by culturing primary mouse OPCs. We generated undifferentiated OPCs from neurospheres derived from cortical neural stem cells. We then cultured the OPCs in the presence of maturation inducing growth factors FGF, CNTF, and T3, as well as different subunits of IL-12 family cytokines. Transcript numbers for markers of mature oligodendrocytes *Myrf* and *Mbp* were lower when OPCs were differentiated in the presence of p80 cytokine (**Figure 5.2A-B**). The p80 dimer is the eponymous cytokine of the IL-12 family. Because we saw decreased differentiation in response to IL-12 and IL12Rβ2 that seems to correlate with myelin formation in patients, we obtained constitutive IL12Rβ2$^{-/-}$ mice. The CNS of these mice have previously been characterized by single cell RNAseq in the context of a mouse model of Alzheimer's disease[357]. In the knockout animals, deficiencies were found in myelin programming, so we hoped to observe the same through experimental manipulation. We validated that OPC and oligodendrocyte in vitro cultures of C57Bl/6J mice do have transcripts for *Il12rb2,* which are lacking in both cell types of 12Rβ2$^{-/-}$ mice (**Figure 5.2C**). In vitro cultures from IL12Rβ2$^{-/-}$ mice failed to differentiate (**Figure 5.2D-E**). Together these data indicate that both excess and lack of signaling through IL12Rβ2 disrupts OPC maturation into myelinating oligodendrocytes.

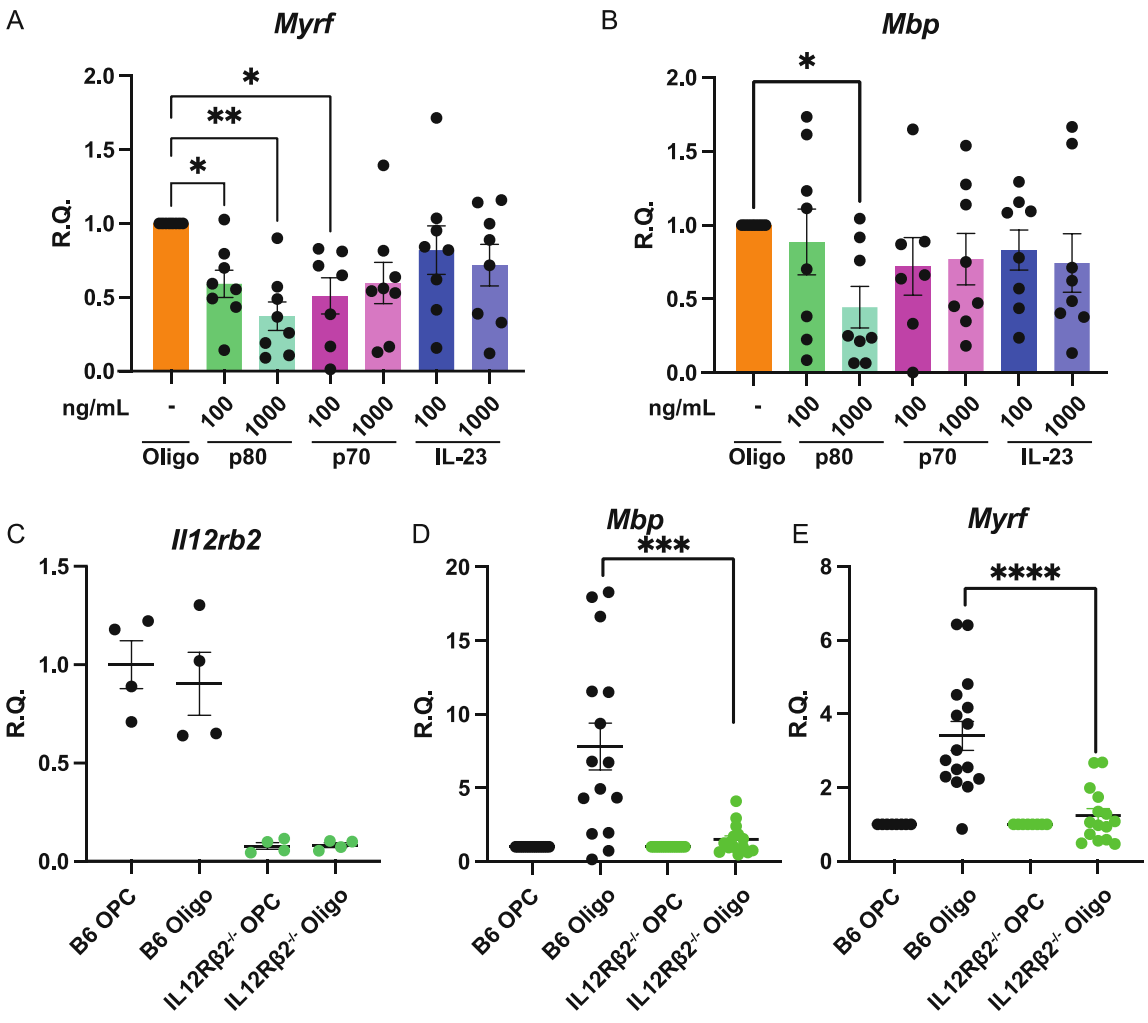

Figure 5.2: OPC differentiation depends on IL-12 signaling. Primary OPC cultures were plated in differentiation media containing growth factors FGF, CNTF, and T4. Cells were incubated along with cytokine for 72 hours and then collected for qPCR. (**A**) *Myrf*, a transcription factor regulating myelin formation, and (**B**) *Mbp,* an integral myelin protein only found in mature oligodendrocytes, were measured. (n=7-8 biological replicated/group; N= 2 experimental replicates; One-way ANOVA). (**C**) C57Bl/6J or IL12Rβ2$^{-/-}$ undifferentiated OPCs and differentiated oligodendrocytes from primary culture were collected, and transcripts of *Il12rb2* (n=4/group; N=1 experimental replicate) (**D**) *Mbp* and (**E**) *Myrf* (n=15-16/group; N=2 experimental replicates) were analyzed by qPCR.

12Rβ2$^{-/-}$ female mice have disrupted myelin formation.

We next aimed to characterize the oligolineage cells of IL12Rβ2$^{-/-}$ mice by using immunofluorescent staining for markers of mature oliogodendrocytes (Olig2+, O4+) and OPCs (PDGFRα+, O4+). The mature oligodendrocytes from IL12Rβ2$^{-/-}$ mice appear to have disrupted morphology in comparison to the C57Bl/6J controls. Especially in female mice, Olig2+ cells do not seem to follow the axonal tracts in the corpus collosum; rather, they have a much more amoeboid appearance, and have less consistent coverage (**Figure 5.3A**). In contrast, the OPCs appear to be more ramified in ILRβ2 deficient mice in comparison with control mice. The OPCs also seem to elongate along the axonal tracts of the corpus collosum more than those of the C57Bl/6J controls (**Figure 5.3A**). Again, this phenotype appears to be stronger in female mice than in male mice (**Figure 5.3B**). Visualization of myelin basic protein (MBP) does not show disruptions in myelin coverage in either male or female mice (**Figure 5.3C-D**). Upon quantification of these attributes, we find more OPCs in the corpus collosom of 12Rβ2$^{-/-}$ female mice than controls, but no differences in male mice or in the number of mature oligodendrocytes (**Figure 5.4A**). In the cortex, IL12Rβ2$^{-/-}$ female mice have higher numbers of both OPCs and oligodendrocytes compared to C57Bl/6J mice while there are no differences noted in male mice (**Figure 5.4B**). Together, these data suggest both morphological and proliferative changes in the absence of IL12Rβ2 signaling that may be sex dependent.

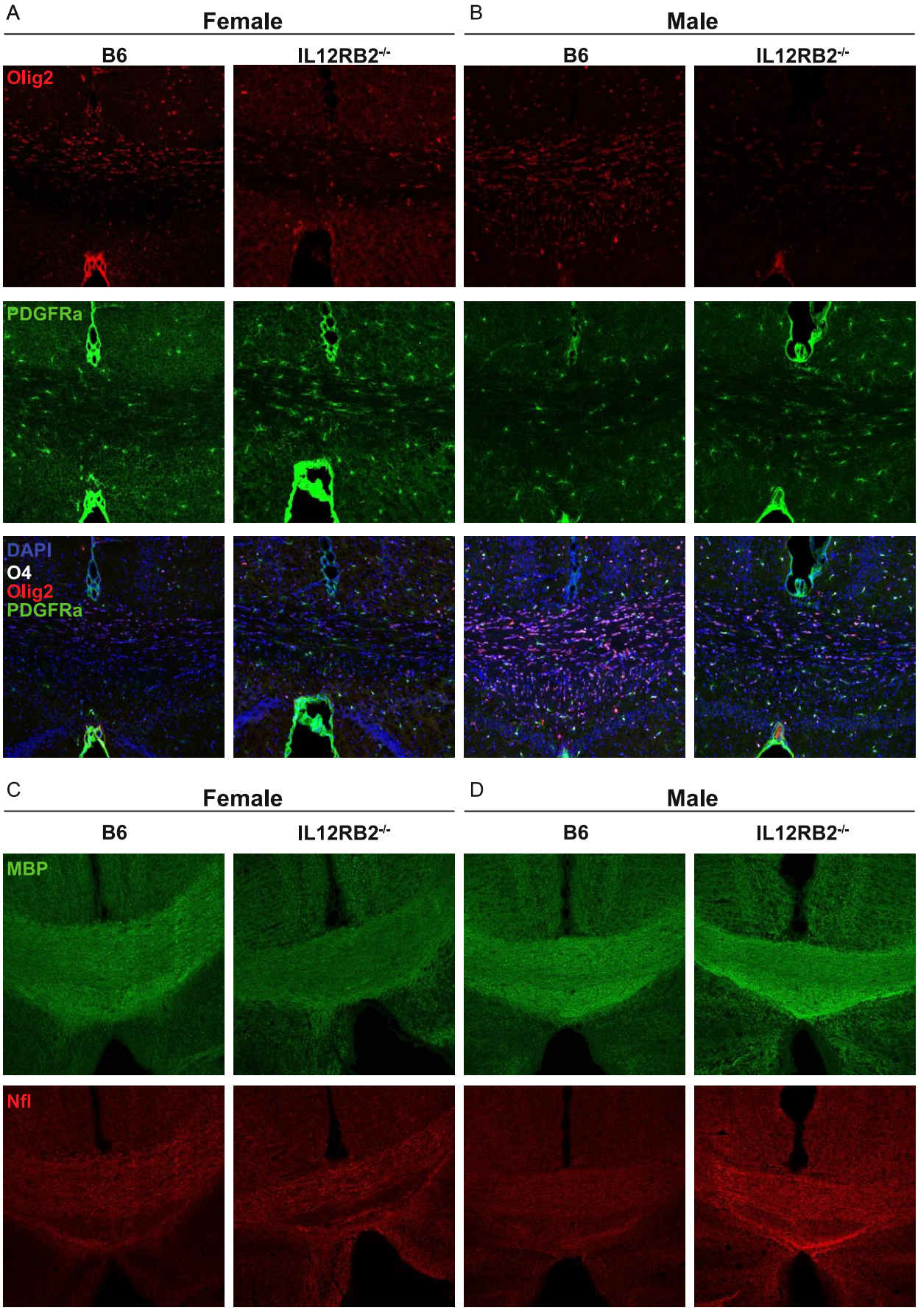
A
Female
B
Male
B6
IL12RB2-/-
B6
IL12RB2-/-
Olig2
PDGFRa
DAPI
O4
Olig2
PDGFRa
C
Female
D
Male
B6
IL12RB2-/-
B6
IL12RB2-/-
MBP
Nfl

Figure 5.3: Morphological differences in OPCs and oligodendrocytes of female 12Rβ2$^{-/-}$ mice. Representative images of the corpus collosum from 10-15 week old (**A**) female and (**B**) male mice were stained with oligodendrocyte markers Olig2 and O4 and OPC markers PDGFRα and O4. Representative images from 10-15 week old (**A**) female and (**B**) male mice were stained with MBP and neurofilament.

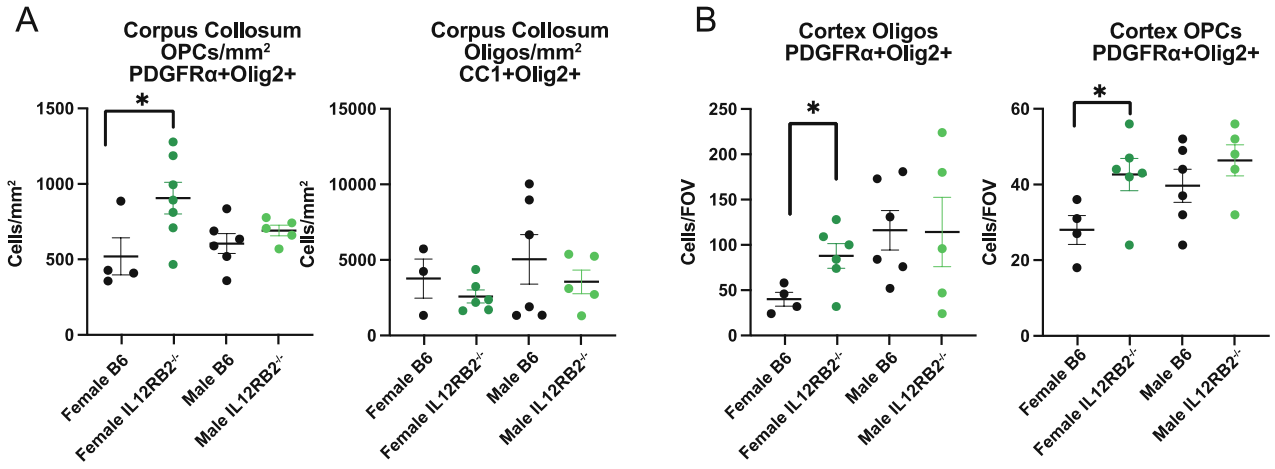

Figure 5.4: Female 12Rβ2$^{-/-}$ mice have more OPCs and oligodendrocytes than wildtype controls. (**A**) Quantification of the images from Figure 3A-B. (**B**) Quantification of oligodendrocyte and OPC numbers in the cortex of male and female 12Rβ2$^{-/-}$ and control mice. (n=3-6 mice/group; N=2 experimental replicates; Two-way ANOVA)

Female 12Rβ2$^{-/-}$ mice do not demyelinate in response to cuprizone.

Unlike many models of demyelination, cuprizone-mediated demyelination can occur independently from the immune system. As we are manipulating a primary immune signal, this was an ideal model. IL12Rβ2$^{-/-}$ and control mice were fed cuprizone chow for five weeks to initiate demyelination, after which the mice were returned to normal chow for four days to allow for partial remyelination. In male mice, the percent of MBP coverage in the corpus collosum of both control and IL12Rβ2$^{-/-}$ mice decreased as expected after demyelination. Both groups recovered MBP coverage over the next four days with no differences between genotypes (**Figure 5.5A**). Female mice, however,

differed in presentation. Control mice responded to demyelination and recovery like the male mice, but MBP expression in IL12Rβ2$^{-/-}$ female mice never changed (**Figure 5.5B**). MBP staining in the corpus collosum seemed stable across the time course, indicating that the combination the female brain and suppressing signaling through IL12Rβ2 creates resistance to cuprizone-mediated demyelination. These data were further supported by measurement of the thickness of the corpus collosum, as male mice experience increased thickness in the corpus collosum with demyelination that began to return to baseline levels after four days (**Figure 5.5C**). Female control mice experienced the same corpus collosum thickening, but the IL12Rβ2$^{-/-}$ remained thin (**Figure 5.5D**). Cuprizone-mediated demyelination was thought to occur by copper chelation, however recent work has put this in doubt[358]. Currently, the mechanism of white matter destruction is currently unknown.

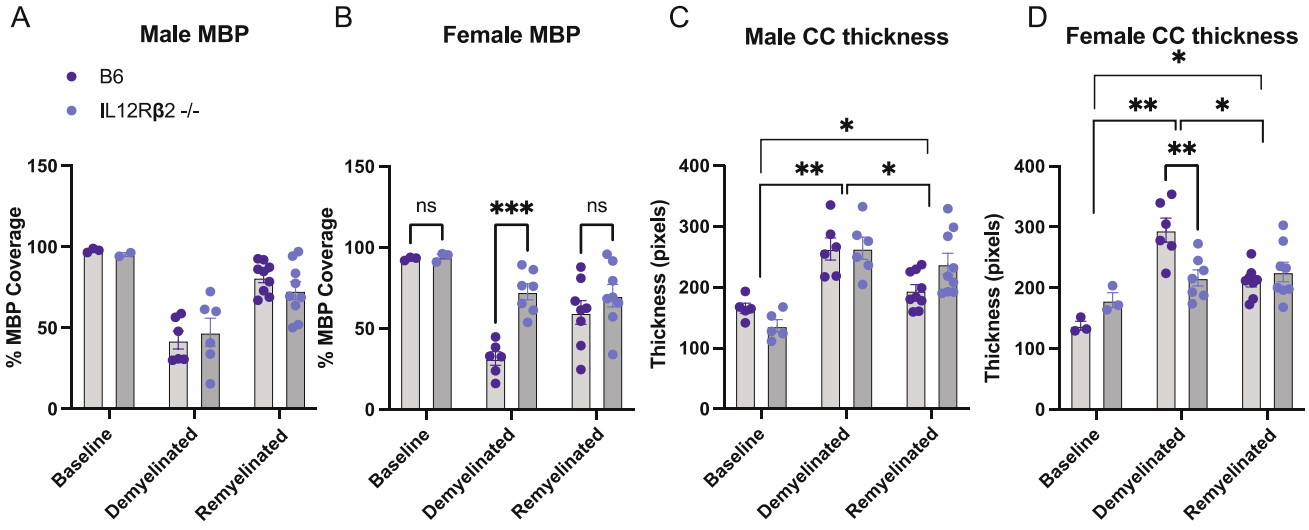

Figure 5.5: IL12Rβ2 knockout protects female mice from cuprizone-mediated demyelination. Mice were given mouse chow with 0.3% cuprizone by weight for five weeks. They were returned to normal mouse chow for four days. Four sections 300µm apart from across the corpus collosum were stained for MBP. Quantification of MBP coverage of the corpus collosum was completed using unbiased thresholding by a blinded scorer, and values were averaged across the four sections. Each dot represents a mouse. Quantification of MBP for (**A**) male (male mice n=5-9mice/group; N=2 experimental replicates) and (**B**) female mice was performed at baseline, at 5 weeks of demyelination, and after four days of remyelination

(female mice n= 3-8 mice/group; N=2 experimental replicates). The thickness of the corpus collosum was measured at the midline across four sections, 300µm apart. The thickness was averaged across images in (**C**)males and (**D**) females.

5.3 Discussion

Homeostatic cytokine signaling in brain resident cells is not a novel concept, but researchers continue to describe new roles for these molecules. Here we show that appropriate IL-12 signaling to IL-12Rβ2 on oligolineage cells is necessary to promote normal myelination. Additionally, we show that overstimulation with the p40 subunit of IL-12 can also have detrimental effects on OPC differentiation. Constitutive knockout of IL-12Rβ2 leads to disruptions in myelin and oligolineage morphogenesis, especially in female mice. Lastly, we have found a synergistic protective effect of blocking IL-12 signal transduction in the female brain. In summary, these data suggest that appropriate IL-12 signaling in oligolineage cells is necessary for proper development.

No sex differences in demyelination due to cuprizone have been reported in C57BL/6J mice. Estrogen receptor knockout does not have an impact on demyelination[359]. However, evidence of potential sex-specific effects of cuprizone demyelination include the disruption of the estrus cycle in mice and increased neurotoxicity in male rats [359,360]. Furthermore, female SJL mice are less sensitive to cuprizone demyelination and 17β-estadiol is protective in this strain[361]. We hypothesize that in C57Bl/6J mice, there may be mild sex differences that are only revealed with the additional disruption of IL-12 receptors.

Differential immune responses between sexes have been fairly well characterized[362]. The first report of IL-12 hyper-sensitivity in females, was by Mon and colleagues in 2019 and has since been corroborated in models of Alzheimer's disease[363,364]. Our current lack of understanding of the sex differences in immune communication is a roadblock for finding effective treatments across a wide variety of diseases and disorders. Specifically, research into sex differences in multiple sclerosis, which primarily affects females, is necessary to fully understand the etiology of this disorder.

Anti-IL-12/27/23 neutralizing antibodies have been proposed for use in the clinic in MS, but these studies have largely been unsuccessful[365,366]. Many have posed that the therapy is occurring too late to interfere with the early immune events that often present before diagnosis[367]. These therapies may be better suited to immunomodulation in the early stages of autoimmunity, but perhaps the

route of administration should be reconsidered. These neutralizing antibodies are not able to cross the blood brain barrier in any appreciable sense, so administration directly to the CSF may increase the chances of modulating the pro-myelinating effect.

Overall, further translational testing is needed, and IL-12 modulation should next be tested in various models of myelin disorders. These myelin disorders can include demyelinating degenerative disorders like multiple sclerosis, optic neuritis, and Alzheimer's disease or abnormal myelin development like leukodystrophy and Alexander's disease. Better understandings of the mechanisms of basic physiology and development will give insight to novel therapeutic approaches.

Chapter 6:

Discussion and Open Questions

A scientist sits at her desk, exhausted and drained,
Her eyes heavy with fatigue, her mind nearly strained,
She's spent years researching the gut and the brain,
In the hopes of therapies soon to be gained.

There were days when it seemed impossible,
The data was murky and the theories implausible,
But with the help of her team, and the support of her friends,
She was able to push through and now comprehends.

They encouraged her through each and every trial,
Helped her to see that her work was worthwhile.
When she was tired, they picked her up,
And when she was stuck, they helped her to unstuck.

Now the scientist sits at her desk, and looks back,
At the years of hard work and dedication, with a sense of pride and gratitude,
For she knows that she could not have done it alone,
Her success is her mentors', her team's, all sharing her goals.

She takes a deep breath, and reflects on the journey,
Filled with ups and downs, moments of glory and moments of uncertainty,
But with her work now complete, she feels content,
For her contribution to science, is what she is meant.

As she closes her eyes and rests her weary head,
She knows that the future holds many more questions unsaid,
But for now, she will rest and be proud,
As there is as much science to be done as time allows.

-Andrea Merchak and ChatGPT

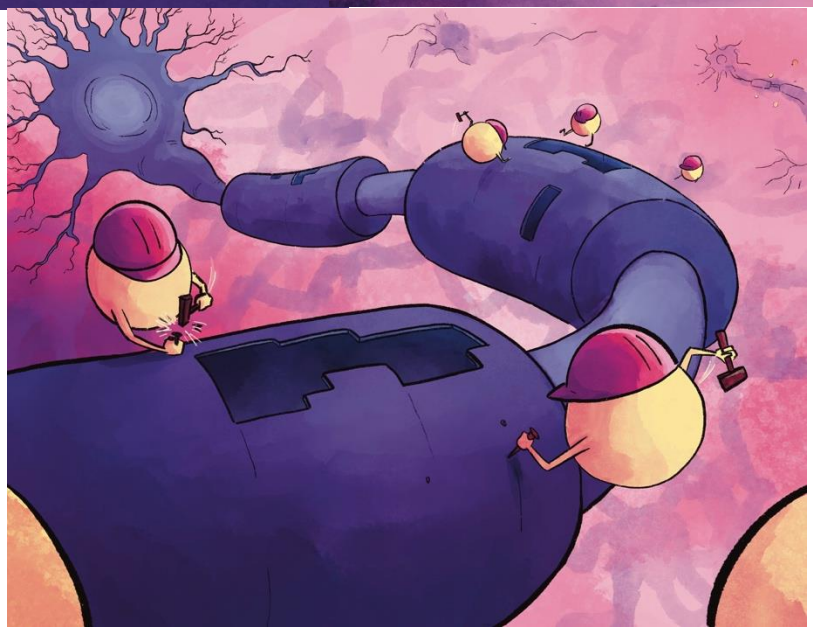

The microbiome changes in response to neurological and psychological disorders. This idea is well established and broadly accepted in the scientific community. A consensus has yet to be made about whether the microbiome will be an effective point of intervention to treat these disorders. Throughout this thesis work, I seek to demonstrate that not only does the microbiome influence both behavior and immune regulation, but that it may also be an effective point of therapeutic intervention.

I first aimed to understand the mechanism by which *Lactobacillus* can interrupt the cycle of environmental stress leading to mood and behavioral disruption. I hypothesized that it operated through bacterial-derived small molecules activating the aryl hydrocarbon receptor in T cells. I established that this signaling modality was not necessary for the development of behavioral disruptions. Our team next hypothesized that Th17 cells may be an immune trigger necessary to facilitate the cycle of stress to behavioral disruption. This hypothesis was based on data collected over the past ten years by our group and others. We established that Th17 cells are not in fact necessary for the development of stress-induced depression. With these two hypotheses struck down by the negative data collected, we next utilized a novel tool to use a more exploratory approach.

To better explain how *Lactobacillus* influences stress responses, I created gnotobiotic mice lacking *Lactobacillus*. This tool allowed us to experimentally manipulate developmental microbiome-immune interactions. I confirmed that *Lactobacillus* does lead to behavioral resilience to environmental stressors. I also isolated that Type 1 immunity that was being modulated in the lamina propria of the intestines. This change in Type 1 immunity led to systemic effects that mirrored the decreased IFNγ concentrations in germ-free mice that had been colonized by the microbiome from stressed mice. In all, I was able to eliminate two of the leading hypotheses in the field about the immunogenic theory of mood disorders. I was also able to develop a novel tool which will facilitate future microbiome research.

For the second portion of my thesis work, I applied built upon the AHR work presented earlier to study the interplay between the gut and the immune system in the autoimmune disorder multiple sclerosis. AHR activation has been well characterized as an immune modulator in various cell types including T cells, dendritic cells, astrocytes, and microglia. My work explored beyond the direct effects on the immune system and found that AHR activation in T cells regulates the gut microenvironment. I found that this gut microenvironment is pro-inflammatory and disruption can lead to recovery from

paralysis in the mouse model, EAE. I identified the lack of bile acid reabsorption and degradation by bacteria as key to establishing this phenotype though the gut microenvironment's effects on host physiology are likely occurring through several routes. Furthermore, oral treatment with bile acids was sufficient to promote recovery. I am in the process of translating these findings into a clinical setting and believe that it will be a promising new avenue for disease modifying intervention.

Finally, I stumbled across a surprising finding that in the spinal cords of mice that recovered from EAE, cytokine IL-12 was reduced. Rarely has IL-12 been characterized as having an endogenous role in the tissue of the central nervous system. Preliminary work has shown that IL-12 signaling is important for the development of normal morphology of myelin and is necessary for the differentiation and maturation of oligodendrocyte progenitor cells. Much of our data also supports a sex-specific effect in which female mice respond to IL-12 signaling more strongly than male mice. This supports research showing that estrogen signaling and IL-12 signaling can act synergistically. One of the most surprising findings from this work is that cuprizone-mediated demyelination be completely ameliorated without IL-12 signaling in females only. Our data may help to shed light on the mechanism cuprizone demyelination. These data together suggest a novel signaling cascade that is important for myelin and oligolineage health and development, one that will be applicable to a range of demyelinating diseases from multiple sclerosis to Alzheimer's disease.

6.1 Next Steps:

The next steps for these projects are diverse as my thesis has spanned several disciplines. Here I will discuss some future avenues for research, however, these avenues are by no means the only possible paths of discovery.

Starting with work on mood disorders and the microbiome, some mechanistic questions remain. First, there remains a gap in knowledge about how *Lactobacillus* is communicating with the immune system. While I have eliminated direct activation of T cells, there may be direct signaling in the brain or indirect activation via antigen presentation. These questions will be likely straightforward to elucidate in the near future. The mechanism by which IFNγ impacts behavior will be more difficult to discern. There are several groups currently working on this question; the answers down the line potentially could be avenues for new therapies.

In the course of working with ASF mice, I made a surprising discovery that deserves some additional investigation. I found that mice that were given ASF(-L) microbiomes in adulthood rather than during development had behavioral phenotypes opposite than expected. These mice were more resistant to stress than germ-free mice colonized with ASF(+L). The data indicated that there are likely different mechanisms influencing psychological resilience via immune education in early in life and adulthood. Additionally, the differences between early life and adult colonization are important to consider when developing therapies for mood disorders which primarily affect people in adolescence and adulthood. Because these data are also in conflict with probiotic supplement data in SPF mice, I am inclined to believe that this result is an artifact of working with germ-free animals, but it will still be important for investigation.

Beyond investigating these direct next steps, I would also be interested in discovering how current treatment options for mood disorders operate in conjunction with probiotic supplementation. Some promising work has been completed in the clinical setting, but we are still short of understanding which part of *Lactobacillus* colonization is integral to treating mood disorders. Later, we could utilize work from other groups with genetically engineered bugs to increase the output of biologically important metabolites or simply isolate the molecules that drive recovery and deliver them as a pharmaceutical product. Overall, my work reinforces the need for understanding the interconnections between the brain, the body, and the environment in regulating mood.

Multiple sclerosis a highly debilitating disease and patients are desperate for new therapies. We, as researchers, have a responsibility to both embody hope while also managing expectations. This has been one of the hardest aspects of completing my thesis work as I started to interface with hopeful patients. I am proud to say that we are currently taking steps to give patients access to bile acid sequestrants in the clinic. These are a class of drugs that are currently approved by the FDA and are mostly used to manage cholesterol. The side effects are usually limited to problems with digestion. I hope that in conjunction with the clinical teams at UVA and a few other sites, we will be able to pair these drugs with current standard care to aid patients with multiple sclerosis.

On a more mechanistic level, cytokine signaling in homeostatic brain function is a current area of interest for cellular biologists of the brain. A coworker in my own lab is examining IL-6 signaling in myelin formation. This area has been understudied for decades as scientists have segregated based

on body systems. Because neuroscientists and immunologists have now become one entity in some respects, I am hopeful that we will have a deeper understanding of brain function in health and disease. My work on IL-12 thus far has been very descriptive and mechanistic, with little translational value. The next steps will be to disentangle the role of IL-12 family signaling in the periphery verses the central nervous system in demyelinating diseases. This is likely to be difficult in models of multiple sclerosis, as the disease is a primarily immune event, but with cell specific genetic modification, I believe this avenue of research will be important to pursue. Additionally, the demyelination that occurs prior to cognitive impairment in several forms of dementia has been overlooked to some extent. It would be very informative to probe this early biological process to discover, perhaps, modalities for early interventions.

6.2 Beyond:

Following is a summary of topics that I believe are going to be critical for moving the study of the gut-microbiome forward. Several groups have already begun this work and as these methods are validated and used across more diverse samples, we as researchers will have novel tools to move science forward.

Mapping the Metabolic output of Microbial Communities

The metabolic web of a healthy microbiome has not been fully mapped, but efforts using computer modeling are getting closer to understanding what small molecules are being produced in the gut and how they are being used within it. The availability of the small molecules not only depends on how much is being produced but also how much is being utilized by bacteria in the same environmental niche[368]. The bacteria have a codependent metabolic pattern in which metabolites produced by some are used by others.

The challenges facing researchers aiming to understand the metabolic interactions of microorganisms and the host require collaboration between several fields ranging from microbiology to endocrinology. The complexity of the microbe-host crosstalk requires that researchers continue to develop new methods of mapping and experimenting. While experimental work has focused on the neuroactivity of select metabolites, hundreds of unique molecules are crossing our gut walls every day[369]. Historically, we have looked outside of our bodies to things ranging from fungi, to plants, to

pig pancreases to find ways to treat disease. It is essential, however, to continue to identify molecules within our own bodies that could be modulating our health. This will give us a better understanding for therapeutics and novel medications that will supplement the production of our microbiota.

Understanding how population-level changes influence the immune system

In addition, emphasis should be placed on understanding how bacterial metabolites work in concert with host sensing. Some integral receptors, like AHR, have such a diverse range of specificity and nuanced effects, that in order to understand homeostatic immune states, we must examine how many of these small molecules compete and interact, mediating AHR function.

While there may be bioactive effects that mediate the gut-immune system, there is also a high probability that bacterial metabolites are able to cross the blood-brain barrier and may, as in the case of SCFAs, directly influence the cells in the brain. A starting point of this complex work is to determine the biological effects of the metabolites and small molecules released by a single commensal microbe in health and disease.

Understanding the Heterogeneity of Disease

Finally, segregation of the different etiologies of major depressive disorder and multiple sclerosis is critical to the fields of immunology, neuroscience, and psychology. Both are heterogenous diseases with significantly diverse presentations between patients. Historically, doctors have separated patients based on surrounding life events and presentations. This may not, however, reflect the physiological etiologies of the disorders. Meta-analysis of immunophenotyping data of patients with similar symptoms may allow for better physiological characterization of these complex disorders.

These important open questions will require significant scientific inquiry over a number of years. Personally, I aim to expand my knowledge of the immune-gut-microbiome interactions in other disorders. I believe that being well versed in both animal models and clinical presentations of diverse neurological and psychological disorders will enable me to approach research of these areas more creatively. Integrating our understanding of physiology across biological systems is ultimately the next frontier in biomedical sciences.

Chapter 7:

Materials and Methods

All methods were performed in accordance with guidelines and regulations of the University of Virginia and approved by the University of Virginia Animal Care and Use Committee.

7.1 Chapter 2 Methods

Mice: B6.Cg-Tg(Cd4-cre)1Cwi/BfluJ (CD4Cre)[370] (#022071), B6(Cg)-*Rorc*^{tm3Litt}/J (Roryt^{fl})[231] (#008771), and *AHR*$^{tm3.1Bra}$/J (Ahr^{fx}) (#006203)[371] mice were purchased from Jackson Laboratories. Mice were bred in-house. Mice were kept on a 12-h light/dark schedule. All behavioral interventions were performed between 8 am and 3 pm and animals were sacrificed between 7 am and 1 pm. All mice were housed in cages of up to 5 animals from birth until initiation of the stress protocol. All mice exposed to stress were at least 8 weeks of age and age matched to control animals. Stressed mice were housed individually without enrichment to enhance stress[372]. Naïve animals were housed in standard cages in groups of 2–5 mice of the same sex. All procedures were approved by the University of Virginia ACUC (protocol #3918). All experiments were conducted and reported according to ARRIVE guidelines (https://arriveguidelines.org/arrive-guidelines).

Experimental autoimmune encephalomyelitis: EAE was induced in 6–8-week old female *Cd4 Cre Ahr*$^{F/F}$ and *Ahr*$^{F/F}$ mice as previously described[373]. Briefly, mice were subcutaneously injected with MOG 35-55 and Complete Freund's Adjuvant. Two intraperitoneal injections of pertussis toxin were administered on days 0 and 1. Thirty-minute videos of mice were taken at day 25 post immunization and used for analysis. Healthy controls were age-matched females.

Stress experiments: In our model of Unpredictable Chronic Stress (UCS), mice were exposed to a 2 h period of a daily stressor (restraint, strobe light, or white noise). After the daily stressor, mice were placed in an overnight stress (cage tilt, 24 h light exposure, wet bedding, or 2 × cage change) until the next induction of 2 h stress (Supplemental Table 2.2). UCS protocols were maintained for 3 weeks.

For Unpredictable Chronic Restraint Stress (UCRS) experiments, mice were exposed to chronic restraint (ventilated 50 mL conical vials) for a period of 2 h daily for a period of three weeks. Once removed from restraint, an overnight stressor of either cage tilt, wet bedding, or 2 × cage change was used (Supplemental Table 2.2). All daily stressors were carried out between 8 am and 5 pm. Overnight stressors were started upon removal from the daily stressor and remained in place until the next day's daily stressor.

Behavioral tests: The forced swim, tail suspension, sucrose preference, open field, elevated plus maze, novel object recognition, marble burying, and three chamber social preference tests were performed as previously described. All testing was recorded on a Hero Session 5 GoPro and analyzed with Noldus behavioral analysis software.

DeepLabCut

Animal pose estimation: Animal pose estimation was performed by using a deep-learning package, DeepLabCut[245] (https://github.com/DeepLabCut/DeepLabCut). We generated a DeepLabCut convolutional neural network to analyze open field test videos, which is trained in a supervised manner: 16 manually labeled points were selected as references of transfer learning. 15 randomly selected videos were used for building a training dataset. Finally, the performance of the neural network is evaluated by researchers.

Unsupervised behavior classification: Estimated mouse poses from DeepLabCut were further analyzed by Variational Animal Motion Embedding (VAME)[374], which classifies animal behavior in an unsupervised manner (https://github.com/LINCellularNeuroscience/VAME). We trained a unique VAME recursive neural network for each experiment, which classifies each frame of the open field test video into 1 of the 35 behavioral motifs. Then, all behavior motifs were annotated and evaluated by blinded researchers. With annotated frames, we were able to calculate the percentage of time usage of each motif, which is then used for principal component analysis and Kullback–Leibler divergence analysis.

RNA extraction and quantitative PCR: For RNA extraction, cultured cells were pelleted, frozen, and lysed. RNA was extracted using the Bioline Isolate II RNA mini kit as per manufacture's protocol

(BIO-52073). RNA was quantified with a Biotek Epoch Microplate Spectrophotometer. Normalized RNA was reverse transcribed to cDNA with either the Bioline SensiFast cDNA Synthesis Kit (BIO-65054) or Applied Sciences High-Capacity cDNA Reverse Transcriptase Kit (43-688-13). cDNA was amplified using the Bioline SensiFast NO-ROX kit (BIO-86020), according to manufacturer's instructions. The TaqMan GAPDH probe (Mm99999915_g1) was used as a housekeeping gene for each sample. The TaqMan probes Cyp1a1 (Mm00487218_m1), Ahr (Mm00478932_m1), Rorc (Mm01261019_g1), and Il17a (Mm00439618_m1) were used to measure transcript levels from the samples. Results were analyzed with the relative quantity (ΔΔCq) method.

CD4 T cells isolation and differentiation: Naïve CD4 T cells were harvested and skewed as previously described[375]. After skewing, cells were washed and frozen for qPCR analysis or treated with an Ahr agonist (I_3S-250 µM, Sigma-Aldrich I3875), antagonist (CH223191-10 µM, Tocris Bioscience 301326-22-7), or vehicle control (DMSO-Fisher Scientific D128-1) for 24 h prior to freezing.

Tissue harvest and digestion: After experimental manipulation, mice were perfused with 0.9% saline plus 5 units/mL heparin (Medefil; MIH-3333) and tissues of interest were harvested and processed for flow cytometry as described below.

Small intestine

Whole small intestine was collected from the animals, flayed open and rinsed with ice cold HBSS -/- (Gibco, 14175-095). Tissue was cut into ~ 2 cm pieces and stored in 30 mL of 5% FBS (R&D systems, S12450H) in HBSS until processing. Small intestine was shaken at 37 °C for 20 min to remove mucus and debris. Gut pieces were filtered over mosquito net, placed in fresh 30 mL of 5% FBS in HBSS, and shaken at 37 °C for another 20 min. Samples were again filtered over mosquito net. Pieces were cut using a razor blade until fine slurry was created. Slurry was incubated in gut digestion buffer: Collagenase 8 (Sigma, C2139-5G), DNAse (Worthington, LS002139) in 5% FBS in HBSS for 40 min, shaken at 150 rpm at 37 °C. Once digested, the solution was filtered through a 70 µm filter and washed three times with 5% FBS in HBSS.

Lymph nodes and Peyer's patches

A single cell suspension in RPMI was prepared from Peyer's Patches and lymph nodes after fat removal by mechanical dissociation and subsequent filtration using sterile 70 µm filters.

Meninges

Meninges were dissected from skull caps in ice cold RPMI and digested in the digestion buffer: Collagenase 2 (Gibco, 17101-015), collagenase D (Sigma, 11088882001) and DNAse (Worthington, LS002139) for 20 min at 37 °C. Once digested, meninges were physically dissociated with a 1 mL pipette and filtered through a sterile 70 µm filter.

Flow cytometry: Single cell suspensions were incubated with CD16/32 Fc Block and then stained with a 1:200 antibody dilution (1:100 for transcription factors). For intranuclear staining, the eBioscience FoxP3/Transcription Factor Staining Kit (00-5523-00) was used per manufacturer's instructions. Antibodies used were as follows: 488-conjugated CD8 (53-008182), APCe780-conjugated TCRβ (47-5961-82), e450-conjugated CD4 (48-0042-820, PE-conjugated RORγγt (12-6981-82), and PE-Cy7-conjugated FoxP3 (25-5773-82), all purchased from Invitrogen. APC-conjugated CD45.2 (109813) was purchased from BioLegend. A Live/Dead discrimination dye Ghost Dye Violet 510 (Tonbo Biosciences; 13-0870) was used on all samples. OneComp eBeads (Thermo Fisher Scientific, 01-111-42) were used for all color controls except for the viability dye in which cells were used. Flow cytometry was performed using a Beckman Coulter Gallios flow cytometer and data were analyzed with FlowJo software v10.7.1.

Statistical analysis: All statistical analyses-except those associated with DeepLabCut-were performed in GraphPad Prism 9. Analyses involving two groups were performed using a two-tailed T test. If the variances between groups were significantly different, a Welch's correction was applied. Outliers were excluded if they fell more than two standard deviations from the mean. For all analyses, the threshold for significance was at $p < 0.05$. Repeats for each experiment are specified in the figure legend corresponding to the respective panel.

7.2 Chapter 3 Methods

Mice: C57BL/6J (#000664) were purchased from Jackson Laboratory. Germ free mice (B6NTac), ASF(+L), and ASF(-L) mice were purchased from Taconic and maintained in Flexible Film Isolators (Class Biologically Clean) with a monthly QC to confirm germ status. Microbiomes were validated by Taconic, upon arrival, and periodically in-house. Mice were sterile-transferred to Semi-Rigid Isolators (PARKBIO Inc.) for all experimental manipulations. All mice have a 12-hour light/dark schedule. All procedures were approved by the University of Virginia ACUC (protocol #1918).

Chronic Restraint Stress: For the duration of the CRS, mice were housed individually. Mice were exposed to two hours of daily restraint at a different time of day. Additionally, they were exposed to one of three random overnight stressors that included moist bedding, tilted cage, or two cage changes in a 24 hour period[17,264]. After three weeks of stress, behavioral assays were performed and fecal collection began for microbiome transfer. The CRS and fecal collection were continued for another two weeks.

Microbiome Transfer: For two weeks, dirty bedding from each group was transferred daily to the cages of female germ free C57BL/6J mice. Two weeks passed before the ex-germ-free animals were used for experiments.

Acute and Subclinical Stress: Mice were housed in sterile semirigid isolators. For the mild acute stressor, mice were removed from the isolator, placed in a biological safety cabinet, and restrained in 50mL conical vials with ventilation holes for three hours. During this time, naïve controls remained in their home cages in the semi-rigid isolator. Approximately 30 min to 1 hour after stress, the mice were euthanized and brains were collected for c-Fos staining. For the subclinical chronic stress, autoclaved 50mL conical vials with ventilation holes were passed into the semi-rigid isolators. Mice were restrained in the conical vials for two hours daily at a different time of day for seven consecutive days. On the eighth day, behavioral testing began.

c-Fos Staining: Mice were perfused with saline containing heparin (10,000U/L; Sigma; H-3125) followed by 4% paraformaldehyde. Brains were dissected and drop fixed in paraformaldehyde for 24 hours at which point they were transferred to 30% sucrose solution and mounted in cryomolds with OCT (Tissue-Tek; 4583). Cryosections (30µm thickness) were stained with rabbit anti-c-Fos (abcam; ab190289) and secondary AlexaFluor 488 tagged anti-Rabbit (Life Technologies; A21206). Sections were mounted using Prolong Gold Anti-Fade Reagent (Life Technologies, P36980) and imaged with a Leica TCS SP8 confocal microscope. Images were analyzed and c-Fos positive cells were counted by a blinded researcher using unbiased thresholding using Imaris version 9.9.1.

Behavioral Tests: Prior to all behavioral tests, animals were acclimated for 1 hour to the room in a biological safety cabinet. Animals were kept in the biological safety cabinet until testing after which they were returned to the biological safety cabinet. All tools were cleaned before testing with MinnCare Disinfectant. Between mice, tools were cleaned with 70% ethanol and between groups tools were cleaned again with MinnCare Disinfectant.

Tail Suspension: Mice were taped by the tip of a tail to a surface two feet high for six minutes. Two minutes were used for acclimation and only the last four minutes were used for analysis. Video was recorded on a Hero Session 5 GoPro and analyzed with Noldus behavioral analysis software.

Nestlet Shred: Animals were placed into newly autoclaved cages with corncob bedding and allowed to acclimate for 30 minutes. A pre-weighed nestlet was placed in the center of the cage and left for 30 minutes. The nestlet was removed from the cage and weighed again.

Elevated Plus Maze: Mice were placed in the center of an elevated plus maze and tracked using video recorded from a Hero Session 5 GoPro for ten minutes. The amount of time spent in the open arms was calculated using Noldus behavioral analysis software.

16S sequencing: 16S Sequencing was conducted at Microbiome Insights. Initial sequence data was analyzed using the latest version of Quantitative Insights Into Microbial Ecology 2 (Qiime2 v2021.11)[376]. Demultiplexed paired-end sequence reads were preprocessed using DADA2[377]. The first 20 base pairs were trimmed from forward and reverse reads before they were merged to remove adaptors. Taxonomy was assigned to Amplicon Sequence Variants (ASVs) using a Naïve Bayes classifier

trained on full length 16S sequences from the latest Greengenes16S database (13_8) clustered at 99% sequence similarity. Samples were rarified before core diversity analysis. Core diversity metrics were analyzed, including number of ASVs. Nonmetric multidimensional scaling was performed in RStudio using the phyloseq package[378].

Serum Collection and Luminex: Blood was collected by cardiac puncture and transferred to BD Microtainer SST(BD; 365967) to prepare serum per manufacturer's instructions. Samples were stored frozen at -80°C until downstream analysis. Mouse Luminex panel was run per manufacturer's instructions on a MagPix by the University of Virginia Flow Cytometry Core, RRID: DCR_0177829.

Untargeted Metabolomics: Untargeted Metabolomics was performed by Creative Proteomics. Serum was collected by cardiac puncture as described above. Samples were thawed and lyophilized, 200µL of 80% methanol was added. Samples were vortexed and then sonicated for 30 minutes at 4 ºC. Samples were kept at -20 for 1 h, vortexed for 30s and kept at 4 ºC for 15min until they were centrifuged at 12000 rpm at 4 ºC for 15 min. 100µL of the supernatant and 2.5µL of DL-o-Chlorophenylalanine were used for LC-MS analysis. Separation is performed by Ultimate 3000 LC combined with Q Exactive MS (Thermo) and screened with ESI-MS. The LC system is comprised of ACQUITY UPLC HSS T3 (100×2.1mm×1.8 µm) with Ultimate 3000 LC. The mobile phase is composed of solvent A (0.05% formic acid water) and solvent B (acetonitrile) with a gradient elution (0-1.0 min, 5%B; 1.0-12.0 min, 5%-95%B; 12.0-13.5 min, 95%B; 13.5-13.6 min, 95%-5%B; 13.6-16.0 min, 5%B). The flow rate of the mobile phase is 0.3 mL·min-1. The column temperature is maintained at 40°C, and the sample manager temperature is set at 4°C. Mass spectrometry parameters in ESI+ and ESI- mode are listed as follows:

ESI+: Heater Temp 300 °C; Sheath Gas Flow rate, 45arb; Aux Gas Flow Rate, 15arb; Sweep Gas Flow Rate, 1arb; spray voltage, 3.0KV; Capillary Temp, 350 °C; S-Lens RF Level, 30%.
ESI-: Heater Temp 300 °C, Sheath Gas Flow rate, 45arb; Aux Gas Flow Rate, 15arb; Sweep Gas Flow Rate, 1arb; spray voltage, 3.2KV; Capillary Temp,350 °C; S-Lens RF Level,60%.

RNA Extraction and Quantitative PCR: After Euthasol injection, mice were perfused with saline with heparin (10,000U/L; Sigma; H-3125). The duodenum was dissected and 0.5 cm sections were used for RNA extraction. Extraction was conducted using the Bioline Isolate II RNA mini kit per manufacturer's protocol (BIO-52073). RNA was normalized after quantification using the Biotek Epoch Microplate Spectrophotometer and reverse transcribed using the Bioline SensiFast cDNA Synthesis Kit (BIO-65054). Primers for qPCR are listed in the supplemental materials. Results were analyzed using the relative quantity (ΔΔcq) method.

Flow Cytometry: Animals were perfused with saline with heparin (10,000U/L; Sigma; H-3125). Peyer's patches, lymph nodes, and spleens were mashed onto 70 µm filters to achieve single cells suspensions[379].

Dural meninges were dissected from skull caps into RPMI. They were then added to 2 mL of digestion buffer (Collagenase D (2mg/mL; Sigma-Aldrich; 11088882001), Collagenase 11 (2mg/mL; Gibco; 17101-015), DNAse (20U/mL; Worthington; LS002139)) in a 15mL conical vial. They were agitated at 37°C for 30 minutes. We then added 20µL of 0.5M EDTA and filtered through a 70µm filter. 2mL RPMI with 5% FBS was added followed by 5 minutes of centrifugation at 400g. The cells were resuspended in FACS buffer.

Small intestines (jejunum, ilium, duodenum) were dissected, flayed open, and cut into 1cm long pieces. These pieces were washed two times in 30mL of HBSS-/- with 5% FBS via agitation at 37°C for 20 minutes. After each wash, tissue was filtered over a mosquito net. After washing, the tissue was minced and added to a new 50mL conical vial with 20mL of digestion buffer (HBSS-/-, 5% FBS, Collagenase 8 (900U/mL; Milipore; C2139), DNAse (20U/mL; Worthington; LS002139). These were agitated at 37°C for 30 minutes then vigorously vortexed and filtered through 70µm filter. 30mL of HBSS-/- with 5% FBS was added to halt digestion and centrifuged at 400g for 5 minutes. The pellet was resuspended in 50mL of HBSS-/- with 5% FBS and centrifuged again at 400g for 5 minutes. The pellet was resuspended in 1mL of FACS and 200µL was used for flow staining.

For staining, single cell suspensions were incubated with Fc Block CD16/32 (Invitrogen; 14-0161-85). The cells were then incubated for 30 minutes with the surface antibodies and Live/Dead Ghost Dye Violet 510 (Tonbow Biosciences; 13-0870). Cells were washed and the FoxP3/Transcription Factor Staining Kit (eBioscience; 00-5523-00) was used per manufacturer's instructions in order to do intracellular staining. OneComp eBeads (Thermo Fisher Scientific; 01-111-42) were used for single color controls. Flow cytometry was performed on a Beckman Coulter Gallios flow cytometer and the data were analyzed with FlowJo software v10.7.1.

Modified LB media: Modified LB media consisted of LB Base (Sigma, L3022-250G) supplemented with 0.25 g/L L-cysteine (filter sterilized; Sigma, 30120-10G) and sterilized. Prior to culture the media was also supplemented with 10 mL/L hemin solution (filter sterilized 0.5 g/L dissolved in 1% NaOH, 99% deionized water; Sigma H9030-1G), 100 µL/L vitamin K1 solution (0.5% vitamin K1 dissolved in 95% ethanol; Sigma, V3501-1G), 10 mL/L lactose solution (filter sterilized5 mg/mL dissolved in deionized water; cat), 10 mL/L Tween 20 (filter sterilized 1mg/mL dissolved in deionized water; cat), 39mL/L of a mineral salts solution (containing 6 g/L KH2PO4, 6 g/L (NH4)2SO4, 12g/L NaCl, 2.5g/L MgSO4,7H2O, 1.6 g/L CaCl2,2H2O (cat), all dissolved in deionized water and filter sterilized).

Lactobacillus EV isolation: Whole intestines (small, cecum, and colon) from two pooled ASF or ASF-L mice were sterile harvested and passed into an aerobic chamber. Under anaerobic conditions the intestines were flayed open and shaken in modified LB media. Solids were removed using a sterile 70 µm filter and cultured shaking for 36 hours at 37°C. Bacterial cultures were removed from the aerobic chamber and pelleted by centrifugation at 10,000g for 20 min. Supernatant was passed through a 0.22 µm filter. Filtrate was concentrated using 10KDa concentrators (Amicon; UFC901024) by spinning at 3000g at 4°C until the original 250mL was reduced to around 15mL. Extracellular vesicles were pelleted by ultracentrifugation at 150,000g for 3 hours at 4°C. Pellets were resuspended in filtered PBS and centrifuged again at 150,000g for 3 hours at 4°C. Pellet was resuspended in 550µL filtered PBS, protein was quantified using a BCA assay and samples were stored at -80°C until use.

Isolation and Preparation of T cells: Mesenteric, inguinal, axial, and brachial lymph nodes plus the spleen were dissected from the C57/BL6 mice after CO_2 euthanasia. They were then dissociated through sterile 70 μm filters and lysed with ACK lysis buffer (Quality Biological, 118-156-101). An EasySep Mouse CD4+ T cell Isolation Kit (Stem Cell Technologies, #19852) was used per manufacturer's protocol to sort naïve CD4+ T cells. The cells were incubated at $1x10^6$ cells/mL in skew media in anti-CD28 (InVivoMab, BE0015-5) and anti-CD3 (InVivoMab, BE0001-1) coated plates as previously described[380]. T_H1 and T_H2 media contained RPMI (Gibco, 11875-093) supplemented with 10% FBS (Optima, S12450H), 0.5% Pen/Strep (Gibco, 15240-062), 1mM sodium pyruvate (Gibco, 11360-070), 2mM L-glutamine (Gibco, 25030081), 10mM HEPES (Gibco, 15603-080), 1:100 NEAA (Gibco, 11140-050), and 50uM B-mercaptoethanol (Fisher Scientific, O3446I-100). Treg and T_H17 media contained IMDM (Gibco, 12440-053) using the same supplements. T_H1 skew media contained IL-2 (100U/mL; Tecin, 23-6019), IL-12 (10ng/mL; PeproTech, 210-12), and anti-IL-4 (10ug/mL; InVivoMab, BE0045). T_H2 skew media contained IL-2 (100U/mL; Tecin, 23-6019), IL-4 (10ng/mL; InVivoMab, BE0045), and anti-IFNγ (10ug/mL; InVivoMab BE0054). Treg skew media contained TGF-B (5ng/mL; BioLegend, 763102) and anti-CD28 (2ug/mL; InVivoMab, BE0015-5). T_H17 skew media contained IL-6 (20ng/mL; BioLegend, 575704), IL-23 (10ng/mL; Invitrogen, 14-8231), TGF-B (0.3ng/mL; BioLegend, 763102), anti-IL-4 (10ug/mL; InVivoMab, BE0045), and anti-IFNγ (10ug/mL; InVivoMab BE0054). T_H1 and T_H2 cell cultures were expanded on day 3 after plating by transferring cells to larger plates and adding 3x volume of RPMI supplemented media containing IL-2 (100U/mL). On day 5 skewing was complete and cells were washed and plated for downstream assays. Treg and T_H17 cell cultures were not expanded but simply washed and plated for downstream assays on day 4 after plating.

Th1 cells treated with bacterial extracellular vesicles: Prior to initial plating and differentiation, 1.7 million EVs/T cell or similarly treated LB media controls were added by volume to 0.5 million sorted naïve CD4+ T cells in 1mL of differentiation media. Cells were counted at 3 days prior to expansion. After expansion, cells were stimulated as described above by anti-CD3 coated plates for 24 hours. The supernatant was collected for ELISA analysis and the cells were collected for flow cytometry.

ELISA: ELISA for IFNγ was performed as previously described [381]. Antibodies used were as follows: anti-IFNγ (BioLegend; 517902), biotin labeled anti-IFNγ (BioLegend; 505704).

7.3 Chapter 4 Methods

Experimental Design: The objective of these studies was to understand the role of CD4 specific AHR activity in EAE. Immunophenotyping and characterization of the mice occurred in cohoused mice to determine the purely genetic differences. Once no major changes were discovered in the *Ahr* knockout mice, we began to separately house them based on genotype. This allowed us to examine the microbiome-dependent features of autoimmunity and the development of further hypotheses. Sample sizes were determined by power analysis. The final desired n was divided by two and included for each experiment. In this way, we have two independent experiments resulting in appropriate power. Except where otherwise stated, all experiments were conducted twice independently. Data collection for all EAE experiments ended at 30 days- the time point at which we have defined as chronic stage. All experiments were conducted on age- and sex- matched animals. Histological analysis was conducted by a blinded investigator. Clinical scores are reported as the average of two blinded investigators to account for interrater variability. Statistical outliers identified using the ROUT method (Q=1%) are not included in analysis or figures.

Mice: $AHR^{tm3.1Bra}$/J(Ahr^{fx}) (#006203), B6.Cg-Tg(Cd4-cre)1Cwi/BfluJ (CD4Cre) (#022071), and C57BL/6J (#000664) mice were purchased from Jackson Laboratories. Mice were bred in-house with a 12-hour light/dark schedule. Cohoused mice were housed with their littermates of the same sex from birth. Separately housed mice were separated at weaning (3 weeks) based on presence of Cre. Litters born within 4 days of each other were housed together to achieve 2-5 mice per cage. All procedures were approved by the University of Virginia ACUC (protocol #1918).

Experimental autoimmune encephalomyelitis: EAE was induced in both male and female mice between 8 and 12 weeks of age. MOG_{35-55} peptide (100µg, CSBio, CS0681) was emulsified in complete Freund's adjuvant containing *Mycobacterium tuberculosis* (1mg/mL, Sigma, F5881; M. tuberculosis (BD 231141) added to final concentration of 4mg/mL) and was injected subcutaneously (100 µL volume) at the base of the tail. Pertussis toxin (200 ng, List Biologicals, 180) was administered i.p. on the day of and 1 day after MOG immunization. Mice were scored daily by two blinded evaluators using

the following scale: 0-no clinical disease, 1-limp tail, 2-hindlimb incoordination, 3-hindlimb weakness, 4-hindlimb paralysis, 5-moribund. As is standard practice, animals who did not develop any signs of EAE were excluded from analysis. Total incidence including excluded animals is reported in the supplement.

Immunohistochemistry and Fluorescent Microscopy: Spinal cords were prepared as previously described[382]. Slides were deparaffinized using xylenes and an ethanol gradient. IHC antibodies used were anti-CD3 (Dako; A0452) at 1:200 dilution and anti-CD45 (BD Biosciences; 550539) at 1:80 dilution. Adjacent sections were stained with Luxol Fast Blue and Hemtoxylin and Eosin for demyelinating plaques. In short, slides were deparaffinized using xylenes and an ethanol gradient. Slides were stained with Luxol Fast Blue at 56 ºC overnight. Slides were rinsed with distilled water and then 0.05% Lithium carbonate until sharp contrast between white matter and grey matter was evident. Slides were imaged using an EVOS microscope. All images were analyzed with ImageJ by setting a threshold in the negative control and evaluating percent positive area within the white matter of the spinal cord. Luxol Fast Blue alone was used for quantification of myelin coverage while Luxol Fast Blue with H&E images were used in the figure to highlight lesions. Histological analysis was performed by a blinded evaluator.

For TUNEL staining, cryosections (30µm) were stained with anti-CD3 (eBioscience; 50-0032-82) or isotype control (Fisher Scientific; 14-0032-82) as previously described[382]. A positive control slide was treated with DNAse (3000U/mL). After staining, sections were fixed with paraformaldehyde for 15 minutes at room temperature. Sections were washed two times in PBS followed by proteinase K (200ug/mL in PBS) treatment for 10 minutes at room temperature. Sections were washed twice with PBS and incubated with TUNEL reaction mixture (Roche; 12156792910) for 60 minutes at 37 ºC in a humidified chamber. Sections were washed three times in PBS and mounted using Prolong Gold Anti-Fade Reagent (Life Technologies). Slides were imaged with a Leica TCS SP8 confocal microscope. All images were analyzed with ImageJ. Histological analysis was performed by a blinded evaluator.

RNA Extraction and Quantitative PCR: Whole spinal cords or 0.5 cm sections of gut tissue were homogenized using a dounce homogenizer and RNA was extracted using the Bioline Isolate II RNA mini kit as per manufacture's protocol (BIO-52073). RNA was quantified with a Biotek Epoch Microplate Spectrophotometer. Normalized RNA was reverse transcribed to cDNA with the Bioline SensiFast

cDNA Synthesis Kit (BIO-65054). For the qPCR array, two spinal cords per group were pooled and analyzed as described by the manufacturer (Demyelinating Diseases Tier 1-4 M384; 10038953). Primers for targeted qPCR are listed in the supplemental materials (S1 Data). Results were analyzed with the relative quantity (ΔΔCq) method.

Isolation and Preparation T cells: Mesenteric, inguinal, axial, and brachial lymph nodes plus the spleen were dissected from the mice after CO_2 euthanasia. They were then dissociated through sterile 70 μm filters and lysed with ACK lysis buffer (Quality Biological, 118-156-101). Naïve CD4+ T cells were then sorted using an EasySep Mouse CD4+ T cell Isolation Kit (Stem Cell Technologies, #19852). The cells were incubated at $1x10^6$ cells/mL in skew media in anti-CD28 (InVivoMab, BE0015-5) and anti-CD3 (InVivoMab, BE0001-1) coated plates as previously described[380]. T_H1 and T_H2 media contained RPMI (Gibco, 11875-093) supplemented with 10% FBS (Optima, S12450H), 0.5% Pen/Strep (Gibco, 15240-062), 1mM sodium pyruvate (Gibco, 11360-070), 2mM L-glutamine (Gibco, 25030081), 10mM HEPES (Gibco, 15603-080), 1:100 NEAA (Gibco, 11140-050), and 50uM B-mercaptoethanol (Fisher Scientific, O3446I-100). Treg and T_H17 media contained IMDM (Gibco, 12440-053) using the same supplements. T_H1 skew media contained IL-2 (100U/mL; Tecin, 23-6019), IL-12 (10ng/mL; PeproTech, 210-12), and anti-IL-4 (10ug/mL; InVivoMab, BE0045). T_H2 skew media contained IL-2 (100U/mL; Tecin, 23-6019), IL-4 (10ng/mL; InVivoMab, BE0045), and anti-IFNγ (10ug/mL; InVivoMab BE0054). Treg skew media contained TGF-B (5ng/mL; BioLegend, 763102) and anti-CD28 (2ug/mL; InVivoMab, BE0015-5). T_H17 skew media contained IL-6 (20ng/mL; BioLegend, 575704), IL-23 (10ng/mL; Invitrogen, 14-8231), TGF-B (0.3ng/mL; BioLegend, 763102), anti-IL-4 (10ug/mL; InVivoMab, BE0045), and anti-IFNγ (10ug/mL; InVivoMab BE0054). T_H1 and T_H2 cell cultures were expanded on day 3 after plating by transferring cells to larger plates and adding 3x volume of RPMI supplemented media containing IL-2 (100U/mL). On day 5 skewing was complete and cells were washed and plated for downstream assays. Treg and T_H17 cell cultures were not expanded but simply washed and plated for downstream assays on day 4 after plating.

Apoptosis and Cytokines Production Assay: Skewed T cells were plated with respective treatments at $1x10^6$ cells/mL in 48 well plates coated with anti-CD3. After 24 hours, the supernatant was collected for ELISA assay or cells were collected for Annexin V staining. In short, cells were stained with Ghost Live Dead (Tonbo Biosciences; 13-0870), Annexin V (Fisher Scientific; BDB556420) per

manufacturer's instructions (Annexin V, fixed using the FoxP3 permeabilization, fixation kit (eBioscience; 00-5523-00), and stained with RORgt PE. Results were gated on singlets, RORgt+, and Annexin V+, L/D negative.

Enzyme-linked immunosorbent Assay: ELISA for IFNγ, IL-4, IL-17, and IL-10 were performed as previously described[381]. Antibodies used were as follows: anti-IFNγ (BioLegend; 517902), biotin labeled anti-INFγ (BioLegend; 505704), anti-IL-4 (Thermo Fisher; 14-7041-85), biotin labeled anti-IL-4 (Thermo Fisher; 13-7042-85), anti-IL-17 (eBioscience; 14-7175-85), biotin labeled anti-IL-17(eBioscience; 13-7177-85), anti-IL-10 (BioLegend; 505002), biotin labeled anti-IL-10 (BioLegend; 505004).

Isolation of Cecal Contents: For both metabolomics and *in vitro* analysis, the cecal contents were resuspended in 1mL of IMDM by vortexing. Preparations were then sequentially processed using first syringe filters to remove insoluble materials (70 μm, 40 μm, .22 μm) and then protein concentrators (50 and 3 kDa from Thermo Fischer scientific) to exclude macromolecules with a molecular weight > 3kDa. Preparations were used immediately, or flash frozen at -80C for up to 3 weeks.

Spinal Cord Dissociation Spinal cords were collected in 2.5 mL ice cold HBSS (Gibco, 14025134). Equal amounts of 4mg/mL collagenase 4 (Worthington; LS002139) with 50U/mL DNase (Worthington, LS002139) were added and samples were shaken three times at 37ºC for 15 minutes, triturating in between. Spinal cords were strained through a 70mm filter into 10mL DMEM (Gibco, 11965-092) with 10% FBS (R&D Systems; S12450H). The samples were then centrifuged at 260 g for 8 minutes. The pellet was resuspended in a 15mL tube in 12 mL of Percoll (GE Healthcare, 17-0891-01). The sample was then centrifuged at 650g for 25 min without brake. The myelin layer and supernatant were aspirated and the pellet was resuspended in 2mL of FACS buffer.

Spinal Cord Luminex Mice were perfused with PBS containing heparin (5U/mL; Sigma; H-3125) solution. Spinal cords were dissected and flash frozen. Frozen spinal cords were homogenized in 1mL of PBS with protease inhibitor (MedChem Express; HY-K0010) using a Dounce homogenizer. Triton X-100 was added to final concentration of 0.2% and samples were vortexed. Samples were centrifuged at 10,000g for 5 minutes at 4 °C and 200 □L was acquired from the top layer to be flash frozen for later

analysis. Mouse T_H17 Luminex was run per manufacturer's instructions on a MagPix by the University of Virginia Flow Cytometry Core , RRID: SCR_017829.

Microbiome Transfer Female C57BL6/J mice were given drinking water containing 1g/L Ampicillin (Sigma-Aldrich; A8351-25G), 1g/L Neomycin (Sigma-Aldrich; N6386-25G), 1g/L Metronidazol (Sigma-Aldrich; M1547-25G), 500mg/mL Vancomycin (Sigma-Aldrich; V1130-5G), and 8mg/mL Splenda for two weeks. Mice were then orally gavaged with fresh filtered (40µm) cecal contents from pooled donor animals on day 0, day 2, and day 4 after removal from antibiotics. On the day of antibiotics withdrawal, a naïve microbiome donor animal was added to the cage and remained for the duration of the experiment. EAE was induced 2 weeks post reconstitution.

Bile Acid Supplement Female and male C57BL6/J mice were immunized with MOG as described above. Daily gavage of either 100µL of 125 mg/mL taurocholic acid (in saline) or 100µL of saline started on day 4 and continued through day 10. Mice were then monitored and scored as described earlier.

Flow Cytometry Single cell suspensions were incubated with Fc Block CD16/32 (Invitrogen, 14-0161-85). The cells were then incubated with a 1:200 dilution of antibody for surface stains and A Live/Dead Ghost Dye Violet 510 (Tonbo Biosciences; 13-0870). Surface antibodies: 488-conjugated CD8 (Invitrogen; 53-008182), APCe780-conjugated TCRβ (Invitrogen; 47-5961-82), e450-conjugated CD4 (Invitrogen; 48-0042-820), 488 conjugated- CD11b (Invitrogen; 53-0112-82), and APC-conjugated CD45.2 (Biolegend; 109813). For transcription factor staining, the eBioscience FoxP3/Transcription Factor Staining Kit (00-5523-00) was used per manufacturer's instructions with intracellular antibodies: PE-conjugated RORγT (Invitrogen; 12-6981-82), PE-Cy7- conjugated FoxP3 (Invitrogen; 25-5773-82), PE-conjugated GATA3 (Invitrogen; 12-9966-42), PE-Cy7-conjugated Tbet (Biolegend; 644824). OneComp eBeads (Thermo Fisher Scientific, 01-111-42) were used for color controls. Flow cytometry was performed using a Beckman Coulter Gallios flow cytometer and data were analyzed with FlowJo software v10.7.1.

LC-MS Untargeted Metabolomics was performed by Creative Proteomics. Cecal samples (<3kDa) were prepared and concentrated as before as described before. Samples were thawed and lyophilized, 200µL of 80% methanol was added. Samples were vortexed and then sonicated for 30

minutes at 4 ºC. Samples were kept at -20 for 1 h, vortexed for 30s and kept at 4 ºC for 15min until they were centrifuged at 12000 rpm at 4 ºC for 15 min. 100µL of the supernatant and 2.5µL of DL-o-Chlorophenylalanine were used for LC-MS analysis. Separation is performed by Ultimate 3000 LC combined with Q Exactive MS (Thermo) and screened with ESI-MS. The LC system is comprised of ACQUITY UPLC HSS T3 (100×2.1mm×1.8 µm) with Ultimate 3000 LC. The mobile phase is composed of solvent A (0.05% formic acid water) and solvent B (acetonitrile) with a gradient elution (0-1.0 min, 5%B; 1.0-12.0 min, 5%-95%B; 12.0-13.5 min, 95%B; 13.5-13.6 min, 95%-5%B; 13.6-16.0 min, 5%B). The flow rate of the mobile phase is 0.3 mL·min-1. The column temperature is maintained at 40°C, and the sample manager temperature is set at 4°C. Mass spectrometry parameters in ESI+ and ESI- mode are listed as follows:

ESI+: Heater Temp 300 °C; Sheath Gas Flow rate, 45arb; Aux Gas Flow Rate, 15arb; Sweep Gas Flow Rate, 1arb; spray voltage, 3.0KV; Capillary Temp, 350 °C; S-Lens RF Level, 30%.
ESI-: Heater Temp 300 °C, Sheath Gas Flow rate, 45arb; Aux Gas Flow Rate, 15arb; Sweep Gas Flow Rate, 1arb; spray voltage, 3.2KV; Capillary Temp,350 °C; S-Lens RF Level,60%.

LC-MS Data Processing LC-MS data was processed using R studio. Analysis was conducted using POMA Shiny version 1.4.0[383]. In short, we removed features with more than 20% missing values, normalized with log scaling and then completed sparse partial least squares discriminate analysis (sPLS-DA). Top ranked products were utilized in MetaMapp[384,385] analysis to produce a web of chemically and biologically related compounds. Finally, the top ranked products were also inputted into Metaboanalyst to complete pathway enrichment and determine mouse KEGG terms.

16S Sequencing Data Processing 16S Sequencing was conducted at Microbiome Insights (Cohoused Feces), ZymoBIOMICS (Separately Housed Cecum), and at the University of Virginia Genomics Core (Separately housed Feces). Initial sequence data was analyzed using the latest version of Quantitative Insights Into Microbial Ecology 2 (Qiime2 v2021.11)[376]. Demultiplexed paired-end sequence reads were preprocessed using DADA2[377]. The first 20 base pairs were trimmed from forward and reverse reads before they were merged to remove adaptors. Taxonomy was assigned to Amplicon Sequence Variants (ASVs) using a Naïve Bayes classifier trained on full length 16S sequences from the latest Greengenes16S database (13_8) clustered at 99% sequence similarity. Samples were rarified before core diversity analysis. Rarefied sampling depth was 16000 for cecal contents, 30000

for separately housed fecal contents, and 10,411 for cohoused fecal contents. Core diversity metrics were analyzed, including number of ASVs. Nonmetric multidimensional scaling was performed in RStudio using the phyloseq package[378].

Statistical Analysis Unless otherwise noted, all statistical tests were run on Graph Pad Prism 9 Version 9.1.0. Statistical tests and p-values for each comparison are listed in the figure legends or in the supplementary report. In the figure legends, n denotes the total number of animals displayed in the figure used in analysis. In the figure legends, N denotes the total number of replicates that were completed for the given experiment. Testing level of α=0.05 was used throughout.

7.4 Chapter 5 Methods

Mice: C57BL/6J (#000664) and B6;129S1-*Il12rb2*^{tm1Jm}/J (#003248) were purchased from Jackson Laboratory. All mice have a 12-hour light/dark schedule. All procedures were approved by the University of Virginia ACUC (protocol #1918).

Cuprizone Model of Demyelination: Adult male and female mice between 10 and 20 weeks of age were fed regular mouse chow, ground and mixed with 0.3% cuprizone (Sigma; 14690) ad libitum for 5 weeks to induce demyelination as previously described[386]. Brains were dissected directly following demyelination and at 4 days after the return to normal diet.

Immunofluorescent Staining: Animals were perfused with saline with heparin (10,000U/L; Sigma; H-3125), followed by perfusion with 4% paraformaldehyde. Dissected brains were drop fixed in 4% paraformaldehyde for 24 hours. After 24 hours, the brains were transferred to 30% sucrose solution and mounted in cryomolds with OCT (Tissue-Tek; 4583). Thirty µm cryosections were stained floating. Sections were mounted using Prolong Gold Anti-Fade Reagent (Life Technologies, P36980) and imaged with a Leica TCS SP8 confocal microscope. Image processing and threshold quantification was done using ImageJ version 2.1.0/1.53c.

Primary OPC Culture: OPC cultures were prepared as previously described from P4-P8 pups[387]. In short, cortices were dissected and the meninges were removed. They were then digested in 2mL of Accutase (Thermo Fisher; A1110501) supplemented with 50U/mL DNase (Worthington Biochemical, LS002139) for 45 minutes at 37°C, triturating every 15 minutes for a total of 3 titurations. The digested tissue was then filtered through a sterile 70 µm strainer, and grown in suspension media consisting of DMEM/F12 (Gibco; 11320082), B27 (Gibco; 17504044), Pen/Strep (Gibco; 15140122), and 10ng/mL EGF (Preprotech; 315-09). Cells were expanded as neurospheres and then transferred to oligosphere media consisting of DMEM/F12 (Gibco; 11320082), B27 (Gibco; 17504044), Pen/Strep (Gibco; 15140122), 10ng/mL FGF (Preprotech; 450-33), and 10ng/mL PDGFRα (Preprotech, 315-17). Cells grew in suspension for at least two days and then plated on 0.01% Poly-L-Lysine coated plates (Electron Microscopy Sciences; 193320-B). After 12 hours, media was replaced with treatment indicated. Differentiation media consisted of DMEM/F12 (Gibco; 11320082), B27 (Gibco; 17504044), Pen/Strep (Gibco; 15140122), 10ng/mL FGF (Preprotech; 450-33), and 10ng/mL CNTF (Preprotech; 450-13), and 40ng/mL T3 (Sigma; T6397). Cells were incubated with differentiation media and/or treatment for 72 hours and cell pellets were collected.

RNA Extraction and Quantitative PCR: RNA from cell pellets was extracted using the Bioline Isolate II RNA mini kit per manufacturer's protocol (BIO-52073). RNA was normalized after quantification using the Biotek Epoch Microplate Spectrophotometer and reverse transcribed using the Bioline SensiFast cDNA Synthesis Kit (BIO-65054). Primers for qPCR are listed in the supplemental materials. Results were analyzed using the relative quantity (ΔΔcq) method. GAPDH was used as a housekeeping gene.

Funding Sources: This work has been funded through the National Institutes of Health (T32 NS115657, R33 MH108156, F31 AI174782), the Owens Family Foundation, and the UVA Trans University Microbiome Initiative pilot grant.

Acknowledgements:

First and foremost, I would like to acknowledge my mentor and labmates (past and present) without whom this work would not have been possible: Alban Gaultier, Hannah Cahill, Lucy Brown, Alisha Thakur, Deniz Olgun, Anthony Fernandez-Casteñeda, A Rosen, Rebecca Beiter, Courtney Rivet-Noor, Ryan Brown, Tula Raghavan, Sam Wachamo, Stephanie Moy, and Naudia Gay. Special thanks to Brett Moreau and Sihan Li who also contributed to this work. Thank you to my committee Scott Zeitlan, Tajie Harris, Melanie Rutkowski, Hui Zong, and Barry Condron for all of our fruitful discussions and scientific contributions.

I would next like to thank everyone who contributed to the production and editing of this thesis including Katriel Cho who created all of the original artwork and my editors: Sharon Walsh, Jack Piunti, Kelly Piunti, and Helen Benet.

I would also like to thank all of the mice whose lives were sacrificed in the pursuit of finding cures for human diseases. This work would be impossible without them and all of the animal care takers at the University of Virginia vivarium.

Finally, I would like to thank all who supported me through the five years this work took. There are too many to name all, but I would especially like to thank the following people. My family, Patrick Merchak, Sharon Walsh, Elise Merchak, and Chris Merchak, who supported me no only through this thesis but also got me to this point. My friends both in the Biomedical Sciences Program and out. And finally, I would like to thank the individuals who have given me more moral support than they can ever understand: Jack Piunti, Olyver, Morty, Mercy, and Ragnar.

Works Cited

1. World Health Organization, Depression. 2018; https://www.who.int/news-room/fact-sheets/detail/depression
2. Dudek KA, Dion-Albert L, Lebel M, et al. Molecular adaptations of the blood–brain barrier promote stress resilience vs. Depression. *Proc Natl Acad Sci U S A*. 2020;117(6):3326-3336. doi:10.1073/pnas.1914655117
3. Menard C, Pfau ML, Hodes GE, et al. Social stress induces neurovascular pathology promoting depression. *Nat Neurosci*. 2017;20(12):1752-1760. doi:10.1038/s41593-017-0010-3
4. Abernethy J. No Title. The Abernethian code of health and longevity. doi:61360010R
5. Dinan TG, Cryan JF. The Microbiome-Gut-Brain Axis in Health and Disease. *Gastroenterol Clin North Am*. 2017;46(1):77-89. doi:10.1016/j.gtc.2016.09.007
6. Qin J, Li R, Raes J, et al. A human gut microbial gene catalogue established by metagenomic sequencing. *Nature*. 2010;464(7285):59-65. doi:10.1038/nature08821
7. Jiang H, Ling Z, Zhang Y, et al. Altered fecal microbiota composition in patients with major depressive disorder. *Brain Behav Immun*. 2015;48:186-194. doi:10.1016/j.bbi.2015.03.016
8. Kelly JR, Borre Y, O' Brien C, et al. Transferring the blues: Depression-associated gut microbiota induces neurobehavioural changes in the rat. *J Psychiatr Res*. 2016;82:109-118. doi:10.1016/j.jpsychires.2016.07.019
9. Naseribafrouei A, Hestad K, Avershina E, et al. Correlation between the human fecal microbiota and depression. *Neurogastroenterol Motil*. 2014;26(8):1155-1162. doi:10.1111/nmo.12378
10. Huang R, Wang K, Hu J. Effect of probiotics on depression: A systematic review and meta-analysis of randomized controlled trials. *Nutrients*. 2016;8(8). doi:10.3390/nu8080483
11. Ng QX, Peters C, Ho CYX, Lim DY, Yeo WS. A meta-analysis of the use of probiotics to alleviate depressive symptoms. *J Affect Disord*. 2018;228:13-19. doi:10.1016/j.jad.2017.11.063
12. Nadeem I, Rahman MZ, Ad-Dab'bagh Y, Akhtar M. Effect of probiotic interventions on depressive symptoms: A narrative review evaluating systematic reviews. *Psychiatry Clin Neurosci*. 2019;73(4):154-162. doi:10.1111/pcn.12804

13. Sudo N, Chida Y, Aiba Y, et al. Postnatal microbial colonization programs the hypothalamic-pituitary-adrenal system for stress response in mice. *J Physiol*. 2004;558(1):263-275. doi:10.1113/jphysiol.2004.063388
14. Clarke G, Grenham S, Scully P, et al. The microbiome-gut-brain axis during early life regulates the hippocampal serotonergic system in a sex-dependent manner. *Mol Psychiatry*. 2013;18(6):666-673. doi:10.1038/mp.2012.77
15. Matsumoto M, Kibe R, Ooga T, et al. Cerebral Low-Molecular Metabolites Influenced by Intestinal Microbiota: A Pilot Study. *Front Syst Neurosci*. 2013;7(APR 2013):9. doi:10.3389/fnsys.2013.00009
16. Bailey MT, Coe CL. Maternal separation disrupts the integrity of the intestinal microflora in infant rhesus monkeys. *Dev Psychobiol*. 1999;35(2):146-155. doi:10.1002/(SICI)1098-2302(199909)35:2<146::AID-DEV7>3.0.CO;2-G
17. Marin IA, Goertz JE, Ren T, et al. Microbiota alteration is associated with the development of stress-induced despair behavior. *Sci Rep*. 2017;7(1):43859. doi:10.1038/srep43859
18. Bravo JA, Forsythe P, Chew M V., et al. Ingestion of Lactobacillus strain regulates emotional behavior and central GABA receptor expression in a mouse via the vagus nerve. *Proc Natl Acad Sci U S A*. 2011;108(38):16050-16055. doi:10.1073/pnas.1102999108
19. Sun J, Wang F, Hu X, et al. Clostridium butyricum Attenuates Chronic Unpredictable Mild Stress-Induced Depressive-Like Behavior in Mice via the Gut-Brain Axis. *J Agric Food Chem*. 2018;66(31):8415-8421. doi:10.1021/acs.jafc.8b02462
20. Galeazzi GM, Ferrari S, Giaroli G, et al. Psychiatric disorders and depression in multiple sclerosis outpatients: impact of disability and interferon beta therapy. *Neurol Sci*. 2005;26(4):255-262. doi:10.1007/S10072-005-0468-8
21. Figved N, Klevan G, Myhr KM, et al. Neuropsychiatric symptoms in patients with multiple sclerosis. *Acta Psychiatr Scand*. 2005;112(6):463-468. doi:10.1111/J.1600-0447.2005.00624.X
22. Khan F, McPhail T, Brand C, Turner-Stokes L, Kilpatrick T. Multiple sclerosis: Disability profile and quality of life in an Australian community cohort. *Int J Rehabil Res*. 2006;29(2):87-96. doi:10.1097/01.MRR.0000194393.56772.62
23. Maglione A, Zuccalà M, Tosi M, Clerico M, Rolla S. Host Genetics and Gut Microbiome:

Perspectives for Multiple Sclerosis. *Genes 2021, Vol 12, Page 1181*. 2021;12(8):1181. doi:10.3390/GENES12081181

24. Miyake S, Kim S, Suda W, et al. Dysbiosis in the gut microbiota of patients with multiple sclerosis, with a striking depletion of species belonging to clostridia XIVa and IV clusters. *PLoS One*. 2015;10(9). doi:10.1371/journal.pone.0137429
25. Berer K, Gerdes LA, Cekanaviciute E, et al. Gut microbiota from multiple sclerosis patients enables spontaneous autoimmune encephalomyelitis in mice. *Proc Natl Acad Sci U S A*. 2017;114(40):10719-10724. doi:10.1073/pnas.1711233114
26. Chen J, Chia N, Kalari KR, et al. Multiple sclerosis patients have a distinct gut microbiota compared to healthy controls. *Sci Rep*. 2016;6. doi:10.1038/SREP28484
27. Berer K, Mues M, Koutrolos M, et al. Commensal microbiota and myelin autoantigen cooperate to trigger autoimmune demyelination. *Nature*. 2011;479(7374):538-541. doi:10.1038/nature10554
28. Lécuyer E, Rakotobe S, Lengliné-Garnier H, et al. Segmented filamentous bacterium uses secondary and tertiary lymphoid tissues to induce gut IgA and specific T helper 17 cell responses. *Immunity*. 2014;40(4):608-620. doi:10.1016/j.immuni.2014.03.009
29. Lee YK, Menezes JS, Umesaki Y, Mazmanian SK. Proinflammatory T-cell responses to gut microbiota promote experimental autoimmune encephalomyelitis. *Proc Natl Acad Sci U S A*. 2011;108 Suppl 1(Suppl 1):4615-4622. doi:10.1073/PNAS.1000082107
30. Johanson DM, Goertz JE, Marin IA, Costello J, Overall CC, Gaultier A. Experimental autoimmune encephalomyelitis is associated with changes of the microbiota composition in the gastrointestinal tract. *Sci Rep*. 2020;10(1). doi:10.1038/s41598-020-72197-y
31. Macfarlane GT, Macfarlane S. Bacteria, colonic fermentation, and gastrointestinal health. *J AOAC Int*. 2012;95(1):50-60. doi:10.5740/jaoacint.SGE_Macfarlane
32. Rechkemmer G, Rönnau K, von Engelhardt W. Fermentation of polysaccharides and absorption of short chain fatty acids in the mammalian hindgut. *Comp Biochem Physiol A Comp Physiol*. 1988;90(4):563—568. doi:10.1016/0300-9629(88)90668-8
33. Stilling RM, van de Wouw M, Clarke G, Stanton C, Dinan TG, Cryan JF. The neuropharmacology of butyrate: The bread and butter of the microbiota-gut-brain axis? *Neurochem Int*.

2016;99:110-132. doi:10.1016/j.neuint.2016.06.011

34. Macfarlane S, Macfarlane GT. Regulation of short-chain fatty acid production. *Proc Nutr Soc*. 2003;62:67-72. doi:10.1079/PNS2002207

35. Miyauchi S, Gopal E, Fei YJ, Ganapathy V. Functional Identification of SLC5A8, a Tumor Suppressor Down-regulated in Colon Cancer, as a Na+-coupled Transporter for Short-chain Fatty Acids. *J Biol Chem*. 2004;279(14):13293-13296. doi:10.1074/jbc.C400059200

36. Stumpff F. A look at the smelly side of physiology: transport of short chain fatty acids. *Pflugers Arch Eur J Physiol*. 2018;470(4):571-598. doi:10.1007/s00424-017-2105-9

37. Schönfeld P, Wojtczak L. Short- and medium-chain fatty acids in energy metabolism: The cellular perspective. *J Lipid Res*. 2016;57(6):943-954. doi:10.1194/jlr.R067629

38. De Vadder F, Kovatcheva-Datchary P, Goncalves D, et al. Microbiota-generated metabolites promote metabolic benefits via gut-brain neural circuits. *Cell*. 2014;156(1-2):84-96. doi:10.1016/j.cell.2013.12.016

39. Fukumoto S, Tatewaki M, Yamada T, et al. Short-chain fatty acids stimulate colonic transit via intraluminal 5-HT release in rats. *Am J Physiol - Regul Integr Comp Physiol*. 2003;284(5 53-5). doi:10.1152/ajpregu.00442.2002

40. Reigstad CS, Salmonson CE, Rainey JF, et al. Gut microbes promote colonic serotonin production through an effect of short-chain fatty acids on enterochromaffin cells. *FASEB J*. 2015;29(4):1395-1403. doi:10.1096/fj.14-259598

41. Goswami C, Iwasaki Y, Yada T. Short-chain fatty acids suppress food intake by activating vagal afferent neurons. *J Nutr Biochem*. 2018;57:130-135. doi:10.1016/j.jnutbio.2018.03.009

42. Haase S, Haghikia A, Wilck N, Müller DN, Linker RA. Impacts of microbiome metabolites on immune regulation and autoimmunity. *Immunology*. 2018;154(2):230-238. doi:10.1111/imm.12933

43. Volmar CH, Wahlestedt C. Histone deacetylases (HDACs) and brain function. *Neuroepigenetics*. 2015;1:20-27. doi:10.1016/j.nepig.2014.10.002

44. Marks PA, Richon VM, Miller T, Kelly WK. Histone deacetylase inhibitors. *Adv Cancer Res*. 2004;91:137-168. doi:10.1016/S0065-230X(04)91004-4

45. Sarkar A, Chachra P, Kennedy P, et al. Hippocampal HDAC4 contributes to postnatal

fluoxetine-evoked depression-like behavior. *Neuropsychopharmacology*. 2014;39(9):2221-2232. doi:10.1038/npp.2014.73

46. Fischer A, Sananbenesi F, Wang X, Dobbin M, Tsai LH. Recovery of learning and memory is associated with chromatin remodelling. *Nature*. 2007;447(7141):178-182. doi:10.1038/nature05772

47. Govindarajan N, Agis-Balboa RC, Walter J, Sananbenesi F, Fischer A. Sodium butyrate improves memory function in an alzheimer's disease mouse model when administered at an advanced stage of disease progression. *J Alzheimer's Dis*. 2011;26(1):187-197. doi:10.3233/JAD-2011-110080

48. Covington HE, Maze I, LaPlant QC, et al. Antidepressant actions of histone deacetylase inhibitors. *J Neurosci*. 2009;29(37):11451-11460. doi:10.1523/JNEUROSCI.1758-09.2009

49. Renthal W, Maze I, Krishnan V, et al. Histone Deacetylase 5 Epigenetically Controls Behavioral Adaptations to Chronic Emotional Stimuli. *Neuron*. 2007;56(3):517-529. doi:10.1016/j.neuron.2007.09.032

50. Hollis F, Wang H, Dietz D, Gunjan A, Kabbaj M. The effects of repeated social defeat on long-term depressive-like behavior and short-term histone modifications in the hippocampus in male Sprague-Dawley rats. *Psychopharmacology (Berl)*. 2010;211(1):69-77. doi:10.1007/s00213-010-1869-9

51. Chandramohan Y, Droste SK, Arthur JSC, Reul JMHM. The forced swimming-induced behavioural immobility response involves histone H3 phospho-acetylation and c-Fos induction in dentate gyrus granule neurons via activation of the *N* -methyl-d-aspartate/extracellular signal-regulated kinase/mitogen- and stress-activated kinase signalling pathway. *Eur J Neurosci*. 2008;27(10):2701-2713. doi:10.1111/j.1460-9568.2008.06230.x

52. Bilang-Bleuel A, Ulbricht S, Chandramohan Y, De Carli S, Droste SK, Reul JMHM. Psychological stress increases histone H3 phosphorylation in adult dentate gyrus granule neurons: involvement in a glucocorticoid receptor-dependent behavioural response. *Eur J Neurosci*. 2005;22(7):1691-1700. doi:10.1111/j.1460-9568.2005.04358.x

53. Ferland CL, Schrader LA. Regulation of histone acetylation in the hippocampus of chronically stressed rats: A potential role of sirtuins. *Neuroscience*. 2011;174:104-114.

doi:10.1016/j.neuroscience.2010.10.077

54. Uchida S, Hara K, Kobayashi A, et al. Epigenetic status of Gdnf in the ventral striatum determines susceptibility and adaptation to daily stressful events. *Neuron*. 2011;69(2):359-372. doi:10.1016/j.neuron.2010.12.023

55. Schroeder FA, Lin CL, Crusio WE, Akbarian S. Antidepressant-Like Effects of the Histone Deacetylase Inhibitor, Sodium Butyrate, in the Mouse. *Biol Psychiatry*. 2007;62(1):55-64. doi:10.1016/j.biopsych.2006.06.036

56. Yamawaki Y, Fuchikami M, Morinobu S, Segawa M, Matsumoto T, Yamawaki S. Antidepressant-like effect of sodium butyrate (HDAC inhibitor) and its molecular mechanism of action in the rat hippocampus. *World J Biol Psychiatry*. 2012;13(6):458-467. doi:10.3109/15622975.2011.585663

57. Le Poul E, Loison C, Struyf S, et al. Functional characterization of human receptors for short chain fatty acids and their role in polymorphonuclear cell activation. *J Biol Chem*. 2003;278(28):25481-25489. doi:10.1074/jbc.M301403200

58. Onyszkiewicz M, Gawrys-Kopczynska M, Konopelski P, et al. Butyric acid, a gut bacteria metabolite, lowers arterial blood pressure via colon-vagus nerve signaling and GPR41/43 receptors. *Pflügers Arch - Eur J Physiol*. 2019;471(11-12):1441-1453. doi:10.1007/s00424-019-02322-y

59. Lal S, Kirkup AJ, Brunsden AM, Thompson DG, Grundy D. Vagal afferent responses to fatty acids of different chain length in the rat. *Am J Physiol - Gastrointest Liver Physiol*. 2001;281(4 44-4). doi:10.1152/ajpgi.2001.281.4.g907

60. Bonini JA, Anderson SM, Steiner DF. Molecular cloning and tissue expression of a novel orphan G protein-coupled receptor from rat lung. *Biochem Biophys Res Commun*. 1997;234(1):190-193. doi:10.1006/bbrc.1997.6591

61. Nøhr MK, Egerod KL, Christiansen SH, et al. Expression of the short chain fatty acid receptor GPR41/FFAR3 in autonomic and somatic sensory ganglia. *Neuroscience*. 2015;290:126-137. doi:10.1016/j.neuroscience.2015.01.040

62. Bender DA. Effects of a dietary excess of leucine on the metabolism of tryptophan in the rat: a mechanism for the pellagragenic action of leucine. *Br J Nutr*. 1983;50(1):25-32.

doi:10.1079/bjn19830068

63. McCreanor GM, Bender DA. The metabolism of high intakes of tryptophan, nicotinamide and nicotinic acid in the rat. *Br J Nutr*. 1986;56(3):577-586. doi:10.1079/bjn19860138

64. Satyanarayana U, Narasinga Rao BS. Effect of dietary protein level on some key enzymes of the tryptophan-NAD pathway. *Br J Nutr*. 1977;38(1):39-45. doi:10.1079/bjn19770059

65. Moffett JR, Namboodiri MA. Tryptophan and the immune response. *Immunol Cell Biol*. 2003;81(4):247-265. doi:10.1046/j.1440-1711.2003.t01-1-01177.x

66. Suzuki Y, Suda T, Asada K, et al. Serum indoleamine 2,3-dioxygenase activity predicts prognosis of pulmonary tuberculosis. *Clin Vaccine Immunol*. 2012;19(3):436-442. doi:10.1128/CVI.05402-11

67. Divanovic S, Sawtell NM, Trompette A, et al. Opposing Biological Functions of Tryptophan Catabolizing Enzymes During Intracellular Infection. *J Infect Dis*. 2011;205:152-161. doi:10.1093/infdis/jir621

68. Mcmenamy RH, Meyer EJ. *Binding of Indole Analogues to Human Serum Albumin EFFECTS OF FATTY ACIDS**. Vol 240.; 1965.

69. Madras BK, Cohen EL, Fernstrom JD, Larin F, Munro HN, Wurtman RJ. Dietary carbohydrate increases brain tryptophan and decreases free plasma tryptophan. *Nature*. 1973;244(5410):34-35. doi:10.1038/244034a0

70. Madras BK, Cohen EL, Messing R, Munro HN, Wurtman RJ. Relevance of free tryptophan in serum to tissue tryptophan concentrations. *Metabolism*. 1974;23(12):1107-1116. doi:10.1016/0026-0495(74)90027-4

71. Clark SM, Pocivavsek A, Nicholson JD, et al. Reduced kynurenine pathway metabolism and cytokine expression in the prefrontal cortex of depressed individuals. *J Psychiatry Neurosci*. 2016;41(6):386-394. doi:10.1503/jpn.150226

72. Busse M, Busse S, Myint AM, et al. Decreased quinolinic acid in the hippocampus of depressive patients: evidence for local anti-inflammatory and neuroprotective responses? *Eur Arch Psychiatry Clin Neurosci*. 2015;265(4):321-329. doi:10.1007/s00406-014-0562-0

73. Steiner J, Walter M, Gos T, et al. Severe depression is associated with increased microglial quinolinic acid in subregions of the anterior cingulate gyrus: Evidence for an immune-

modulated glutamatergic neurotransmission? *J Neuroinflammation*. 2011;8(1):94. doi:10.1186/1742-2094-8-94

74. Stone TW, Addae JI. The pharmacological manipulation of glutamate receptors and neuroprotection. *Eur J Pharmacol*. 2002;447(2-3):285-296. doi:10.1016/S0014-2999(02)01851-4

75. Hardingham GE. Coupling of the NMDA receptor to neuroprotective and neurodestructive events. *Biochem Soc Trans*. 2009;37(6):1147-1160. doi:10.1042/BST0371147

76. Danysz W, Parsons CG. Alzheimer's disease, β-amyloid, glutamate, NMDA receptors and memantine - searching for the connections. *Br J Pharmacol*. 2012;167(2):324-352. doi:10.1111/j.1476-5381.2012.02057.x

77. Guillemin GJ. Quinolinic acid, the inescapable neurotoxin. *FEBS J*. 2012;279(8):1356-1365. doi:10.1111/J.1742-4658.2012.08485.X@10.1002/(ISSN)1742-4658(CAT)FREEREVIEWCONTENT(VI)REVIEWS1213

78. Lovelace MD, Varney B, Sundaram G, et al. Recent evidence for an expanded role of the kynurenine pathway of tryptophan metabolism in neurological diseases. *Neuropharmacology*. 2017;112:373-388. doi:10.1016/j.neuropharm.2016.03.024

79. Harris CA, Miranda AF, Tanguay JJ, Boegman RJ, Beninger RJ, Jhamandas K. Modulation of striatal quinolinate neurotoxicity by elevation of endogenous brain kynurenic acid. *Br J Pharmacol*. 1998;124(2):391-399. doi:10.1038/sj.bjp.0701834

80. Stone TW, Darlington LG. The kynurenine pathway as a therapeutic target in cognitive and neurodegenerative disorders. *Br J Pharmacol*. 2013;169(6):1211-1227. doi:10.1111/bph.12230

81. Sapko MT, Guidetti P, Yu P, Tagle DA, Pellicciari R, Schwarcz R. Endogenous kynurenate controls the vulnerability of striatal neurons to quinolinate: Implications for Huntington's disease. *Exp Neurol*. 2006;197(1):31-40. doi:10.1016/j.expneurol.2005.07.004

82. Wang J, Simonavicius N, Wu X, et al. Kynurenic acid as a ligand for orphan G protein-coupled receptor GPR35. *J Biol Chem*. 2006;281(31):22021-22028. doi:10.1074/jbc.M603503200

83. Fukui S, Schwarcz R, Rapoport SI, Takada Y, Smith QR. Blood–Brain Barrier Transport of Kynurenines: Implications for Brain Synthesis and Metabolism. *J Neurochem*. 1991;56(6):2007-2017. doi:10.1111/j.1471-4159.1991.tb03460.x

84. Gershon MD. 5-Hydroxytryptamine (serotonin) in the gastrointestinal tract. *Curr Opin Endocrinol Diabetes Obes*. 2013;20(1):14-21. doi:10.1097/MED.0b013e32835bc703
85. Cervenka I, Agudelo LZ, Ruas JL. Kynurenines: Tryptophan's metabolites in exercise, inflammation, and mental health. *Science (80-)*. 2017;357(6349). doi:10.1126/science.aaf9794
86. Mawe GM, Hoffman JM. Serotonin signalling in the gut-functions, dysfunctions and therapeutic targets. *Nat Rev Gastroenterol Hepatol*. 2013;10(8):473-486. doi:10.1038/nrgastro.2013.105
87. Yano JM, Yu K, Donaldson GP, et al. Indigenous bacteria from the gut microbiota regulate host serotonin biosynthesis. *Cell*. 2015;161(2):264-276. doi:10.1016/j.cell.2015.02.047
88. Ramírez LA, Pérez-Padilla EA, García-Oscos F, Salgado H, Atzori M, Pineda JC. A new theory of depression based on the serotonin/kynurenine relationship and the hypothalamicpituitary-adrenal axis. *Biomedica*. 2018;38(3):437-450. doi:10.7705/biomedica.v38i3.3688
89. HU B, HISSONG BD, CARLIN JM. Interleukin-1 Enhances Indoleamine 2,3-Dioxygenase Activity by Increasing Specific mRNA Expression in Human Mononuclear Phagocytes. *J Interf Cytokine Res*. 1995;15(7):617-624. doi:10.1089/jir.1995.15.617
90. Connor TJ, Starr N, O'Sullivan JB, Harkin A. Induction of indolamine 2,3-dioxygenase and kynurenine 3-monooxygenase in rat brain following a systemic inflammatory challenge: A role for IFN-γ? *Neurosci Lett*. 2008;441(1):29-34. doi:10.1016/j.neulet.2008.06.007
91. Myint AM, Kim YK. Cytokine-serotonin interaction through IDO: A neurodegeneration hypothesis of depression. *Med Hypotheses*. 2003;61(5-6):519-525. doi:10.1016/S0306-9877(03)00207-X
92. Guillemin GJ, Smith DG, Kerr SJ, et al. Characterisation of kynurenine pathway metabolism in human astrocytes and implications in neuropathogenesis. *Redox Rep*. 2000;5(2-3):108-111. doi:10.1179/135100000101535375
93. Guillemin GJ, Smythe G, Takikawa O, Brew BJ. Expression of indoleamine 2,3-dioxygenase and production of quinolinic acid by human microglia, astrocytes, and neurons. *Glia*. 2005;49(1):15-23. doi:10.1002/glia.20090
94. Ganong AH, Cotman CW. Kynurenic acid and quinolinic acid act at N-methyl-D-aspartate receptors in the rat hippocampus. *J Pharmacol Exp Ther*. 1986;236(1):293-299.

95. Neale SA, Copeland CS, Salt TE. Effect of VGLUT inhibitors on glutamatergic synaptic transmission in the rodent hippocampus and prefrontal cortex. *Neurochem Int*. 2014;73(1):159-165. doi:10.1016/j.neuint.2013.10.001

96. Stone TW, Stoy N, Darlington LG. An expanding range of targets for kynurenine metabolites of tryptophan. *Trends Pharmacol Sci*. 2013;34(2):136-143. doi:10.1016/j.tips.2012.09.006

97. Müller N, Schwarz MJ. The immune-mediated alteration of serotonin and glutamate: Towards an integrated view of depression. *Mol Psychiatry*. 2007;12(11):988-1000. doi:10.1038/sj.mp.4002006

98. Carpenedo R, Pittaluga A, Cozzi A, et al. Presynaptic kynurenate-sensitive receptors inhibit glutamate release. *Eur J Neurosci*. 2001;13(11):2141-2147. doi:10.1046/j.0953-816X.2001.01592.x

99. Kessler M, Baudry M, Lynch G. Quinoxaline derivatives are high-affinity antagonists of the NMDA receptor-associated glycine sites. *Brain Res*. 1989;489(2):377-382. doi:10.1016/0006-8993(89)90875-5

100. Scharfman HE, Hodgkins PS, Lee SC, Schwarcz R. Quantitative differences in the effects of de novo produced and exogenous kynurenic acid in rat brain slices. *Neurosci Lett*. 1999;274(2):111-114. doi:10.1016/S0304-3940(99)00690-4

101. Jahr CE, Yoshioka K. Ia afferent excitation of motoneurones in the in vitro new-born rat spinal cord is selectively antagonized by kynurenate. *J Physiol*. 1986;370(1):515-530. doi:10.1113/jphysiol.1986.sp015948

102. Bijak M, Jarolimek W, Misgeld U. Effects of antagonists on quisqualate and nicotinic receptor-mediated currents of midbrain neurones in culture. *Br J Pharmacol*. 1991;102(3):699-705. doi:10.1111/j.1476-5381.1991.tb12236.x

103. Perrins R, Roberts A. Nicotinic and muscarinic ACh receptors in rhythmically active spinal neurones in the Xenopus laevis embryo. *J Physiol*. 1994;478(2):221-228. doi:10.1113/jphysiol.1994.sp020244

104. Bertolino M, Kellar KJ, Vicini S, Gillis RA. Nicotinic receptor mediates spontaneous GABA release in the rat dorsal motor nucleus of the vagus. *Neuroscience*. 1997;79(3):671-681. doi:10.1016/S0306-4522(97)00026-2

105. Hilmas C, Pereira EFR, Alkondon M, Rassoulpour A, Schwarcz R, Albuquerque EX. The brain metabolite kynurenic acid inhibits α7 nicotinic receptor activity and increases non-α7 nicotinic receptor expression: Physiopathological implications. *J Neurosci*. 2001;21(19):7463-7473. doi:10.1523/jneurosci.21-19-07463.2001

106. Stone TW. Kynurenic acid blocks nicotinic synaptic transmission to hippocampal interneurons in young rats. *Eur J Neurosci*. 2007;25(9):2656-2665. doi:10.1111/j.1460-9568.2007.05540.x

107. Dobelis P, Staley KJ, Cooper DC. Lack of modulation of Nicotinic Acetylcholine alpha-7 receptor currents by Kynurenic acid in adult hippocampal interneurons. *PLoS One*. 2012;7(7). doi:10.1371/journal.pone.0041108

108. Chu ZG, Zhou FM, Hablitz JJ. Nicotinic acetylcholine receptor-mediated synaptic potentials in rat neocortex. *Brain Res*. 2000;887(2):399-405. doi:10.1016/S0006-8993(00)03076-6

109. Arnaiz-Cot JJ, González JC, Sobrado M, et al. Allosteric modulation of α7 nicotinic receptors selectively depolarizes hippocampal interneurons, enhancing spontaneous GABAergic transmission. *Eur J Neurosci*. 2008;27(5):1097-1110. doi:10.1111/j.1460-9568.2008.06077.x

110. Mok MHS, Fricker AC, Weil A, Kew JNC. Electrophysiological characterisation of the actions of kynurenic acid at ligand-gated ion channels. *Neuropharmacology*. 2009;57(3):242-249. doi:10.1016/j.neuropharm.2009.06.003

111. Stone TW. Does kynurenic acid act on nicotinic receptors? An assessment of the evidence. *J Neurochem*. 2020;152(6):627-649. doi:10.1111/jnc.14907

112. Cosi C, Mannaioni G, Cozzi A, et al. G-protein coupled receptor 35 (GPR35) activation and inflammatory pain: Studies on the antinociceptive effects of kynurenic acid and zaprinast. *Neuropharmacology*. 2011;60(7-8):1227-1231. doi:10.1016/j.neuropharm.2010.11.014

113. Alfawaz H, Al-Onazi M, Bukhari SI, et al. The Independent and Combined Effects of Omega-3 and Vitamin B12 in Ameliorating Propionic Acid Induced Biochemical Features in Juvenile Rats as Rodent Model of Autism. *J Mol Neurosci*. 2018;66(3):403-413. doi:10.1007/s12031-018-1186-z

114. Romano KA, Vivas EI, Amador-Noguez D, Rey FE. Intestinal microbiota composition modulates choline bioavailability from diet and accumulation of the proatherogenic metabolite trimethylamine-N-oxide. *MBio*. 2015;6(2). doi:10.1128/mBio.02481-14

115. Bennett BJ, Vallim TQDA, Wang Z, et al. Trimethylamine-N-Oxide, a metabolite associated with atherosclerosis, exhibits complex genetic and dietary regulation. *Cell Metab*. 2013;17(1):49-60. doi:10.1016/j.cmet.2012.12.011
116. Koeth RA, Wang Z, Levison BS, et al. Intestinal microbiota metabolism of l-carnitine, a nutrient in red meat, promotes atherosclerosis. *Nat Med*. 2013;19(5):576-585. doi:10.1038/nm.3145
117. Del Rio D, Zimetti F, Caffarra P, et al. The Gut Microbial Metabolite Trimethylamine-N-Oxide Is Present in Human Cerebrospinal Fluid. *Nutrients*. 2017;9(10):1053. doi:10.3390/nu9101053
118. Xu R, Wang QQ. Towards understanding brain-gut-microbiome connections in Alzheimer's disease. *BMC Syst Biol*. 2016;10. doi:10.1186/s12918-016-0307-y
119. Tseng HC, Graves DJ. Natural methylamine osmolytes, trimethylamine N-oxide and betaine, increase tau-induced polymerization of microtubules. *Biochem Biophys Res Commun*. 1998;250(3):726-730. doi:10.1006/bbrc.1998.9382
120. Drewes G, Ebneth A, Preuss U, Mandelkow EM, Mandelkow E. MARK, a novel family of protein kinases that phosphorylate microtubule- associated proteins and trigger microtubule disruption. *Cell*. 1997;89(2):297-308. doi:10.1016/S0092-8674(00)80208-1
121. Praveenraj SS, Sonali S, Anand N, et al. The Role of a Gut Microbial-Derived Metabolite, Trimethylamine N-Oxide (TMAO), in Neurological Disorders. *Mol Neurobiol 2022 5911*. 2022;59(11):6684-6700. doi:10.1007/S12035-022-02990-5
122. Cakmak YO. Provotella-derived hydrogen sulfide, constipation, and neuroprotection in Parkinson's disease. *Mov Disord*. 2015;30(8):1151-1151. doi:10.1002/mds.26258
123. Kida K, Yamada M, Tokuda K, et al. Inhaled hydrogen sulfide prevents neurodegeneration and movement disorder in a mouse model of Parkinson's disease. *Antioxidants Redox Signal*. 2011;15(2):343-352. doi:10.1089/ars.2010.3671
124. Hu L-F, Lu M, Tiong CX, Dawe GS, Hu G, Bian J-S. Neuroprotective effects of hydrogen sulfide on Parkinson's disease rat models. *Aging Cell*. 2010;9(2):135-146. doi:10.1111/j.1474-9726.2009.00543.x
125. Clarke G, Stilling RM, Kennedy PJ, Stanton C, Cryan JF, Dinan TG. Minireview: Gut microbiota: The neglected endocrine organ. *Mol Endocrinol*. 2014;28(8):1221-1238. doi:10.1210/me.2014-1108

126. Hsiao EY, McBride SW, Hsien S, et al. Microbiota modulate behavioral and physiological abnormalities associated with neurodevelopmental disorders. *Cell*. 2013;155(7):1451-1463. doi:10.1016/j.cell.2013.11.024

127. Zhao Y, Qin G, Sun Z, Che D, Bao N, Zhang X. Effects of soybean agglutinin on intestinal barrier permeability and tight junction protein expression in weaned piglets. *Int J Mol Sci*. 2011;12(12):8502-8512. doi:10.3390/ijms12128502

128. Ying C, Chunmin Y, Qingsen L, et al. Effects of simulated weightlessness on tight junction protein occludin and Zonula Occluden-1 expression levels in the intestinal mucosa of rats. *J Huazhong Univ Sci Technol - Med Sci*. 2011;31(1):26-32. doi:10.1007/s11596-011-0145-5

129. Qiao Z, Li Z, Li J, Lu L, Lv Y, Li J. Bacterial translocation and change in intestinal permeability in patients after abdominal surgery. *J Huazhong Univ Sci Technol - Med Sci*. 2009;29(4):486-491. doi:10.1007/s11596-009-0419-3

130. Sheedy JR, Wettenhall REH, Scanlon D, et al. Increased D-lactic acid intestinal bacteria in patients with chronic fatigue syndrome. *In Vivo (Brooklyn)*. 2009;23(4):621-628.

131. Skowrońska M, Albrecht J. Alterations of blood brain barrier function in hyperammonemia: An overview. *Neurotox Res*. 2012;21(2):236-244. doi:10.1007/s12640-011-9269-4

132. Ninan J, Feldman L. Ammonia levels and hepatic encephalopathy in patients with known chronic liver disease. *J Hosp Med*. 2017;12(8):659-661. doi:10.12788/jhm.2794

133. Alleva FR, Balazs T. Age-dependent sensitivity of the rat to neurotoxic effects of streptomycin. *Toxicol Lett*. 1980;6(6):385-389. doi:10.1016/0378-4274(80)90111-3

134. Li W, Wu X, Hu X, et al. Structural changes of gut microbiota in Parkinson's disease and its correlation with clinical features. *Sci China Life Sci*. 2017;60(11):1223-1233. doi:10.1007/s11427-016-9001-4

135. Wikoff WR, Anfora AT, Liu J, et al. Metabolomics analysis reveals large effects of gut microflora on mammalian blood metabolites. *Proc Natl Acad Sci U S A*. 2009;106(10):3698-3703. doi:10.1073/pnas.0812874106

136. Cho JHJ, Irwin MR, Eisenberger NI, Lamkin DM, Cole SW. Transcriptomic predictors of inflammation-induced depressed mood. *Neuropsychopharmacology*. 2019;44(5):923-929. doi:10.1038/s41386-019-0316-9

137. Rainville JR, Tsyglakova M, Hodes GE. Deciphering sex differences in the immune system and depression. *Front Neuroendocrinol*. 2018;50:67-90. doi:10.1016/j.yfrne.2017.12.004

138. Pryce CR, Fontana A, Dantzer R, Capuron L. Depression in Autoimmune Diseases. *Curr Top Behav Neurosci*. 2017;31(31):139-154. doi:10.1007/7854_2016_7

139. Herbert TB, Cohen S. Depression and immunity: A meta-analytic review. *Psychol Bull*. 1993;113(3):472-486. doi:10.1037/0033-2909.113.3.472

140. Miller AH, Raison CL. The role of inflammation in depression: From evolutionary imperative to modern treatment target. *Nat Rev Immunol*. 2016;16(1):22-34. doi:10.1038/nri.2015.5

141. Shu-Kuang Hu, Mitcho YL, Rath NC. Effect of estradiol on interleukin 1 synthesis by macrophages. *Int J Immunopharmacol*. 1988;10(3):247-252. doi:10.1016/0192-0561(88)90055-0

142. Smith RS. The macrophage theory of depression. *Med Hypotheses*. 1991;35(4):298-306. doi:10.1016/0306-9877(91)90272-Z

143. Belowski D, Kowalski J, Madej A, et al. SHORT COMMUNICATION INFLUENCE OF ANTIDEPRESSANT DRUGS ON MACROPHAGE CYTOTOXIC ACTIVITY IN RATS Influence of antidepressant drugs on macrophage cytotoxic activity in rats. *Polish J Pharmacol Pol J Pharmacol*. 2004;56:837-842.

144. Wang X, Sundquist K, Palmér K, Hedelius A, Memon AA, Sundquist J. Macrophage Migration Inhibitory Factor and microRNA-451a in Response to Mindfulness-based Therapy or Treatment as Usual in Patients with Depression, Anxiety, or Stress and Adjustment Disorders. *Int J Neuropsychopharmacol*. 2018;21(6):513-521. doi:10.1093/ijnp/pyy001

145. Suzuki H, Savitz J, Kent Teague T, et al. Altered populations of natural killer cells, cytotoxic T lymphocytes, and regulatory T cells in major depressive disorder: Association with sleep disturbance. *Brain Behav Immun*. 2017;66:193-200. doi:10.1016/j.bbi.2017.06.011

146. Gimeno D, Kivimäki M, Brunner EJ, et al. Associations of C-reactive protein and interleukin-6 with cognitive symptoms of depression: 12-Year follow-up of the Whitehall II study. *Psychol Med*. 2009;39(3):413-423. doi:10.1017/S0033291708003723

147. Jamilian M, Samimi M, Mirhosseini N, et al. The influences of vitamin D and omega-3 co-supplementation on clinical, metabolic and genetic parameters in women with polycystic

ovary syndrome. *J Affect Disord*. 2018;238:32-38. doi:10.1016/j.jad.2018.05.027

148. Bufalino C, Hepgul N, Aguglia E, Pariante CM. The role of immune genes in the association between depression and inflammation: A review of recent clinical studies. *Brain Behav Immun*. 2013;31:31-47. doi:10.1016/j.bbi.2012.04.009
149. Khandaker GM, Zammit S, Burgess S, Lewis G, Jones PB. Association between a functional interleukin 6 receptor genetic variant and risk of depression and psychosis in a population-based birth cohort. *Brain Behav Immun*. 2018;69:264-272. doi:10.1016/j.bbi.2017.11.020
150. Hung YY, Kang HY, Huang KW, Huang TL. Association between toll-like receptors expression and major depressive disorder. *Psychiatry Res*. 2014;220(1-2):283-286. doi:10.1016/j.psychres.2014.07.074
151. Maes M, Lambrechts J, Bosmans E, et al. Evidence for a systemic immune activation during depression: Results of leukocyte enumeration by flow cytometry in conjunction with monoclonal antibody staining. *Psychol Med*. 1992;22(1):45-53. doi:10.1017/S0033291700032712
152. Grosse L, Hoogenboezem T, Ambrée O, et al. Deficiencies of the T and natural killer cell system in major depressive disorder. T regulatory cell defects are associated with inflammatory monocyte activation. *Brain Behav Immun*. 2016;54:38-44. doi:10.1016/j.bbi.2015.12.003
153. Eyre HA, Stuart MJ, Baune BT. A phase-specific neuroimmune model of clinical depression. *Prog Neuro-Psychopharmacology Biol Psychiatry*. 2014;54:265-274. doi:10.1016/j.pnpbp.2014.06.011
154. Barnes J, Mondelli V, Pariante CM. Genetic Contributions of Inflammation to Depression. *Neuropsychopharmacology*. 2017;42(1):81-98. doi:10.1038/npp.2016.169
155. Borzabadi S, Oryan S, Eidi A, et al. *The Effects of Probiotic Supplementation on Gene Expression Related to Inflammation, Insulin and Lipid in Patients with Parkinson's Disease: A Randomized, Double-Blind, Placebo-Controlled Trial*. Vol 21.; 2018.
156. Gaykema RPA, Goehler LE, Hansen MK, Maier SF, Watkins LR. Subdiaphragmatic vagotomy blocks interleukin-1β-induced fever but does not reduce IL-1β levels in the circulation. In: *Autonomic Neuroscience: Basic and Clinical*. Vol 85. Elsevier; 2000:72-77. doi:10.1016/S1566-0702(00)00222-8

157. Quan N, Banks WA. Brain-immune communication pathways. *Brain Behav Immun*. 2007;21(6):727-735. doi:10.1016/j.bbi.2007.05.005

158. Zong Y, Zhu S, Zhang S, Zheng G, Wiley JW, Hong S. Chronic stress and intestinal permeability: Lubiprostone regulates glucocorticoid receptor-mediated changes in colon epithelial tight junction proteins, barrier function, and visceral pain in the rodent and human. *Neurogastroenterol Motil*. 2019;31(2). doi:10.1111/nmo.13477

159. Vanuytsel T, Van Wanrooy S, Vanheel H, et al. Psychological stress and corticotropin-releasing hormone increase intestinal permeability in humans by a mast cell-dependent mechanism. *Gut*. 2014;63(8):1293-1299. doi:10.1136/gutjnl-2013-305690

160. Maes M, Kubera M, Leunis JC, Berk M. Increased IgA and IgM responses against gut commensals in chronic depression: Further evidence for increased bacterial translocation or leaky gut. *J Affect Disord*. 2012;141(1):55-62. doi:10.1016/j.jad.2012.02.023

161. Lee H, Chang MJ, Kim SH. Effects of poly-γ-glutamic acid on serum and brain concentrations of glutamate and GABA in diet-induced obese rats. *Nutr Res Pract*. 2010;4(1):23-29. doi:10.4162/nrp.2010.4.1.23

162. Lee K, Hwang S, Paik DJ, Kim WK, Kim JM, Youn J. Bacillus-derived poly-γ-glutamic acid reciprocally regulates the differentiation of T helper 17 and regulatory T cells and attenuates experimental autoimmune encephalomyelitis. *Clin Exp Immunol*. 2012;170(1):66-76. doi:10.1111/j.1365-2249.2012.04637.x

163. Unger MM, Spiegel J, Dillmann KU, et al. Short chain fatty acids and gut microbiota differ between patients with Parkinson's disease and age-matched controls. *Park Relat Disord*. 2016;32:66-72. doi:10.1016/j.parkreldis.2016.08.019

164. Zeng Q, Junli Gong, Liu X, et al. Gut dysbiosis and lack of short chain fatty acids in a Chinese cohort of patients with multiple sclerosis. *Neurochem Int*. 2019;129:104468. doi:10.1016/j.neuint.2019.104468

165. Caspani G, Swann J. Small talk: microbial metabolites involved in the signaling from microbiota to brain. *Curr Opin Pharmacol*. 2019;48:99-106. doi:10.1016/j.coph.2019.08.001

166. Wang L, Christophersen CT, Sorich MJ, Gerber JP, Angley MT, Conlon MA. Elevated fecal short chain fatty acid and ammonia concentrations in children with autism spectrum disorder. *Dig*

Dis Sci. 2012;57(8):2096-2102. doi:10.1007/s10620-012-2167-7

167. Dalile B, Van Oudenhove L, Vervliet B, Verbeke K. The role of short-chain fatty acids in microbiota–gut–brain communication. *Nat Rev Gastroenterol Hepatol*. 2019;16(8):461-478. doi:10.1038/s41575-019-0157-3
168. Karaki SI, Mitsui R, Hayashi H, et al. Short-chain fatty acid receptor, GPR43, is expressed by enteroendocrine cells and mucosal mast cells in rat intestine. *Cell Tissue Res*. 2006;324(3):353-360. doi:10.1007/s00441-005-0140-x
169. Maslowski KM, Vieira AT, Ng A, et al. Regulation of inflammatory responses by gut microbiota and chemoattractant receptor GPR43. *Nature*. 2009;461(7268):1282-1286. doi:10.1038/nature08530
170. Tazoe H, Otomo Y, Karaki SI, et al. Expression of short-chain fatty acid receptor GPR41 in the human colon. *Biomed Res*. 2009;30(3):149-156. doi:10.2220/biomedres.30.149
171. Dalile B, Van Oudenhove L, Vervliet B, Verbeke K. The role of short-chain fatty acids in microbiota–gut–brain communication. *Nat Rev Gastroenterol Hepatol*. May 2019:1. doi:10.1038/s41575-019-0157-3
172. Corrêa-Oliveira R, Fachi JL, Vieira A, Sato FT, Vinolo MAR. Regulation of immune cell function by short-chain fatty acids. *Clin Transl Immunol*. 2016;5(4). doi:10.1038/cti.2016.17
173. Chang P V., Hao L, Offermanns S, Medzhitov R. The microbial metabolite butyrate regulates intestinal macrophage function via histone deacetylase inhibition. *Proc Natl Acad Sci U S A*. 2014;111(6):2247-2252. doi:10.1073/pnas.1322269111
174. Gurav A, Sivaprakasam S, Bhutia YD, Boettger T, Singh N, Ganapathy V. Slc5a8, a Na+-coupled high-affinity transporter for short-chain fatty acids, is a conditional tumour suppressor in colon that protects against colitis and colon cancer under low-fibre dietary conditions. *Biochem J*. 2015;469(2):267-278. doi:10.1042/BJ20150242
175. Kim CH, Park J, Kim M. Gut Microbiota-Derived Short-Chain Fatty Acids, T Cells, and Inflammation. *Immune Netw*. 2014;14(6):277. doi:10.4110/in.2014.14.6.277
176. Park J, Kim M, Kang SG, et al. Short-chain fatty acids induce both effector and regulatory T cells by suppression of histone deacetylases and regulation of the mTOR-S6K pathway. *Mucosal Immunol*. 2015;8(1):80-93. doi:10.1038/mi.2014.44

177. Delgoffe GM, Kole TP, Zheng Y, et al. The mTOR Kinase Differentially Regulates Effector and Regulatory T Cell Lineage Commitment. *Immunity*. 2009;30(6):832-844. doi:10.1016/j.immuni.2009.04.014

178. Chen S, Liu D, Wu J, et al. Effect of inhibiting the signal of mammalian target of rapamycin on memory T cells. *Transplant Proc*. 2014;46(5):1642-1648. doi:10.1016/j.transproceed.2013.10.063

179. Arpaia N, Campbell C, Fan X, et al. Metabolites produced by commensal bacteria promote peripheral regulatory T-cell generation. *Nature*. 2013;504(7480):451-455. doi:10.1038/nature12726

180. Paley EL, Merkulova-Rainon T, Faynboym A, Shestopalov VI, Aksenoff I. Geographical distribution and diversity of gut microbial NADH: Ubiquinone oxidoreductase sequence associated with Alzheimer's disease. *J Alzheimer's Dis*. 2018;61(4):1531-1540. doi:10.3233/JAD-170764

181. Zheng S, Yu M, Lu X, et al. Urinary metabonomic study on biochemical changes in chronic unpredictable mild stress model of depression. *Clin Chim Acta*. 2010;411(3-4):204-209. doi:10.1016/j.cca.2009.11.003

182. Chen J jun, Zhou C juan, Zheng P, et al. Differential urinary metabolites related with the severity of major depressive disorder. *Behav Brain Res*. 2017;332:280-287. doi:10.1016/j.bbr.2017.06.012

183. Bampi SR, Casaril AM, Fronza MG, et al. The selenocompound 1-methyl-3-(phenylselanyl)-1H-indole attenuates depression-like behavior, oxidative stress, and neuroinflammation in streptozotocin-treated mice. *Brain Res Bull*. 2020;161:158-165. doi:10.1016/j.brainresbull.2020.05.008

184. Hamid HA, Ramli ANM, Yusoff MM. Indole alkaloids from plants as potential leads for antidepressant drugs: A mini review. *Front Pharmacol*. 2017;8(FEB). doi:10.3389/fphar.2017.00096

185. Bansal T, Alaniz RC, Wood TK, Jayaraman A. The bacterial signal indole increases epithelial-cell tight-junction resistance and attenuates indicators of inflammation. *Proc Natl Acad Sci U S A*. 2010;107(1):228-233. doi:10.1073/pnas.0906112107

186. Denison MS, Nagy SR. Activation of the Aryl Hydrocarbon Receptor by Structurally Diverse Exogenous and Endogenous Chemicals. *Annu Rev Pharmacol Toxicol*. 2003;43(1):309-334. doi:10.1146/annurev.pharmtox.43.100901.135828

187. Lamas B, Natividad JM, Sokol H. Aryl hydrocarbon receptor and intestinal immunity review-article. *Mucosal Immunol*. 2018;11(4). doi:10.1038/s41385-018-0019-2

188. Rothhammer V, Quintana FJ. The aryl hydrocarbon receptor: an environmental sensor integrating immune responses in health and disease. *Nat Rev Immunol*. February 2019:1. doi:10.1038/s41577-019-0125-8

189. Quintana FJ, Basso AS, Iglesias AH, et al. Control of Treg and TH17 cell differentiation by the aryl hydrocarbon receptor. *Nature*. 2008. doi:10.1038/nature06880

190. Rutz S, Noubade R, Eidenschenk C, et al. Transcription factor c-Maf mediates the TGF-β-dependent suppression of IL-22 production in TH17 cells. *Nat Immunol*. 2011. doi:10.1038/ni.2134

191. Schmidt J V., Bradfield CA. AH Receptor Signalling Pathways. *Annu Rev Cell Dev Biol*. 1996;12(1):55-89. doi:10.1146/annurev.cellbio.12.1.55

192. Vogel CFA, Sciullo E, Matsumura F. Involvement of RelB in aryl hydrocarbon receptor-mediated induction of chemokines. *Biochem Biophys Res Commun*. 2007;363(3):722-726. doi:10.1016/j.bbrc.2007.09.032

193. Dietrich C, Kaina B. The aryl hydrocarbon receptor (AhR) in the regulation of cell-cell contact and tumor growth. *Carcinogenesis*. 2010;31(8):1319-1328. doi:10.1093/carcin/bgq028

194. Xing X, Bi H, Chang AK, et al. SUMOylation of AhR modulates its activity and stability through inhibiting its ubiquitination. *J Cell Physiol*. 2012;227(12):3812-3819. doi:10.1002/jcp.24092

195. Hahn ME, Allan LL, Sherr DH. Regulation of constitutive and inducible AHR signaling: Complex interactions involving the AHR repressor. *Biochem Pharmacol*. 2009;77(4):485-497. doi:10.1016/J.BCP.2008.09.016

196. Ouyang W, Kolls JK, Zheng Y. The Biological Functions of T Helper 17 Cell Effector Cytokines in Inflammation. *Immunity*. 2008;28(4):454-467. doi:10.1016/j.immuni.2008.03.004

197. Qiu J, Guo X, Chen ZE, et al. Group 3 Innate Lymphoid Cells Inhibit T-Cell-Mediated Intestinal Inflammation through Aryl Hydrocarbon Receptor Signaling and Regulation of Microflora.

Immunity. 2013;39(2):386-399. doi:10.1016/J.IMMUNI.2013.08.002

198. Godinho-Silva C, Domingues RG, Rendas M, et al. Light-entrained and brain-tuned circadian circuits regulate ILC3s and gut homeostasis. *Nature*. 2019;574(7777):254-258. doi:10.1038/s41586-019-1579-3
199. Aguiniga LM, Yang W, Yaggie RE, Schaeffer AJ, Klumpp DJ. Acyloxyacyl hydrolase modulates depressive-like behaviors through aryl hydrocarbon receptor. *Am J Physiol Integr Comp Physiol*. 2019;317(2):R289-R300. doi:10.1152/ajpregu.00029.2019
200. Liu D, Ray B, Neavin DR, et al. Beta-defensin 1, aryl hydrocarbon receptor and plasma kynurenine in major depressive disorder: Metabolomics-informed genomics. *Transl Psychiatry*. 2018;8(1):1-13. doi:10.1038/s41398-017-0056-8
201. Mezrich JD, Fechner JH, Zhang X, Johnson BP, Burlingham WJ, Bradfield CA. An Interaction between Kynurenine and the Aryl Hydrocarbon Receptor Can Generate Regulatory T Cells. *J Immunol*. 2010. doi:10.4049/jimmunol.0903670
202. Zelante T, Iannitti RG, Cunha C, et al. Tryptophan catabolites from microbiota engage aryl hydrocarbon receptor and balance mucosal reactivity via interleukin-22. *Immunity*. 2013. doi:10.1016/j.immuni.2013.08.003
203. Rothhammer V, Borucki DM, Tjon EC, et al. Microglial control of astrocytes in response to microbial metabolites. *Nature*. 2018;557:724-728. doi:10.1038/s41586-018-0119-x
204. Turski MP, Turska M, Zgrajka W, Kuc D, Turski WA. Presence of kynurenic acid in food and honeybee products. *Amino Acids*. 2009;36(1):75-80. doi:10.1007/s00726-008-0031-z
205. Achtyes E, Keaton SA, Smart LA, et al. Inflammation and kynurenine pathway dysregulation in post-partum women with severe and suicidal depression. *Brain Behav Immun*. 2020;83:239-247. doi:10.1016/j.bbi.2019.10.017
206. Rudzki L, Ostrowska L, Pawlak D, et al. Probiotic Lactobacillus Plantarum 299v decreases kynurenine concentration and improves cognitive functions in patients with major depression: A double-blind, randomized, placebo controlled study. *Psychoneuroendocrinology*. 2019;100:213-222. doi:10.1016/j.psyneuen.2018.10.010
207. Heyes MP, Chen CY, Major EO, Saito K. Different kynurenine pathway enzymes limit quinolinic acid formation by various human cell types. *Biochem J*. 1997;326(2):351-356.

doi:10.1042/bj3260351

208. Zang X, Zheng X, Hou Y, et al. Regulation of proinflammatory monocyte activation by the kynurenine–AhR axis underlies immunometabolic control of depressive behavior in mice. *FASEB J*. 2017. doi:10.1096/fj.201700853R

209. Laumet G, Edralin JD, Chiang ACA, Dantzer R, Heijnen CJ, Kavelaars A. Resolution of inflammation-induced depression requires T lymphocytes and endogenous brain interleukin-10 signaling. *Neuropsychopharmacology*. 2018;43(13):2597-2605. doi:10.1038/s41386-018-0154-1

210. Hassanain HH, Chon SY, Gupta SL. Differential Regulation of Human Indoleamine 2,3-dioxygenase Gene Expression by Interferons-Gamma and -Alpha. Analysis of the Regulatory Region of the Gene and Identification of an Interferon-Gamma-Inducible DNA-binding Factor. *J Biol Chem*. 1993;268(7):5077-5084.

211. Chaves ACL, Cerávolo IP, Gomes JAS, Zani CL, Romanha AJ, Gazzinelli RT. IL-4 and IL-13 regulate the induction of indoleamine 2,3-dioxygenase activity and the control of Toxoplasma gondii replication in human fibroblasts activated with IFN-γ. *Eur J Immunol*. 2001;31(2):333-344. doi:10.1002/1521-4141(200102)31:2<333::AID-IMMU333>3.0.CO;2-X

212. Martin-Gallausiaux C, Larraufie P, Jarry A, et al. Butyrate Produced by Commensal Bacteria Down-Regulates Indolamine 2,3-Dioxygenase 1 (IDO-1) Expression via a Dual Mechanism in Human Intestinal Epithelial Cells. *Front Immunol*. 2018;9:2838. doi:10.3389/fimmu.2018.02838

213. Ohtake F, Baba A, Takada I, et al. Dioxin receptor is a ligand-dependent E3 ubiquitin ligase. *Nature*. 2007;446(7135):562-566. doi:10.1038/nature05683

214. Papoutsis AJ, Selmin OI, Borg JL, Romagnolo DF. Gestational exposure to the AhR agonist 2,3,7,8-tetrachlorodibenzo- *p* -dioxin induces BRCA-1 promoter hypermethylation and reduces BRCA-1 expression in mammary tissue of rat offspring: Preventive effects of resveratrol. *Mol Carcinog*. 2015;54(4):261-269. doi:10.1002/mc.22095

215. Frauenstein K, Sydlik U, Tigges J, et al. Evidence for a novel anti-apoptotic pathway in human keratinocytes involving the aryl hydrocarbon receptor, E2F1, and checkpoint kinase 1. *Cell Death Differ*. 2013;20(10):1425-1434. doi:10.1038/cdd.2013.102

216. Malhi GS, Mann JJ. Depression. *Lancet*. 2018;392(10161):2299-2312. doi:10.1016/S0140-6736(18)31948-2

217. Mulinari S. Monoamine Theories of Depression: Historical Impact on Biomedical Research. *http://dx.doi.org/101080/0964704X2011623917*. 2012;21(4):366-392. doi:10.1080/0964704X.2011.623917

218. Ban TA. Pharmacotherapy of depression: A historical analysis. *J Neural Transm*. 2001;108(6):707-716. doi:10.1007/S007020170047/METRICS

219. Tissot R. The Common Pathophysiology of Monoaminergic Psychoses: a New Hypothesis. *Neuropsychobiology*. 1975;1(4):243-260. doi:10.1159/000117498

220. Blier P. Neurobiology of Depression and Mechanism of Action of Depression Treatments. *J Clin Psychiatry*. 2016;77(3):26392. doi:10.4088/JCP.13097TX3C

221. Sampson TR, Debelius JW, Thron T, et al. Gut Microbiota Regulate Motor Deficits and Neuroinflammation in a Model of Parkinson's Disease. *Cell*. 2016;167(6):1469-1480.e12. doi:10.1016/j.cell.2016.11.018

222. Lammert CR, Frost EL, Bolte AC, et al. Cutting Edge: Critical Roles for Microbiota-Mediated Regulation of the Immune System in a Prenatal Immune Activation Model of Autism. *J Immunol*. 2018;201(3):845-850. doi:10.4049/JIMMUNOL.1701755

223. Jiang H yin, Zhang X, Yu Z he, et al. Altered gut microbiota profile in patients with generalized anxiety disorder. *J Psychiatr Res*. 2018;104:130-136. doi:10.1016/j.jpsychires.2018.07.007

224. Li N, Wang Q, Wang Y, et al. Fecal microbiota transplantation from chronic unpredictable mild stress mice donors affects anxiety-like and depression-like behavior in recipient mice via the gut microbiota-inflammation-brain axis. *https://doi.org/101080/10253890201916172 67*. 2019;22(5):592-602. doi:10.1080/10253890.2019.1617267

225. Pearson-Leary J, Zhao C, Bittinger K, et al. The gut microbiome regulates the increases in depressive-type behaviors and in inflammatory processes in the ventral hippocampus of stress vulnerable rats. *Mol Psychiatry 2019 255*. 2019;25(5):1068-1079. doi:10.1038/s41380-019-0380-x

226. Zheng P, Zeng B, Zhou C, et al. Gut microbiome remodeling induces depressive-like behaviors through a pathway mediated by the host's metabolism. *Mol Psychiatry 2016 216*.

2016;21(6):786-796. doi:10.1038/mp.2016.44

227. Merchak A, Gaultier A. Microbial metabolites and immune regulation: New targets for major depressive disorder. *Brain, Behav Immun - Heal*. 2020;9:100169. doi:10.1016/j.bbih.2020.100169

228. Smith AK, Ratanatharathorn A, Maihofer AX, et al. Epigenome-wide meta-analysis of PTSD across 10 military and civilian cohorts identifies methylation changes in AHRR. *Nat Commun 2020 111*. 2020;11(1):1-9. doi:10.1038/s41467-020-19615-x

229. Omenetti S, Pizarro TT. The Treg/Th17 axis: A dynamic balance regulated by the gut microbiome. *Front Immunol*. 2015;6(DEC):639. doi:10.3389/FIMMU.2015.00639/BIBTEX

230. Beurel E, Harrington LE, Jope RS. Inflammatory T helper 17 cells promote depression-like behavior in mice. *Biol Psychiatry*. 2013;73(7):622-630. doi:10.1016/j.biopsych.2012.09.021

231. Choi GB, Yim YS, Wong H, et al. The maternal interleukin-17a pathway in mice promotes autism-like phenotypes in offspring. *Science (80-)*. 2016;351(6276):933-939. doi:10.1126/SCIENCE.AAD0314/SUPPL_FILE/PAPV2.PDF

232. Westfall S, Caracci F, Zhao D, et al. Microbiota metabolites modulate the T helper 17 to regulatory T cell (Th17/Treg) imbalance promoting resilience to stress-induced anxiety- and depressive-like behaviors. *Brain Behav Immun*. 2021;91:350-368. doi:10.1016/J.BBI.2020.10.013

233. Saraykar S, Cao B, Barroso LS, et al. Plasma IL-17A levels in patients with late-life depression. *Rev Bras Psiquiatr*. 2017;40(2):212-215. doi:10.1590/1516-4446-2017-2299

234. Tsuboi H, Sakakibara H, Minamida Y, et al. Elevated Levels of Serum IL-17A in Community-Dwelling Women with Higher Depressive Symptoms. *Behav Sci (Basel, Switzerland)*. 2018;8(11). doi:10.3390/bs8110102

235. Köhler CA, Freitas TH, Maes M, et al. Peripheral cytokine and chemokine alterations in depression: a meta-analysis of 82 studies. *Acta Psychiatr Scand*. 2017;135(5):373-387. doi:10.1111/ACPS.12698

236. Davami MH, Baharlou R, Ahmadi Vasmehjani A, et al. Elevated IL-17 and TGF-β Serum Levels: A Positive Correlation between T-helper 17 Cell-Related Pro-Inflammatory Responses with Major Depressive Disorder. *Basic Clin Neurosci*. 2016;7(2):137-142.

doi:10.15412/J.BCN.03070207

237. Kim J-W, Kim Y-K, Hwang J-A, et al. Plasma Levels of IL-23 and IL-17 before and after Antidepressant Treatment in Patients with Major Depressive Disorder. *Psychiatry Investig*. 2013;10(3):294-299. doi:10.4306/pi.2013.10.3.294

238. LIU Y, HO RC-M, MAK A. The role of interleukin (IL)-17 in anxiety and depression of patients with rheumatoid arthritis. *Int J Rheum Dis*. 2012;15(2):183-187. doi:10.1111/j.1756-185X.2011.01673.x

239. Chevalier G, Siopi E, Guenin-Macé L, et al. Effect of gut microbiota on depressive-like behaviors in mice is mediated by the endocannabinoid system. *Nat Commun 2020 111*. 2020;11(1):1-15. doi:10.1038/s41467-020-19931-2

240. Jianguo L, Xueyang J, Cui W, Changxin W, Xuemei Q. Altered gut metabolome contributes to depression-like behaviors in rats exposed to chronic unpredictable mild stress. *Transl Psychiatry 2019 91*. 2019;9(1):1-14. doi:10.1038/s41398-019-0391-z

241. Schiering C, Wincent E, Metidji A, et al. Feedback control of AHR signalling regulates intestinal immunity. *Nat 2017 5427640*. 2017;542(7640):242-245. doi:10.1038/nature21080

242. Ambrée O, Ruland C, Zwanzger P, et al. Social defeat modulates T helper cell percentages in stress susceptible and resilient mice. *Int J Mol Sci*. 2019;20(14). doi:10.3390/ijms20143512

243. Alves de Lima K, Rustenhoven J, Da Mesquita S, et al. Meningeal γδ T cells regulate anxiety-like behavior via IL-17a signaling in neurons. *Nat Immunol 2020 2111*. 2020;21(11):1421-1429. doi:10.1038/s41590-020-0776-4

244. Yang X, Solomon S, Fraser LR, et al. Constitutive regulation of CYP1B1 by the aryl hydrocarbon receptor (AhR) in pre-malignant and malignant mammary tissue. *J Cell Biochem*. 2008;104(2):402-417. doi:10.1002/JCB.21630

245. Mathis A, Mamidanna P, Cury KM, et al. DeepLabCut: markerless pose estimation of user-defined body parts with deep learning. *Nat Neurosci 2018 219*. 2018;21(9):1281-1289. doi:10.1038/s41593-018-0209-y

246. Albert PR. Why is depression more prevalent in women? *J Psychiatry Neurosci*. 2015;40(4):219-221. doi:10.1503/JPN.150205

247. McEwen BS, Nasca C, Gray JD. Stress Effects on Neuronal Structure: Hippocampus, Amygdala,

and Prefrontal Cortex. *Neuropsychopharmacol 2016 411*. 2015;41(1):3-23. doi:10.1038/npp.2015.171

248. Behrens-Wittenberg E, Wedegaertner F. Identifying Individuals at High Risk for Permanent Disability From Depression and Anxiety. *Front Psychiatry*. 2020;11:740. doi:10.3389/FPSYT.2020.00740/BIBTEX
249. McGeachy MJ, Cua DJ, Gaffen SL. The IL-17 Family of Cytokines in Health and Disease. *Immunity*. 2019;50(4):892-906. doi:10.1016/J.IMMUNI.2019.03.021
250. Monin L, Gaffen SL. Interleukin 17 Family Cytokines: Signaling Mechanisms, Biological Activities, and Therapeutic Implications. *Cold Spring Harb Perspect Biol*. 2018;10(4):a028522. doi:10.1101/CSHPERSPECT.A028522
251. Khan D, Ahmed SA. Regulation of IL-17 in autoimmune diseases by transcriptional factors and microRNAs. *Front Genet*. 2015;6(JUL):236. doi:10.3389/FGENE.2015.00236/BIBTEX
252. Gałecka M, Bliźniewska-Kowalska K, Orzechowska A, et al. Inflammatory versus Anti-Inflammatory Profiles in Major Depressive Disorders—The Role of IL-17, IL-21, IL-23, IL-35 and Foxp3. *J Pers Med 2021, Vol 11, Page 66*. 2021;11(2):66. doi:10.3390/JPM11020066
253. KA Y, ITO R, NOZU R, et al. Establishment of a human microbiome- and immune system-reconstituted dual-humanized mouse model. *Exp Anim*. 2023:23-0025. doi:10.1538/EXPANIM.23-0025
254. Daoust L, Choi BSY, Agrinier AL, et al. Gnotobiotic mice housing conditions critically influence the phenotype associated with transfer of faecal microbiota in a context of obesity. *Gut*. 2023;72(5). doi:10.1136/GUTJNL-2021-326475
255. Zhu R, Fang Y, Li H, et al. Psychobiotic Lactobacillus plantarum JYLP-326 relieves anxiety, depression, and insomnia symptoms in test anxious college via modulating the gut microbiota and its metabolism. *Front Immunol*. 2023;14. doi:10.3389/FIMMU.2023.1158137
256. Kim S-Y, Woo S-Y, Raza S, et al. Association between gut microbiota and anxiety symptoms: A large population-based study examining sex differences. *J Affect Disord*. April 2023. doi:10.1016/J.JAD.2023.04.003
257. Radjabzadeh D, Bosch JA, Uitterlinden AG, et al. Gut microbiome-wide association study of depressive symptoms. *Nat Commun 2022 131*. 2022;13(1):1-10. doi:10.1038/s41467-022-

34502-3

258. Rieder R, Wisniewski PJ, Alderman BL, Campbell SC. Microbes and mental health: A review. *Brain Behav Immun*. 2017;66:9-17. doi:10.1016/j.bbi.2017.01.016

259. Bravo JA, Forsythe P, Chew M V., et al. Ingestion of Lactobacillus strain regulates emotional behavior and central GABA receptor expression in a mouse via the vagus nerve. *Proc Natl Acad Sci U S A*. 2011;108(38):16050-16055. doi:10.1073/pnas.1102999108

260. Jang HM, Lee KE, Kim DH. The Preventive and Curative Effects of Lactobacillus reuteri NK33 and Bifidobacterium adolescentis NK98 on Immobilization Stress-Induced Anxiety/Depression and Colitis in Mice. *Nutr 2019, Vol 11, Page 819*. 2019;11(4):819. doi:10.3390/NU11040819

261. Slykerman RF, Hood F, Wickens K, et al. Effect of Lactobacillus rhamnosus HN001 in Pregnancy on Postpartum Symptoms of Depression and Anxiety: A Randomised Double-blind Placebo-controlled Trial. *EBioMedicine*. 2017;24:159-165. doi:10.1016/J.EBIOM.2017.09.013

262. Xu M, Tian P, Zhu H, et al. Lactobacillus paracasei CCFM1229 and Lactobacillus rhamnosus CCFM1228 Alleviated Depression-and Anxiety-Related Symptoms of Chronic Stress-Induced Depression in Mice by Regulating Xanthine Oxidase Activity in the Brain. *Nutrients*. 2022;14(6). doi:10.3390/NU14061294/S1

263. Dewhirst FE, Chien CC, Paster BJ, et al. Phylogeny of the defined murine microbiota: altered Schaedler flora. *Appl Environ Microbiol*. 1999;65(8):3287-3292. doi:10.1128/AEM.65.8.3287-3292.1999

264. Rivet-Noor CR, Merchak AR, Li S, et al. Stress-induced despair behavior develops independently of the Ahr-RORγt axis in CD4 + cells. *Sci Reports 2022 121*. 2022;12(1):1-10. doi:10.1038/s41598-022-12464-2

265. Yang C, Fujita Y, Ren Q, Ma M, Dong C, Hashimoto K. Bifidobacterium in the gut microbiota confer resilience to chronic social defeat stress in mice OPEN. *Nat Publ Gr*. 2017. doi:10.1038/srep45942

266. Bercik P, Denou E, Collins J, et al. The Intestinal Microbiota Affect Central Levels of Brain-Derived Neurotropic Factor and Behavior in Mice. *Gastroenterology*. 2011;141(2):599-609.e3. doi:10.1053/J.GASTRO.2011.04.052

267. Hu Y, Xie Y, Wang Y, Chen X, Smith DE. Development and Characterization of a Novel

MouseLine Humanized for the Intestinal Peptide Transporter PEPT1. *Mol Pharm*. 2014;11(10):3737. doi:10.1021/MP500497P

268. Guo Y, Li H, Liu Z, et al. Impaired intestinal barrier function in a mouse model of hyperuricemia. *Mol Med Rep*. 2019;20(4):3292-3300. doi:10.3892/MMR.2019.10586/HTML
269. Luczynski P, Neufeld KAMV, Oriach CS, Clarke G, Dinan TG, Cryan JF. Growing up in a Bubble: Using Germ-Free Animals to Assess the Influence of the Gut Microbiota on Brain and Behavior. *Int J Neuropsychopharmacol*. 2016;19(8):1-17. doi:10.1093/IJNP/PYW020
270. Filiano AJ, Xu Y, Tustison NJ, et al. Unexpected role of interferon-γ in regulating neuronal connectivity and social behaviour. *Nature*. 2016;535(7612):425-429. doi:10.1038/NATURE18626
271. Stögerer T, Stäger S. Innate Immune Sensing by Cells of the Adaptive Immune System. *Front Immunol*. 2020;11:1081. doi:10.3389/FIMMU.2020.01081
272. Bose S, Aggarwal S, Singh DV, Acharya N. Extracellular vesicles: An emerging platform in gram-positive bacteria. *Microb Cell*. 2020;7(12):312. doi:10.15698/MIC2020.12.737
273. Guo M, Liu T, Guo JC, Jiang XL, Chen F, Gao YS. Study on serum cytokine levels in posttraumatic stress disorder patients. *Asian Pac J Trop Med*. 2012;5(4):323-325. doi:10.1016/S1995-7645(12)60048-0
274. Chourbaji S, Urani A, Inta I, et al. IL-6 knockout mice exhibit resistance to stress-induced development of depression-like behaviors. *Neurobiol Dis*. 2006;23(3):587-594. doi:10.1016/J.NBD.2006.05.001
275. Litteljohn D, Cummings A, Brennan A, et al. Interferon-gamma deficiency modifies the effects of a chronic stressor in mice: Implications for psychological pathology. *Brain Behav Immun*. 2010;24(3):462-473. doi:10.1016/J.BBI.2009.12.001
276. Gustafsson B. GERM-FREE REARING OF RATS. *Cells Tissues Organs*. 1946;2(3-4):376-391. doi:10.1159/000140222
277. Bhattarai Y, Kashyap PC. Germ-free mice model for studying host–microbial interactions. *Methods Mol Biol*. 2016;1438:123-135. doi:10.1007/978-1-4939-3661-8_8/COVER
278. Sharvin BL, Aburto MR, Cryan JF. Decoding the neurocircuitry of gut feelings: Region-specific microbiome-mediated brain alterations. *Neurobiol Dis*. 2023;179:106033.

doi:10.1016/J.NBD.2023.106033

279. Fiebiger U, Bereswill S, Heimesaat MM. Dissecting the interplay between intestinal microbiota and host immunity in health and disease: Lessons learned from germfree and gnotobiotic animal models. *Eur J Microbiol Immunol*. 2016;6(4):253-271. doi:10.1556/1886.2016.00036
280. Choi J, Kim YK, Han PL. Extracellular Vesicles Derived from Lactobacillus plantarum Increase BDNF Expression in Cultured Hippocampal Neurons and Produce Antidepressant-like Effects in Mice. *Exp Neurobiol*. 2019;28(2):158-171. doi:10.5607/EN.2019.28.2.158
281. Kawashima T, Hayashi K, Kosaka A, et al. Lactobacillus plantarum strain YU from fermented foods activates Th1 and protective immune responses. *Int Immunopharmacol*. 2011;11(12):2017-2024. doi:10.1016/J.INTIMP.2011.08.013
282. Cross ML. Immunoregulation by probiotic lactobacilli: pro-Th1 signals and their relevance to human health. *Clin Appl Immunol Rev*. 2002;3(3):115-125. doi:10.1016/S1529-1049(02)00057-0
283. Mohr DC, Genain C. Social support as a buffer in the relationship between treatment for depression and T-cell production of interferon gamma in patients with multiple sclerosis. *J Psychosom Res*. 2004;57(2):155-158. doi:10.1016/S0022-3999(03)00601-9
284. Pinto R, Belsky J, Baptista J, et al. Mothers' distress exposure and children's withdrawn behavior – A moderating role for the Interferon Gamma gene (IFNG). *Dev Psychobiol*. 2020;62(6):783-791. doi:10.1002/DEV.21955
285. Hashioka S, Klegeris A, Schwab C, McGeer PL. Interferon-γ-dependent cytotoxic activation of human astrocytes and astrocytoma cells. *Neurobiol Aging*. 2009;30(12):1924-1935. doi:10.1016/J.NEUROBIOLAGING.2008.02.019
286. Folkerth RD, Keefe RJ, Haynes RL, Trachtenberg FL, Volpe JJ, Kinney HC. Interferon-gamma expression in periventricular leukomalacia in the human brain. *Brain Pathol*. 2004;14(3):265-274. doi:10.1111/J.1750-3639.2004.TB00063.X
287. Compston A, Coles A. Multiple sclerosis. *Lancet*. 2008;372(9648):1502-1517. doi:10.1016/S0140-6736(08)61620-7
288. Aaen G, Belman A, Benson L, et al. Associations between the gut microbiota and host immune markers in pediatric multiple sclerosis and controls. *BMC Neurol*. 2016;16(1).

doi:10.1186/S12883-016-0703-3

289. Jangi S, Gandhi R, Cox LM, et al. Alterations of the human gut microbiome in multiple sclerosis. *Nat Commun 2016 71*. 2016;7(1):1-11. doi:10.1038/ncomms12015

290. Boziki MK, Kesidou E, Theotokis P, et al. Microbiome in multiple sclerosis; where are we, what we know and do not know. *Brain Sci*. 2020;10(4). doi:10.3390/brainsci10040234

291. Levinthal DJ, Rahman A, Nusrat S, O'Leary M, Heyman R, Bielefeldt K. Adding to the Burden: Gastrointestinal Symptoms and Syndromes in Multiple Sclerosis. *Mult Scler Int*. 2013;2013:1-9. doi:10.1155/2013/319201

292. Cox LM, Maghzi AH, Liu S, et al. Gut Microbiome in Progressive Multiple Sclerosis. *Ann Neurol*. 2021;89(6):1195-1211. doi:10.1002/ana.26084

293. Jangi S, Gandhi R, Cox LM, et al. Alterations of the human gut microbiome in multiple sclerosis. *Nat Commun*. 2016;7. doi:10.1038/ncomms12015

294. Barroso A, Mahler JV, Fonseca-Castro PH, Quintana FJ. The aryl hydrocarbon receptor and the gut-brain axis. *Cell Mol Immunol*. 2021;18:259-268. doi:10.1038/s41423-020-00585-5

295. Hubbard TD, Murray IA, Bisson WH, et al. Adaptation of the human aryl hydrocarbon receptor to sense microbiota-derived indoles. *Sci Rep*. 2015;5. doi:10.1038/srep12689

296. Jin U-H, Lee S-O, Sridharan G, et al. Microbiome-Derived Tryptophan Metabolites and Their Aryl Hydrocarbon Receptor-Dependent Agonist and Antagonist Activities. *Mol Pharmacol*. 2014;85(5). doi:10.1124/mol.113.091165

297. Denison MS, Faber SC. And now for something completely different: Diversity in ligand-dependent activation of Ah receptor responses. *Curr Opin Toxicol*. 2017;2. doi:10.1016/j.cotox.2017.01.006

298. Ott M, Avendanõ-Guzmán E, Ullrich E, et al. Laquinimod, a prototypic quinoline-3-carboxamide and aryl hydrocarbon receptor agonist, utilizes a CD155-mediated natural killer/dendritic cell interaction to suppress CNS autoimmunity. *J Neuroinflammation*. 2019;16(1):1-14. doi:10.1186/S12974-019-1437-0/FIGURES/6

299. Kaye J, Piryatinsky V, Birnberg T, et al. Laquinimod arrests experimental autoimmune encephalomyelitis by activating the aryl hydrocarbon receptor. *Proc Natl Acad Sci U S A*. 2016;113(41):E6145-E6152. doi:10.1073/PNAS.1607843113/ASSET/7F61B05C-3626-44AA-

A009-1BEAC4E447B3/ASSETS/GRAPHIC/PNAS.1607843113FIG07.JPEG

300. Korecka A, Dona A, Lahiri S, et al. Bidirectional communication between the Aryl hydrocarbon Receptor (AhR) and the microbiome tunes host metabolism. *npj Biofilms Microbiomes 2016 21*. 2016;2(1):1-10. doi:10.1038/npjbiofilms.2016.14

301. Yang F, DeLuca JAA, Menon R, et al. Effect of diet and intestinal AhR expression on fecal microbiome and metabolomic profiles. *Microb Cell Fact*. 2020;19(1):1-18. doi:10.1186/S12934-020-01463-5/TABLES/1

302. Murray IA, Nichols RG, Zhang L, Patterson AD, Perdew GH. Expression of the aryl hydrocarbon receptor contributes to the establishment of intestinal microbial community structure in mice. *Sci Rep*. 2016;6. doi:10.1038/srep33969

303. Fling RR, Zacharewski TR. Aryl hydrocarbon receptor (Ahr) activation by 2,3,7,8-tetrachlorodibenzo-p-dioxin (tcdd) dose-dependently shifts the gut microbiome consistent with the progression of non-alcoholic fatty liver disease. *Int J Mol Sci*. 2021;22(22). doi:10.3390/IJMS222212431/S1

304. Abdulla OA, Neamah W, Sultan M, et al. The Ability of AhR Ligands to Attenuate Delayed Type Hypersensitivity Reaction Is Associated With Alterations in the Gut Microbiota. *Front Immunol*. 2021;12:2505. doi:10.3389/FIMMU.2021.684727/BIBTEX

305. Kurschus FC. T cell mediated pathogenesis in EAE: Molecular mechanisms. *Biomed J*. 2015;38(3):183-193. doi:10.4103/2319-4170.155590

306. Ehrlich AK, Pennington JM, Bisson WH, Kolluri SK, Kerkvliet NI. TCDD, FICZ, and Other High Affinity AhR Ligands Dose-Dependently Determine the Fate of CD4+ T Cell Differentiation. *Toxicol Sci*. 2018;161(2):310-320. doi:10.1093/toxsci/kfx215

307. Hong CH, Lin SH, Clausen BE, Lee CH. Selective AhR knockout in langerin-expressing cells abates Langerhans cells and polarizes Th2/Tr1 in epicutaneous protein sensitization. *Proc Natl Acad Sci U S A*. 2020;117(23):12980-12990. doi:10.1073/PNAS.1917479117

308. Duarte JH, Di Meglio P, Hirota K, Ahlfors H, Stockinger B. Differential Influences of the Aryl Hydrocarbon Receptor on Th17 Mediated Responses in vitro and in vivo. *PLoS One*. 2013;8(11):e79819. doi:10.1371/JOURNAL.PONE.0079819

309. Quintana FJ, Murugaiyan G, Farez MF, et al. An endogenous aryl hydrocarbon receptor ligand

acts on dendritic cells and T cells to suppress experimental autoimmune encephalomyelitis. *Proc Natl Acad Sci U S A*. 2010;107(48):20768-20773. doi:10.1073/PNAS.1009201107/SUPPL_FILE/PNAS.201009201SI.PDF

310. Angelou CC, Wells AC, Vijayaraghavan J, et al. Differentiation of Pathogenic Th17 Cells Is Negatively Regulated by Let-7 MicroRNAs in a Mouse Model of Multiple Sclerosis. *Front Immunol*. 2020;10:3125. doi:10.3389/FIMMU.2019.03125/BIBTEX
311. Bhargava P, Smith MD, Mische L, et al. Bile acid metabolism is altered in multiple sclerosis and supplementation ameliorates neuroinflammation. *J Clin Invest*. 2020;130(7):3467. doi:10.1172/JCI129401
312. Sayin SI, Wahlström A, Felin J, et al. Gut microbiota regulates bile acid metabolism by reducing the levels of tauro-beta-muricholic acid, a naturally occurring FXR antagonist. *Cell Metab*. 2013;17(2):225-235. doi:10.1016/J.CMET.2013.01.003/ATTACHMENT/43CC1338-7BAD-48DF-9A11-35D134DCD18E/MMC1.PDF
313. Ma C, Han M, Heinrich B, et al. Gut microbiome–mediated bile acid metabolism regulates liver cancer via NKT cells. *Science (80-)*. 2018;360(6391). doi:10.1126/SCIENCE.AAN5931/SUPPL_FILE/AAN5931_MA_SM.PDF
314. MA Z, N S, PM M, et al. Butyrate suppresses colonic inflammation through HDAC1-dependent Fas upregulation and Fas-mediated apoptosis of T cells. *Am J Physiol Gastrointest Liver Physiol*. 2012;302(12). doi:10.1152/AJPGI.00543.2011
315. Kurita-Ochiai T, Ochiai K, Fukushima K. Butyric Acid-Induced T-Cell Apoptosis Is Mediated by Caspase-8 and -9 Activation in a Fas-Independent Manner. *Clin Diagn Lab Immunol*. 2001;8(2):325. doi:10.1128/CDLI.8.2.325-332.2001
316. Lewis ND, Patnaude LA, Pelletier J, et al. A GPBAR1 (TGR5) Small Molecule Agonist Shows Specific Inhibitory Effects on Myeloid Cell Activation In Vitro and Reduces Experimental Autoimmune Encephalitis (EAE) In Vivo. *PLoS One*. 2014;9(6):e100883. doi:10.1371/JOURNAL.PONE.0100883
317. Ho PP, Steinman L. Obeticholic acid, a synthetic bile acid agonist of the farnesoid X receptor, attenuates experimental autoimmune encephalomyelitis. *Proc Natl Acad Sci U S A*. 2016;113(6):1600. doi:10.1073/PNAS.1524890113

318. Duarte JH, Di Meglio P, Hirota K, Ahlfors H, Stockinger B. Differential Influences of the Aryl Hydrocarbon Receptor on Th17 Mediated Responses in vitro and in vivo. 2013;8(11):e79819. doi:10.1371/journal.pone.0079819
319. Shin JH, Moreno-Nieves UY, Zhang LH, et al. AHR Regulates NK Cell Migration via ASB2–Mediated Ubiquitination of Filamin A. *Front Immunol*. 2021;12:94. doi:10.3389/FIMMU.2021.624284/BIBTEX
320. Wang C, Ye Z, Kijlstra A, Zhou Y, Yang P. Activation of the aryl hydrocarbon receptor affects activation and function of human monocyte-derived dendritic cells. *Clin Exp Immunol*. 2014;177(2):521-530. doi:10.1111/CEI.12352
321. Quintana FJ, Murugaiyan G, Farez MF, et al. An endogenous aryl hydrocarbon receptor ligand acts on dendritic cells and T cells to suppress experimental autoimmune encephalomyelitis. *Proc Natl Acad Sci U S A*. 2010;107(48):20768-20773. doi:10.1073/pnas.1009201107
322. Lee Y, Awasthi A, Yosef N, et al. Induction and molecular signature of pathogenic T H 17 cells. *Nat Immunol*. 2012. doi:10.1038/ni.2416
323. McAleer JP, Fan J, Roar B, Primerano DA, Denvir J. Cytokine Regulation in Human CD4 T Cells by the Aryl Hydrocarbon Receptor and Gq-Coupled Receptors. *Sci Reports 2018 81*. 2018;8(1):1-12. doi:10.1038/s41598-018-29262-4
324. Rothhammer V, Mascanfroni ID, Bunse L, et al. Type i interferons and microbial metabolites of tryptophan modulate astrocyte activity and central nervous system inflammation via the aryl hydrocarbon receptor. *Nat Med*. 2016;22(6). doi:10.1038/nm.4106
325. Parker A, Fonseca S, Carding SR. Gut microbes and metabolites as modulators of blood-brain barrier integrity and brain health. *Gut Microbes*. 2020;11(2):135. doi:10.1080/19490976.2019.1638722
326. Keogh CE, Kim DHJ, Pusceddu MM, et al. Myelin as a regulator of development of the microbiota-gut-brain axis. *Brain Behav Immun*. 2021;91:437-450. doi:10.1016/J.BBI.2020.11.001
327. Hoban AE, Stilling RM, Ryan FJ, et al. Regulation of prefrontal cortex myelination by the microbiota. *Transl Psychiatry*. 2016;6(4). doi:10.1038/TP.2016.42
328. Lycke NY, Bemark M. The regulation of gut mucosal IgA B-cell responses: recent

developments. *Mucosal Immunol 2017 106*. 2017;10(6):1361-1374. doi:10.1038/mi.2017.62

329. Vaidyanathan B, Chaudhry A, Yewdell WT, et al. The aryl hydrocarbon receptor controls cell-fate decisions in B cells. *J Exp Med*. 2017;214(1):197. doi:10.1084/JEM.20160789
330. Araujo A, Safronova A, Burger E, et al. Ifn-g mediates paneth cell death via suppression of mtor. *Elife*. 2021;10. doi:10.7554/ELIFE.60478
331. Kamioka M, Goto Y, Nakamura K, et al. Intestinal commensal microbiota and cytokines regulate Fut2+ Paneth cells for gut defense. *Proc Natl Acad Sci U S A*. 2022;119(3). doi:10.1073/PNAS.2115230119/SUPPL_FILE/PNAS.2115230119.SAPP.PDF
332. Šarenac TM, Mikov M. Bile acid synthesis: From nature to the chemical modification and synthesis and their applications as drugs and nutrients. *Front Pharmacol*. 2018;9(SEP):939. doi:10.3389/FPHAR.2018.00939/BIBTEX
333. Duc D, Vigne S, Bernier-Latmani J, et al. Disrupting Myelin-Specific Th17 Cell Gut Homing Confers Protection in an Adoptive Transfer Experimental Autoimmune Encephalomyelitis. *Cell Rep*. 2019;29(2):378-390.e4. doi:10.1016/J.CELREP.2019.09.002
334. JG B, MV T, NL D, et al. Regulation of autoimmune myocarditis by host responses to the microbiome. *Exp Mol Pathol*. 2017;103(2):141-152. doi:10.1016/J.YEXMP.2017.08.003
335. Bergot AS, Giri R, Thomas R. The microbiome and rheumatoid arthritis. *Best Pract Res Clin Rheumatol*. 2019;33(6). doi:10.1016/J.BERH.2020.101497
336. KL G, BP A, EMM Q. The microbiome and inflammatory bowel disease. *J Allergy Clin Immunol*. 2020;145(1):16-27. doi:10.1016/J.JACI.2019.11.003
337. J O-R, TO K, LH K. The Gut Microbiome and Multiple Sclerosis. *Cold Spring Harb Perspect Med*. 2018;8(6). doi:10.1101/CSHPERSPECT.A029017
338. YJ H, HA B. The microbiome in asthma. *J Allergy Clin Immunol*. 2015;135(1):25-30. doi:10.1016/J.JACI.2014.11.011
339. Duncan ID, Radcliff AB, Heidari M, Kidd G, August BK, Wierenga LA. The adult oligodendrocyte can participate in remyelination. *Proc Natl Acad Sci U S A*. 2018;115(50):E11807-E11816. doi:10.1073/PNAS.1808064115/SUPPL_FILE/PNAS.1808064115.SAPP.PDF
340. Neely SA, Williamson JM, Klingseisen A, et al. New oligodendrocytes exhibit more abundant and accurate myelin regeneration than those that survive demyelination. *Nat Neurosci 2022*

254. 2022;25(4):415-420. doi:10.1038/s41593-021-01009-x

341. Fernández-Castañeda A, Chappell MS, Rosen DA, et al. The active contribution of OPCs to neuroinflammation is mediated by LRP1. *Acta Neuropathol*. 2020;139(2):365-382. doi:10.1007/S00401-019-02073-1/METRICS

342. Kirby L, Jin J, Cardona JG, et al. Oligodendrocyte precursor cells present antigen and are cytotoxic targets in inflammatory demyelination. *Nat Commun 2019 101*. 2019;10(1):1-20. doi:10.1038/s41467-019-11638-3

343. Beiter RM, Rivet-Noor C, Merchak AR, et al. Evidence for oligodendrocyte progenitor cell heterogeneity in the adult mouse brain. *Sci Reports 2022 121*. 2022;12(1):1-15. doi:10.1038/s41598-022-17081-7

344. Aloisi F, Penna G, Cerase J, Menéndez Iglesias B, Adorini L. IL-12 production by central nervous system microglia is inhibited by astrocytes. *J Immunol*. 1997;159(4):1604-1612. doi:10.4049/JIMMUNOL.159.4.1604

345. Andreadou M, Ingelfinger F, Feo D De, et al. Neuroprotective tissue adaptation induced by IL-12 attenuates CNS inflammation. *bioRxiv*. September 2022:2022.09.14.506749. doi:10.1101/2022.09.14.506749

346. Turka LA, Goodman RE, Rutkowski JL, et al. Interleukin 12: A potential link between nerve cells and the immune response in inflammatory disorders. *Mol Med*. 1995;1(6):690-699. doi:10.1007/BF03401609/FIGURES/7

347. Ireland DDC, Reiss CS. Expression of IL-12 Receptor by Neurons. *https://home.liebertpub.com/vim*. 2004;17(3):411-422. doi:10.1089/VIM.2004.17.411

348. Sorensen EW, Gerber SA, Frelinger JG, Lord EM. IL-12 Suppresses Vascular Endothelial Growth Factor Receptor 3 Expression on Tumor Vessels by Two Distinct IFN-γ–Dependent Mechanisms. *J Immunol*. 2010;184(4):1858. doi:10.4049/JIMMUNOL.0903210

349. Fancy SPJ, Baranzini SE, Zhao C, et al. Dysregulation of the Wnt pathway inhibits timely myelination and remyelination in the mammalian CNS. *Genes Dev*. 2009;23(13):1571-1585. doi:10.1101/GAD.1806309

350. Kessaris N, Fogarty M, Iannarelli P, Grist M, Wegner M, Richardson WD. Competing waves of oligodendrocytes in the forebrain and postnatal elimination of an embryonic lineage. *Nat*

Neurosci 2005 92. 2005;9(2):173-179. doi:10.1038/nn1620

351. Jakovcevski I, Filipovic R, Mo Z, Rakic S, Zecevic N. Oligodendrocyte Development and the Onset of Myelination in the Human Fetal Brain. *Front Neuroanat*. 2009;3(JUN). doi:10.3389/NEURO.05.005.2009
352. Flechsig Of Leipsic P. Developmental (Myelogenetic) Localisation of the Cerebral Cortex in the Human Subject. *Lancet*. 1901;158(4077):1027-1030. doi:10.1016/S0140-6736(01)01429-5
353. Hill RA, Li AM, Grutzendler J. Lifelong cortical myelin plasticity and age-related degeneration in the live mammalian brain. *Nat Neurosci*. 2018;21(5):683. doi:10.1038/S41593-018-0120-6
354. Hughes EG, Orthmann-Murphy JL, Langseth AJ, Bergles DE. Myelin remodeling through experience-dependent oligodendrogenesis in the adult somatosensory cortex. *Nat Neurosci*. 2018;21(5):696. doi:10.1038/S41593-018-0121-5
355. Miller JA, Ding SL, Sunkin SM, et al. Transcriptional landscape of the prenatal human brain. *Nature*. 2014;508(7495):199-206. doi:10.1038/NATURE13185
356. Jäkel S, Agirre E, Mendanha Falcão A, et al. Altered human oligodendrocyte heterogeneity in multiple sclerosis. *Nat 2019 5667745*. 2019;566(7745):543-547. doi:10.1038/s41586-019-0903-2
357. Schneeberger S, Kim SJ, Eede P, et al. The neuroinflammatory interleukin-12 signaling pathway drives Alzheimer's disease-like pathology by perturbing oligodendrocyte survival and neuronal homeostasis. *bioRxiv*. April 2021:2021.04.25.441313. doi:10.1101/2021.04.25.441313
358. Morgan ML, Teo W, Hernandez Y, et al. Cuprizone-induced Demyelination in Mouse Brain is not due to Depletion of Copper. doi:10.1177/17590914221126367
359. Taylor LC, Gilmore W, Ting JPY, Matsushima GK. Cuprizone induces similar demyelination in male and female C57BL/6 mice and results in disruption of the estrous cycle. *J Neurosci Res*. 2010;88(2):391-402. doi:10.1002/JNR.22215
360. Ünsal C, Özcan M. Neurotoxicity of Cuprizone in Female and Male Rats: Electrophysiological Observations. *Neurophysiology*. 2018;50(2):108-115. doi:10.1007/S11062-018-9724-4/METRICS
361. Taylor LC, Matsushima GK, Grobin C, Lysle D, Markovic-Plese S, Ting JPY. Sex differences and the protective influence of estrogen in a mouse model of demyelinating disease. 2008.

doi:10.17615/5T0S-5K20

362. Pujantell M, Altfeld M. Consequences of sex differences in Type I IFN responses for the regulation of antiviral immunity. *Front Immunol*. 2022;13:5303. doi:10.3389/FIMMU.2022.986840/BIBTEX

363. Eede P, Obst J, Benke E, et al. Interleukin-12/23 deficiency differentially affects pathology in male and female Alzheimer's disease-like mice. *EMBO Rep*. 2020;21(3):e48530. doi:10.15252/EMBR.201948530

364. Mon KJY, Goldsmith E, Watson NB, Wang J, Smith NL, Rudd BD. Differential Sensitivity to IL-12 Drives Sex-Specific Differences in the CD8+ T Cell Response to Infection. *ImmunoHorizons*. 2019;3(4):121. doi:10.4049/IMMUNOHORIZONS.1800066

365. Vollmer TL, Wynn DR, Alam SM, Valdes J. A phase 2, 24-week, randomized, placebo-controlled, double-blind study examining the efficacy and safety of an anti-interleukin-12 and -23 monoclonal antibody in patients with relapsing–remitting or secondary progressive multiple sclerosis. *http://dx.doi.org/101177/1352458510384496*. 2010;17(2):181-191. doi:10.1177/1352458510384496

366. Segal BM, Constantinescu CS, Raychaudhuri A, Kim L, Fidelus-Gort R, Kasper LH. Repeated subcutaneous injections of IL12/23 p40 neutralising antibody, ustekinumab, in patients with relapsing-remitting multiple sclerosis: a phase II, double-blind, placebo-controlled, randomised, dose-ranging study. *Lancet Neurol*. 2008;7(9):796-804. doi:10.1016/S1474-4422(08)70173-X

367. Longbrake EE, Racke MK. Why did IL-12/IL-23 antibody therapy fail in multiple sclerosis? *http://dx.doi.org/101586/1473717593319*. 2014;9(3):319-321. doi:10.1586/14737175.9.3.319

368. Nussinov R, Papin JA. How can computation advance microbiome research? *PLoS Comput Biol*. 2017;13(9). doi:10.1371/journal.pcbi.1005547

369. Kunzelmann K, Mall M. Electrolyte transport in the mammalian colon: Mechanisms and implications for disease. *Physiol Rev*. 2002;82(1):245-289. doi:10.1152/physrev.00026.2001

370. Lee PP, Fitzpatrick DR, Beard C, et al. A critical role for Dnmt1 and DNA methylation in T cell development, function, and survival. *Immunity*. 2001;15(5):763-774. doi:10.1016/S1074-7613(01)00227-8

371. Walisser JA, Glover E, Pande K, Liss AL, Bradfield CA. Aryl hydrocarbon receptor-dependent liver development and hepatotoxicity are mediated by different cell types. *Proc Natl Acad Sci U S A*. 2005;102(49):17858-17863. doi:10.1073/PNAS.0504757102/ASSET/B629CAB0-231D-4792-BC40-71780F173F40/ASSETS/GRAPHIC/ZPQ0470502960006.JPEG

372. Fox C, Merali Z, Harrison C. Therapeutic and protective effect of environmental enrichment against psychogenic and neurogenic stress. *Behav Brain Res*. 2006;175(1):1-8. doi:10.1016/J.BBR.2006.08.016

373. Fernández-Castañeda A, Chappell MS, Rosen DA, et al. The active contribution of OPCs to neuroinflammation is mediated by LRP1. *Acta Neuropathol*. 2020;139(2):365-382. doi:10.1007/s00401-019-02073-1

374. Luxem K, Mocellin P, Fuhrmann F, et al. Identifying behavioral structure from deep variational embeddings of animal motion. *Commun Biol 2022 51*. 2022;5(1):1-15. doi:10.1038/s42003-022-04080-7

375. Seki SM, Posyniak K, McCloud R, et al. Modulation of PKM activity affects the differentiation of TH17 cells. *Sci Signal*. 2020;13(655). doi:10.1126/SCISIGNAL.AAY9217/SUPPL_FILE/AAY9217_SM.PDF

376. Bolyen E, Rideout JR, Dillon MR, et al. Reproducible, interactive, scalable and extensible microbiome data science using QIIME 2. *Nat Biotechnol 2019 378*. 2019;37(8):852-857. doi:10.1038/s41587-019-0209-9

377. Callahan BJ, McMurdie PJ, Rosen MJ, Han AW, Johnson AJA, Holmes SP. DADA2: High-resolution sample inference from Illumina amplicon data. *Nat Methods 2016 137*. 2016;13(7):581-583. doi:10.1038/nmeth.3869

378. McMurdie PJ, Holmes S. phyloseq: An R Package for Reproducible Interactive Analysis and Graphics of Microbiome Census Data. *PLoS One*. 2013;8(4):e61217. doi:10.1371/JOURNAL.PONE.0061217

379. Merchak AR, Cahill HJ, Brown LC, et al. The activity of the aryl hydrocarbon receptor in T cells tunes the gut microenvironment to sustain autoimmunity and neuroinflammation. *PLOS Biol*. 2023;21(2):e3002000. doi:10.1371/JOURNAL.PBIO.3002000

380. Seki SM, Stevenson M, Rosen AM, et al. Lineage-Specific Metabolic Properties and

Vulnerabilities of T Cells in the Demyelinating Central Nervous System. *J Immunol*. 2017;198(12):4607-4617. doi:10.4049/jimmunol.1600825

381. Remick DG, Bolgos GR, Siddiqui J, Shin J, Nemzek JA. Six at six: interleukin-6 measured 6 h after the initiation of sepsis predicts mortality over 3 days. *Shock*. 2002;17(6):463-467. doi:10.1097/00024382-200206000-00004
382. Chuang TY, Guo Y, Seki SM, et al. LRP1 expression in microglia is protective during CNS autoimmunity. *Acta Neuropathol Commun*. 2016;4(1):68. doi:10.1186/S40478-016-0343-2
383. Castellano-Escuder P, Andrés-Lacueva C, Sánchez-Pla A. POMA: User-friendly Workflow for Metabolomics and Proteomics Data Analysis. *PLoS Comput Biol*. 2021;17(7):e1009148.
384. Hartman AL, Lough DM, Barupal DK, et al. Human gut microbiome adopts an alternative state following small bowel transplantation. *Proc Natl Acad Sci U S A*. 2009;106(40):17187-17192. doi:10.1073/PNAS.0904847106
385. Barupal DK, Haldiya PK, Wohlgemuth G, et al. MetaMapp: mapping and visualizing metabolomic data by integrating information from biochemical pathways and chemical and mass spectral similarity. *BMC Bioinformatics*. 2012;13(1):1-15. doi:10.1186/1471-2105-13-99/FIGURES/5
386. Sachs HH, Bercury KK, Popescu DC, Narayanan SP, Macklin WB. A new model of Cuprizone-Mediated demyelination/remyelination. *ASN Neuro*. 2014;6(5). doi:10.1177/1759091414551955/ASSET/IMAGES/LARGE/10.1177_1759091414551955-FIG7.JPEG
387. Emery B, Dugas JC. Purification of Oligodendrocyte Lineage Cells from Mouse Cortices by Immunopanning. *Cold Spring Harb Protoc*. 2013;2013(9):pdb.prot073973. doi:10.1101/PDB.PROT073973

Supplementary Materials

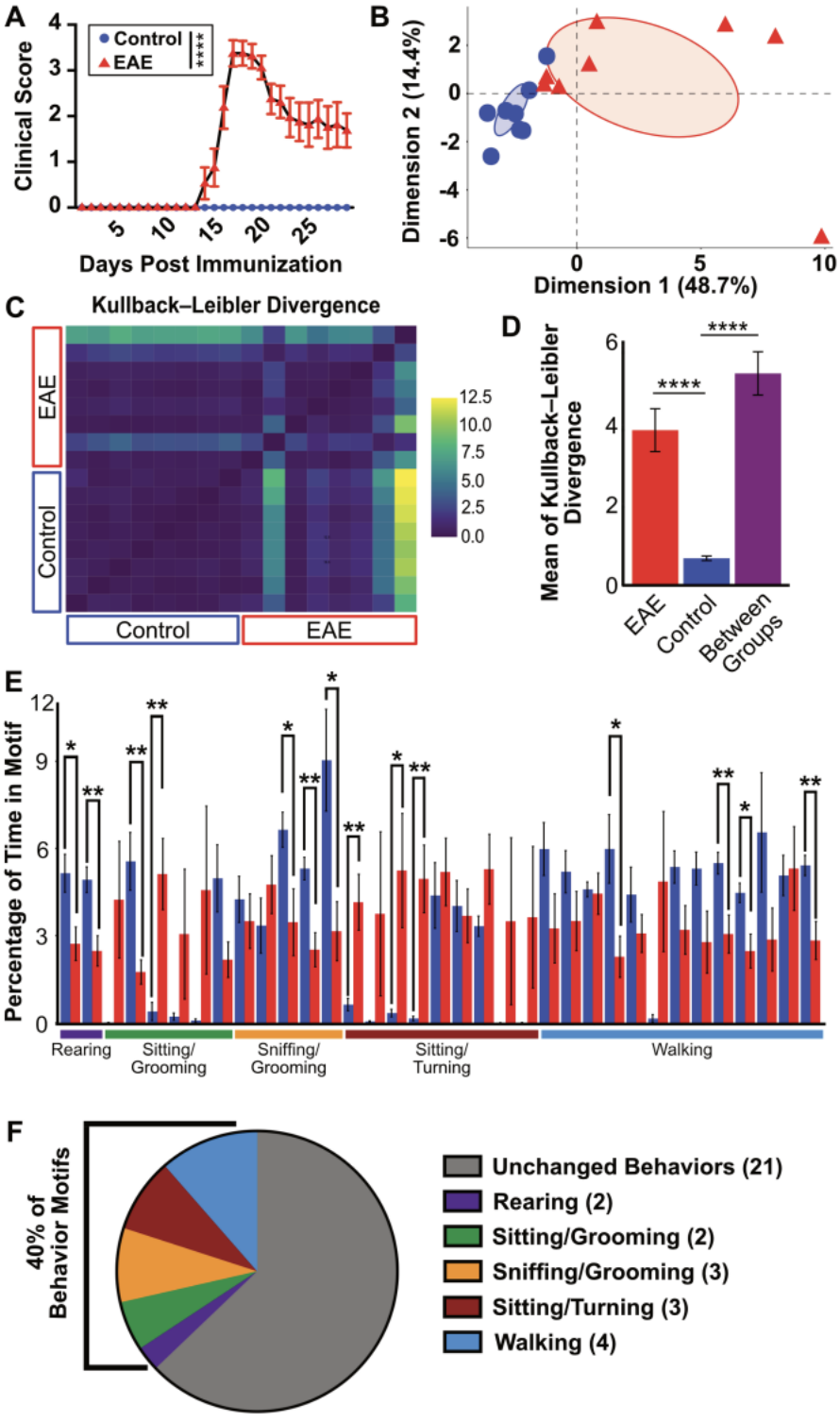

Supplemental Figure 2.1: Validation of DeepLabCut in EAE Mice. (A) Average clinical scores of EAE and control mice (n=8/group). Mann-Whitney U Test (p= <0.0001 1) . (B) PCA and (C) Kullback-Leibler Divergence plots representing differences between EAE and control animals (n=8/group). (D) Means of Kullback-Leibler Divergence scores in control mice, EAE mice, and between groups. Multiple T tests (p= <0.0001). (E) Percentage and grouping of motif usage by EAE vs control mice in DeepLabCut analyzed videos (n=8/group). T tests (Supplemental Table 1). (F) Quantification and grouping of significantly changed motifs (by % usage) in EAE vs control mice. N=1, All female mice.

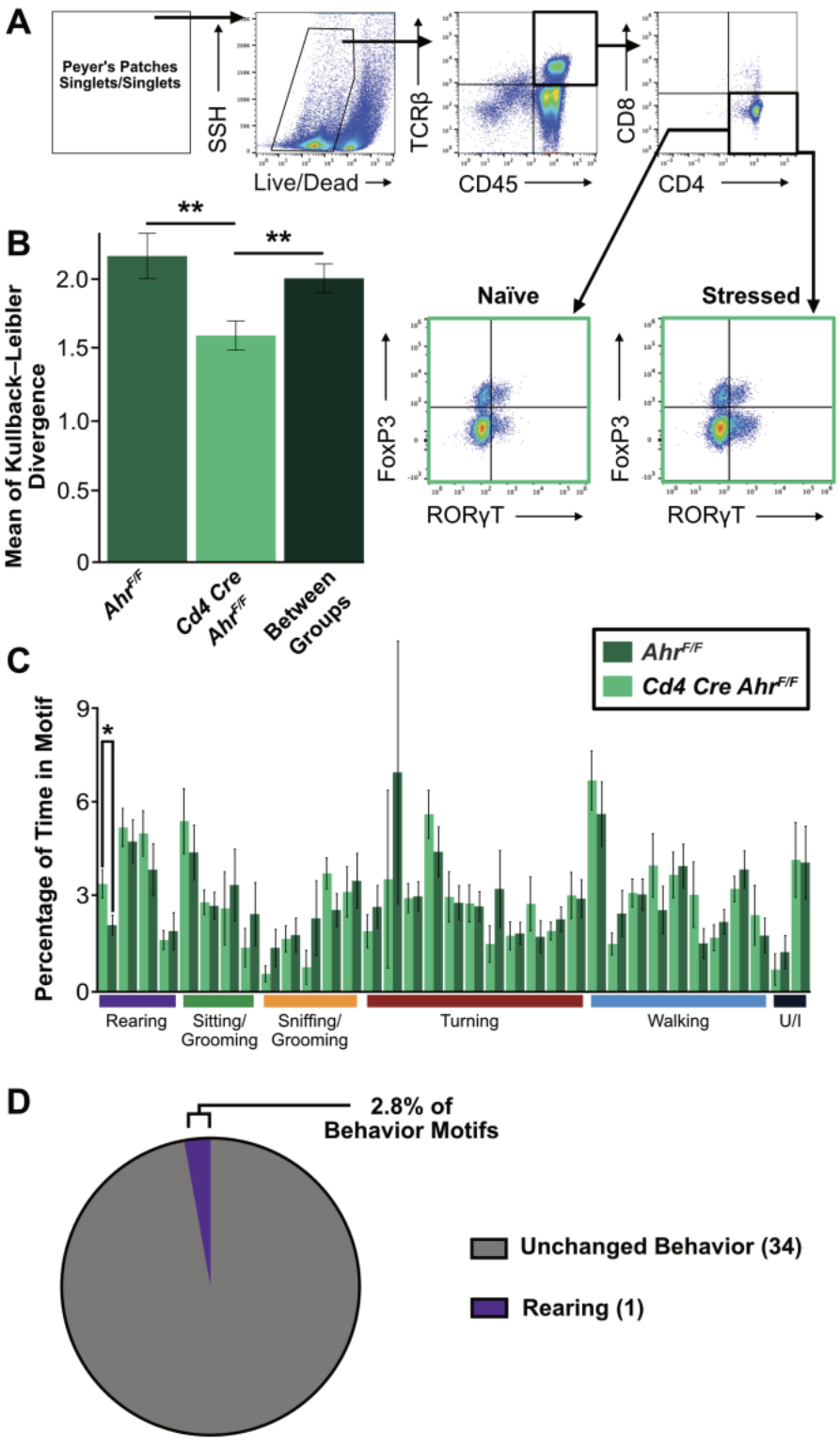
A
Peyer's Patches
Singlets/Singlets
SSH
Live/Dead
TCRβ
CD45
CD8
CD4
B
Mean of Kullback–Leibler Divergence
2.0
1.5
1.0
0.5
0
**
**
Ahr F/F
Cd4 Cre Ahr F/F
Between Groups
Naïve
Stressed
FoxP3
RORγT
C
Ahr F/F
Cd4 Cre Ahr F/F
Percentage of Time in Motif
9
6
3
0
*
Rearing
Sitting/ Grooming
Sniffing/ Grooming
Turning
Walking
U/I
D
2.8% of Behavior Motifs
Unchanged Behavior (34)
Rearing (1)

Supplemental Figure 2.2: *Ahr* Depletion does not Impact Subtle Behaviors After Stress Exposure. (A) Representative flow cytometry gating strategy for Th17s in naïve vs stressed mice. (B) Graphical quantification of mean of Kullback-Leibler Divergence scores in *Ahr* KO, littermate controls, and between groups. Multiple T tests (p= 0.0034 and p= 0.0056). (C) Percentage and grouping of motif usage from DeepLabCut analyzed behaviors between *Ahr* KO and littermate controls (n= 13-14/group). T tests (Supplemental Table 1). (D) Percentage and grouping of significantly changed motifs (by % usage) between *Ahr* KO and control groups.

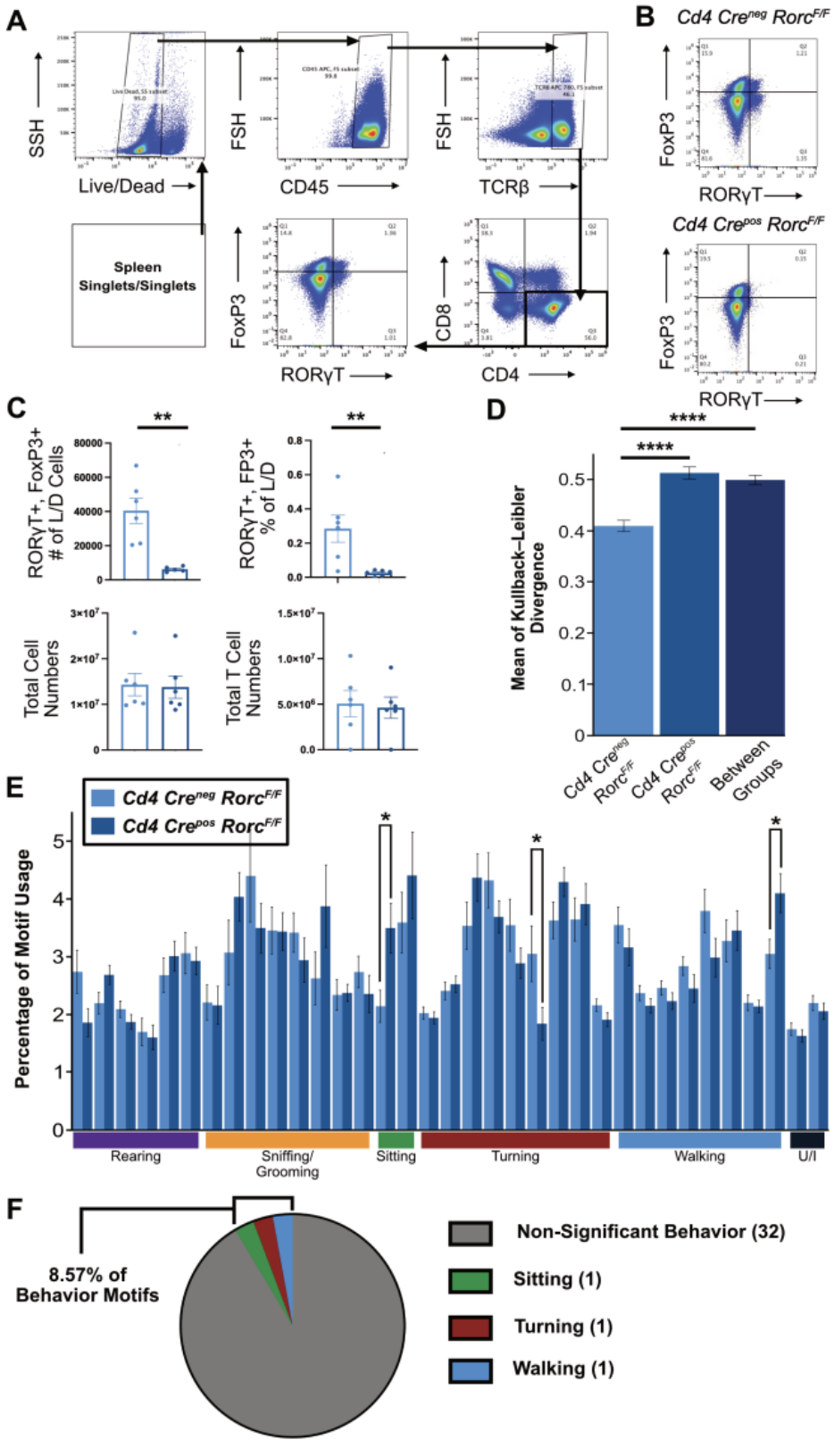
A
SSH
Live/Dead
FSH
CD45
FSH
TCRβ
Spleen
Singlets/Singlets
FoxP3
RORγT
CD8
CD4
B
Cd4 Cre^neg Rorc^F/F
FoxP3
RORγT
Cd4 Cre^pos Rorc^F/F
FoxP3
RORγT
C
RORγT+, FoxP3+ # of L/D Cells
**
RORγT+, FP3+ % of L/D
**
Total Cell Numbers
Total T Cell Numbers
D
****
****
Mean of Kullback–Leibler Divergence
Cd4 Cre^neg Rorc^F/F
Cd4 Cre^pos Rorc^F/F
Between Groups
E
Cd4 Cre^neg Rorc^F/F
Cd4 Cre^pos Rorc^F/F
Percentage of Motif Usage
Rearing
Sniffing/ Grooming
Sitting
Turning
Walking
U/I
F
8.57% of Behavior Motifs
Non-Significant Behavior (32)
Sitting (1)
Turning (1)
Walking (1)

Supplemental Figure 2.3: *Rorc* Depletion does not Impact Subtle Behaviors in Male Mice at Baseline. (A) Representative gating strategy for spleen Foxp3 and RORγT positive cells between *Rorc* KO and control animals. (B) Representative flow cytometry quadrants for FoxP3 and RORγT+ cells between Rorc KO and littermate controls. (C) Quantification of the number and percent of mesenteric RORγT+ and FoxP3+ cells and total cell and T cell numbers between *Rorc* KO and littermate controls (n=5-6/group). T tests (Number of RORγT, FP3+ cells: p= 0.0048, RORγt, FoxP3+ % of L/D: p= 0.0085). (D) Means of Kullback-Leibler Divergence scores in littermate controls, *Rorc* KO mice, and between groups (n=22 or 32/group). Multiple T tests (p= <0.0001). (E) Percentage and grouping of motif usage by Rorc KO vs littermate controls in DeepLabCut analyzed videos (n=22 or 32/group). T tests (Supplemental Table 1). (F) Quantification and grouping of significantly changed motifs (by % usage) in Rorc KO vs littermate controls. Male mice.

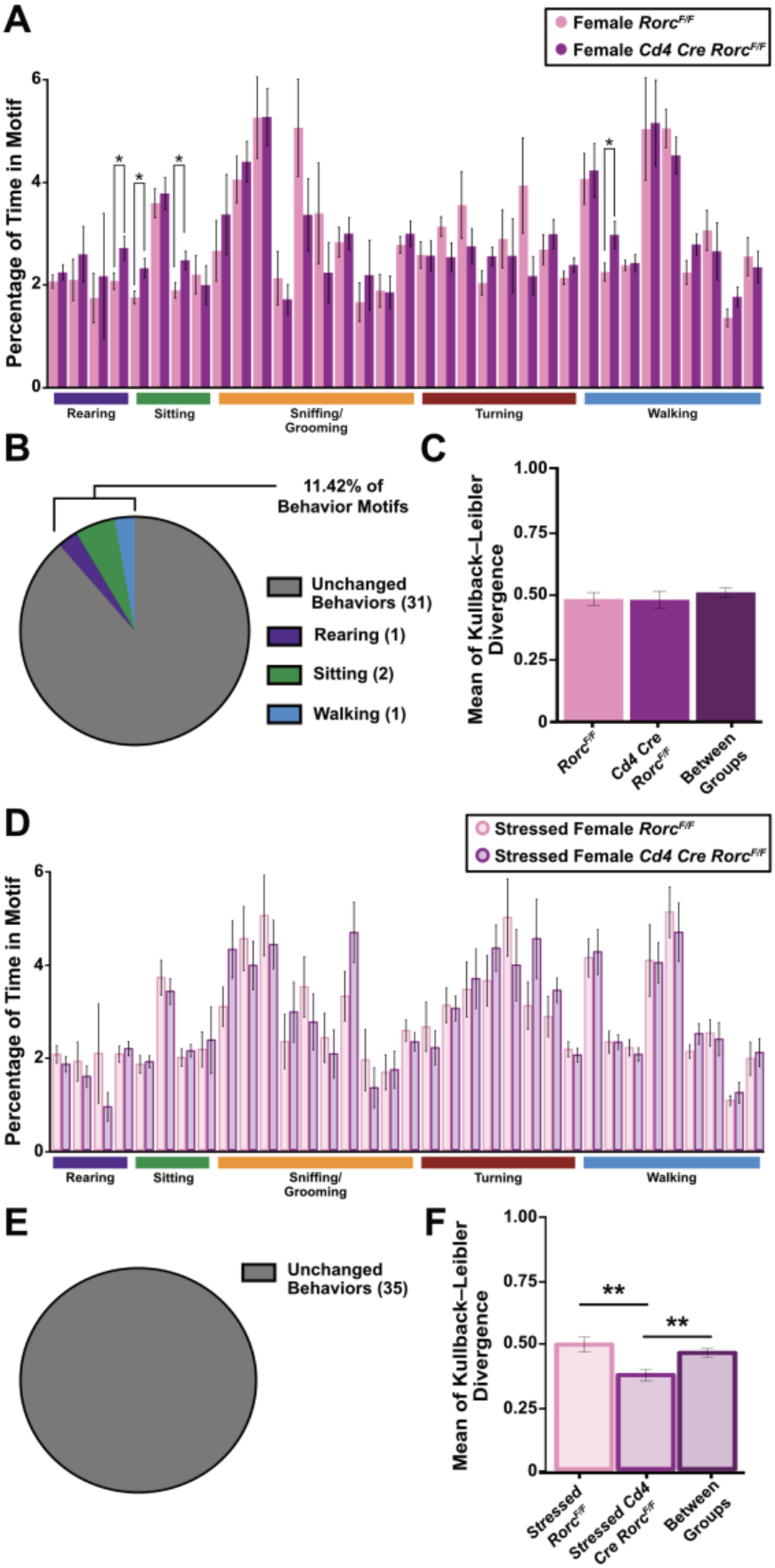
A
Female Rorc F/F
Female Cd4 Cre Rorc F/F
Percentage of Time in Motif
Rearing
Sitting
Sniffing/ Grooming
Turning
Walking
B
11.42% of Behavior Motifs
Unchanged Behaviors (31)
Rearing (1)
Sitting (2)
Walking (1)
C
Mean of Kullback–Leibler Divergence
Rorc F/F
Cd4 Cre Rorc F/F
Between Groups
D
Stressed Female Rorc F/F
Stressed Female Cd4 Cre Rorc F/F
Percentage of Time in Motif
Rearing
Sitting
Sniffing/ Grooming
Turning
Walking
E
Unchanged Behaviors (35)
F
Mean of Kullback–Leibler Divergence
Stressed Rorc F/F
Stressed Cd4 Cre Rorc F/F
Between Groups

Supplemental Figure 2.4: *Rorc* Depletion does not Impact Subtle Behaviors in Female Mice at Baseline or after Stress. (A) Percentage and grouping of baseline motif usage by female *Rorc* KO vs littermate controls in DeepLabCut analyzed videos (n=12/group). T tests (Supplemental Table 1). (B) Means of baseline Kullback-Leibler Divergence scores in female littermate controls, *Rorc* KO mice, and between groups (n=12/group). Multiple T tests (Supplemental Table 1). (C) Quantification and grouping of significantly changed motifs (by % usage) at baseline in female *Rorc* KO vs littermate controls. (D) Percentage and grouping of motif usage by stressed female *Rorc* KO vs stressed female littermate controls after 3 weeks of UCRS in DeepLabCut analyzed videos (n=12/group). T tests (Supplemental Table c1). (E) Quantification and grouping of significantly changed motifs (by % usage) after 3 weeks of UCRS in female *Rorc* KO vs littermate controls. (F) Means of Kullback-Leibler Divergence scores after 3 weeks of UCRS in female littermate controls, *Rorc* KO mice, and between groups (n=12/group). Multiple T tests (p= 0.0015, p= 0.0032).

Day	UCS Stress Procedure
1	Restraint + Cage Tilt
2	Cage Crowding + 2x Cage Change
3	Strobe Light + Wet Bedding
4	White Noise + 24hr Light Exposure
5	Restraint + 2x Cage Change
6	Cage Crowding + Wet Bedding
7	Strobe Light + Cage Tilt

Supplemental Table 2.2: Unpredictable Chronic Stress Protocol Table

Day	UCRS Stress Procedure
1	Restraint + Cage Tilt
2	Restraint + 2x Cage Change
3	Restraint + Wet Bedding
4	Restraint + Cage Tilt
5	Restraint + 2x Cage Change
6	Restraint + Wet Bedding
7	Restraint + Cage Tilt

Supplemental Table 2.3: Unpredictable Chronic Restraint Stress Protocol Table.

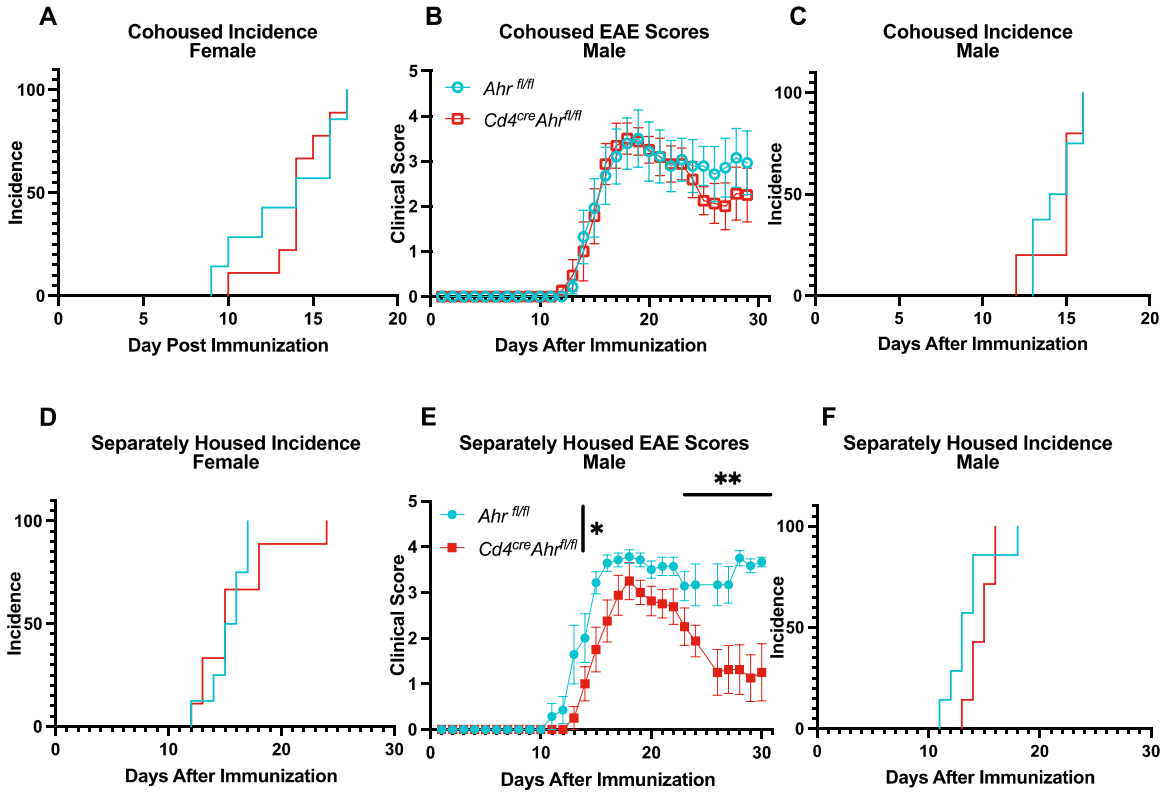

Supplement Figure 4.1 Separately housed *Cd4*^{cre}*Ahr*$^{fl/fl}$ recover from EAE phase.

(A) No genotype differences in EAE incidence from the experiment shown in **Figure 4.1A. (B)** No differences in EAE clinical score or (**C**) incidence in cohoused male mice (males; *n* = 7–8; *N* = 1; Mann–Whitney U Test [*p* = 0.5680]). (**D**) No genotype differences in EAE incidence from the experiment shown in **Figure 4.1D.** (E) Separately housed male *Cd4*^{cre}*Ahr*$^{fl/fl}$ mice recover from EAE, while *Ahr*$^{fl/fl}$ mice maintain paralysis. (Males; *n* = 7–8/group; *N* = 1; Mann–Whitney U Test on total scores reported in legend [*p* = 0.0010] and on single days reported on plot.) (F) No difference in incidence of cohoused male mice.

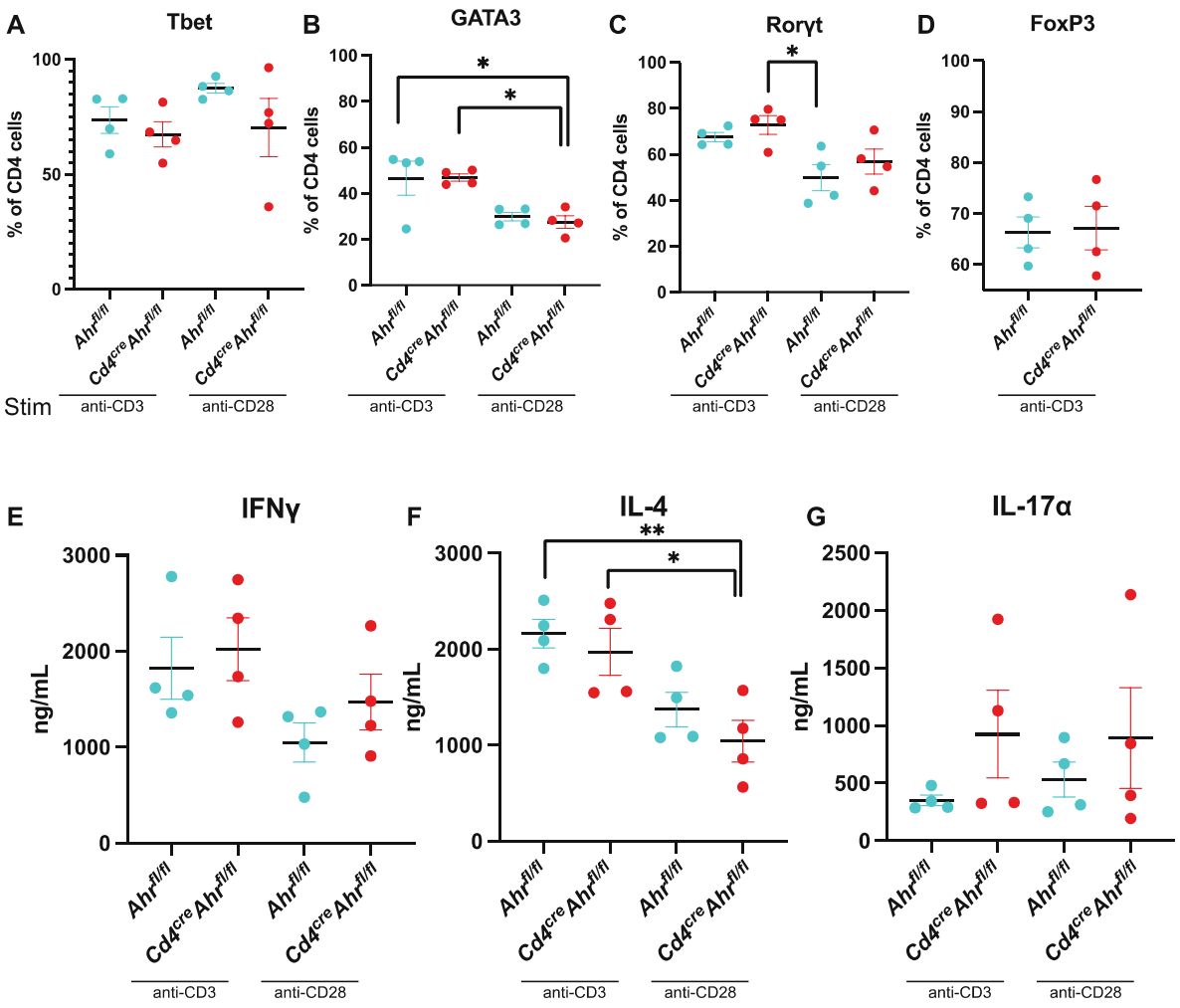
A
Tbet
B
GATA3
C
Rorγt
D
FoxP3
% of CD4 cells
Stim
anti-CD3
anti-CD28
Ahrfl/fl
Cd4cre Ahrfl/fl
E
IFNγ
F
IL-4
G
IL-17α
ng/mL

Supplement Figure 4.2 Lack of AHR in T cells isolated from separately housed mice does not impact differentiation capacity or cytokine production.

Naïve T cells were isolated from separately housed at weaning animals and differentiated toward T_H1, T_H2, T_H17, and T_{reg} in vitro. Transcription factor expression was quantified by flow cytometry. (A) Quantification of Tbet+ cells differentiated to T_H1 cell type and stimulated for 24 h with either anti-CD3 (anti-CD3) or a combination of anti-CD28 and anti-CD3 (anti-CD28) (*n* = 4 mice/group; *N* = 1 experiment; Ordinary one-way ANOVA [*p* = 0.2927]). (B) Quantification of GATA3+ cells differentiated to T_H2 cell type and stimulated for 24 h with either anti-CD3 (anti-CD3) or a combination of anti-CD28 and anti-CD3 (anti-CD28) (*n* = 4 mice/group; *N* = 1 experiment; Ordinary one-way ANOVA [*p* = 0.0076] followed by Tukey's post hoc). (C) Quantification of RORγt+ cells differentiated to T_H17 cell type and stimulated for 24 h with either anti-CD3 or anti-CD28 (*n* = 4 mice/group; *N* = 1 experiment; Ordinary one-way ANOVA [*p* = 0.0163] followed by Tukey's post hoc). (D) Quantification of FoxP3+ cells differentiated to T_{reg} cell type and stimulated for 24 h with either anti-CD3 or anti-CD28 (*n* = 4 mice/group; *N* = 1 experiment; Ordinary one-way ANOVA [*p* = 0.8801]). (E) IFNγ ELISA on supernatant of differentiated T_H1 cells stimulated for 24 h with either anti-CD3 (anti-CD3) or a combination of anti-CD28 and anti-CD3 (anti-CD28) (*n* = 4 mice/group; *N* = 1 experiment; Ordinary one-way ANOVA [*p* = 0.8639]). (F) IL-4 ELISA on supernatant of differentiated T_H2 cells stimulated for 24 h with either anti-CD3 or anti-CD28 (*n* = 4 mice/group; *N* = 1 experiment; Ordinary one-way ANOVA [*p* = 0.0064] followed by Tukey's post hoc). (G) IL-17a ELISA on supernatant of differentiated T_H17 cells stimulated for 24 h with either anti-CD3 or anti-CD28 (*n* = 4 mice/group; *N* = 1 experiment; Ordinary one-way ANOVA [*p* = 0.4826]).

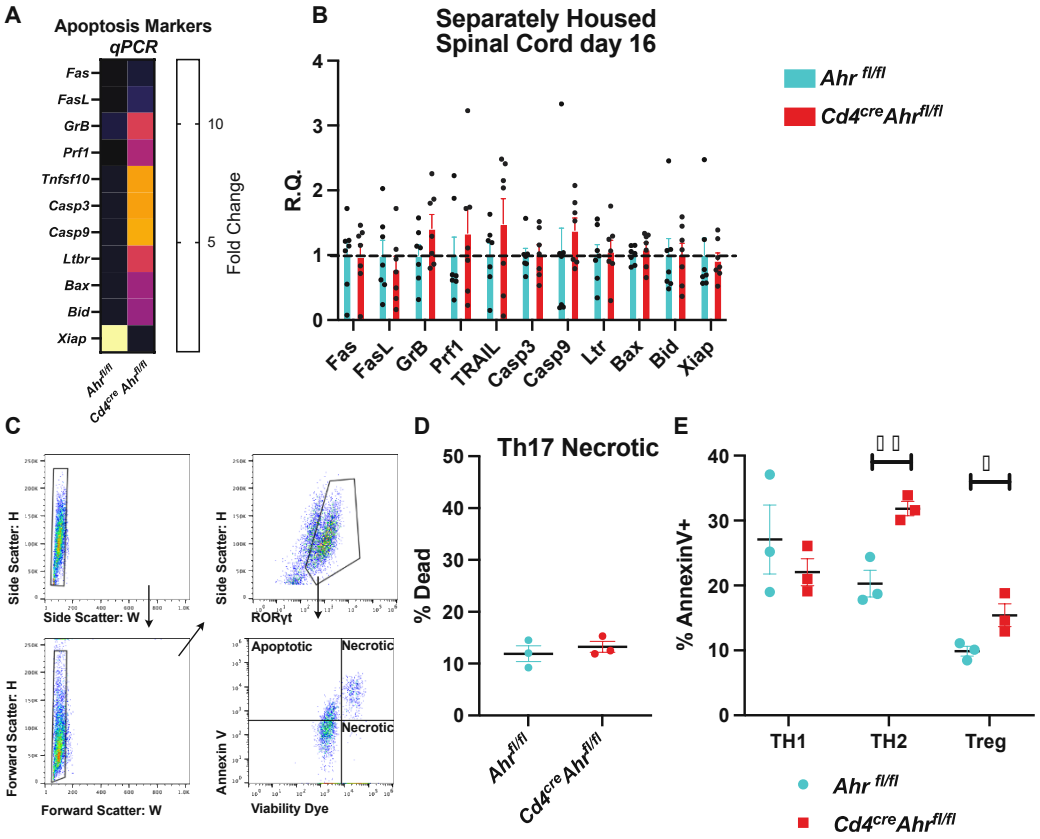

Supplement Figure 4.3 Higher apoptosis in CD4 T cells lacking AHR.

(**A**) Gene expression analysis (qPCR array) performed on spinal cord RNA prepared from separately housed *Cd4*^{cre}*Ahr*$^{fl/fl}$ mice and *Ahr*$^{fl/fl}$ littermate controls at the peak of disease (day 16) shows increased pro-apoptotic transcripts and decreased anti-apoptotic transcript (cDNA prepared from 2 spinal cords were pooled for each sample). (**B**) Gating strategy for Annexin V+ apoptotic and necrotic cells shown in show in Figures 4.4 and Supplement Figure 4.3C and Supplement Figure 4.3D. (**C**) Quantification of total dead cells in separately housed T_H17 differentiated cells (n = 3 mice/group; N = 1 experiment; unpaired t test [p = 0.5130]). (**D**) T cells differentiated to T_H1, T_H2, or T_{reg} in vitro from separately housed *Cd4*^{cre}*Ahr*$^{fl/fl}$ mice have higher expression of the apoptotic marker Annexin V after 24 h of CD3 stimulation. (n = 3/group; N = 1 experiment; unpaired t tests [p = 0.4276, 0.0078, 0.0442]).

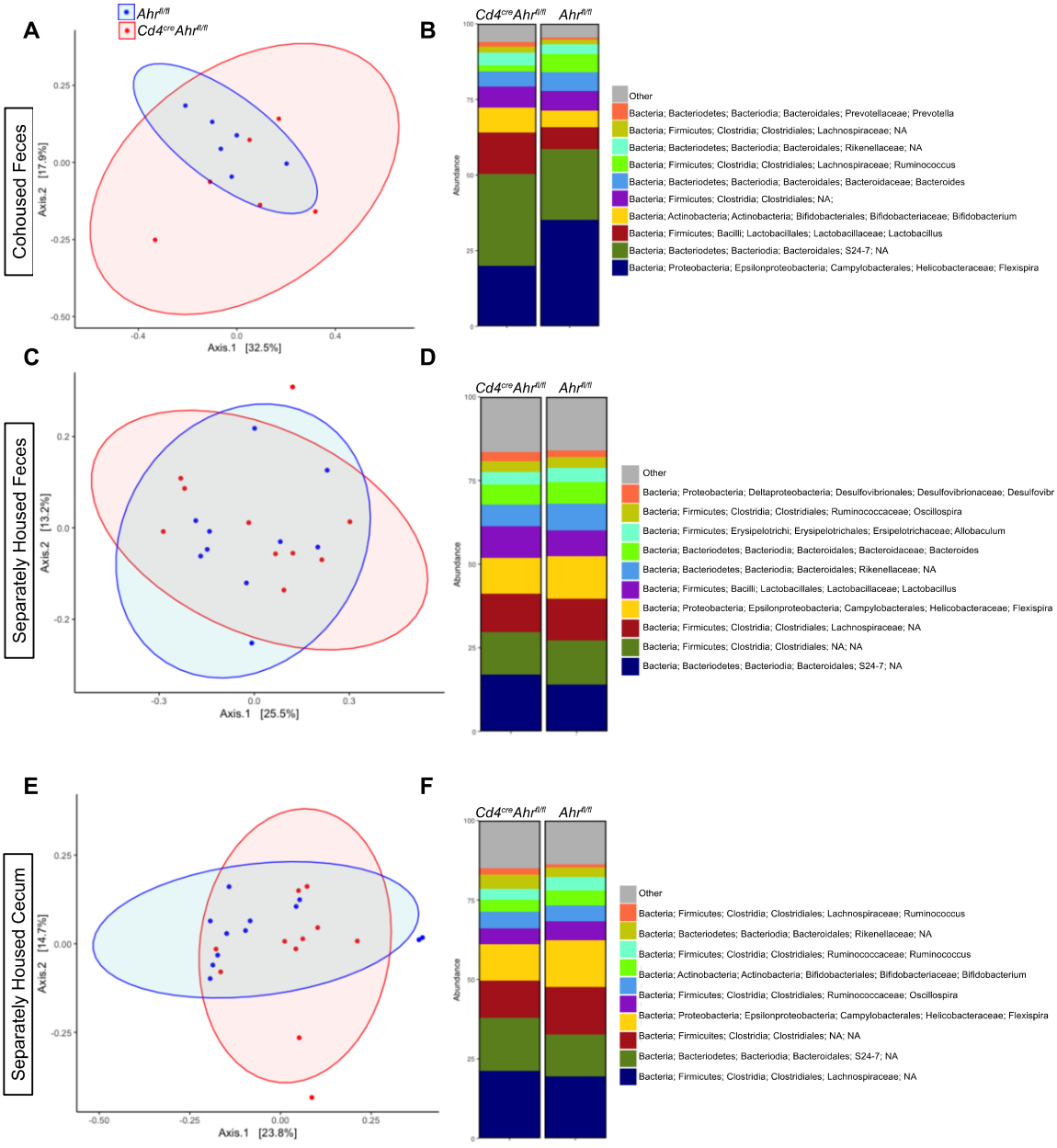

Supplement Figure 4.4 Only subtle microbiota population changes in *Cd4*^{cre}*Ahr*$^{fl/fl}$ mice.

(**A**) PCA plot and (**B**) microbiome composition at the genus level obtained from 16S sequencing performed on feces collected from cohoused animals. (Males; *n* = 6/group) (**C**) PCA plot and (**D**) microbiome composition at the genus level obtained from 16S sequencing performed on feces collected from separately housed animals. (Males and females; *n* = 10/group) (**E**) PCA plot and (**F**) microbiome composition at the genus level obtained from 16S sequencing performed on cecum collected from separately housed animals. (Males and females; *n* = 12/group). Raw data are available

in the NCBI Gene Expression Omnibus repository accession number GSE200440; https://www.ncbi.nlm.nih.gov/geo/query/acc.cgi?acc=GSE200440. https://doi.org/10.1371/journal.pbio.3002000.s004